DISTINCT DNA REPLICATION PROGRAMS IN *TETRAHYMENA THERMOPHILA*

A Dissertation

by

XIANGZHOU MENG

Submitted to the Office of Graduate and Professional Studies of
Texas A&M University
in partial fulfillment of the requirements for the degree of

DOCTOR OF PHILOSOPHY

Chair of Committee,	Geoffrey Kapler
Committee Members,	Sarah Bondos
	Pingwei Li
	David Peterson
Head of Department,	Gregory Reinhart

May 2015

Major Subject: Biochemistry

ABSTRACT

DNA replication is a vital process to duplicate genetic material for inheritance. A conventional mitotic cell cycle is composed of G1, S, G2 and M phases, and DNA is replicated during S phase. Besides the conventional cell cycle, there are other distinct replication programs. Here in my dissertation, I used the organism *Tetrahymena thermophila* to study DNA replication because it employs alternative DNA replication programs, such as genome-wide endoreplication, locus-specific gene amplification and an unprecedented DNA replication program in cells that are recovered from hydroxyurea (HU) induced replication stress.

In my dissertation research, I determined that ribosomal DNA (rDNA) minichromosome amplification occurs when non-rDNA chromosomes are undergoing endoreplication during *Tetrahymena* development, and that both programs are shut down simultaneously. I found that rDNA amplification is then switched to endoreplication upon refeeding when the levels of the initiation proteins, the origin recognition complex (ORC) and the minichromosome maintenance protein complex (MCM2-7) are dramatically reduced. During this stage, the rDNA origin is not utilized, and a higher origin density was observed on a genome-wide scale. These data indicate that origin utilization is altered for endoreplication and suggest an ORC-independent initiation mechanism. More importantly, rDNA replication intermediates that are accumulated in both wild type endoreplication and vegetative S phase of a histone monomethyltransferase defective strain TXR1Δ share the same signature, suggesting

epigenetic modifications may be involved in replication initiation and elongation during endoreplication.

As part of my dissertation research, I studied a DNA replication program that occurs after ORC and MCM proteins are degraded in hydroxyurea treated cells. I found that replication forks are arrested rather than slowed down upon HU treatment, when the protein levels of ORC and MCMs are degraded. I detected new origin firing on a genome-wide scale upon HU removal, before the protein levels of ORC and MCMs are restored. Moreover, the rDNA origin that is used for vegetative S phase is not utilized in this specialized replication program. The collective data suggest that an ORC-independent initiation is utilized.

In summary, my research has led to new discoveries of distinct DNA replication initiation and elongation mechanisms in eukaryotes.

DEDICATION

I would like to dedicate this dissertation to my beloved grandparents.

ACKNOWLEDGEMENTS

I would like to express my deepest gratitude to my advisor Dr. Geoffrey Kapler for his endless support. He is always very patient with me and tries his best to help me in my studies and my life. I could not have completed my graduate studies without his guidance and encouragement.

I am grateful to my committee members, Dr. Sarah Bondos, Dr. Pingwei Li and Dr. David Peterson for their guidance and great suggestions on my research. I would like to thank Dr. Dorothy Shippen for her critical advice and encouragement throughout the course of my graduate studies and research. I would also like to thank Dr. Xiuren Zhang and Dr. Jun-yuan Ji for their advice on my research.

I want to thank my colleagues, Dr. Po-Hsuen Lee, Dr. Marcella Cervantes, Dr. Jeong Chan Moon, Dr. Brian Berquist, and Dr. Pamela Sandoval for their help and suggestions.

I want to thank my friends, Guo Fu, Cai Jiang, Cheng Cheng, Hengyi Xu, Shanshan Yang, and Fuqu Hu, who help me a lot and bring me so much fun.

I would like to thank my parents, sister, brother and grandparents for their constant support, encouragement and love.

Finally, I want to thank my wife Yanping Cui for her understanding and support during the past few years, and thank my little daughter for bringing me a lot of joy.

TABLE OF CONTENTS

Page

Page

LIST OF FIGURES

Page

Page

Page

LIST OF TABLES

Page

CHAPTER I

INTRODUCTION

Overview

The focus of my dissertation research is to gain insight into the control of different replication programs in eukaryotes. In order to provide a framework for my research, in this chapter I will first give an overview of eukaryotic DNA replication initiation and how it is controlled to prevent re-replication. Different DNA replication programs in eukaryotes, such as endoreplication and gene amplification will then be presented. Finally, I will introduce the model organism *Tetrahymena thermophila* used for my dissertation study.

DNA replication initiation

Duplication of the genome is an important biological process which needs to be strictly regulated in cells. The first model that was proposed to explore the mechanism of replication regulation is the "replicon" model introduced in 1963 in bacteria (Jacob et al, 1963). In this model, a replicon contains two genetic determinants: a gene encodes a trans-acting regulatory factor, named the "initiator", and the specific DNA sites that the initiator act on, the "replicator", also termed the origin of replication. While there is often a single replication origin in bacterial or archaeal genomes, eukaryotic genomes contain multiple origins for the much larger linear chromosomes. Origins in most eukaryotes do not have sequence specificity; however, the initiator, the origin recognition complex (ORC) is highly conserved across eukaryotes (Bell & Stillman,

1992; Gossen et al, 1995; Moon et al, 1999; Rowles et al, 1996). The manner of ORC binding to origins is distinct in different eukaryotes.

Origins and ORC

In budding yeast *Saccharomyces cerevisiae*, the first chromosomal replicator was identified based on its ability to provide plasmids autonomous replication (Stinchcomb et al, 1979). The DNA element was named autonomous replication sequence 1 (ARS1), and further studies on ARS1 showed that ARSs contained an 11 bp AT-rich sequence ARS consensus sequence (ACS) (Marahrens & Stillman, 1992), extended to 17 bp later on (Theis & Newlon, 1997). The A-T rich ACSs are the essential core of all ARSs and are specifically recognized and bound by ORC. Although ACSs define origins of replication in *S. cerevisiae*, only a small fraction of them are used in a single S phase (Linskens & Huberman, 1988). Additional DNA elements close to the ACS also play important roles in determining functional origins, such as the B domains, B1, B2 and B3 elements. In ARS1, the B1 element is involved in ORC binding to DNA (Rao & Stillman, 1995). ORC contains six subunits, named Orc1 through Orc6 in a decreasing order of molecular mass. Multiple subunits of ORC are involved in contacting DNA (Lee & Bell, 1997). The B2 element has been proposed to act as a DNA unwinding element (DUE) (Huang & Kowalski, 1993), and it is important for binding of minichromosome maintenance complex 2-7 (MCM2-7) to the origin and assembly of pre-replication complex (pre-RC) (Wilmes & Bell, 2002). The B3 element serves as the binding site for transcription factor Abf1 (ARS binding factor 1) which is involved in transcription activation and chromatin remodeling (Marahrens & Stillman, 1992; Miyake

et al, 2002). More importantly, the B3 element serves as a boundary element that creates a nucleosome-free ARS.

In the fission yeast *Schizosaccharomyces pombe* (Sp), similar ARS assays were used to identify replicons (Clyne & Kelly, 1995). In contrast to *S. cerevisiae*, *S. pombe* frequently has larger replicons (0.5-1 kb), and concensus sequences have not been identified. However, genetic dissection analyses of the origins demonstrated that *S. pombe* ARSs are composed of several functional A-T rich elements. These elements consist of clustered adenine/thymine stretches, and the number of stretches and degree of the clustering may determine the activity of a given origin (Okuno et al, 1999). Genome-wide analysis revealed later that approximately 90% of the A+T-rich islands co-localize with active origins (Segurado et al, 2003). In *S. pombe*, the specialized structure of SpOrc4 subunit is utilized for SpORC binding to degenerate A+T-rich sequences (Chuang & Kelly, 1999). The N-terminal domain of SpOrc4 is composed of nine copies of the AT-hook motif which binds to the minor groove of A+T-rich stretches. Both *in vivo* and *in vitro* studies revealed that the AT-hook domain is essential for SpORC binding to the origin (Kong & DePamphilis, 2001; Lee et al, 2001).

Similar to yeasts, metazoan DNA replication starts at specific sites; however, the sequence feature of replication origins is still largely incomprehensible. Studies on individual origins have revealed some characteristics. Some sequence-specific sites function as origins and can also act at ectopic sites, such as human lamin B2 origin and human β-globin locus origin. A 1.2 kb DNA segment of human lamin B2 replicon overlaps with the 3' end of the lamin B2 gene and the promoter of the downstream gene.

This region contains the start site of replication, and a nearby CpG island which positively influence the efficiency of initiation (Paixao et al, 2004). The replication initiation region of human β-globin locus contains two 2-3 kb adjacent, redundant replicators, and each can initiate replication independently at ectopic sites. Initiation of the replicator at ectopic sites shows similar requirement with initiation at native locus. In addition, non-redundant sequences within each replicator work cooperatively to determine replicator activity (Wang et al, 2004). In contrast, other origins are not confined sites, but exist as broad initiation zones, such as the Chinese hamster dihydrofolate reductase (DHFR) locus. The DHFR origin region contains a 55 kb intergenic segment with more than 40 initiation sites that are unevenly dispersed and are utilized with different efficiencies. In metazoans, there is no sequence specificity for ORC binding to origins (Remus et al, 2004; Vashee et al, 2003). The mechanisms of the recruitment are still not well defined.

Genome-wide analysis on replication origins in *S. pombe* shows that there are approximately 400 strong origins and 500 putative weaker origins in mitotic cell cycles with the average inter-origin distance of 14 kb (Heichinger et al, 2006). In mammals, about 30,000-50,000 origins are active in each cell cycle (Huberman & Riggs, 1966). Recent genome-wide analysis of replication origins in *Drosophila* and mouse cells revealed that origin G-rich repeated elements (OGREs) exist in 90% of the DNA replication origins in mouse and human cells and 67% in *Drosophila* origins (Cayrou et al, 2012a). These elements are GC-rich and have the potential to form G-quadruplex structures which may facilitate their function. The biological functions of these OGREs

at metazoan origins are still unknown. Metazoan DNA replication origins are organized in large replicons with high density and are utilized with low efficiency (Cayrou et al, 2011). Approximately 20% of licensed origins are activated in each cell cycle in mouse embryonic fibroblast cells. In addition, origin-rich regions replicate early, whereas origin-poor regions are late replicating (Cayrou et al, 2011).

Epigenetic effect on replication initiation

Epigenetic factors also play important roles in regulating replication initiation, such as nucleosome positioning and histone modifications. In *S. cerevisiae*, the core sequences of the ARS1 origin has been found in nucleosome-free region by nucleosome mapping studies, and is flanked by well positioned nucleosomes (Thoma et al, 1984). The positioning of the flanking nucleosomes is important for the origin activity. When the ARS1 is moved into the central DNA region with a nucleosome core particle, the origin's activity on an episome is compromised (Simpson, 1990). The significance of nucleosome positioning has been tested at the endogenous ARS1 locus on the chromosome (Lipford & Bell, 2001). It was demonstrated that ORC is needed for maintenance of nucleosome positioning at the origin. When the nucleosomal arrangement is disrupted, ORC still can associate with the origin, but pre-RC formation is inhibited. Therefore, the positioning of nucleosomes can affect origin activity and replication initiation. Recently, genome-wide analysis revealed that a conserved pattern of nucleosome positioning exists at most origins of replication in budding yeast (Berbenetz et al, 2010; Eaton et al, 2010). *In vitro* nucleosome reconstitution without any trans-acting factors coupled with high-throughput sequencing has demonstrated that

the intrinsic DNA sequence rather than ORC binding to the origin determines the nucleosome occupancy at ORC binding sites (Kaplan et al, 2009). In higher eukaryotes, ORC binding sites is also related to nucleosome occupancy. In *Drosophila*, ORC-associated sequences localize to highly accessible regions with open chromatin that is enriched for the replication-independent histone variant H3.3 (MacAlpine et al, 2010). Histone variant H3.3 marks regions with active chromatin remodeling and depleted for bulk nucleosomes. In Chinese hamster cells, ORC also associates with nucleosome-free regions in the DHFR initiation zone (Lubelsky et al, 2011).

Epigenetic modifications, such as post-translational histone acetylation and methylation are often associated with replication timing. Genome-wide analysis in *Drosophila* has demonstrated that activating chromatin marks, such as H3K27ac, H3K18ac, or H3K4me, are associated with replication early in S phase (Eaton et al, 2011). Histone acetylation is also critical for specifying origins during the developmental transition from global replication to the amplification of chorion genes (Aggarwal & Calvi, 2004). ORC binding sites are enriched with hyperacetylated histones. Mutation of histone deacetylase Rpd3 triggers global hyperacetylation and redistribution of ORC2. In *S. cerevisiae*, histone deacetylase Rpd3 is involved in regulating replication timing, especially for late firing origins (Knott et al, 2009). Another deacetylase, Sir2, is responsible for heterochromatin silencing also plays a negative role in modulating pre-RC formation at some origins (Pappas et al, 2004). On the other hand, histone acetyltransferase Hbo1 (histone acetylase binding to Orc1) interacts with various components of the pre-RC, such as Orc1, Mcm2 and Cdt1, and

involves in pre-RC formation (Burke et al, 2001; Doyon et al, 2006; Iizuka et al, 2006). Hbo1 is H4-specific histone acetylase, and H4 acetylation and MCM2-7 loading are impaired when Hbo1 activity is inactivated (Miotto & Struhl, 2010). In addition, when Rpd3 is tethered to the origin of chorion genes, the origin activity decreases, but the origin activity increases when Hbo1 is used (Aggarwal & Calvi, 2004).

In early *Xenopus* embryos, rDNA replication initiates randomly in 9-12 kb intervals in both coding regions and non-coding regions, without showing any sequence specificity, when there is no rDNA transcription (Hyrien et al, 1995). During the mid-blastula transition, the chromatin is remodeled and rDNA transcription starts. Replication initiation within coding regions is repressed, restricting origin firing to intergenic regions, so inter-origin distances increase dramatically. This study indicates that change in chromosome structure could alter origin utilization.

Genome-wide analysis in *Drosophila*, mouse and human cells revealed that origins cluster near CpG islands regardless of methylation status (Cadoret et al, 2008; Cayrou et al, 2011; MacAlpine et al, 2004; Sequeira-Mendes et al, 2009). Origins tend to replicate in early S phase if adjacent genes are actively transcribed.

Control of replication initiation

DNA replication occurs at thousands of origins in eukaryotic cells in order to replicate large genomes in brief periods of time. Origin usage needs to be strictly coordinated to make sure that the genome is replicated only once per cell cycle. There are two temporally separated steps to initiate replication and prevent re-replication (Blow & Dutta, 2005): helicase loading and helicase activation. The process of helicase

loading, also refered to as pre-RC assembly, results in origin licensing. The pre-RC was first identified in *S. cerevisiae* by using an *in vivo* DnaseI protection assay, and the appearance of pre-RC is cell cycle-regulated (Diffley et al, 1994). Researchers have identified a conserved pathway for replication origin licensing. Cyclin-dependent kinases (CDKs) are the key players in the regulation of pre-RC assembly. Origin licensing takes place during late mitosis and early G1 phase when S-phase CDK activity is low, allowing ORC binding to replication origins (Figure 1.1). In G1 phase, after ORC is bound to replication origins, Cdc6 and Cdt1 are recruited to the site and MCM2-7, the replicative helicase is loaded onto DNA to form the "licensed" pre-RC ORC and Cdc6 are no longer required for MCM binding to DNA once MCM is loaded. Two MCM2-7 molecules form an inactive ring-structured head-to-head dimer surrounding double-stranded DNA (Evrin et al, 2009; Remus et al, 2009). In S phase, the MCM2-7 complex is activated by the action of cyclin-dependent kinase (CDK) and Dbf4-dependent kinase (DDK) (Labib, 2010). Firstly, DDK phosphorylates MCM subunits to load Cdc45 and Sld3 (Heller et al, 2011; Sheu & Stillman, 2006). Mcm4 and Mcm6 are the only crucial subunits for phosphorylation by DDK (Randell et al, 2010). In addition, DDK promotes S phase activation of the helicase by removal of inhibitory activity of the Mcm4 N-terminal domain (Sheu & Stillman, 2010). Next, CDK phosphorylates Sld2 and Sld3 to generate the binding sites for BRCT-repeat protein Dpb11 (Tanaka et al, 2007b; Zegerman & Diffley, 2007). This complex then promotes GINS recruitment. Finally, binding of Cdc45 and GINS to Mcm2-7 leads to the formation of Cdc45-Mcm2-7-GINS complex and helicase activation (Ilves et al, 2010). These changes at the origin allow

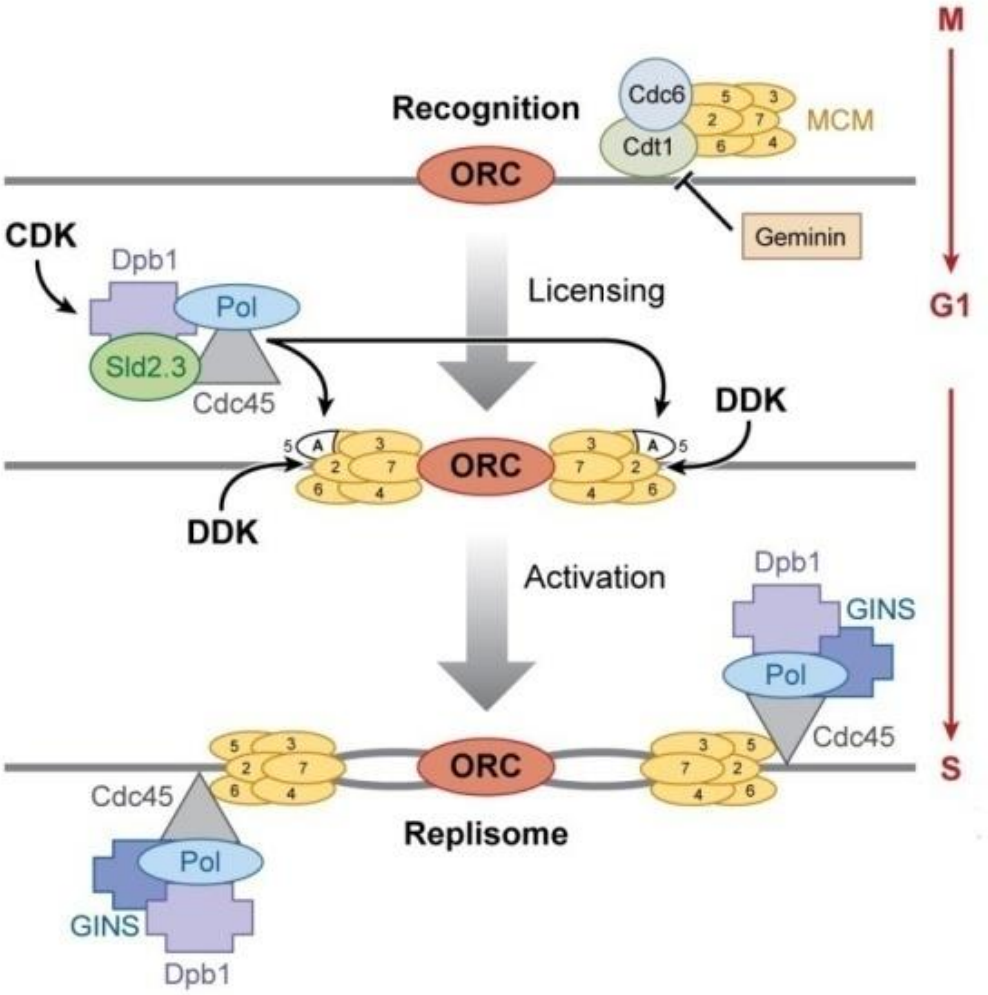

Figure 1.1. Model of the regulation of eukaryotic DNA replication. This figure is modified from Sclafani & Holzen, 2007.

other components of the replisome, such as DNA polymerase α and primase to be recruited.

In eukaryotes, separation of helicase loading and activation is the strategy to prevent re-replication. There are basically two different ways to achieve this. One way is to degrade or inactivate the pre-RC components, like ORC, Cdc6 and Cdt1. Another way is to export pre-RC components out of the nuclei or released from chromatin once they have performed their task, such as exporting MCM2-7 from the nucleus in *S. cerevisiae*. In S phase, once helicases are activated, licensing is stringently blocked through different mechanisms. In *S. cerevisiae*, Cdc6 (or Cdc18 in *S. pombe*) is phosphorylated by CDK, marking this protein for ubiquitylation by SCF^{Cdc4} ligase (SCF^{Pop1} in *S. pombe*), and it triggers destruction by the proteasome (Drury et al, 1997; Drury et al, 2000; Jallepalli et al, 1997). Moreover, in budding yeast, mitotic CDK binds the N-terminal domain of Cdc6 to block its licensing activity (Mimura et al, 2004). CDKs also phosphorylate ORC subunits Orc2 and Orc6 to inhibit its ability to initiate re-replication (Nguyen et al, 2001; Vas et al, 2001). In addition, it was reported that CDKs interact directly with ORC at origins to keep the inactive state of ORC during S and G2 phases (Wilmes et al, 2004; Wuarin et al, 2002). In *S. cerevisiae*, the MCM2-7 complex is exported from the nucleus promoted by CDK phosphorylation (Labib et al, 1999; Nguyen et al, 2000) but not in higher eukaryotes. Cdt1 is also exported to the cytoplasm during S phase since it is associated with MCM2-7 (Tanaka & Diffley, 2002). In *S. pombe*, Cdt1 is regulated by proteolysis in S and G2 phases in a manner similar to Cdc6/Cdc18 (Nishitani et al, 2000).

In metazoans, like in *S. cerevisiae*, phosphorylation or degradation of Orc1p is one way to prevent re-replication (Fernandez-Cid et al, 2013). In human cells, Orc1 is ubiquitinated once cells enter S phase, and degraded through the proteasome (Mendez et al, 2002). Cdt1 is another major target for cells to prevent licensing during S and G2 phases. Cdt1 activity is down-regulated at two levels: degradation of the Cdt1 protein and activation of a Cdt1 inhibitory protein termed geminin. There is more than one pathway for Cdt1 proteolysis. One pathway is regulated by phosphorylation of Cdt1 by CDK, which is similar to the degradation of Cdt1 in *S. pombe*. Phosphorylation of Cdt1 labels it for the SCF^{Skp2} E3 ubiquitin ligase (Li et al, 2003; Liu et al, 2004). Another pathway for Cdt1 proteolysis utilizes the Cul4-Ddb1-Cdt2 E3 ubiquitin ligase complex and depends on proliferating cell nuclear antigen (PCNA) (Arias & Walter, 2006; Nishitani et al, 2006; Senga et al, 2006). PCNA, which is loaded onto chromatin during replication, directly binds Cdt1, so Cdt1 proteolysis is coupled with DNA replication. In higher eukaryotes, in addition to degradation of Cdt1, down-regulation of Cdt1 is also achieved via Geminin (Tada et al, 2001; Wohlschlegel et al, 2000). Geminin binds to Cdt1 during S and G2 phases to sequester it on chromatin. As a result, Cdt1 is prevented from associating with MCM2-7, and therefore pre-PC reassembly is inhibited. DNA re-replication is triggered when Geminin is depleted in cells (Mihaylov et al, 2002; Quinn et al, 2001; Zhu et al, 2004).

Alternative DNA replication programs: endoreplication and gene amplification

Endoreplication

In eukaryotic cells, the genome is duplicated once and only once in preparation for cell division. Endocycling is an alternative DNA replication program consisting of alternate Gap (G) phase and S phase without cell division. Endocycles and polyploidy have been found not only in plant and animal tissues, but also in single celled organisms, such as ciliates (Fox & Duronio, 2013). Endoreplication is often observed during eukaryotic development and serves the purpose of generating polyploid cells that provide nutrients and proteins to support the development of the embryo. During *Drosophila* larval growth, most tissues contain polyploid cells, the best studied example of which is the giant salivary gland. In these cells, DNA copy numbers reach around 1350 C after ten round of endoreplication (Hammond & Laird, 1985). Another example is the *Drosophila* follicle cells which proliferate mitotically until stage 6 of oogenesis. After that, three rounds of endoreplication occur from stage 7 to stage 10A (Calvi et al, 1998).

Studies on endocycles in *Drosophila* follicle cells have shown that Notch signaling is the regulator for transition from mitotic cell cycles to endocycles (Deng et al, 2001; Lopez-Schier & St Johnston, 2001). In follicle cells, the Notch signaling ligand Delta activates Notch transmembrane receptor. The intracellular domain of Notch is cleaved and enters the nucleus to control transcription of Notch-responsive genes. Notch mutant follicle cell clones cannot achieve the transition from mitotic cell cycle to endocycle (Deng et al, 2001; Lopez-Schier & St Johnston, 2001). Notch signaling

promotes this transition through upregulation of Fzr/Cdh1 and downregulation of Dacapo and String/Cdc25 (Schaeffer et al, 2004; Shcherbata et al, 2004). Fzr/Cdh1 is an activator of anaphase-promoting complex/cyclosome (APC/C); therefore, induced Fzr/Cdh1 promotes ubiquitin-mediated degradation of mitotic cyclins. Dacapo is the S-phase CDK (CycE/Cdk2) inhibitor, and String is a protein phosphatase which can remove inhibitory phosphates from Cdk1 to promote mitosis. Hence, downregulation of Dacapo and String blocks mitosis and promotes endoreplciation.

Studies have shown that oscillation of Cyclin E/Cdk2 activity is the main factor driving endoreplication. CyclinE/Cdk2 is required for cells to enter S phase. During *Drosophila* embryogenesis, endoreplication is detected in late wild-type embryos, but not in cyclin E (*DmcycE*) mutant embryos (Knoblich et al, 1994). Cyclin E is required for both mitotic cycles and endocycles. In addition, ectopic overexpression of *DmcycE* can drive quiescent endoreplicating cells generated by starvation into S phase (Britton & Edgar, 1998). Similarly, in the mouse, Cyclin E1 and E2 which are mostly unnecessary for mouse development are required for endoreplication of trophoblast giant (TG) cells and megakaryocytes (Geng et al, 2003). The double knockout placenta has a normal phenotype in general, but the DNA content in the nuclei of TG cells is dramatically reduced (Parisi et al, 2003). Moreover, depletion of Cdk2 prevents endoreplication in trophoblast stem (TS) cells (Ullah et al, 2008). Although CyclinE/Cdk2 activity is required for endoreplication, continuous overexpression of *DmcycE* in *Drosophila* salivary glands inhibits progression through endocycles (Follette et al, 1998; Weiss et al,

1998). These studies indicate that oscillation of CycE/Cdk2 activity is the driving force for endoreplication.

In metazoans, Cyclin E expression is controlled by E2F transcription factors. For example, in *Drosophila*, there are two E2Fs, E2F1, which is an activator, and E2F2, which is a repressor. E2F1 is required for both the expression and oscillation of *Drosophila* cyclin E, and it is has been shown that disruption of the E2F1 gene causes endoreplication arrest in *Drosophila* cells (Zielke et al, 2011). E2F1 also oscillates during the cell cycle: high E2F1 protein levels are observed during G1 phase and the protein is degraded in S phase. Oscillation of E2F1 protein during cell cycle is controlled by the CRL4/Cdt2 E3 ubiquitin ligase which can be activated by chromatin bound-PCNA (Arias & Walter, 2006). Therefore the CRL4/Cdt2 E3 ligase is activated only when DNA replication occurs, and E2F1 protein is downregulated by degradation in the proteasome. By this autoregulatory feedback loop, the oscillation of cyclin E is achieved and endoreplication occurs. Overexpression of E2F1 accelerates endocycling in salivary glands, but stabilization of E2F1 by PIP box mutations blocks endocycling (Zielke et al, 2011). It has not been shown that the same regulatory mechanisms are taken by plants or mammals. Other mechanisms to control oscillation of CDK activity might be utilized.

It is suggested that a distinct initiation program must be utilized for endoreplication in *Drosophila*, since in the *Drosophila* salivary gland, ORC is dispensable for endoreplication (Park & Asano, 2008), though ORC is associated with chromosomes during endocycling (Sher et al, 2013). So far, there is no direct evidence on whether ORC is required for endoreplication during *Tetrahymena* development.

Gene amplification

Gene amplification is a specialized program to increase the amount of a certain DNA segment in the genome by firing origins at specific loci many times. One type of gene amplification, associated with development, such as amplification of *Drosophila* chorion genes (Calvi et al, 1998), *Sciara* cocoon genes (Wu et al, 1993), and the *Tetrahymena* rDNA gene (Yao et al, 1974). The purpose of developmental gene amplification is to increase DNA template at specific loci for transcription to generate the large quantities of rRNAs and structural proteins required during development. Developmental gene amplification is often associated with endoreplication. In *Drosophila* follicle cells, after three rounds of endoreplication, follicle cells switch into gene amplification at stage 10B. This switch results in higher copy numbers for chorion genes, which are required for eggshell synthesis (Calvi et al, 1998).

In *Drosophila* and Sciara, origins fire repeatedly to amplify the genes, and finally the "onionskin" structure with a gradient of amplified DNA is formed (Calvi et al, 1998; Liang et al, 1993; Osheim et al, 1988). Although the amplification levels among different amplified regions vary in *Drosophila*, ranging from a few folds to 60-80 fold, all amplicons share similar size of the amplification gradient, which is about 80-100 kb (Claycomb et al, 2004; Spradling, 1981). In *Drosophila* follicle cells, the timing of gene amplification is strictly controlled, and the origin firing and fork elongation are separated. Origin firing occurs only during stages 10B and 11, and existing forks elongate during stages 12 and 13 (Claycomb et al, 2002). One exception is the amplicon DAFC-62D, with an additional round of origin firing during stage 13 to provide more

template for late gene transcription (Claycomb et al, 2004). Replication initiation must be stringently regulated for transition from genome-wide endoreplication to site specific gene amplification.

In contrast to *Drosophila melanogaster* ovarian follicle cells, gene amplification of the rDNA and endoreplication of the macronuclear chromosomes during *Tetrahymena* development is not linked to terminal differentiation. Once development is completed, cells need to switch back to normal cell cycle control during vegetative growth. In addition, endoreplication and gene amplification are temporally separated in Drosophila follicle cells. Gene amplification occurs after the completion of endocycles; however, in *Tetrahymena*, there are two periods of endocycles during development: the occurrence of the second endoreplication period depends on re-feeding, and amplification of the rDNA is not temporally separated from endoreplication.

Besides the natural developmental regulated gene amplification, gene amplification also exists in drug resistant cells and cancer cells. Amplification of DHFR genes has been documented in methotrexate-resistant murine cells long time ago (Alt et al, 1978). Methotrexate is an analog of folic acid and it can competitively inhibit DHFR which is involved in synthesis of purines, thymidylic acid and glycine. Therefore, the drug can inhibit DNA synthesis and used for chemotherapy. In methotrexate resistant cells, increase of DHRF gene copy number is one way to achieve resistance.

DNA damage induced checkpoint response

DNA damage checkpoint responses are the feedback response of the cell cycle progression when DNA is damaged. In order to ensure complete replication of the entire

genome, cell cycle progression stops temporarily until damaged DNA is repaired. The DNA damage checkpoint responses are coordinated primarily by two kinase signaling cascades, orchestrated by ATM (ataxia-telangiectasia mutated) and ATR (ATM- and Rad3-Related) kinases. ATM and ATR recognized different DNA structures: ATM primarily binds to double-strand breaks (DSBs) and ATR is recruited on single-stranded DNA (ssDNA) (Figure 1.2). Chk1 and Chk2, both of which are the serine-threonine checkpoint effector kinases, are the substrates of ATR and ATM respectively. In addition, there is crosstalk between these two signaling pathways.

ATM exists as inactive homodimer in the cells without DSBs. In response to DSBs, ATM autophosphorylates at serine 1981 and forms partially active monomers (Bakkenist & Kastan, 2003). After further phosphorylation at serine 367 and 1893, ATM monomers are recruited to DSBs via interactions with Mre11-Rad50-Nbs1 (MRN) sensor complex (Lee & Paull, 2005) and fully activated. ATM locally phosphorylates the histone variant H2A.X at serine 139 (Burma et al, 2001). The phosphorylated H2A.X (γ-H2A.X) is bound by the mediator of DNA damage checkpoint protein 1 (MDC1) which recruits more ATM/MRN complexes and promotes further phosphorylation of H2A.X (Stucki et al, 2005). ATM phosphorylates Chk2 at threonine 68, resulting in intermolecular trans-autophosphorylation at threonine 383 and 387 and activation of Chk2 (Ahn et al, 2002; Lee & Chung, 2001; Oliver et al, 2006). Activated Chk2 phosphorylates phosphatase CDC25 (Falck et al, 2001). CDC25 is responsible for removing the inhibitory phosphorylations on cyclin-dependent kinases and promotes cell cycle progression. Phosphorylated CDC25 is targeted for ubiquitin-dependent

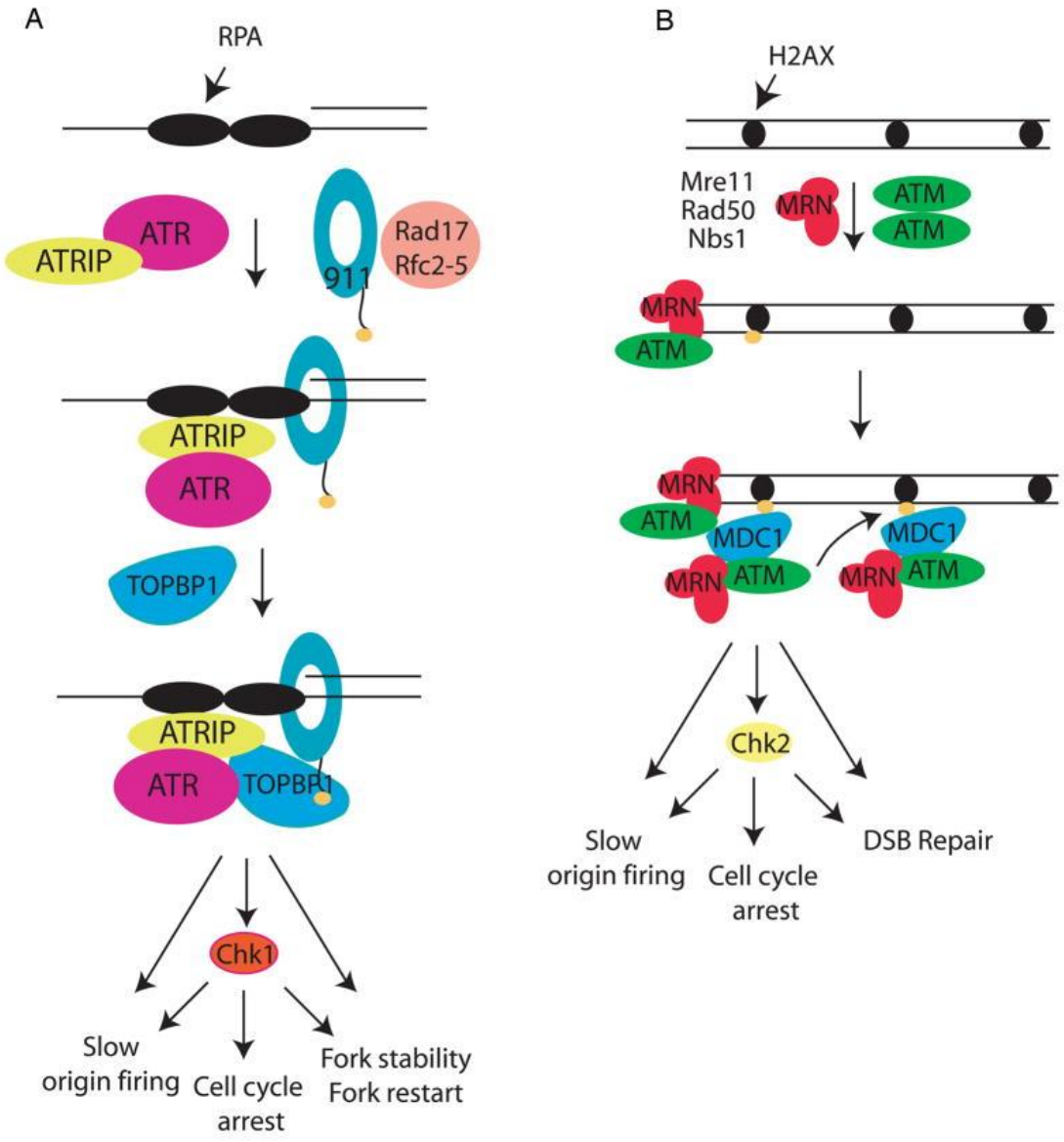

Figure 1.2. Simple models for ATR and ATM activation. This figure is adapted from Cimprich & Cortez, 2008.

degradation and CDK activation is prevented, resulting in cell cycle arrest (Mailand et al, 2000). Besides, both ATM and Chk2 phosphorylate, and thus stabilize and activate the tumor suppressor protein p53 (Chehab et al, 2000). Activated p53 induces transcription of CDK inhibitor p21 and leads to cell cycle arrest or apoptosis.

In contrast to ATM, ATR signaling is often activated when DNA replication forks stall under certain replication stress, such as nucleotide depletion. When replication is impeded, DNA polymerase is uncoupled from MCM helicases, resulting in ssDNA (Byun et al, 2005). ssDNA is coated by Replication Protein A (RPA), and ATR is recruited to the RPA coated ssDNA tracts via the partner protein ATRIP (Zou & Elledge, 2003). To activate ATR signaling, ATR-ATRIP complex needs to localize with the RAD9: RAD1: HUS1 (9-1-1) checkpoint clamp. The PCNA-like 9-1-1 complex then brings an ATR activator TOPBP1 to the sites of DNA damage to stimulate ATR activity (Delacroix et al, 2007). Once ATR is activated, Chk1 is activated through phosphorylation by ATR at serine 317 and 345. A mediator protein Claspin is required for Chk1 activation (Kumagai & Dunphy, 2000). Similar to Chk2, activated Chk1 promotes cell cycle arrest through phosphorylation of phosphatase CDC25 (Furnari et al, 1997; Shimuta et al, 2002).

In addition to the role in cell cycle arrest, ATR is also critical for regulating DNA replication. Under replication stress, DNA synthesis is slowed down or arrested due to suppression of replication initiation or reduced fork progression (Alvino et al, 2007; Feijoo et al, 2001; Shirahige et al, 1998; Tercero & Diffley). How ATR regulates DNA replication is still unknown. The MCM2-7 helicase is one target for ATR

phosphorylation (Cortez et al, 2004), and may T be involved in regulation of DNA replication. Once the replication stress is gone, dormant origins are utilized to complete replication (Ge et al, 2007; Ibarra et al, 2008).

Tetrahymena thermophila as a model for DNA replication and other aspects of chromosome biology

Two nuclei in a single cell

In my dissertation research, the model organism *Tetrahymena thermophila* was used to investigate distinct DNA replication programs. *Tetrahymena*, like other ciliates, contains two different nuclei in a single cell, which makes it a powerful model system for studying DNA replication. The two nuclei, the micronucleus (MIC) and macronucleus (MAC), are structurally and functionally distinct. The germline MIC contains five chromosomes and is diploid. The MIC chromosomes are packaged into heterochromatin and are transcriptionally silent during the vegetative phase of the life cycle (Gorovsky & Woodard, 1969; Mayo & Orias, 1981; Yao & Gorovsky, 1974). The MIC functions as the reservoir of genetic material and is responsible for the transmission of genetic material to progeny during the sexual life cycle. The MIC undergoes normal mitosis and meiosis, respectively, during vegetative and sexual life cycles. The somatic macronucleus (MAC), with approximately 180 actively transcribed chromosomes (Karrer, 2012), provides coding information for RNA transcripts and is the phenotype determinant. These chromosomes are generated by fragmentation and rearrangement of micronuclear chromosomes during development. The MAC does not have functional centromeres, and divides amitotically. During vegetative cell cycle, the macronucleus

elongates and constricts, and distributes about half of the DNA to each daughter nucleus (Orias, 1991). Successive unequal divisions of the MAC can generate a sub-population homozygous at a particular locus. This phenomenon is termed phenotypic assortment. It eventually causes elimination of one of the two alleles from parents (Merriam & Bruns, 1988).

Macronuclear development

Besides the vegetative cell cycle, *Tetrahymena* has a complex sexual life cycle (Figure 1.3). To initiate conjugation, *Tetrahymena* cells must be of different mating types. About 70 cell divisions are required for the progeny of previously mated cells to reach sexual maturity. Starvation conditions are also necessary (Allewell et al, 1976) (Figure 1.3a). During conjugation, cells form mating pairs, and a conjugation junction develops between two partner cells to facilitate pronuclei exchange and fusion (Wolfe, 1982) (Figure 1.3b). After formation of mating pairs, the micronucleus first elongates and forms a crescent shaped structure (Figure 1.3c). It has been suggested that chromosomes within the crescent take up a polarized arrangement similar to the chromosomal bouquet arrangement, promoting chromosome pairing and recombination (Loidl & Scherthan, 2004). The crescent then becomes more condensed and goes through normal meiosis to generate four pronuclei (Figure 1.3d-e). One of the pronuclei is selected and moves toward the anterior end of the cell. The other three move to the posterior end of the cell and are degraded through programmed nuclear death (PND) (Akematsu & Endoh, 2010; Cole & Sugai, 2012) (Figure 1.3f). Then, the selected nucleus undergoes one round of mitosis and generate two genetically identical pronuclei

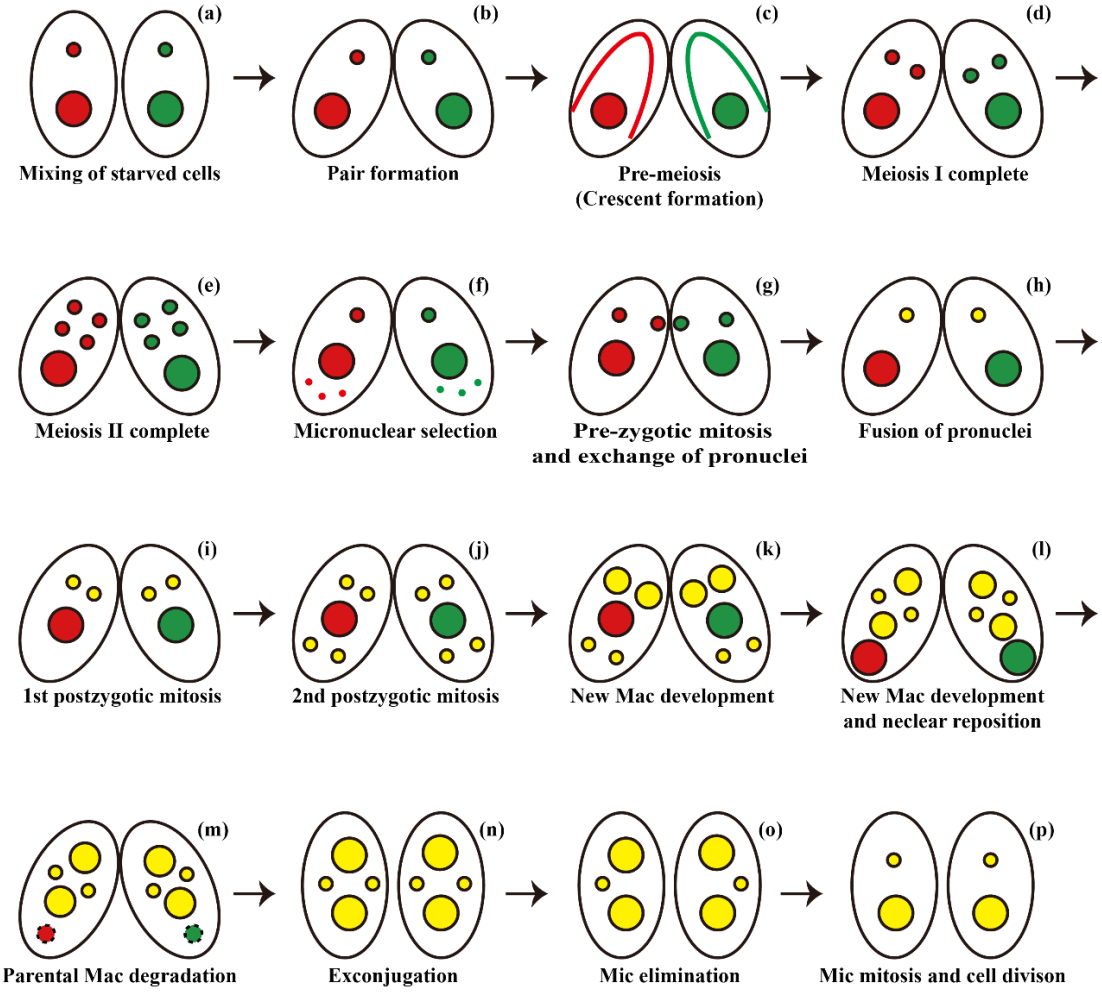

Figure 1.3. Schematic of nuclear events during *Tetrahymena* conjugation

(Figure 1.3g). One pronucleus is transferred to the mating partner and the other one still remains in the original cell which will fuse with the exchanged pronucleus to form the zygotic micronucleus (Figure 1.3h). After two rounds of post-zygotic mitosis, the cell finally contains four micronuclei (Figure 1.3i-j). Two of these four nuclei remain as micronuclei, and the other two nuclei will develop into new macronuclei. The two developing nuclei are named anlagen and this process is called macronuclear development (Figure 1.3k-n). While anlagen MAC is developing, the parental MAC are degraded through PND (Akematsu & Endoh, 2010) (Figure 1.3m). After separation of the mating pairs, one of the two MIC is degraded, and the cell contains two new MACs and one MIC in the end (Figure 1.3n-o). The remaining MIC undergoes one round of mitosis once cells are re-fed with nutrients. Cells will divide to generate two daughter cells containing one MIC and one MAC, before entry into the vegetative cell cycle (Figure 1.3p).

During macronuclear development, micronuclear chromosomes undergo rearrangements. There are two major types of DNA rearrangements: chromosome breakage which is associated with *de novo* telomere addition and the removal of internal eliminated sequences (IES) (Chalker & Yao, 2011). Micronuclear chromosome breakage occurs at specific sites containing chromosomal breakage sequence (CBS). The CBS is a conserved 15 bp sequence, and is necessary and sufficient for chromosome breakage (Yao et al, 1990; Yao et al, 1987). There are approximately 200 breakage sites in *Tetrahymena* micronuclear genome (Altschuler & Yao, 1985). *De novo* addition of telomeres follows fragmentation of micronuclear chromosomes, and around 180

macronuclear chromosomes are generated. Previous studies revealed that the size of macrounuclear chromosomes range from 200 kb to over 1000 kb (Altschuler & Yao, 1985; Conover & Brunk, 1986; Preer & Preer, 1979).

In contrast to chromosome breakage, which results in elimination of a very small fraction of the DNA sequence (<50 bp) (Yao et al, 1987), the second type of DNA rearrangement - internal DNA elimination - plays a major role in reducing sequence complexity. Internal DNA sequences from 5,000-6,000 sites in the micronuclear chromosomes are eliminated, ranging in size from a few hundred bp to over 10 kb. These sequences account for overall approximately 15% of micronuclear genome (Yao et al, 1984; Yao & Gorovsky, 1974). Most IESs are located within intergenic regions and consist of repetitive DNA sequences. Many IES resemble transposons (Cherry & Blackburn, 1985; Patil et al, 1997). Non-coding RNAs are used to determine which sequences are targeted for elimination (Yao & Chao, 2005). The small RNA involved in this process is named scan RNA (scnRNA). The ~28 nt scnRNAs are processed from germ line transcripts by the Dicer-liker protein (Dcl1) in meiotic micronuclei during conjugation (Malone et al, 2005). The scnRNAs are exported into the cytoplasm and then associated with the Argonaute protein, Twi1p (Mochizuki et al, 2002). Twi1p-associated scnRNAs are subsequently transported into the old parental macronucleus to scan the macronuclear genome, and RNAs that can base pair with the genomic DNA are degraded. The remaining scnRNAs correspond to the IESs that were eliminated in the previous generation. These RNAs migrate to the anlagen macronucleus and induce methylation of histone lysine 9 (Taverna et al, 2002). Then, the chromodomain of

programmed DNA degradation protein 1 (Pdd1) binds to H3K9 to promote DNA elimination (Taverna et al, 2002).

During chromosome fragmentation, the 10.3 kb single copy of ribosomal DNA (rDNA) locus is excised from flanking DNA, and rearranged in a head-to-head configuration to generate a 21 kb palindromic rDNA minichromosome (Yasuda & Yao, 1991) (Figure 1.4). The rDNA minichromosome, which only contains the ribosomal RNA genes, undergoes gene amplification and reaches a final copy number of 9,000 C. Non-rDNA macronuclear chromosomes increase their copy number during two stages of endoreplication, Endoreplication I (Endo I) and Endoreplication II (Endo II): the final copy number for these chromosomes eventually average 45 C. Anlagen Stage Induced 2 (ASI2), is a developmentally regulated gene in *Tetrahymena* and encodes a putative signal transduction receptor. ASI2 is not essential for vegetative growth, but it is required during development for the Mac anlagen to generate viable progeny. ASI2 is up-regulated during macronuclear development and endocycling is arrested in an ASI2 knockout mutant (Li et al, 2006; Yin et al, 2010).

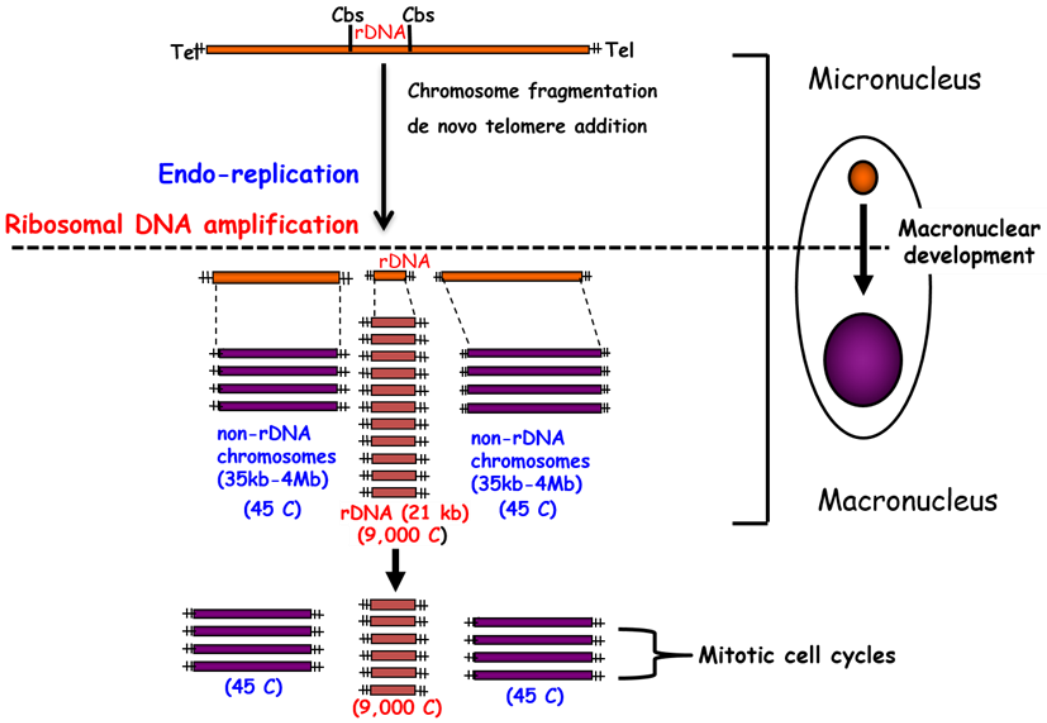

Figure 1.4. Schematic of macronuclear development, endoreplication and rDNA amplification.

Replicons in Tetrahymena

DNA replication of the 21 kb macronuclear rDNA minichromosome has been extensively studied. rDNA replication occurs in different replication programs, including cell cycle-regulated rDNA replication and developmental regulated rDNA amplification. rDNA replication initiates from the 1.9 kb 5' non-transcribed spacer (5' NTS) (Cech & Brehm, 1981) (Figure 1.5). The 5' NTS contains three nucleosome-free regions: Domain I, Domain II and the promoter region (Palen & Cech, 1984). Domain I and Domain II functions as DNA replication initiation sites (Zhang et al, 1997). There are important cis-elements in the 5' NTS, such as type I elements and pause site elements (PSEs). Type I elements are required for both rDNA amplification during development and vegetative replication (Zhang et al, 1997). There are four type I elements in the 5'NTS. Two of them reside in replication origins: Ia in Domain I, and Ib in domain II, and the other two situate at the promoter region: Ic and Id (Figure 1.5). Type Ic and Id elements are part of the rDNA promoter, regulating both rDNA replication and rRNA transcription (Gallagher & Blackburn, 1998; Pan et al, 1995). PSEs regulate DNA replication through transiently pausing fork movement at these sites (MacAlpine et al, 1997).

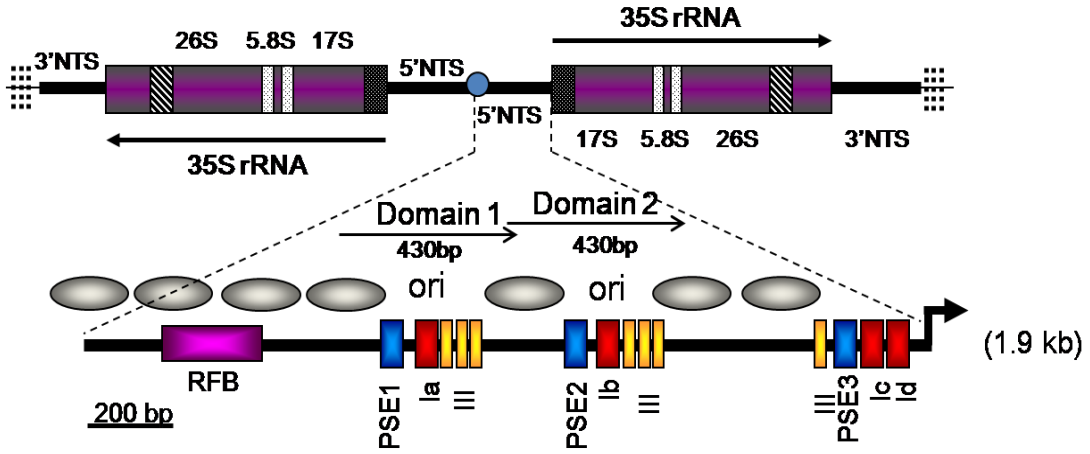

Figure 1.5. Schematic of the *T. thermophila* rDNA minichromosome. (Top) rDNA minichromosomes are composed of two copies of the rDNA molecules in an inverted orientation. The 35S rRNA precursor encodes the 17S, 5.8S and 26S rRNAs. (Bottom) 5' NTS: gray ovals, positioned nucleosomes in vegetative rDNA minichromosomes; red boxes, type I elements (Ia–Id); blue boxes, pause site elements (PSE1–3); yellow boxes, type III elements; purple box, developmentally regulated replication fork barrier (RFB); Terminal arrow, rRNA promoter.

Previous *in vitro* biochemical studies identified four sequence specific Type I element binding factors, TIF1 through TIF4, all of which bind exclusively to single strand DNA (Mohammad et al, 2000; Mohammad et al, 2003; Saha & Kapler, 2000). TIF4, which specifically binds to the type I element T-rich strand in an ATP-dependent manner, was then revealed as the *Tetrahymena* ORC (TtORC). TtORC contains an integral RNA subunit, named 26T RNA corresponding to the terminal 282 nucleotides of 26S rRNA. TtORC binding to the Type I element is mediated by Watson-Crick base pairing between 26T RNA and the Type I element T-rich strand (Mohammad et al, 2007).

Besides the rDNA origin, one non-rDNA *Tetrahymena* replicator has been identified in our lab. This 6.7 kb non-rDNA fragment, named ARS1, does not show sequence complementarity to 26T RNA, indicating that ORC binding to non-rDNA chromosomes may utilize a different mechanism. In addition, ORC exclusively binds to the rDNA origins throughout the cell cycle, but ORC binding to non-rDNA chromosomes is cell cycle regulated. During G2 phase, ORC binds non-specifically to the non-rDNA ARS1 chromosome, while the binding switches to ARS1 locus in the next G1 phase (Donti et al, 2009).

CHAPTER II

DEVELOPMENTAL REGULATION OF THE *TETRAHYMENA THERMOPHILA* ORIGIN RECOGNITION COMPLEX*

Overview

The *Tetrahymena thermophila* DNA replication machinery faces unique demands due to the compartmentalization of two functionally distinct nuclei within a single cytoplasm, and a complex developmental program. Here we present evidence for programmed changes in ORC and MCM abundance that are not consistent with conventional models for DNA replication. As a starting point, we show that ORC dosage is critical during the vegetative cell cycle and development. A moderate reduction in Orc1p induces genome instability in the diploid micronucleus, aberrant division of the polyploid macronucleus, and failure to generate a robust intra-S phase checkpoint response. In contrast to yeast ORC2 mutants, replication initiation is unaffected; instead, replication fork elongation is perturbed, as Mcm6p levels decline in parallel with Orc1p. Experimentally induced down-regulation of ORC and MCMs also impairs endoreplication and gene amplification, consistent with essential roles during development. Unexpectedly Orc1p and Mcm6p levels fluctuate dramatically in developing wild type conjugants, increasing for early cycles of conventional micronuclear DNA replication and macronuclear anlagen replication (endoreplication phase I, rDNA gene amplification). This increase does not reflect the DNA replication

load, as much less DNA is synthesized during this developmental window compared to vegetative S phase. Furthermore, although Orc1p levels transiently increase prior to endoreplication phase II, Orc1p and Mcm6p levels decline when the replication load increases and unconventional DNA replication intermediates are produced. We propose that replication initiation is re-programmed to meet different requirements or challenges during the successive stages of *Tetrahymena* development.

Introduction

DNA replication initiates at specific sites in chromosomes, termed origins of replication. While the genomic architecture of replication initiation sites varies widely across the eukaryotic lineage, a conserved feature is their association with the six-subunit Origin Recognition Complex (ORC) (Gibson et al, 2006; Mechali, 2010). ORC-dependent licensing is required for replication initiation and provides a mechanism to prevent re-replication of chromosomes during S phase. Pre-replicative complex (pre-RC) assembly is mediated by transient interactions between ORC, Cdc6 and Cdt1, which recruit the MCM2-7 complex- the replicative helicase that unwinds the DNA at replication origins and elongating replication forks. Additional factors (Cdc45, GINS) recruit the DNA polymerase machinery to generate pre-initiation complexes. Phosphorylation and/or degradation of Orc1p prevents new pre-RCs from forming on daughter chromosomes (Fernandez-Cid et al, 2013).

Research with the budding yeast, *Saccharomyces cerevisiae* (Sc), has revealed conserved and unique insights into replication initiation. Sc replicons are short (100-200 bp) and include a conserved 11 bp motif, the ARS consensus sequence (ACS), that is

bound by ORC in an ATP-dependent, sequence-specific manner. With an estimated 20,000 Orc2p molecules per cell (Shimada et al, 2002), and 12,000 ACSs, but only 400 replication origins (Nieduszynski et al, 2006), Sc-ORC appears to be in vast excess. Multiple ORC subunits interact with the DNA, with the ancestral Orc1p contacting the ACS (Chen et al, 2008). Metazoan ORCs exhibit no sequence specificity, and are in modest excess relative to replication origins. In *Drosophila melanogaster*, approximately 30% of *in vivo* ORC binding sites function as early replication origins (MacAlpine et al, 2010). With the exception of Orc1p, the steady state levels of ORC subunits are not differentially regulated in quiescent versus proliferating mammalian cells (Ohtani et al, 1996). Cdc6 and MCM2-7 serve as reliable biomarkers for mammalian cell proliferation (Stoeber et al, 2001). ORC and MCMs are dramatically up-regulated during embryonic development in *Xenopus laevis* to support the rapid S phases prior to the mid-blastula transition (Tugal et al, 1998). Origin density increases by a factor of ~10, as replication initiates in coding and non-coding sequences (Marheineke & Hyrien, 2004). The onset of zygotic transcription and remodeling of chromatin redirects replication initiation to intergenic regions when ORC protein levels decline.

The ciliated protozoan, *Tetrahymena thermophila*, has served as a useful model for examining the molecular organization of eukaryotic replicons, and studying the genetic and epigenetic control of DNA replication (Tower, 2004). A distinguishing feature of ciliates is the cohabitation of two functionally distinct nuclei within the same cytoplasm. This arrangement results in the genesis of different autonomous DNA replication programs. The transcriptionally silent diploid micronucleus serves as the

reservoir of genetic material that is transmitted from parent to progeny during conjugation. The polyploid macronucleus is actively transcribed throughout the vegetative cell cycle and development. Since the macronucleus is destroyed in progeny (Karrer, 2012), a new macronucleus must be generated by differentiation of a post-zygotic micronucleus (Karrer, 2012).

The partitioning of chromosomes into two operationally distinct nuclei places unusual demands on DNA replication, including origin licensing and the coordination of checkpoint responses that maintain genome integrity. The temporal order of DNA replication parallels that of higher order chromatin domains in more typical eukaryotic chromosomes (Aparicio, 2013; Berezney et al, 2000), in that euchromatic macronuclear chromosomes are replicated prior to replication of the heterochromatic micronuclear genome. However, macronuclear S phase precedes micronuclear S (Cole & Sugai, 2012), and cytokinesis is coupled to amitotic macronuclear division (Doerder & DeBault, 1978).

Micro- and macronuclear DNA replication programs are uncoupled in conjugating cells. First, meiosis converts a diploid micronucleus into four haploid pronuclei, three of which are degraded (Cole & Sugai, 2012). The sole survivor replicates and divides to produce genetically identical migratory and stationary pronuclei, which are reciprocally exchanged between mating partners. The diploid zygotic micronucleus undergoes two rounds of DNA replication and mitosis. Two micronuclei exit the DNA replication program, and two differentiate into macronuclei. During macronuclear development, the five micronuclear chromosomes are extensively

remodeled. One third of the genome (including centromeres and retrotransposons) is eliminated by site-specific DNA fragmentation and *de novo* telomere addition, or removal of internal DNA sequences by breakage and rejoining, generating ~180 distinct macronuclear chromosomes. Non-coding RNAs generated in the newly formed micronucleus dictate which internal DNA sequences are eliminated from the developing macronucleus (Yao et al, 2003). Epigenetic reprogramming of histones converts heterochromatic micronuclear chromosomes into macronuclear euchromatin. Through endoreplication, the copy number of macronuclear chromosomes increases to ~45 C, and the 21 kb ribosomal DNA minichromosome is amplified to ~9000 C. Similar to ovarian follicle cells in *Drosophila* (Claycomb & Orr-Weaver, 2005), genome-wide endoreplication precedes selective gene amplification. Once development is completed, micro- and macronuclear chromosomes replicate once per vegetative cell cycle. Although amitotic macronuclear chromosomal segregation and unequal nuclear division can generate genic imbalances (Smith et al, 2004), the copy number of macronuclear chromosomes is maintained in a narrow range. This occurs through the elimination of 'excess DNA' in the form of chromatin extrusion bodies, or partial re-replication of macronuclear chromosomes.

Like yeast and metazoa (Masai et al, 2010), the *Tetrahymena* Origin Recognition Complex (ORC) specifies where replication initiates, recruiting the MCM2-7 helicase to specific sites in chromosomes. *Tetrahymena* ORC is unusual in that it contains an integral RNA subunit, designated 26T RNA, which selectively targets ORC to the amplified rDNA origin through Watson-Crick base pairing (Mohammad et al, 2007).

26T RNA is not complementary to regulatory sequences in non-rDNA origins, and ORC is loaded onto rDNA and non-rDNA origins at different stages of the cell cycle (Donti et al, 2009). Hence, ORC recruitment and licensing differs for rDNA and non-rDNA origins. ORC and MCM transcript levels are elevated in conjugating cells in parallel with other replication proteins, such as Cdt1, PCNA and DNA polymerase α/primase (Miao et al, 2009), suggesting that the demands for these proteins increases during development.

DNA damage and replication stress can irreparably harm *Tetrahymena* chromosomes (Morrison et al, 2005). While deleterious events may be resolved without the need to arrest the cell cycle, *Tetrahymena* elicits a robust DNA damage/replication stress checkpoint response when a threshold is exceeded (Yakisich et al, 2006). In yeast and mammals, the intra-S phase checkpoint is triggered by an apical kinase, MEC1 and ATR, respectively (Cortez, 2005; Nam & Cortez, 2011). Checkpoint activation leads to the phosphorylation of MCM2-7 helicase subunits, blocking both replication initiation and fork elongation (Forsburg, 2008). *Tetrahymena* encodes a single ATR gene, which has been shown to induce cell cycle arrest and prevent micro- and macronuclear genome instability (Yakisich et al, 2006). ATR is also required for the reorganization of chromosomes during meiosis (Loidl & Mochizuki, 2009).

In the work presented here, we examine how programmed and experimentally induced changes in the abundance of ORC affect DNA replication and the intra-S phase checkpoint response. We show that the sustained down regulation of Orc1p in a macronuclear knockdown mutant induces genome instability in the micro- and

macronucleus. Unexpectedly, ORC1 depletion induces defects in replication fork elongation rather than initiation, and fails to activate the intra S-phase checkpoint response. We also document coordinately regulated changes in ORC and MCM protein levels during development, in which the abundance of pre-RC proteins does not correlate with the impending DNA replication load. Finally, we provide evidence for altered replication initiation and/or elongation in endoreplicating macronuclear chromosomes. The collective data demonstrate that the rules for DNA replication change substantially when *Tetrahymena* exits the vegetative cell cycle and commits to its complex developmental program.

Results

Down-regulation of DNA replication components in ORC1 mutants

To evaluate the requirements for ORC during vegetative replication of micro- and macronuclear chromosomes, ORC1 knockdown mutants were generated by targeted gene disruption in the macronucleus (Table 2.2). The random segregation of amitotic chromosomes was exploited to obtain phenotypic assortments with reduced dosage of the wild type locus. Using conditions that select for retention of the paromomycin-resistant disruption allele, only a 5-fold reduction of the wild type ORC1 gene (TTHERM_00865050) was achieved in the 45 C macronucleus. A corresponding reduction in Orc1p was observed in the mutant population (Figure 2.1A, WL). Even less Orc1p was associated with chromatin in the mutant (Figure 2.1A), suggesting that ORC occupancy on chromosomes was ~10% that of wild type *Tetrahymena*. Unexpectedly, Orc2p and Mcm6p levels were also reduced in the ORC1 knockdown strain

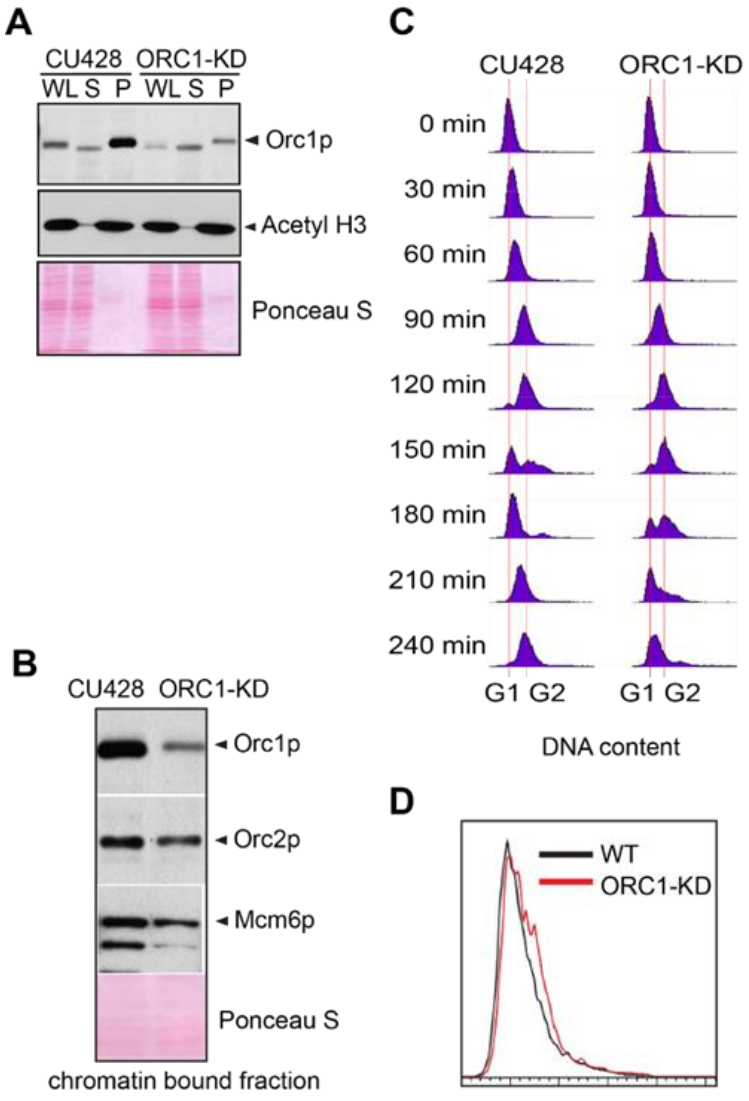

Figure 2.1. ORC1 depletion induces slow cell cycle progression. (A) Western blot analysis of whole cell lysates (WL), NP-40-extractable soluble fractions (S), and nuclear chromatin-bound pellet fractions (P). Samples were prepared from log phase wild type (CU428) and ORC1 knockdown (ORC1-KD) cells, and immunoblotted with rabbit polyclonal anti-Orc1p, anti-Orc2p, anti-Mcm6p, and anti-acetyl Histone H3 antibodies. Each lane corresponds to proteins derived from 10 µl of cultured cells at density of 2 x 10^5 cells/ml. Membranes were stained with Ponceau S to visualize total protein loaded in each lane prior to antibody probing. (B) Western blot analysis of chromatin bound pre-RC components in wild type and ORC1 knockdown strains. A Lowry assay was performed to assure that equivalent amounts of protein (20 µg) were loaded in each lane. Due to the different sizes of target proteins, a single membrane was cut into pieces to probe for each target protein. (C) Cell cycle progression of CU428 and ORC1-KD cells as measured by flow cytometry. 0 min corresponds to G1 phase cells isolated by elutriated centrifugation. (D) Flow cytometry analysis of asynchronous, log phase wild type (CU428) and ORC1 knockdown (ORC1-KD) cells. Vegetative growing cell cultures were harvested at late log phase (cell density: 2.5 x 10^5 cells/ml).

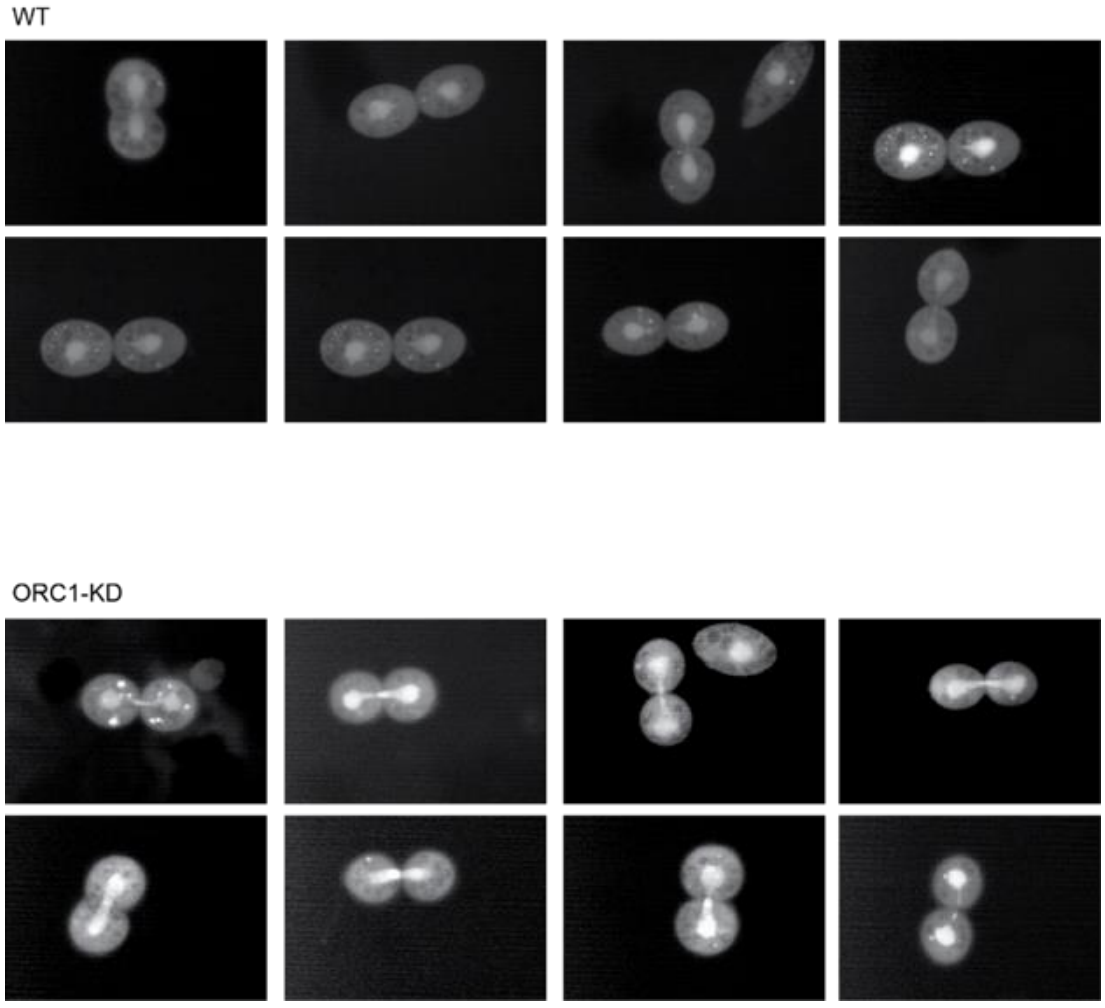

Figure 2.2. Nuclear division in wild type CU428 and ORC1 knockdown cells visualized with acridine orange. Log phase wild type (WT) CU428 and ORC1 knockdown (ORC1-KD) cell cultures were collected and fixed with paraformaldehyde. For apofluor staining, cells were stained with 0.001% acridine orange and observed immediately with fluorescence microscopy. Eight representative images from each strain are shown.

(Figure 2.1B). ORC1 knockdown cells grew more slowly than wild type, exhibiting a prolonged S phase (Figure 2.1C, compare data for 120-210 min time points), consistent with a defect in DNA replication. Asynchronous cultures contained more cells with a high DNA content (Figure 2.1D), and ~90% of dividing mutant cells underwent asymmetric macronuclear division with lagging chromosomes (Figure 2.2, wild type frequency: ~2%). The collective data are consistent with the failure to fully replicate macronuclear chromosomes.

The ORC1 mutant has a diminished intra-S phase checkpoint response

S phase induced DNA damage and replication stress trigger an ATR/MEC1 checkpoint response in eukaryotes that prevents new origins from firing and inhibits the elongation of existing replication forks. Both processes are blocked by the reversible phosphorylation of the MCM2-7 complex (Forsburg, 2008). To assess DNA replication and DNA damage checkpoint responses, G1 synchronized cultures were treated with hydroxyurea (HU) or methylmethanesulphonate (MMS), respectively. Activation of the ATR checkpoint was monitored by flow cytometry and accumulation of Rad51p, which is rapidly up-regulated (Mochizuki et al, 2008; Yakisich et al, 2006). Whereas 20 mM HU inhibited DNA replication in wild type *Tetrahymena*, the ORC1 knockdown strain entered S phase and continued to synthesize DNA (Figure 2.3A), albeit at a slower rate than untreated controls (Figure 2.1C). Similar results were obtained for mutant cells treated with 0.06% MMS (Figure 2.4). The inability to inhibit DNA replication is consistent with compromised DNA replication (HU) and DNA damage (MMS) checkpoint responses. ORC1 mutants were less responsive than wild type cells to HU

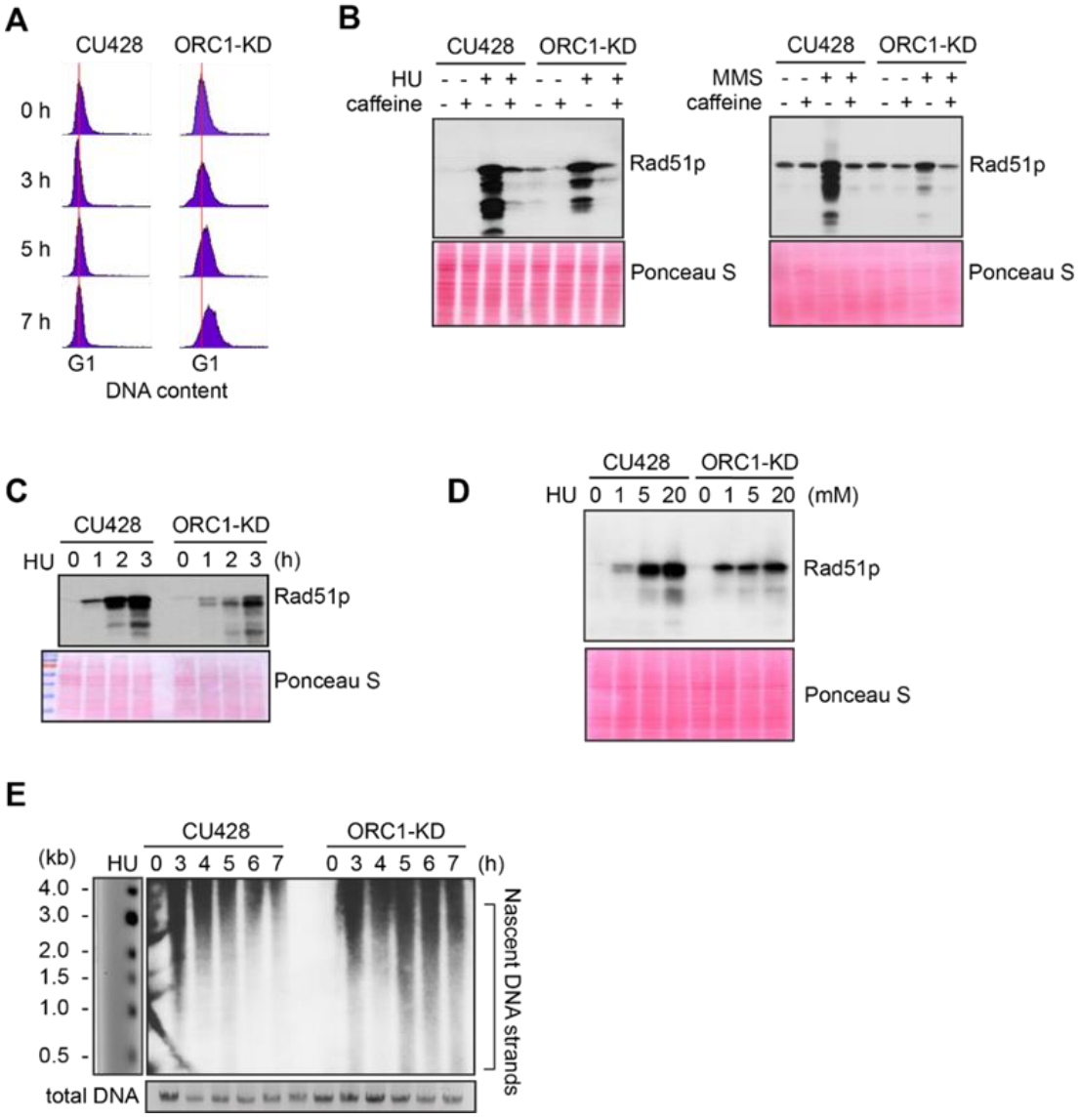

Figure 2.3. Abrogated intra-S phase checkpoint response in ORC1 knockdown cells. (A) Elutriated G1 phase wild type (CU428) and ORC1 knockdown (ORC1-KD) cells were treated with 20 mM HU and samples were collected at the indicated intervals for flow cytometry analysis. (B) G1 synchronized cells were released into fresh medium containing 20 mM HU or 0.06% MMS +/- 1 mM caffeine (1 mM) for 4 h. Whole cell lysates were subjected to western blot analysis of Rad51p. (C) G1 synchronized cells were incubated in medium containing 20 mM HU. Whole cell lysates were prepared at timed intervals and subjected to western blot analysis with anti-Rad51 antibody. (D) G1 synchronized cells were incubated in the presence of HU (1-20 mM) for 4 h and subjected to western blot analysis. (E) Alkaline gel electrophoresis of nascent DNA strands accumulated under HU treatment. G1 synchronized cells were cultured in 20 mM HU and genomic DNA was isolated at indicated time points. RIs were released under alkaline condition and resolved in a 1% alkaline agarose gel. RIs from the rDNA 5' NTS origin region were visualized by Southern blot analysis.

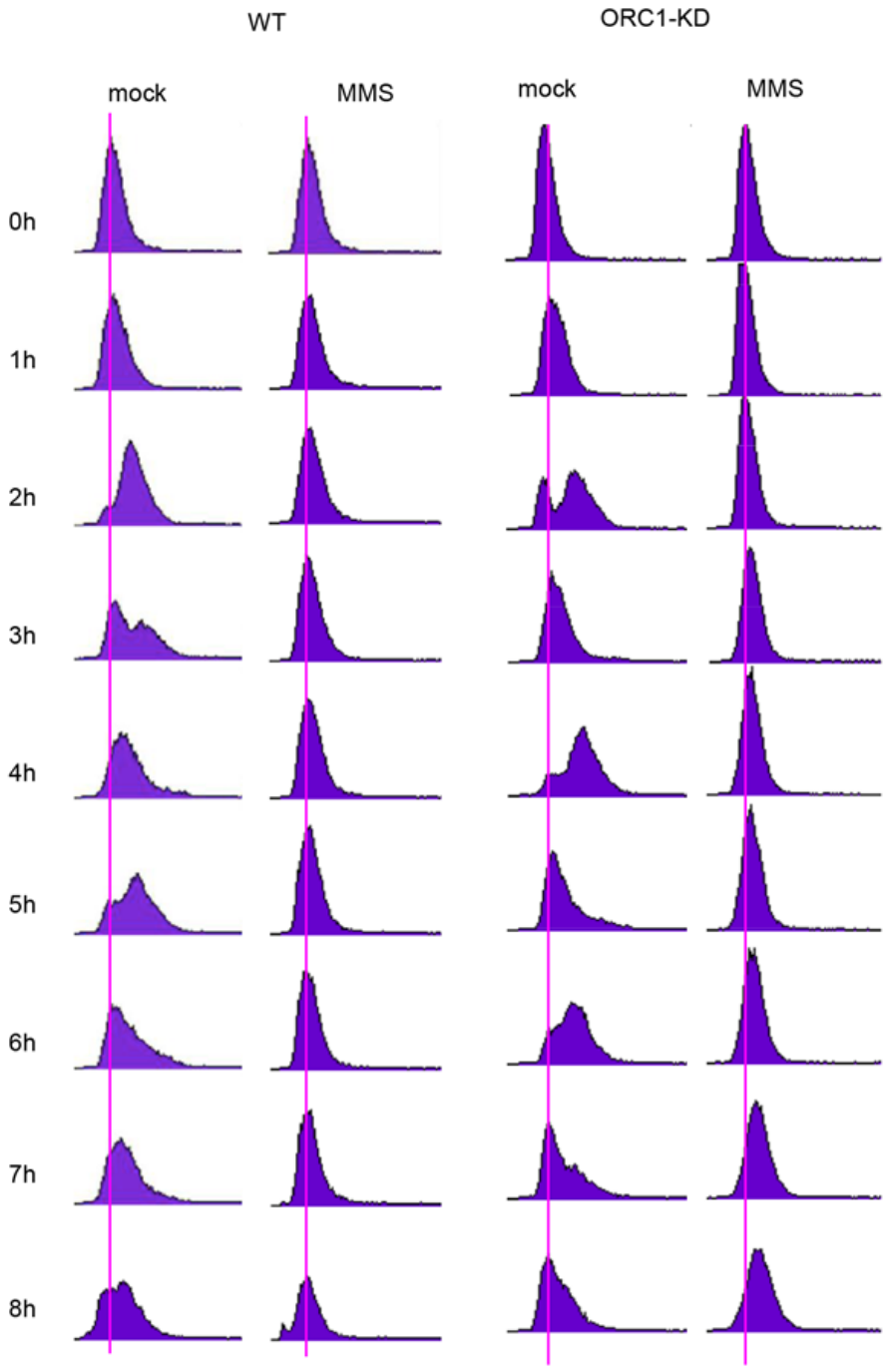

Figure 2.4. Abrogated intra-S phase checkpoint response in ORC1 knockdown cells (supplemental). Elutriated G1 phase wild type (CU428) and ORC1 knockdown (ORC1-KD) cells were treated with 0.06% MMS and samples were collected at the indicated intervals for flow cytometry analysis.

exposure time (Figure 2.3C) or dosage (Figure 2.3D). While MMS was a more potent inducer of Rad51p production, HU and MMS responses were inhibited by the addition of caffeine (Figure 2.3B), consistent with the involvement of ATR.

Alkaline gel electrophoresis was used to visualize nascent DNA strands derived from the rDNA origin region. G1 synchronized cells were incubated for 1-7 h in media containing 20 mM HU and nascent strands were detected by Southern blot analysis with a 5' non-transcribed spacer (NTS) probe (Figure 2.3E). Wild type *Tetrahymena* generated short nascent strands that gradually chased into high molecular weight species. We interpret this to indicate that fork elongation was slowed down by HU, and that new origin firing was suppressed. In contrast, low molecular weight nascent strands were evident at all time points in HU-treated ORC1 mutant cultures, suggesting that replication initiation was not repressed. The collective data (Figure 2.3A-E) indicate that the intra-S phase checkpoint response is compromised in ORC1 knockdown mutant.

Altered replication fork progression in ORC1 knockdown cells

The *S. cerevisiae* ORC2-1 mutant is defective in MEC1-dependent checkpoint activation, generating fewer elongating replication forks due to decreased replication initiation. Consequently, the average distance between initiation sites increases from 45 kb to 65 kb (Shimada et al, 2002). To better understand the impact of ORC1 depletion on the *Tetrahymena* checkpoint response, two-dimensional gel electrophoresis and DNA combing were used to study DNA replication of the amplified 21 kb rDNA minichromosome and larger non-rDNA macronuclear chromosomes. No differences were evident in the rDNA 5' NTS replication intermediate (RI) patterns of wild type and

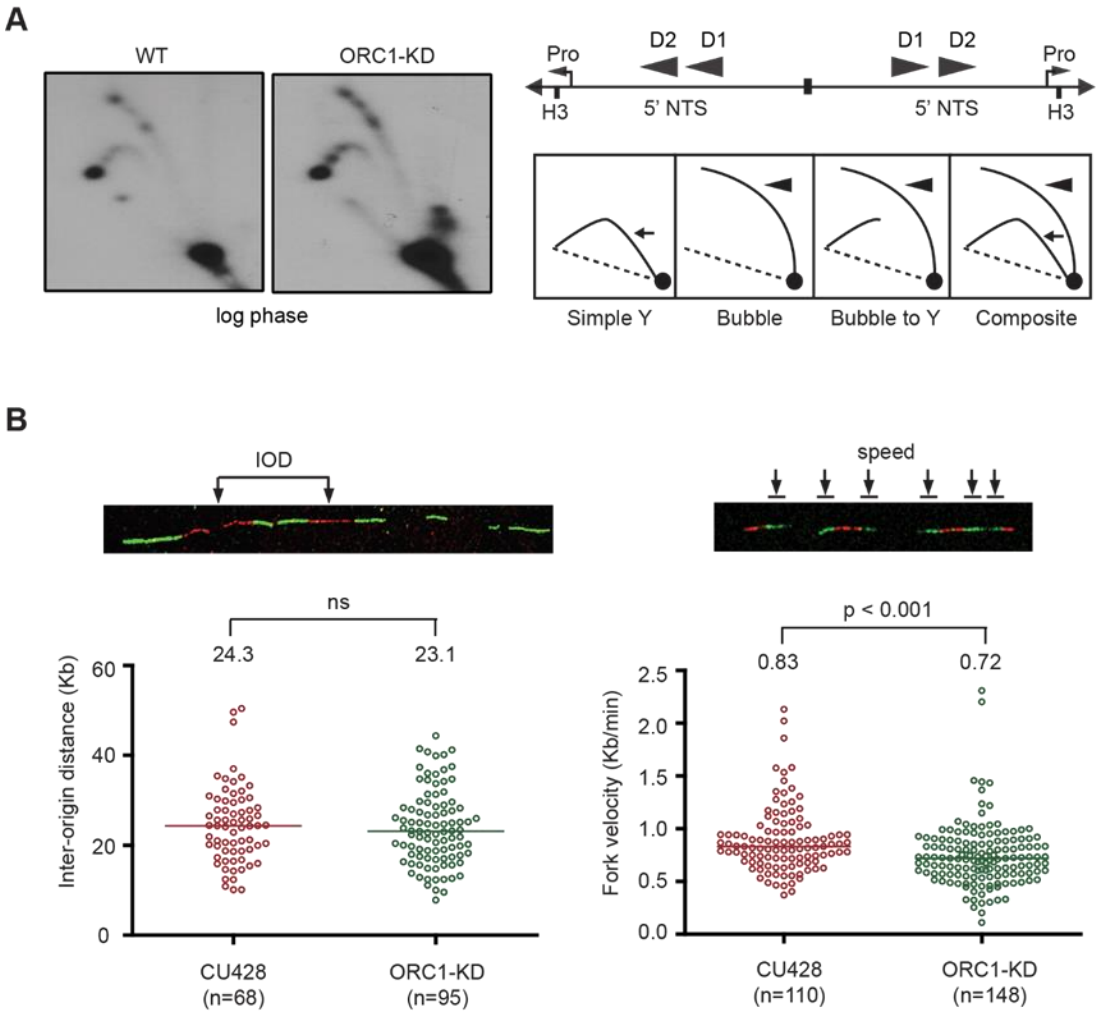

Figure 2.5. Altered cell cycle distribution and replication fork progression in ORC1 knockdown cells. (A) DNA samples from log phase cultures were subjected to neutral-neutral 2D gel analysis following digestion with *HindIII* and enrichment for RIs on BND cellulose. Left panels: blots were probed with the rDNA 5' NTS probe (wild type (WT) and ORC1 knockdown (ORC1-KD) strains). Right panel, schematic of the palindromic *HindIII* fragment spanning the two inverted copies of the 5' NTS, promoter (pro) and replication origins (D1 and D2). (B) Representative images for DNA fibers sequentially labeled with IdU and CldU. Inter-origin distance and fork velocity were measured in log phase CU428 and ORC1-KD cells (see Materials and Methods for details).

mutant strains (Figure 2.5A). Bubble-to-Y arc RIs were generated in the mutant and no complete Y arcs were observed, consistent with initiation from known ORC binding sites in the 5' NTS. The pattern of accumulated RIs on the bubble-to-Y arcs is consistent with the transient pausing of replication forks at conserved PSE elements (MacAlpine et al, 1997). Hence, within the limits of resolution, rDNA origin utilization is unaffected. DNA fiber analysis also revealed no change in origin utilization in non-rDNA chromosomes, as the median distance between non-rDNA origins (inter-origin distance, IOD) was unaltered (Figure 2.5B; WT IOD: 24.3 kb; ORC1 mutant IOD: 23.1 kb). However, the rate for replication fork elongation (RFE) was significantly reduced in the mutant (Figure 2.5B; WT RFE rate: 0.83 kb/min; ORC1 mutant RFE rate: 0.72 kb/min; 14% reduction; $p < 0.001$). These data suggest that the primary defect in the ORC1 mutant occurs downstream of replication initiation.

Mitotic and meiotic micronuclear genome instability in ORC1 knockdown mutants

Since the macronucleus directs all gene expression, the loss of micronuclear chromosomes can be tolerated during the vegetative phase of the life cycle, leading to the genesis of aneuploid micronuclei (Bruns & Brussard, 1981). To assess micronuclear genome instability in ORC1 knockdown cells, PCR was performed with primer sets that span 10 of the chromosome fragmentation sites used to convert the 5 mitotic micronuclear chromosomes into ~180 amitotic macronuclear counterparts (one primer set per micronuclear chromosome arm) (Yakisich et al, 2006). Ten clonal ORC1 knockdown lines were generated and propagated for further analysis. All 10 lines failed to produce PCR products at 120 fissions for primer sets diagnostic for the left and right

arms of chromosome 2 (Figure 2.6A, left panel). Additional micronuclear DNA markers were lost in a subset of clonal lines at 250 fissions (micronuclear chromosome arms 1L, 3R, 4L, 5L, 5R) (Figure 2.6A, clones 1 and 7; right panel). While chromosome instability is expected to be stochastic, with new events displaying a clonal inheritance pattern, our ability to detect chromosome loss did not require repeated sub-cloning, as was previously reported for mutations in cis-acting rDNA determinants (Yakisich & Kapler, 2006) and trans-acting factors (Yakisich et al, 2006).

To assess the effect of Orc1p dosage on meiotic chromosome transmission and subsequent rounds of DNA replication associated with development, early passage knockdown clones that tested positive for all 10 micronuclear chromosome markers were mated to a wild type strain. Strains were pre-incubated with mitotracker dyes to determine the identity of each partner in mating pairs. DAPI was used to follow the fate of micro- and macronuclei. The mutant partner exhibited a temporal delay in formation of the micronuclear crescent, an elongated structure with centromeres and telomeres at opposite ends (Figure 2.6B, 3 h and 4 h time points) (Mochizuki et al, 2008). Sampling at later time points identified progeny in which post-zygotic micronuclear division was either arrested or developmentally delayed in the mutant. The programmed differentiation of micronuclei into macronuclear anlagen was also perturbed. When post-zygotic defects were detected, both progeny in a mating pair were affected (Figure 2.6B, 7 h and 8 h). Since progeny inherit two wild type copies of the ORC1 gene, the macronuclear development program was further examined at the molecular level.

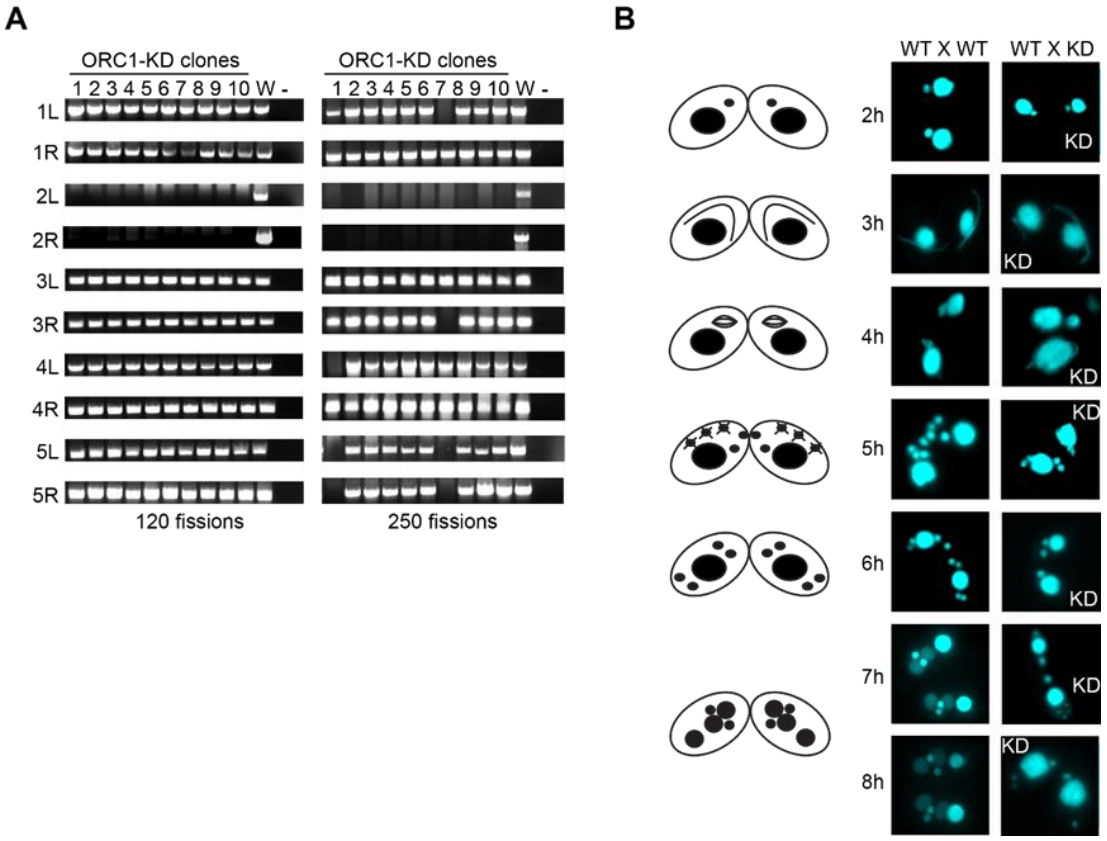

Figure 2.6. Micronuclear genome instability in ORC1 knockdown cells. (A) ORC1 knockdown (ORC1-KD) cells were propagated following the establishment of clonal lines. Genomic DNA was isolated at 120 and 250 fissions and subjected to PCR amplification with the primer sets that span sites for chromosome breakage sequence (CBS)-mediated chromosome fragmentation in the developing macronucleus. PCR primers derived from the right (R) and left (L) arms of all five micronuclear chromosomes were tested. 1–10, clonal ORC1-KD; W, wild type strain CU427; (-), PCR reactions in the absence of template DNA. (B) Cytological examination of crosses between wild type strains (CU427 X CU428), or CU427 X ORC1-KD. Nuclei were visualized with the DNA staining dye DAPI. Cartoons depict the progression of wild type mating cells during development. 3 h: micronuclear elongation (crescent); 4 h: micronuclear meiosis; 5 h: four haploid meiotic micronuclei, three of which subsequently undergo programmed nuclear death (PND); 6 h: postzygotic division; 7-8 h: macronuclear anlagen differentiation. Prior to mating, one of the parental strains was incubated with mitotracker red dye to determine the identity of each partner in mating pairs.

Endoreplication and gene amplification defects in ORC mutant strains

Endoreplication occurs in two temporally separable stages in the developing macronucleus, both of which require expression of the ASI2 gene (Yin et al, 2010). The first period (endoreplication phase I) involves two rounds of DNA replication and generates an 8 C macronucleus (Figure 2.7A). In matings between wild type strains, the first increase in DNA content occurs between 6-18 h (Figure 2.9B). Upon re-feeding, a second re-replication period (endoreplication phase II) is initiated in an ASI2-dependent manner (Yin et al, 2010), generating a macronuclear DNA content of 32-64 C (Figure 2.9B, Figure 2.10B). Endoreplication phase II was delayed in mating between ORC1-KD and a wild type partner (CU427), and was arrested in crosses with the wild type strain SB1934 (A). The parental/old macronucleus (OM) was not destroyed in ORC1 mutant x SB1934 progeny (Figure 2.7A), further evidence for arrest of the developmental program. DAPI images of mating cells corroborated these findings (Figure 2.7B). In wild type mating cultures (24 h mating, mated and re-fed for 4 and 8 h), the vast majority of exconjugant progeny exhibited robust DAPI staining of the two macronuclear anlagen (SB1934 x CU428). In contrast, the macronuclear DAPI signal was very faint in progeny from crosses with the ORC1 mutant.

To determine if depletion of Orc1p affected rDNA amplification, Southern blot analysis was used to assess C3 rDNA production in a mating between the ORC1 mutant and wild type C3 rDNA strain, SB1934 (Kapler & Blackburn, 1994). The SB1934 heterokaryon contains two copies of the integrated C3 rDNA locus in its micronucleus and ~9000 copies of the B rDNA allele in the macronucleus. Since the ORC1

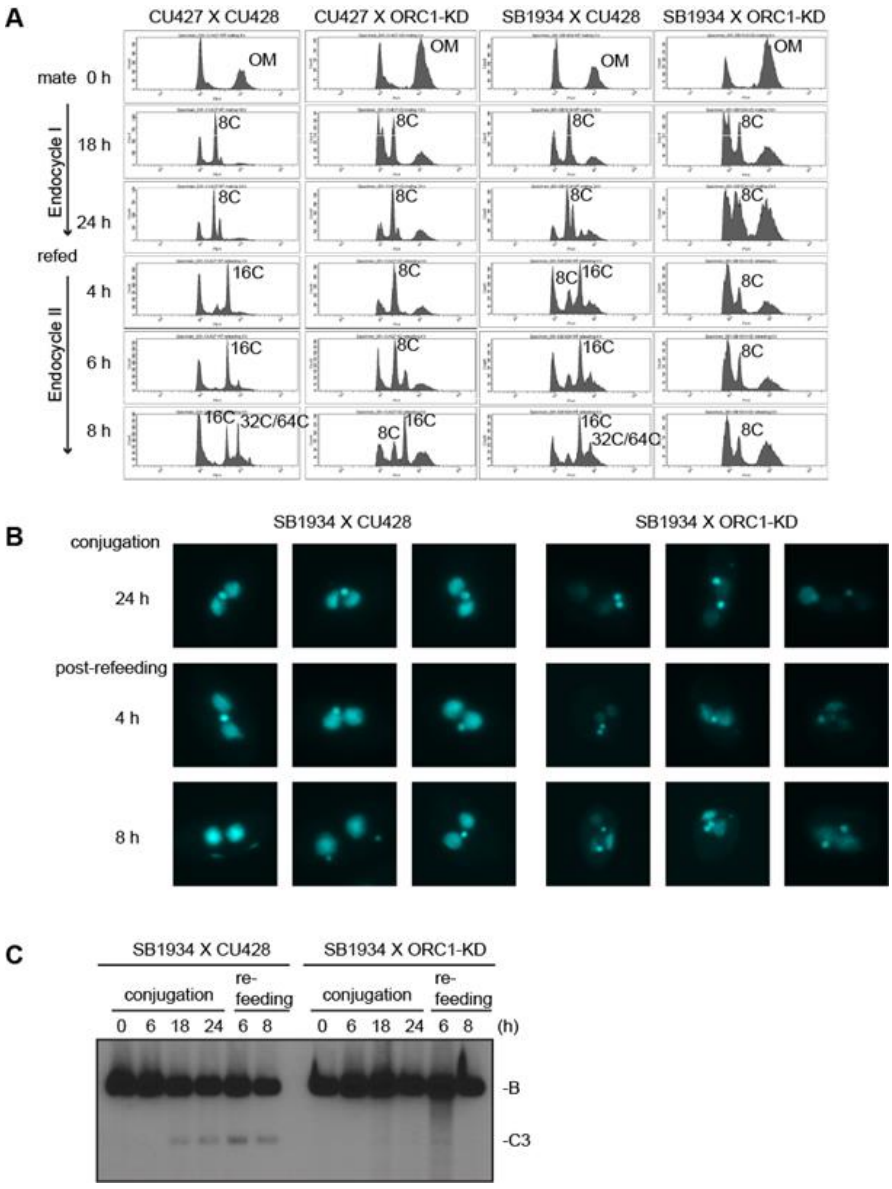

Figure 2.7. Endoreplication and rDNA amplification during *Tetrahymena* development. (A) Flow cytometry analysis of matings between wild type and ORC1-KD strains. Nuclei were isolated and stained with propidium iodide for flow cytometric analysis. Wild type strains: CU427, CU428, SB1934. SB1934 is a heterokaryon, with B rDNA in the macronucleus and C3 rDNA in the micronucleus (Table 2.2). OM, old parental macronucleus, which is degraded in conjugants. (B) Cytological examination of crosses WT X WT (SB1934 and CU428), and WT X mutant (SB1934 and ORC1-KD) with the DNA staining dye, DAPI. Starved mating cultures were re-fed at 24 h. Three representative images are shown for each time point. (C) Southern blot analysis of C3 rDNA gene amplification during development. Mating between wild type SB1934 or CU428 strains with one another (WT x WT) or with the ORC1-KD strain (WT X mutant) were performed and cells were collected at the indicated time points. DNA was digested with *BamHI* and probed with an rDNA 3' NTS probe to distinguish macronuclear B (4.0 kb) and C3 (2.5 kb) rDNA alleles.

knockdown strain encodes B rDNA in both nuclei, exconjugant progeny will contain a mixture of B and C3 rDNA in the developing macronucleus. In a cross between the SB1934 and wild type B rDNA strains, CU428, C3 rDNA was amplified during macronuclear development (Figure 2.7C). In contrast, C3 rDNA was not detected in progeny from the ORC1-KD x SB1934 cross. The collective data demonstrate that the experimentally induced down regulation of ORC1 inhibits global DNA replication and rDNA gene amplification during macronuclear development.

Developmental regulation of ORC and MCMs subunits

Starvation not only induces cell cycle arrest at the macronuclear G1/S border, when Orc1 protein levels are highest during the vegetative cell cycle (Donti et al, 2009), it also prepares cells for conjugation. The earliest rounds of DNA replication in this developmental program are restricted to the micronucleus, while the later rounds create a new polyploid macronucleus. Published microarray profiles revealed two increases in the abundance of ORC and MCM subunit transcripts, peaking 4 h and 14 h after mixing starved cells with different mating types (Figure 2.8 and Table 2.1) (Miao et al, 2009; Xiong et al, 2011). The more prominent early peak is derived from the parental macronucleus, suggesting that these proteins might be stockpiled for later use in the developing macronucleus.

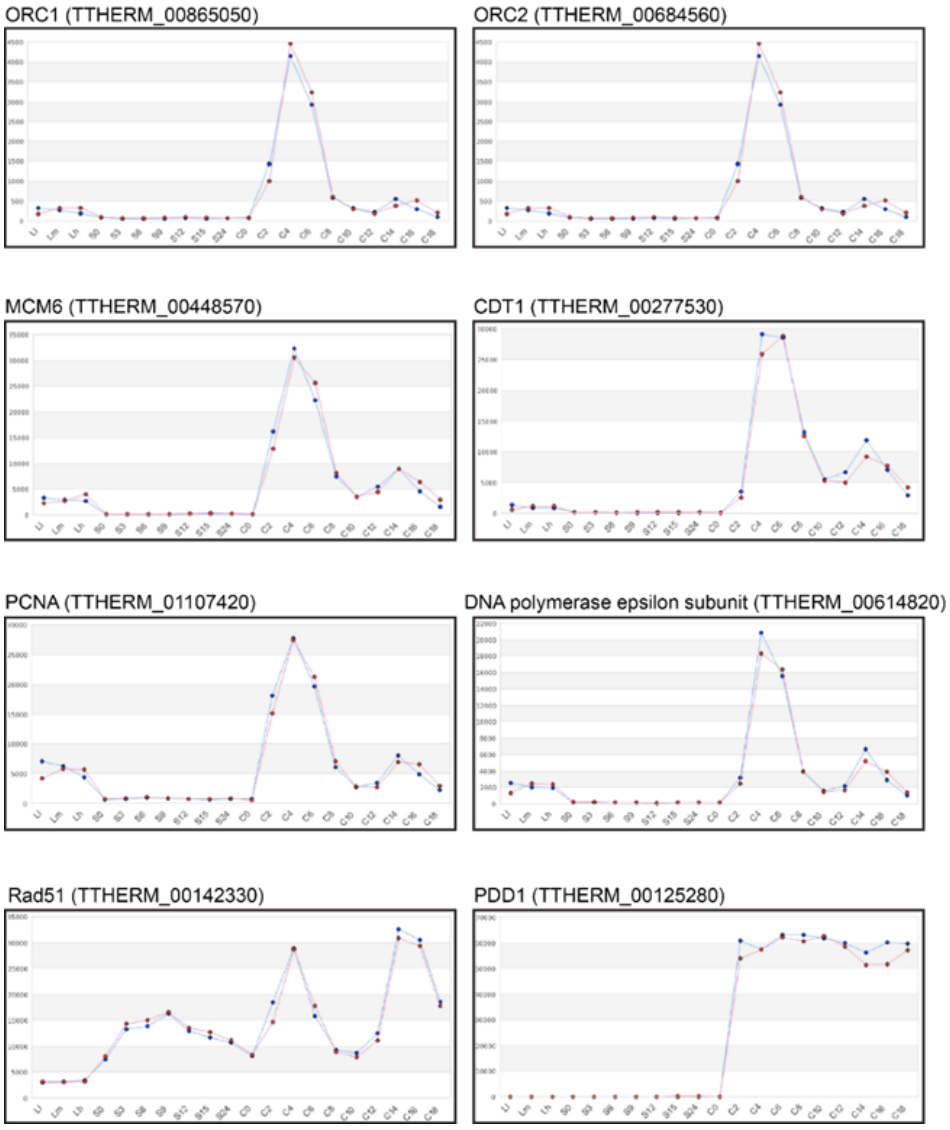

Figure 2.8. Microarray gene expression data of *Tetrahymena* pre-RC components. Gene expression profiles were accessed from the *Tetrahymena* functional genomics database (TetraFGD) (Miao et al, 2009; Xiong et al, 2011). Each profile contains 20 time points during the three physiological and developmental stages of the T. thermophila life cycle, including 3 points in growth (L), 7 points in starvation (S) and 10 points in conjugation (C). For growing cells, L-l, L-m and L-h correspond respectively to 1X105 cells/ml, 3.5 x 105 cells/ml and 1X106 cells/ml. For starved cells, samples were collected at 0, 3, 6, 9, 12, 15 and 24 h (S0 – S24). For conjugation, samples were collected at 0, 2, 4, 6, 8, 10, 12, 14, 16 and 18 h after mating (C0 – C18). Blue and red lines represent the expression values normalized by two different methods. *Tetrahymena* ORC1 (Gene ID: TTHERM_00865050), ORC2 (Gene ID: TTHERM_00684560), MCM6 (Gene ID: TTHERM_00448570), CDT1 (Gene ID: TTHERM_00277530), PCNA (Gene ID: TTHERM_ 01107420), DNA polymerase epsilon, B subunit (GENE ID: TTHERM_00614820), RAD51 (GENE ID: TTHERM_00142330), PDD1 (GENE ID: TTHERM_00125280).

Table 2.1. Coefficients for gene expression. The ORC1 gene expression profile was used as a reference to identify other DNA replication and repair genes with statistically significant coefficients for gene expression. Data were obtained from the TFGD database (http://tfgd.ihb.ac.cn/tool/network).

Gene name	Gene Model Identifier	Z-score* with ORC1	Link to TetraFGD
ORC1	TTHERM_00865050	-	http://tfgd.ihb.ac.cn/search/detail/gene/TTHERM_00865050
ORC2	TTHERM_00684560	6.96	http://tfgd.ihb.ac.cn/search/detail/gene/TTHERM_00684560
MCM2	TTHERM_00554270	8.85	http://tfgd.ihb.ac.cn/search/detail/gene/TTHERM_00554270
MCM3	TTHERM_00092850	9.09	http://tfgd.ihb.ac.cn/search/detail/gene/TTHERM_00092850
MCM4	TTHERM_00277550	8.84	http://tfgd.ihb.ac.cn/search/detail/gene/TTHERM_00277550
MCM5	TTHERM_00069420	5.82	http://tfgd.ihb.ac.cn/search/detail/gene/TTHERM_00069420
MCM6	TTHERM_00448570	8.26	http://tfgd.ihb.ac.cn/search/detail/gene/TTHERM_00448570
MCM7	TTHERM_00011740	7.77	http://tfgd.ihb.ac.cn/search/detail/gene/TTHERM_00011740
MCM8	TTHERM_01031060	NC	http://tfgd.ihb.ac.cn/search/detail/gene/TTHERM_01031060
MCM9	TTHERM_00703910	4.43	http://tfgd.ihb.ac.cn/search/detail/gene/TTHERM_00703910
PCNA	TTHERM_01107420	7.11	http://tfgd.ihb.ac.cn/search/detail/gene/TTHERM_01107420
DNA polymerase alpha/primase	TTHERM_00424700	7.23	http://tfgd.ihb.ac.cn/search/detail/gene/TTHERM_00424700
RFC1	TTHERM_00939110	4.54	http://tfgd.ihb.ac.cn/search/detail/gene/TTHERM_00939110
RFC2	TTHERM_00245150	4.16	http://tfgd.ihb.ac.cn/search/detail/gene/TTHERM_00245150
RFC3	TTHERM_00213600	5.98	http://tfgd.ihb.ac.cn/search/detail/gene/TTHERM_00213600
RFC4	TTHERM_00780750	7.22	http://tfgd.ihb.ac.cn/search/detail/gene/TTHERM_00780750
RFC5	TTHERM_00161180	6.20	http://tfgd.ihb.ac.cn/search/detail/gene/TTHERM_00161180
ATR	TTHERM_01008650	NC	http://tfgd.ihb.ac.cn/search/detail/gene/TTHERM_01008650
RAD51	TTHERM_00142330	NC	http://tfgd.ihb.ac.cn/search/detail/gene/TTHERM_00142330
ASI2	TTHERM_00191480	NC	http://tfgd.ihb.ac.cn/search/detail/gene/TTHERM_00191480
CDT1	TTHERM_00277530	7.79	http://tfgd.ihb.ac.cn/search/detail/gene/TTHERM_00277530

* Z-score: In the *Tetrahymena* Gene Network (TGN) database (http://tfgd.ihb.ac.cn/tool/network), which can be used to identify related genes in the same biological processes or pathways, the Z-score was used in the context likelihood of relatedness (CLR) algorithm based on microarray expression data (Miao et al, 2009; Xiong et al, 2011). The larger of a Z-score between two genes indicated the more similar expression profiles. NC: No correlation; Z-score is below the threshold 3.49.

To assess the abundance of pre-RC components throughout development, western blot analysis was performed with peptide antibodies specific for *Tetrahymena* Orc1p, Orc2p and Mcm6p. Alpha tubulin (Atu1p) and Rad51p were used as reference proteins for comparative analysis. RAD51 generates a distinct RNA profile during development in starved mating cells (Marsh et al, 2000), while Atu1p levels have been reported to fluctuate minimally in starved mating cells (Chung & Yao, 2012). Lowry assays were performed to assure that equivalent amounts of protein were loaded in each lane, and Ponceau S staining was used to monitor protein transfer prior to western blot probing.

Consistent with its RNA profile, Orc1p levels increased dramatically within the synchronized mating cell population, generating a broad peak between 6-15 h (Figure 2.9A). While these time points encompass multiple rounds of micronuclear DNA replication and two rounds of macronuclear anlagen DNA replication (endoreplication phase I) (Figure 2.9B), the cumulative amount of DNA replication is less than half the amount generated during a single vegetative cell cycle. Hence, ORC is in vast excess compared to the vegetative cell cycle. Centrifugal elutriation of a vegetative G1 phase population verified that starvation per se does not appreciably affect the abundance of Orc1p (Figure 2.9C). The decline in Orc1p and Mcm6p levels prior to conjugant re-feeding (18-24 h) indicates that these proteins are not stockpiled for later use. A second wave of Orc1p synthesis was detected in mated re-fed cells. This occurred after the parental macronucleus was destroyed and prior to endoreplication phase II (Figures 2.9A and 2.9B). Similar to Orc1p, Mcm6p levels rose and declined early in development

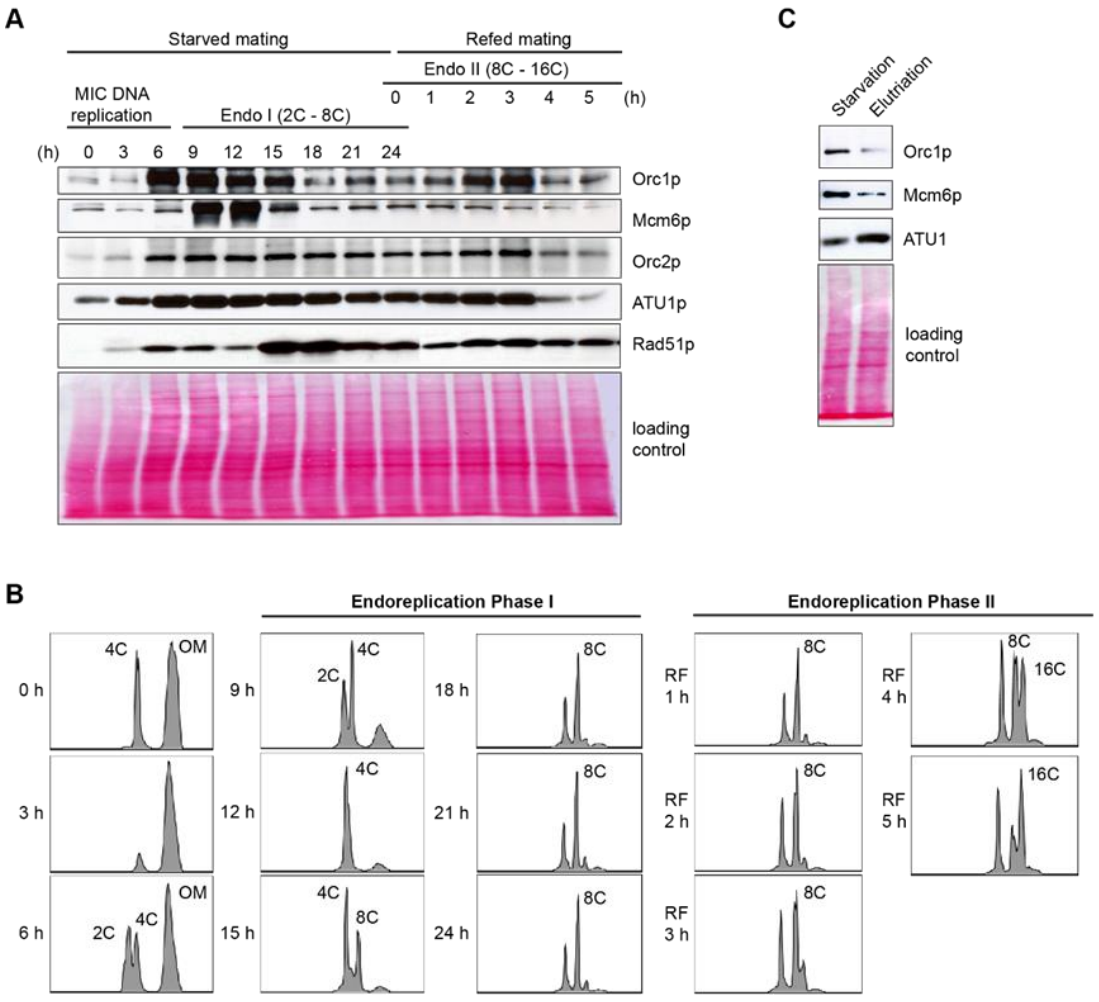

Figure 2.9. Developmental regulation of pre-RC components. Whole cell lysates were prepared from matings between wild type strains, CU427 and CU428, at indicated time points during conjugation. 0-6 h, micronuclear DNA replication; 9-24 h, endoreplication phase I (Endo I). Mating cultures were re-fed at 24 h to complete development (endoreplication phase II; Endo II). Equivalent amounts of total protein (20 μg) were separated by denaturing polyacrylamide gel electrophoresis and subjected to western blot analysis. (B) Flow cytometry analysis samples analyzed in panel A. Nuclei were isolated and stained with propidium iodide. Each histogram represents the number of counted nuclei (x-axis) versus DNA content (y-axis). OM, old parental macronucleus, which is degraded in conjugants. (C) Western blot analysis of wild type cells (CU428) synchronized at the G1/S border by starvation for 18 h or by centrifugal elutriation of a log phase vegetative culture.

(9-12 h). However, Mcm6p levels did not increase in mated/re-fed cells (endoreplication phase II). Like Atu1p, Orc2p levels were relatively constant throughout development. Notably, Rad51p levels peaked when Orc1p levels were low (i.e. endo I (15-18h), endo II 4-5 h) ruling out the possibility that the observed changes in Orc1p abundance can be generalized to all proteins, regardless of their function.

Altered DNA replication during endoreplication phase II

The decline in Orc1p and Mcm6p at later time points during endoreplication phase II (Figure 2.9A, re-fed 4 h and 5 h) prompted us to examine rDNA replication intermediates during this phase. To do so, two heterokaryon strains with a C3 rDNA micronucleus and B rDNA macronucleus were mated and RIs were examined by 2D gel electrophoresis. Western blot analysis and flow cytometry verified the reproducibility for the transient increase and subsequent decline in Orc1p in mated/re-fed cells, and revealed Orc1p levels did not further oscillate prior to the next round of endoreplication (16 C to 32 C) (Figure 2.10A and 2.10B).

To visualize RIs generated in the developing macronucleus, newly synthesized macronuclear C3 rDNA molecules were resolved from B rDNA molecules (derived from the parental macronucleus and non-mating cells within the population) by treating *HindIII*-digested genomic DNA with *SphI*, which cleaves the B rDNA 5' NTS into two smaller fragments. As previously reported (Zhang et al, 1997), the predominant RI pattern detected in the 14-16 h window in mating cells is bubble-to-Y arc (Figure 2.11A, schematic), which is generated from initiation events in one 5' NTS copy in the rDNA palindrome, followed by the transient pausing of replication forks that migrate toward

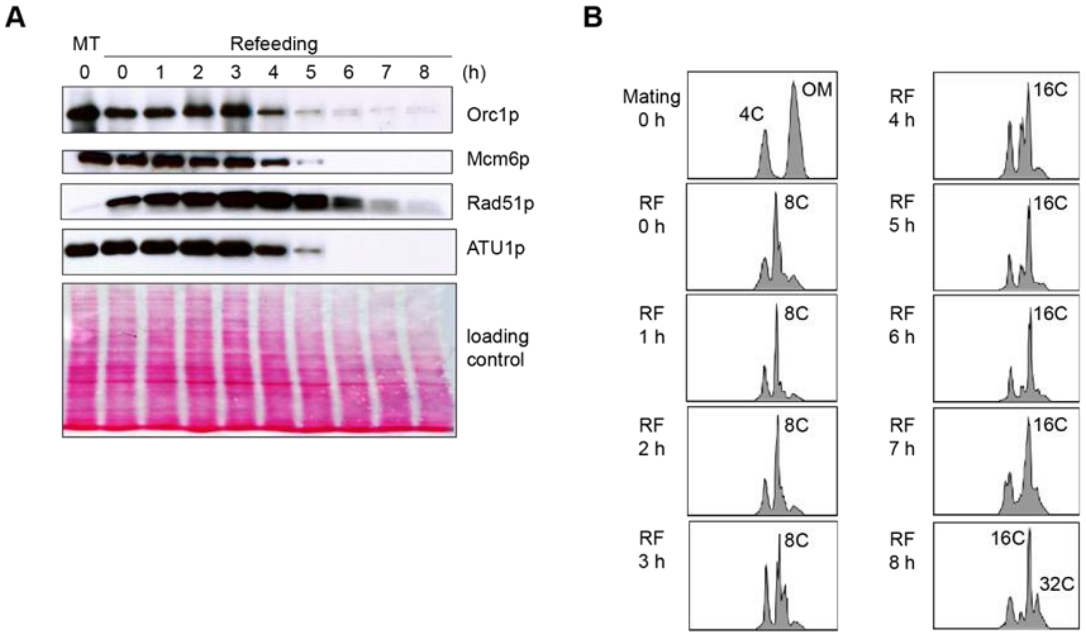

Figure 2.10. Developmental regulation of pre-RC components (supplemental). (A) Whole cell lysates were prepared from matings between wild type strains, CU427 and CU428, at indicated time points during conjugation. MT: mating cells. Mated cells were re-fed at 24 h and samples were collected at 1 h interval for an additional 8 h. Equivalent amounts of total protein (20 μg) were separated by denaturing polyacrylamide gel electrophoresis and subjected to western blot analysis. (B) Flow cytometry analysis samples analyzed in panel A. Nuclei were isolated and stained with propidium iodide. Each histogram represents the number of counted nuclei (x-axis) versus DNA content (y-axis). OM, old parental macronucleus, which is degraded in conjugants.

the telomere (Figure 2.11B) (MacAlpine et al, 1997). This pattern is exclusively observed during vegetative S phase (Figure 2.11B, WT log phase).

The rDNA replication pattern during endoreplication phase II displayed the general features of RIs in mated starved cells (endoreplication phase I) with the following difference: aberrantly migrating RIs were detected on the Y arc during endoreplication phase II (Figure 2.11B, 4-8 h refed mating). Whereas the trajectory of low molecular weight Y arc intermediates in log phase and endoreplication phase I cells intersects the 1N (unreplicated) DNA spot, the trajectory of low molecular weight RIs generated during endoreplication phase II was shifted significantly to the left. Similar aberrant RIs accumulate in *S. cerevisiae* senataxin mutants, which are deficient in an RNA helicase that serves multiple roles in RNA metabolism (Alzu et al, 2012). Like senataxin mutants, the aberrant RIs, termed gapped forks, were eliminated when *Tetrahymena* DNA samples were sequentially treated with RNAse A and Mung Bean nuclease (MBN) (Figure 2.11C). Most notably, the aberrantly migrating RIs are converted to simple Y arcs following MBN-treatment, consistent with the passive replication of the 5' NTS origins. We speculate that these replication origins are not used in a sub-population of endoreplicating rDNA molecules, when ORC protein levels are lowest.

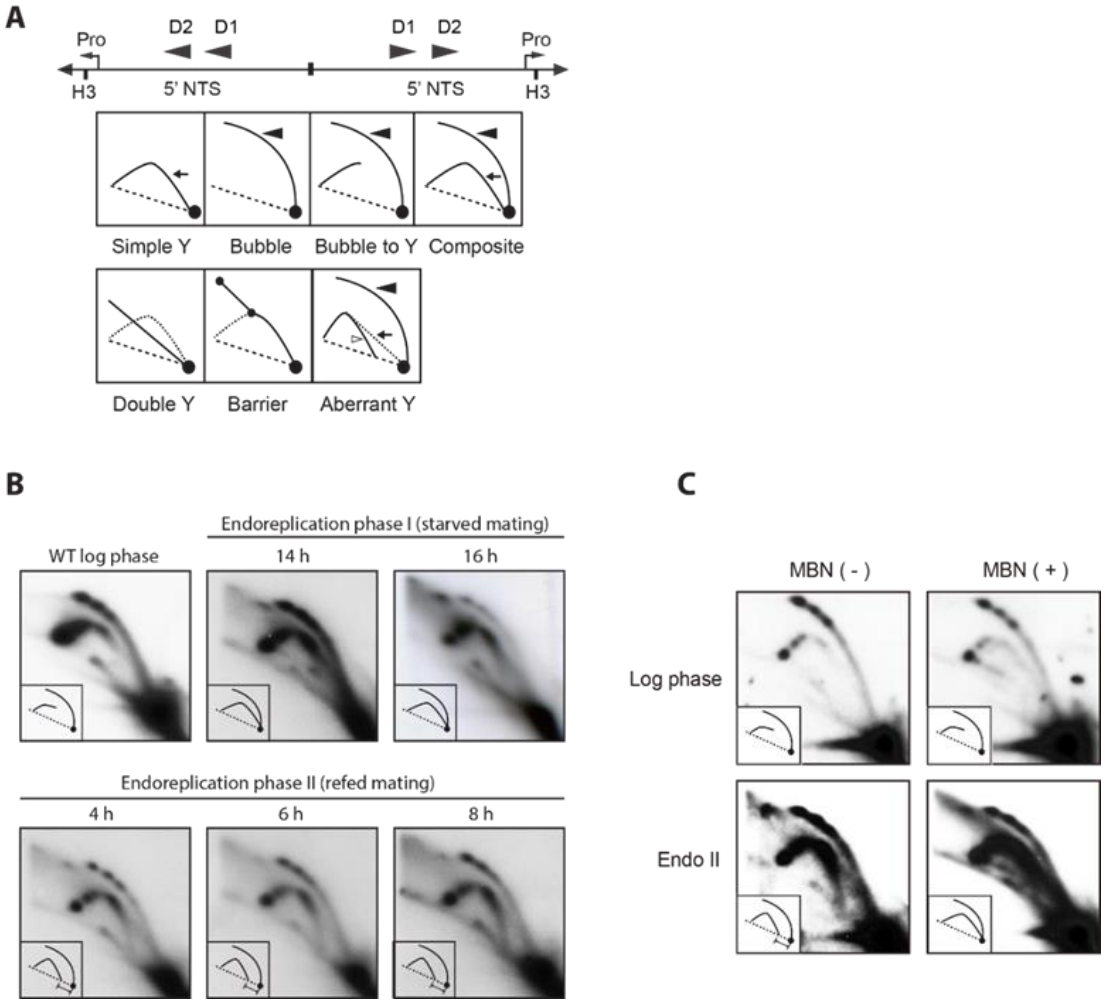

Figure 2.11. Two-dimensional gel analysis of rDNA replication intermediates during development. (A) Schematic of the palindromic rDNA 5'NTS fragment generated by *HindIII* (H3) digestion, and possible replication intermediate patterns resolved by neutral-neutral 2D gel electrophoresis. Pro, promoter; D1 and D2, imperfect 430 bp tandem duplications and harbor the rDNA origins of replication. Simple Y (arrow), passive replication of 5' NTS origins. Bubble (filled arrowhead) or bubble to Y, bidirectional replication within the 5' NTS. Composite (simple Y arc and bubbles), active and passive replication of the 5' NTS. Double Y, two converging forks initiating within or outside the 5' NTS. Barrier, replication of the 5' NTS by converging forks, in which the first fork entered and terminated at a barrier prior to entry of the second fork. Aberrant Y (unfilled arrowhead), simple Y arc containing partially replicated DNA. Diagonal dashed line, migration of linear duplex DNA fragments; dotted arc, reference pattern for simple Y arc intermediates. (B) C3 rDNA amplification replication intermediates after mating for 14 and 16 h, and subsequent refeeding (at 24 h) for an additional 8 h. Mating: strains SB4202 and SB1934. (C) Mung bean nuclease (MBN) digestion on C3 rDNA amplification intermediates in matings between SB4202 and SB1934 collected after refeeding with media for 8 h. DNA samples from log phase SB4204 stain were collected as the control.

Discussion

A distinguishing feature of the early branching eukaryotic phylum, Ciliophora, is the co-habitation of two functionally distinct nuclei within a single cytoplasm. Chromosomes in the somatic macronucleus are actively transcribed and contain euchromatic histone modifications that facilitate this process (i.e. histone H3K29Ac) (Brownell et al, 1996). These same DNA sequences (including replication origins) are packaged into heterochromatin in the transcriptionally silent germ line micronucleus. Whereas chromosomes segregate randomly in the polyploid macronucleus, DNA copy number is maintained through the elimination of excess DNA in the form of chromatin extrusion bodies (Cleffmann, 1980) or re-replication of the genome when a minimal DNA content is not achieved (Doerder & DeBault, 1978). Despite the imprecision of amitosis, macronuclear DNA replication is governed by the same regulatory mechanisms that function in canonical (G1-S-G2-M) cell cycles (Harrison & Haber, 2006; Sclafani & Holzen, 2007). They include ORC-dependent, site-specific initiation of DNA replication (Donti et al, 2009; Mohammad et al, 2007), cell cycle regulated pre-RC assembly (Donti et al, 2009), S phase inactivation of ORC (to prevent re-replication) (Donti et al, 2009; Mohammad et al, 2003), and the presence of a robust ATR-mediated DNA damage/replication stress checkpoint response (Yakisich et al, 2006).

In this study we examined the effect of modulating ORC1 on the execution of micro- and macronuclear DNA replication programs. The moderate reduction in ORC protein levels that was achieved compromised the integrity of chromosomes in micro- and macronuclei during the vegetative cell cycle, yet the deficiencies were not sufficient

to trigger a robust intra-S phase checkpoint response. Remarkably, much greater fluctuations in ORC abundance occur during wild type *Tetrahymena* development. The successive changes in ORC and MCMs protein levels that we uncovered indicate that developmentally regulated replication programs are more complex than previously imagined.

ORC, MCMs and the vegetative cell cycle

The compartmentalization of germ line and somatic functions into micro- and macronuclei poses unique challenges to master regulators of the cell cycle. Micro- and macronuclear S phases are offset during the vegetative cell cycle, daughter chromosomes are partitioned by radically different mechanisms (mitosis and amitosis), and mitotic nuclear division is not coupled to cytokinesis. Indeed, although macronuclear S phase precedes micronuclear S, the order of nuclear division is reversed. We previously showed that ORC (Orc1p, Orc2p and the integral *Tetrahymena*-specific RNA subunit, 26T RNA) dissociates from macronuclear replication origins during S phase, concomitant with the degradation of Orc1p. ORC is subsequently distributed randomly onto daughter chromosomes during G2 phase and re-localizes to origins in G1 phase (Donti et al, 2009). To better illuminate the role(s) of ORC in replication origin licensing, we disrupted the ORC1 gene in the polyploid (45 C) macronucleus. As predicted for an essential gene, complete replacement was not achieved. The 5-fold decrease in ORC1 gene dosage was accompanied by a comparable reduction in Orc1p (Figure 2.1B). An unexpected drop in Orc2p and Mcm6p levels was also observed in the

ORC1 knockdown strain (Figure 2.1B). This may reflect the co-regulation of pre-RC components (see below).

ORC1 mutants exhibited an elongated cell cycle that was typically accompanied by aberrant macronuclear division with lagging chromosomes (Figure 2.1; Figure 2.2). The high incidence of abnormal cell division is consistent with the failure to activate the ATR checkpoint response. In support of this model, HU and MMS did not arrest cell cycle progression or inhibit nascent strand synthesis in the mutant (Figures 2.3A and E), and the induction of Rad51p, a marker for checkpoint activation, was reduced (Figures 2.3B-D). The essential role for ORC in the germ line micronucleus was highlighted by the instability of mitotic chromosomes during vegetative propagation of the mutant. The progressive loss of micronucleus-specific chromosome markers (Figure 2.6A) led to defects in meiotic chromosome transmission (Figure 2.6B) and sterility. Micronuclear chromosome loss failed to trigger cell cycle arrest during the vegetative cell cycle, consistent with previous reports for strains lacking the checkpoint activator protein, TIF1p, or harboring a fragile site in the micronuclear genome (Yakisich & Kapler, 2006; Yakisich et al, 2006). We conclude that a moderate reduction in Orc1p levels profoundly compromises DNA replication in the micro- and macronucleus.

The simplest explanation for these phenotypes is that the reduction in Orc1p compromises replication initiation. Three lines of evidence argue against this model. First, two-dimensional gel analysis showed that rDNA origin site selection and/or usage were unaffected in the ORC1 knockdown strain (Figure 2.5A). Second, DNA fiber imaging of non-rDNA chromosomes revealed no increase in the average inter-origin

distance. Third, DNA fiber imaging uncovered a decrease in the rate of replication fork elongation (Figure 2.5B). We postulate that the slowing of replication forks is linked to the down regulation of MCMs in the ORC1 mutant (Figure 2.1B). Accordingly, the diminished DNA replication checkpoint response may reflect the propensity to maintain proper coupling between the replicative helicase and polymerase. This fork elongation defect is surprising for several reasons. Unlike *Tetrahymena*, down-regulation of *S. cerevisiae* ORC2 has no effect on MCM protein abundance and/or replication fork progression. Instead, origin utilization declines and the inter-origin distance increases in the ORC2-1 mutant strain (Shimada et al, 2002). Furthermore, MCMs are in excess to ORC in other model systems (Edwards et al, 2002; Forsburg, 2004). This stoichiometry has been proposed to facilitate the initial unwinding of replication origins. Furthermore, excess MCMs have been shown to protect chromosomes from replication stress (i.e. stalled or collapsed forks) by activating neighboring dormant origins (Ge et al, 2007; Ibarra et al, 2008). These safeguards may not be necessary in the polyploid amitotic macronucleus of *Tetrahymena*, which employs other correcting mechanisms to maintain genic balance (Cleffmann, 1980; Doerder & DeBault, 1978). Finally, partial depletion of MCMs preferentially inhibits replication initiation in *S. cerevisiae* and cultured *Drosophila* cells (Crevel et al, 2007; Lei et al, 1996), suggesting that this step is most sensitive to MCM dosage. The down regulation of Mcm6p in *Tetrahymena* ORC1 mutants and accompanying effect on replication fork progression argue that elongation is the rate limiting step when ORC and MCM levels are reduced in this species. Whether this reflects how origins are distributed throughout the *Tetrahymena* genome (i.e.

dispersed versus clustered origins (Cayrou et al, 2011)), different requirements for ORC: MCM stoichiometry, or alternative mechanisms for replication initiation in the amitotic macronucleus awaits further studies.

ORC, MCMs and development

In contrast to the vegetative cell cycle, micro- and macronuclear DNA replication programs are uncoupled during *Tetrahymena* development. The increased production of maternal transcripts encoding replication pathway proteins (Figure 2.8) (Miao et al, 2009) suggested that these factors might be stockpiled for later use in progeny, when the demands for DNA replication increase. The earliest rounds of DNA replication in conjugating cells are exclusively devoted to the micronuclear genome. They generate stationary and migratory pronuclei for reciprocal genetic exchange, and produce four genetically equivalent micronuclei in exconjugants. Subsequent rounds of DNA replication are restricted to the macronuclear 'anlagen', as nonconventional DNA replication programs (endoreplication, rDNA gene amplification) are activated.

The developmental oscillations in ORC and MCM protein levels that we uncovered suggest that the rules for DNA replication change at different stages of development. They are intriguing because ORC levels do not correlate with the amount of DNA that is synthesized at a given time. Orc1p levels are highest early in development, when the micronucleus alone is being replicated (Figure 2.9). They start to decline during early rounds of endoreplication in the developing anlagen (4-8 C). Conversely, these proteins are at their lowest level when the demands for macronuclear DNA synthesis peak in late stage endocycling cells (Figure 2.9, Figure 2.10, 16-32 C).

While the purpose for the initial increase in *Tetrahymena* ORC and MCM abundance awaits further investigation, it appears to be distinct from the replication programs associated with early embryonic development in *Xenopus* and *Drosophila* (Blumenthal & Clark, 1977; Tugal et al, 1998). In all three cases, maternally derived proteins support DNA replication prior to cell differentiation. In flies and frogs, ORC and MCM levels are elevated until the mid-blastula transition. They correlate with a transient increase in origin density and occur in transcriptionally silent nuclei. ORC and MCM levels plummet following the onset of zygotic transcription, and subsequent initiation events are primarily relegated to intergenic chromosomal regions. The functional connection between transcriptional silencing and elevated ORC does not hold for *Tetrahymena*. The micronucleus is transcriptionally quiescent during the vegetative stage of the life cycle, and is actively transcribed during development, generating non-coding RNAs that direct the removal of micronuclear-limited sequences in macronuclear anlagen (Chalker & Yao, 2001; Yao et al, 2003). Furthermore, the demands for DNA replication during *Tetrahymena* development are markedly reduced relative to metazoa. In the case of *Drosophila*, successive ten minute cell cycles generate ~6000 nuclei in the developing syncytium. *Tetrahymena* generates only four diploid micronuclei prior to the onset of zygotic transcription. The net increase in synthesized DNA is only 6 C.

Whereas the primary goals of endoreplication phases I and II are the same, to increase DNA content in the newly developing progeny macronucleus, these replication programs have several distinguishing characteristics. Both programs require the ASI2 gene, which encodes a putative transmembrane protein that may function in signal

transduction (Li et al, 2006; Yin et al, 2010), analogous to Notch-dependent signaling in endocycling *Drosophila* follicle cells (Schaeffer et al, 2004). However, unique extrinsic and/or intrinsic requirements must exist, since endoreplication phase I occurs in starved mating cells and endoreplication phase II requires re-feeding. Furthermore, rDNA gene amplification is restricted to endoreplication phase I, and occurs concurrently with the replication of non-rDNA chromosomes (Kapler & Blackburn, 1994; Zhang et al, 1997). Finally, ORC levels are reduced during endoreplication phase II (Figures 2.9 and 2.10), and unconventional DNA replication intermediates are produced at this time (Figure 2.11), indicative of an altered DNA replication program (see below).

Our studies with the ORC1 knockdown strain clearly demonstrate that ORC is required for endoreplication and rDNA gene amplification (Figure 2.7). While the contributions of ORC to endoreplication phase I are well supported, the dependence of ORC during endoreplication phase II is less clear. For example, the rDNA is exclusively replicated from 5' NTS origins during endoreplication phase I (Figure 2.11; bubble-to-Y arc, no simple Y arcs). Endoreplication phase II is much more complicated. While a bubble-to-Y arc pattern is seen, consistent with ORC-mediated initiation, a new pattern of aberrantly migrating 'Y-like' RIs is also observed. The sensitivity of the Y-like RIs to sequential ribonuclease-A (RNase) and Mung Bean nuclease (MBN) treatment supports the idea that single strand DNA or stable RNA-DNA hybrids accumulate in the 5' NTS region during endoreplication phase II. Their nucleolytic conversion to simple Y arc RIs argues that the initiation site is not coincident with the known, ORC-dependent replication origins. By analogy, the impaired activity of an *S. cerevisiae* RNA helicase,

senataxin leads to the accumulation of RNA-DNA hybrids, and generates RNase/MBN-sensitive RIs (Alzu et al, 2012). Moreover, aberrant RIs accumulate when Orc1p levels decline in the developing macronuclear anlagen (Figure 2.10). Since the experimental down regulation of ORC in vegetative cells does not produce this aberrant pattern (Figure 2.5), their genesis may be restricted to *Tetrahymena* development. We propose that the rRNA promoter or a cryptic 5' NTS promoter generates RNA-DNA hybrids in endocycling *Tetrahymena*, and speculate that this RNA might inhibit initiation from the ORC-dependent origin or serve as a primer for DNA synthesis.

How might replication initiation be achieved with limiting amounts of ORC? It is conceivable that ORC might transiently associate with origins to establish pre-RCs and dissociate once MCM complexes are loaded. Live imaging recently revealed that ORC and CDC6 turn over rapidly on chromatin in *C. elegans* embryos, but MCMs do not (Sonneville et al, 2012). Alternatively, replication initiation and elongation might be temporally uncoupled during endoreplication phase II, as was reported for amplification of the chorion gene locus in stage 10-13 *Drosophila* embryos (Claycomb et al, 2002). Our previous studies of the vegetative cell cycle do not support either model in *Tetrahymena*. ChIP analysis of synchronized cell populations demonstrated that ORC is randomly deposited onto chromatin during G2 phase and re-localizes to replication origins during G1 phase, concomitant with the recruitment of MCM complexes (Donti et al, 2009). Fundamental changes in ORC-dependent pre-RC assembly would be required to support endoreplication with diminished amounts of ORC. Furthermore, the aberrant RIs that form during endoreplication phase II are inconsistent with re-initiation of DNA

replication on stalled replication forks (onion skin replication). Indeed, onion skin RIs accumulate very early in the amplification process due to the activation of a developmentally programmed replication fork barrier (Zhang et al, 1997).

A more provocative possibility is that endoreplication occurs by an ORC-independent mechanism. Although ORC normally associates with chromatin in endocycling *Drosophila* salivary gland cells (Sher et al, 2013), the ability of ORC2 mutant clones to support genome-wide re-replication is consistent with this model (Park & Asano, 2008). Furthermore, origin-independent propagation of chromosomes in *S. cerevisiae* (Dershowitz et al, 2007) and *Haloferax volcanii* (Hawkins et al, 2013) demonstrates that recombination-based mechanisms can propagate chromosomes when ORC-mediated pre-RC assembly is perturbed. Advances in genome-wide analysis, such as nascent strand-seq (Cayrou et al, 2012b) should provide fundamental insights in the underlying mechanism for 'alternative' DNA replication programs in *Tetrahymena*.

Material and methods

DNA transformation and propagation of Tetrahymena thermophila *strains*

Tetrahymena strains are described in Table 2.2.

Table 2.2. Genotypes and phenotypes of *T. thermophila* strains used in this study. The micronuclear alleles, chx1-1 and mpr1-1 confer resistance to cycloheximide and 6-methylpurine, respectively. C3 and B rDNA alleles can be distinguished by restriction fragment polymorphisms in the 5' NTS or 3' NTS. Homologous gene replacement of the wild type ORC1 gene with the ORC1::MTT-neo sequence confers resistance to paramomycin due to expression of the cadmium inducible neomycin phosphotransferase gene.

Strain	Micronuclear genotype	Macronuclear phenotype
CU427	*ORC1/ORC1* *chx1-1/chx1-1*	paromomycin-sensitive cycloheximide-sensitive
CU428	*ORC1/ORC1* *mpr1-1/mpr1-1*	paromomycin-sensitive 6-methylpurine-sensitive
ORC1-KD	*ORC1/ORC1* *CHX1/chx1-1* *MPR1/mpr1-1*	paromomycin-resistant; ORC1::MTT-neo* cycloheximide-resistant 6-methylpurine-resistant
SB4202	*ORC1/ORC1* *rDNA [C3]/rDNA [C3]*	paromomycin-sensitive rDNA [B]
SB1934	*ORC1/ORC1* *rDNA [C3]/rDNA [C3]*	paromomycin-sensitive rDNA [B]

* partial replacement

Standard methods were used for mating, transfection and selection of paromomycin (pm) resistant transformants, and for vegetative propagation of wild type and mutant *Tetrahymena* strains (Yakisich et al, 2006). The ORC1 knockdown strain (TD101) was generated by replacing the ORC1 protein coding region with an MTT1-neo gene cassette, using flanking ORC1 sequences for targeted homologous recombination (Donti et al, 2009). Bio-ballistic transformation was used to introduce DNA into the developing macronucleus in a mating between strains CU427 and CU428. Paromomycin (pm) resistant progeny were continuously selected for 'phenotypic assortants' with increased levels of drug resistance (100 μg/ml to 1000 μg/ml), due to replacement of wild type copies of the ORC1 gene with an MTT1-neo disruption allele in the polyploid amitotic macronucleus.

Cell cycle synchronization and flow cytometry

Cell cycle synchronization was achieved by starvation and re-feeding or centrifugal elutriation as previously described (Donti et al, 2009). Flow cytometric analysis was performed to monitor cell cycle progression in vegetative growing cells (Morrison et al, 2005), and to determine the relative DNA content in isolated micro- and macronuclear populations in mating cells. For the later, nuclei were extracted in ice-cold nucleus extraction buffer (10 mM Tris at pH 7.4, 10 mM $MgCl_2$, 3 mM $CaCl_2$, 0.25 M sucrose, 0.2% NP-40, 1 mM dithiothreitol, 1 mM phenylmethylsulfonyl fluoride). Flow cytometry analysis was performed on Becton Dickinson FACSAria II flow cytometer (BD Biosciences). Data were analyzed using BD FACSDiva software. Histograms were

plotted, in which the y-axis represents the number of events and the x-axis represents the relative DNA content.

Cell fractionation and western blot analysis

Whole cell extracts were prepared by lysing cells in 1% SDS lysis buffer (50 mM Tris at pH 8.0, 150 mM NaCl, 1 mM EDTA, 1% NP-40, 1% sodium deoxycholate, 1% SDS) for 15 min on ice. To prepare soluble and chromatin-bound fractions, cells were incubated in 50 µl NP-40 lysis buffer (0.1% NP-40, 20 mM Tris-HCl at pH 8.0, 137 mM NaCl, 10% glycerol, 2 mM EDTA) for 10 min on ice. After centrifugation at 2,000 g for 10 min at 4°C, the supernatant was collected as the 'soluble fraction'. The pellet was resuspended in 50 µl of 1% SDS lysis buffer and designated as 'chromatin-bound fraction'. Protein concentrations were determined using the modified Lowry protein assay reagents (Bio-Rad, cat# 500-0111). Unless otherwise stated, equal amounts of total protein (20 µg) were loaded in each lane and samples were subjected to SDS-PAGE and transferred to nitrocellulose membranes (Whatman Protran BA85, GE Healthcare). Prior to probing, membranes were stained with Ponseau S staining (Sigma-Aldrich) to confirm equivalent sample loading and protein transfer. Immunodetection of *Tetrahymena* Orc1p (1:5,000), Orc2 (1:5,000) and Mcm6p (1:10,000) were carried out using polyclonal rabbit antibodies raised against immunogenic *Tetrahymena* peptides (Covance). Antibodies directed against Rad51 (51RAD01, Thermo Scientific, 1:5,000 dilution), acetyl-histone H3 (Upstate (Invitrogen), 1:10,000 dilution), and alpha tubulin antibodies (Abcam, 1:2,000 dilution) were obtained from the indicated commercial sources. Blots were incubated with the primary antibodies at 4 ℃ overnight, washed and incubated for

3 h at 4 ℃ with horseradish peroxidase-conjugated goat anti-rabbit or anti-mouse IgG (Jackson ImmunoResearch). Membrane bound secondary antibodies were visualized using ECL reagents (PerkinElmer) according to the manufacturer's instructions. Densitometry of blots was performed using ImageJ software (version 1.47v for Macintosh, National Institutes of Health).

Cytological staining and fluorescence microscopy

For mating experiments, wild type strain CU427 was distinguished from its mating partner by incorporation of Mitotracker Red-CMXRos (Molecular Probes, Invitrogen) at a concentration of 500 nM during overnight starvation at 30 ℃. On the next day, starved cell cultures were washed once and resuspended in 10 mM Tris at the density of 2.5 x 10^5 cells/ml. Mating was initiated by mixing CU427 with CU428 or CU427 with ORC1 knockdown cells in equal volume. One-milliliter of mating culture was harvested each hour during development. Cells were fixed in 70% ethanol for at least 1 h. Fixed cells were washed once with PBS and resuspended in 100 µl of 0.1 µg/ml 4',6'-diamidino-2- phenylidole (DAPI, Sigma Chemical) to stain nuclei. To visualize nuclear division, 1 ml of log phase CU427 and ORC1 knockdown cell cultures were harvested and fixed with 2% paraformaldehyde. Acridine orange was added at a concentration of 0.001% to stain nuclei. Cells were examined by conventional fluorescence microscopy.

DNA isolation and enrichment for replication intermediates (RIs)

Total genomic DNA was isolated from *Tetrahymena* cultures as previously described to preserve DNA replication intermediates (Zhang et al, 1997). For RI

enrichment, 200 μg of genomic DNA were digested with *HindIII* for 4 h and applied to the 200-μl packed volume benzoylated naphthoylated DEAE (BND)-cellulose (Sigma-Aldrich). Caffeine-eluted DNA samples were precipitated with isopropanol, using 20 μg glycogen as a carrier. Samples were subsequently digested with *SphI* to resolved C3 and B rDNA fragments as needed. Total DNA recovery was estimated to be ~5% of the input. For mung bean nuclease (MBN) treatment, 3 μg of BND cellulose-enriched RIs was digested with 5 U of MBN (New England BioLabs) at 30 ℃ for 30 min. SDS was added to the final concentration of 0.01% to inactivate MBN (Alzu et al, 2012).

Two-dimensional (2D) gel electrophoresis of DNA replication intermediates

Neutral-neutral 2D gel electrophoresis was performed as previously described (Zhang et al, 1997). Approximately 3-10 μg of BND cellulose-enriched DNA was loaded for each 2D gel experiment. The first dimension gel (0.4% agarose) was run in 1X TAE buffer (40 mM Tris, 20 mM acetic acid, and 1 mM EDTA) at 1.5 V/cm for 20 h at RT. The second dimension gel (1% agarose) was run in 1X TBE buffer (90 mM Tris, 90 mM Boric acid, 2 mM EDTA) containing 0.5 mg/ml ethidium bromide at 3 V/cm for 18 h at 4 ℃. DNA was transferred overnight to a charged nylon membrane (Hybond-XL, Amersham) in alkaline buffer by capillary blotting. Membranes were prehybridized at 37 ℃ for 4 h in 1M NaCl, 1% SDS, 10% dextran sulfate, 5 mM Tris [pH 7.5], 100 μg/ml of denatured salmon sperm DNA and 25% formamide. rDNA 5'NTS probes were labeled by random priming and added directly to the prehybridization solution. After 18 h membranes washed 3 times in 2X SSC/1% SDS solution for 15 min each at 42 ℃, and

once in 0.4X SSC/0.1% SDS solution for 15 min at 42 ℃. Blot were exposed to X-ray film with an intensifying screen at -70 ℃ or analyzed with a phosphorimager.

Alkaline gel electrophoresis

Alkaline gel electrophoresis was performed to examine the replication initiation and elongation under HU treatment. Wild type CU428 and ORC1 knockdown cells were starved overnight to synchronize in G1 phase, and then released into medium containing 20 mM HU. Genomic DNA was isolated by phenol-chloroform extraction as described above from cells harvested at indicated time points under HU treatment. Sixty μg of genomic DNA was loaded in a 1% alkaline gel (40 mM NaOH, 2 mM EDTA at pH 8.0) and separated by electrophoresis in the alkaline buffer (40 mM NaOH, 2 mM EDTA) at 1.5 V/cm for 20 h at 4 ℃ with buffer recirculation to resolve nascent-strand replication intermediates. After electrophoresis, DNA was transferred to a charged nylon membrane (Hybond-XL, Amersham) by capillary blotting and hybridized to the rDNA 5'NTS fragment that was radiolabeled with [α-^{32}P]-dATP as described above.

DNA fiber analysis

Tetrahymena strains CU428 and ORC1-KD were cultured in 2% PPYS media to the density of 1.5x10^5 cell/ml. Cells were pulse labeled with 400 μM IdU (Sigma) at 30 ℃ for 10 min. The media was removed and cells were washed once with 1X PBS. Cells were resuspended in pre-warmed fresh media with 100 μM CldU (MP Biomedicals) and labeled for 10 min. After two washes with PBS, the cell density was adjusted to 1x 10^6 cells/ml. Preparation and immunostaining of DNA fibers was performed as described previously described (Chastain et al, 2006; Schwab &

Niedzwiedz, 2011; Stewart et al, 2012) with the following modifications. Briefly, after fixation and HCl treatment, slides were washed three times with 1X PBS, and blocked with 5% BSA in PBS for 30 min. Mouse anti-BrdU (1:50, Becton Dickson) and rat anti-BrdU (1:100, Accurate Chemical) antibodies in 5% BSA were then added onto slides. After 1 h incubation, the slides wash washed three times again with 1X PBS, and incubated for 30 min with secondary antibodies: Alexa Fluor 568 goat anti-mouse IgG (1:100, Invitrogen/Molecular probes) and Alexa Fluor 488 goat anti-rat IgG (1:100, Invitrogen/Molecular Probes). Finally, slides were washed three times with 1X PBS, dehydrated with an ethanol series, and mounted with SlowFade Gold antifade solution (Invitrogen). During immunostaining, all antibodies were diluted in 5% BSA in 1X PBS, all incubations were performed at 37 ℃, and all wash steps were done at RT. DNA fiber images were taken by a Nikon A1R+ confocal microscope with 600X magnification. Measurements of track length were performed with Nikon NIS-Elements software. Inter-origin distance was defined as the distance between the centers of two red segments in either green-red-green-red-green or green-red-gap-red-green tracks. Fork velocity was determined by measuring the length of the green segment in a red-green track. GraphPad Prism software was used to analyze the statistical significance, and the p-values shown in figures were determined by two-tailed unpaired t-test.

CHAPTER III

CHECKPOINT ACTIVATION OF AN UNCONVENTIONAL DNA REPLICATION PROGRAM IN *TETRAHYMENA*

Overview

The intra-S phase checkpoint kinase of metazoa and yeast, ATR/MEC1, protects chromosomes from DNA damage and replication stress by phosphorylating subunits of the replicative helicase, MCM2-7. Here we describe an unprecedented ATR-dependent pathway in *Tetrahymena thermophila*, in which the essential pre-replicative complex proteins, Orc1p, Orc2p and Mcm6p are degraded in hydroxyurea-treated, S phase-arrested cells. Global changes in chromosomes occur, including phosphorylation of histone H2A.X, deacetylation of histone H3, and an apparent decrease in DNA content. Most remarkably, the cell cycle rapidly resumes upon hydroxyurea removal, and the entire genome is replicated prior to replenishment of ORC and MCMs. While stalled replication forks can be elongated under these conditions, DNA fiber imaging revealed that most replicating molecules are derived from new initiation events. Furthermore, the sole origin in the ribosomal DNA minichromosome is inactive and replication appears to initiate near the rRNA promoter. The collective data are most consistent with an ORC-independent mechanism for replication initiation during the recovery from HU-induced replication stress.

Introduction

A major challenge of the cell cycle is to faithfully transmit chromosomes to daughter cells. This is accomplished through the replication and segregation of

chromosomes during the respective S and M phases. The integrity of chromosomes is under constant assault from extrinsic and intrinsic sources that directly damage DNA or generate roadblocks for the replication machinery. The resulting DNA damage and replication stress can irreparably harm chromosomes. Checkpoint pathways have evolved to combat these problems, arresting the cell cycle when thresholds are exceeded. The phosphatidylinositol-3-OH kinase family members ATM (Ataxia Telangiectasia Mutated) and ATR (ATM-and Rad3-related) function as apical kinases in signal transduction pathways that inhibit DNA replication and promote DNA repair (Cimprich & Cortez, 2008). ATM is activated by double strand breaks (DSBs) and arrests the cell cycle at the G1/S border, while ATR monitors replication stress and other types of DNA damage during S phase. ATR is recruited to exposed stretches of single strand DNA through association with its binding partner, ATRIP. A downstream target for ATR phosphorylation is MCM2-7, the replicative helicase. In response, DNA synthesis at active replication forks arrests or slows down, and new origin firing is suppressed (Cortez et al, 2004; Randell et al, 2010; Snaith et al, 2000). Once the source of stress is removed, new initiation events occur at late replicating or dormant origins (Ge et al, 2007; Ibarra et al, 2008; Levenson & Hamlin, 1993).

While the fundamental components of checkpoint pathways are conserved, eukaryotes exhibit a wide range of responses to DNA damage. For example, hydroxyurea (HU) inhibits initiation from late firing origins and slows elongation of existing replication forks in *S. cerevisiae* (Alvino et al, 2007). In contrast, while fork elongation is suppressed by RAD3/ATR in *S. pombe,* most late firing origins are

regulated by a checkpoint-independent mechanism (Mickle et al, 2007). Meanwhile, mammalian ATR arrests both replication initiation and elongation (Feijoo et al, 2001; Heffernan et al, 2002). Alternative repair mechanisms, such as error prone DNA synthesis and homologous recombination are enlisted to varying degrees across the eukaryotic lineage. *Arabidopsis thaliana* elicits a unique checkpoint response in which double strand breaks do not obligatorily arrest the cell cycle. Instead, the ATR regulated, plant-specific transcription factor, SOG1, activates an alternative DNA replication program involving genome-wide endoreplication (Adachi et al, 2011).

In this study, we explore the intra-S phase checkpoint response in *Tetrahymena thermophila*. As a representative of the Ciliophora lineage, *Tetrahymena* contains two nuclei within a single cytoplasm: the diploid germ line micronucleus and the polyploid (45 C) somatic macronucleus (Karrer, 2012). The transcriptionally silent micronucleus contains all of the genetic information that is transmitted from parent to progeny during the sexual phase of the life cycle. It contains five chromosome pairs, and undergoes conventional mitosis and meiosis. The actively transcribed polyploid macronucleus confers the cellular phenotype and contains ~17,000 chromosomes that randomly segregate at each cell division. The macronucleus is destroyed in mating progeny, and a new macronucleus is generated by extensive processing of germline precursor chromosomes. The ~180 unique macronuclear chromosomes endoreplicate to a copy number of 45 C, and the 21 kb ribosomal DNA (rDNA) minichromosome is amplified to ~9000 C.

Macronuclear chromosomes lack centromeres and the inherent imprecision of amitosis generates genic imbalances. Remarkably, macronuclear chromosome copy number is maintained in a narrow range. 'Excess' DNA is eliminated in the form of chromatin extrusion bodies (Bodenbender et al, 1992) and macronuclear chromosomes re-replicate when copy number falls below an acceptable minimum (Doerder et al, 1981). Although the fundamental components for replication initiation (ORC, MCMs, Cdt1) and the DNA damage/replication stress checkpoint response (ATR, Rad51, gamma H2A.X) are conserved in *Tetrahymena*, their roles in genome maintenance are only partially understood.

We previously identified a caffeine-sensitive DNA damage/replication stress checkpoint pathway that is activated by hydroxyurea (HU) and methylmethanesulphonate (MMS) (Yakisich et al, 2006). Inhibition of this pathway results in aberrant macronuclear division and micronuclear genome instability, consistent with a protective role for chromosomes. A single ATR gene was identified (TTHERM_01008650); however, no obvious ATM candidates were detected (*Tetrahymena* Genome Database, www.ciliate.org). ATR is required for the reorganization of chromosomes during meiosis as well (Loidl & Mochizuki, 2009).

Our analysis of an ORC1 knockdown strain has provided new insights into the regulation of MCM2-7, a major target of ATR (Lee et al, 2015). Like the *S. cerevisiae* orc2-1 mutant (Shimada et al, 2002), a moderate reduction in *Tetrahymena* Orc1p induces genome instability, but fails to trigger an intra-S phase checkpoint response (Lee et al, 2015). In contrast to the budding yeast mutant, replication initiation is unaffected in

the *Tetrahymena* ORC1 knockdown. Instead, the rate of replication fork elongation decreases and Mcm6p levels are reduced, suggesting that the replicative helicase is rate limiting. Since the MCM complex is much more abundant than ORC in other eukaryotes (Takahashi et al, 2005), this fork elongation defect was unanticipated. Moreover, while moderate reductions in pre-replicative complex (pre-RC) components are poorly tolerated during the vegetative cell cycle, ORC and MCM levels oscillate to a much greater degree during development. Paradoxically, these proteins increase in abundance early in development when the DNA replication load is comparatively modest, and decline dramatically when the replication load increases (Lee et al, 2015). At low ORC concentrations, the rDNA origin is frequently bypassed, raising the possibility that alternative initiation sites (cryptic origins) and/or unconventional mechanisms are called into play.

In the work presented here, we document an unprecedented checkpoint response to HU treatment that begins with the targeted degradation of ORC and MCM subunits. We provide evidence for alterations in macronuclear chromosomes that include global deacetylation of histone H3, and manifest as a time-dependent decrease in DNA content in S phase arrested cells. More remarkably, upon HU removal, DNA synthesis resumes and the entire genome is duplicated prior to replenishment of ORC and MCMs. The rDNA minichromosome is replicated, although its ORC-dependent origin is inactive. Non-rDNA chromosomes also initiate bidirectional DNA replication prior to ORC replenishment. These findings argue that a novel program is activated to support

genome-wide DNA replication under conditions in which ORC and MCM proteins are rate limiting.

Results

HU and MMS trigger unconventional checkpoint responses

The DNA damage/replication stress checkpoint response is found throughout the eukaryotic lineage. While the apical kinase, ATR, is conserved, the downstream pathways can deviate in significant ways. *Tetrahymena* provides an opportunity to explore this biological diversity, both as an early branching eukaryote, and as a bi-nucleate organism with conserved and novel mechanisms for DNA replication and chromosome segregation. As previously reported, HU and MMS, arrest cell cycle progression and activate a DNA damage/replication stress checkpoint response in *Tetrahymena*, including induction of the double strand break repair protein, Rad51p (Figure 3.1A, left panel) (Yakisich et al, 2006). Rad51 accumulation was inhibited by the addition of caffeine, consistent with the involvement of an apical PI3-like kinase.

Since MMS activates both ATM and ATR in mammalian species, we used centrifugal elutriation to distinguish between G1/S (ATM-like) and intra-S phase (ATR) checkpoint responses. A mid-log phase culture was subjected to centrifugal elutriation to obtain a pure G1 phase population. Harvested cells were treated immediately with HU or MMS, or the drugs were added 1 h later. After 4 h of treatment of G1 phase cells, the level of Rad51p was elevated by at least ten-fold for HU and two-fold for MMS compared to mock treated cultures (Figure 3.1A, right panel). In order to better monitor the induction of Rad51p, treated samples were monitored every hour after drug addition

Figure 3.1. Characterization of HU and MMS induced checkpoint responses. Western blot analysis of Rad51p for asynchronous log phase cultures (left panel) or elutriated G1 phase cells (right panel) treated for 4 h with 20 mM HU, 0.06% MMS, 1 mM caffeine, or in combination. Equivalent amounts of protein were loaded in each lane. Ponceau S staining was used to verify protein transfer and serve as a crude validation for equal protein loading prior to antibody probing. (B) G1/S and intra-S phase checkpoint analysis. Cells were synchronized at the G1/S border by centrifugal elutriation. 20 mM HU or 0.06% MMS were added immediately (G1 phase, left panel) or 1 h later (mid-S phase, right panel). Western blot analysis was performed with antibodies specific directed against Rad51p and Mcm6p. (C) Flow cytometry analysis of cell populations analyzed in B. The vertical red line demarcates the peak at the time of drug addition. The arrow in cultures treated with HU or MMS during S phase demarcates the newly formed peak at the G1 position. (D) Flow cytometry profiling during an extended HU treatment of S-phase cells. Left panel: mock-treated cells. Right panel: HU-treated cultures in which elutriated G1 cells were grown for 1 h prior to addition of 20 mM HU for 0-6 h. (E) Data from HU-treated mid-S phase cells. Overlay of flow cytometry profiles for mock-treated cells in S phase (red line, 1 h after G1 isolation) and G1+ G2 phase (green line, 2 h after G1 isolation) with cells cultured with HU for 4 h (blue line, HU treatment beginning 1 h after elutriation). Red arrows: newly formed peak at the G1 position in HU-treated cells. Red arrowhead: right shoulder for the cell population at time of HU addition (red profile) and 4 h late (blue profile).

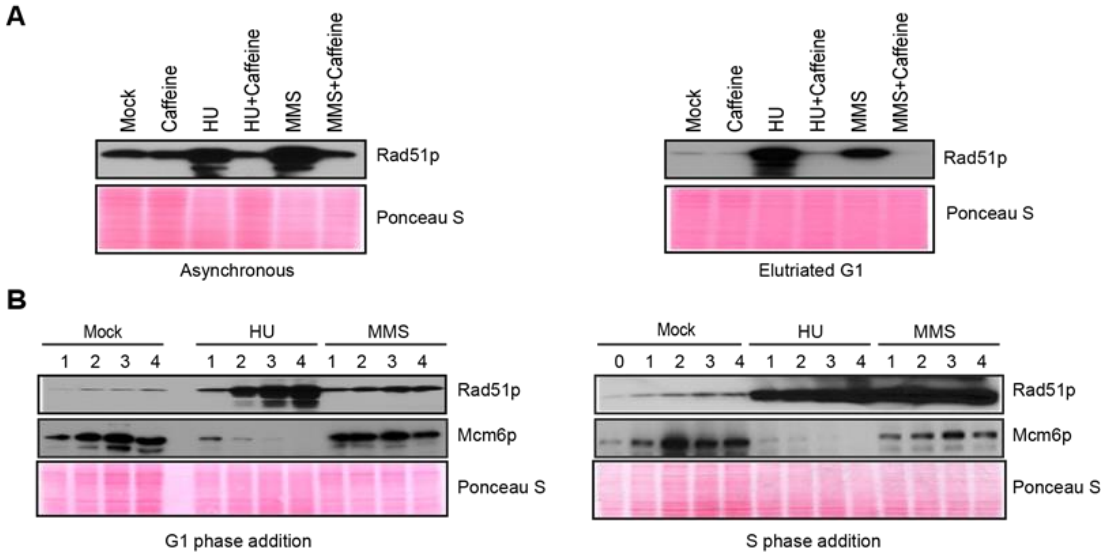
A
Mock
Caffeine
HU
HU+Caffeine
MMS
MMS+Caffeine
Rad51p
Ponceau S
Asynchronous
Elutriated G1
B
Mock
HU
MMS
Rad51p
Mcm6p
Ponceau S
G1 phase addition
S phase addition
C
Elutriated G1 phase addition
Elutriated S phase addition
Hours post elutriation
Hours post drug addition
D
G1+G2
S
G1
E

(Figure 3.1B, left panel). HU elicited a stronger response, presumably reflecting the high fraction of cells that progressed into S phase. To more selectively assess the S phase response, elutriated cells were grown to mid-S phase prior to drug addition (Figure 3.1B, right panel). HU and MMS induced Rad51p under both conditions; however, the MMS response was much more pronounced compared to G1 treated cells. These data suggest that DNA damage is largely averted in G1-treated cells, possibly due to the activation of an ATM-like (G1 arrest) checkpoint response.

Flow cytometry confirmed that DNA synthesis was rapidly inhibited by both drugs regardless of the time of drug addition (G1 versus S phase). The DNA profile for G1 arrested cells was constant over the examined 4 h interval (Figure 3.1C, left panel); however, the profile for S phase treated cells changed in an unanticipated way. An additional peak migrating at the G1 position appeared 1 h after HU addition and became more prominent over time (Figure 3.1C, right panel, arrow). The bimodal distribution suggested that two distinct sub-populations were generated, one arrested in S phase and the other transforming towards an apparent G1 DNA content. MMS-treated cells did not show this bimodal distribution (Figure 3.1C, right). Instead the S phase peak shifted to the left, suggesting that the DNA content of cells within the entire population was reduced. Both results were highly reproducible (n=8). This temporal change in replication profiles was recapitulated in cells synchronized by starvation and re-feeding, with the following variation: bimodal peaks were occasionally observed in MMS-treated S phase cells (Figure 3.2, arrow). The data suggest that that global changes occur at the chromosome level in in S phase arrested cells.

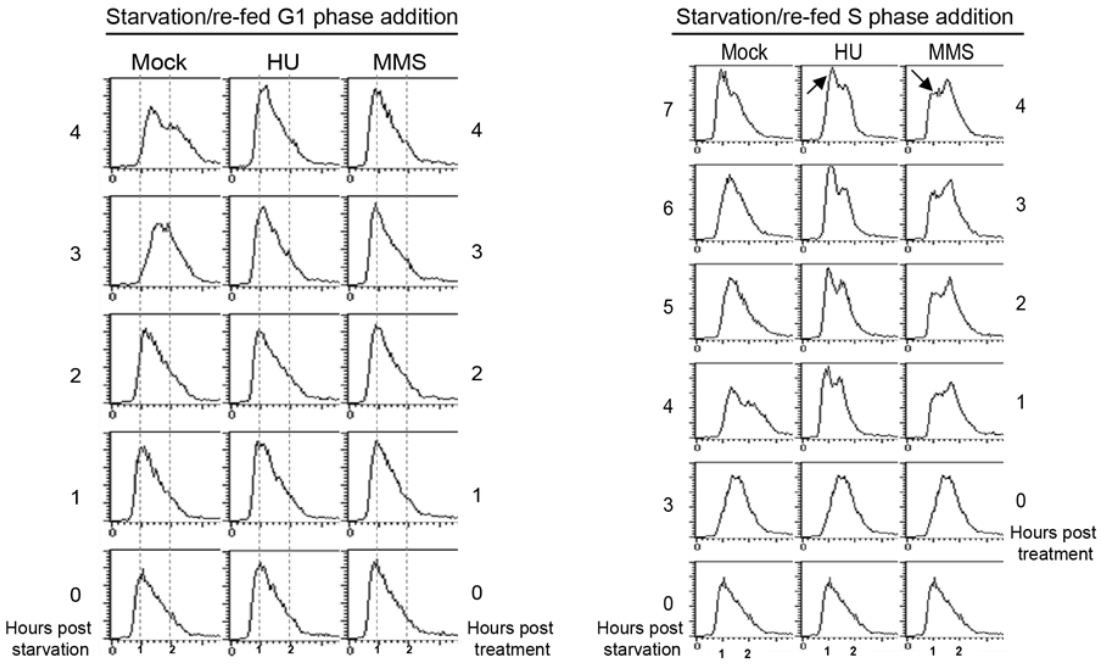

Figure 3.2. Flow cytometry profiles of cells synchronized by starvation and re-feeding (A) Mid- log phase cultures were placed into starvation media (10 mM Tris, pH 7.4) for 12 h to synchronize cells at the G1/S border. 5% PPYS was added to resume cell cycle progression. 20 mM HU or 0.06% MMS was added at the time of re-feeding or 3 h later (B), when cells were in mid-S phase, and DNA content was analyzed by flow cytometry. The arrow in panel B points to the G1 peak generated over time in HU and MMS-treated cells. Note the broad G2 peak that formed 4 h after re-feeding in mock controls did not appear throughout the entire HU or MMS time course. In other representative experiments, MMS-treated cells did not generate a pronounced G1 shoulder. Instead, the entire DNA content profile shifted to the left (lower apparent DNA content).

To investigate this phenomenon further, HU studies were expanded on elutriated cells. Mock-treated G1, S and G2 phase populations (Figure 3.1D, left panel) were used as reference points to evaluate whether the appearance of a G1 peak in HU-treated S phase cells was preceded by the formation of a G2 peak. The data collected over 6 h clearly demonstrate that DNA content does not increase during prolonged exposure to HU (Figure 3.1D). They suggest that the G1 peak is generated without completion of a normal S phase. For better comparison, FACS profiles of mock-treated S and G1+G2 populations were overlaid with the 4 h HU treated sample in another independent experiment (Figure 3.1E). Two features stand out. First, the right shoulder of the HU-treated sample (blue profile) aligned precisely with the right shoulder of the S phase peak (red profile; T=0 h for HU addition in S phase), indicating that that DNA content did not increase in a subpopulation of cells. Second, the peak and left shoulder of the HU-treated profile (blue profile, arrows) aligned with the peak and left shoulder of the G1 profile (green profile), consistent with the idea that cells did not simply exit S phase and divide precociously since no sub-G1 peak was observed. A subsequent flow cytometry profiling at 10 minute intervals showed no evidence for the formation of a G2 peak (Figure 3.3). Consistent with all previous experiments, the left shoulder of the DNA profile (lower DNA content) increased in prominence in a time-dependent manner, and the position of the right shoulder (higher DNA content) was unchanged. The collective data show that the apparent DNA content of HU-treated *Tetrahymena* neither remains constant nor gradually increases, as has been reported for *S. pombe*

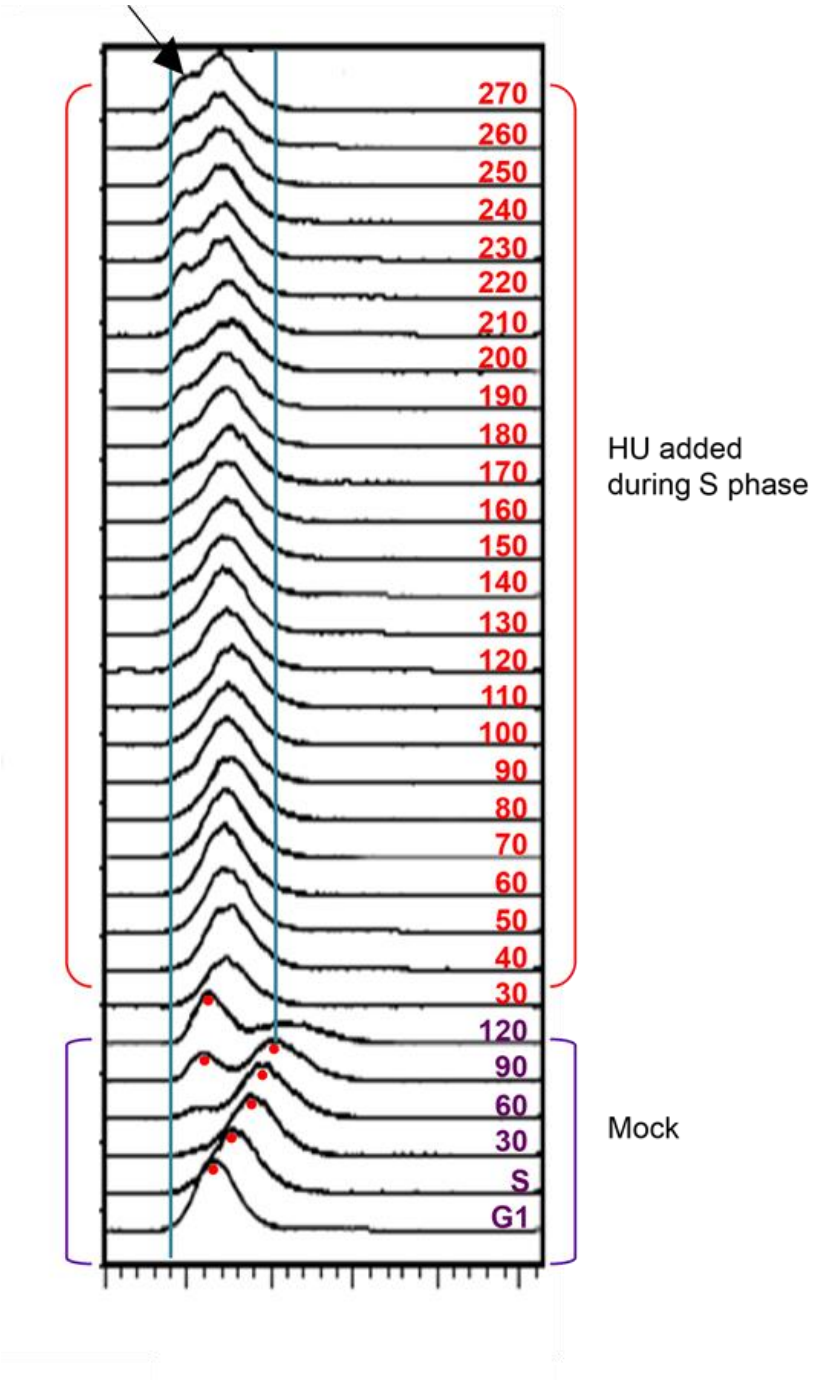

Figure 3.3. Flow cytometry analysis at 10 min intervals. Cells were synchronized at the G1/S border by centrifugal elutriation, and 20 mM HU was added 1 h later, when cells were in mid-S phase (right panel). DNA samples were collect for flow cytometry analysis. Note the pronounced G2 peak in mock-treated cells that appears after the time of HU addition (30/60/90 min). Whereas a G1 peak gradually formed in the HU-treated cells, none of the 25 samples in this time course (30-270 min) exhibited an increase in DNA content after HU addition.

(Meister et al, 2007) and *S. cerevisiae* (Alvino et al, 2007), respectively, but that macronuclear DNA content decreases over time.

HU and MMS do not promote precocious cell division or macronuclear chromatin elimination

Two mechanisms have been previously shown to decrease DNA content during the *Tetrahymena* vegetative cell cycle: asymmetric macronuclear division (Morrison et al, 2005; Smith et al, 2004) and the elimination of 'excess' macronuclear DNA in the form of chromatin extrusion bodies (CEBs) (Cleffmann, 1980). Multiple criteria were used to examine these possibilities in HU or MMS-treated S phase cells. We first monitored cell number. In contrast to mock-treated controls, no increase in cell density was observed in HU or MMS treated cultures (Figure 3.4A). Second, unlike mock-treated cells, cytokinesis was not observed in DAPI-stained, HU-treated cells (Figure 3.4B). By analogy, HU + caffeine treated wild type strains, as well as mock or HU-treated TIF1 (ATR defective) and ORC1 (ATR competent) knockdown mutants continue to divide and exhibit a high frequency of aberrant macronuclear division (Lee et al, 2015; Yakisich et al, 2006). Third, HU-treated S phase cells showed a gradual, steady decline in apparent DNA content (Figure 3.4C, red graph), while the DNA content in mock-treated controls oscillated in conjunction with cell division (Figure 3.4C, blue graph). Fourth, consistent with the absence of cell division, side scatter analysis of flow cytometry profiles detected a substantial increase in the complexity/granularity in the cytoplasm of HU-treated cells (Figure 3.4D red profile; Figure 3.5) compared to mock-treated controls (blue profile). The increase in macromolecular density of HU-treated

Figure 3.4. Physical characterization of cells in mock, 20 mM HU and 0.06% MMS treated cultures. A G1 cell population was obtained by centrifugal elutriation and propagated for 1 h (mid-S phase) prior to the addition of HU or MMS. (A) Cell density analysis by direct counting on a hemocytometer. (B) Visualization of a cytokinetic furrow in fixed DAPI-stained cells. Approximately 40% of mock-treated cells generated a cytokinetic furrow 2 h after G1 phase isolation (1 h after HU or MMS addition in treated samples). T=4 h, mock versus HU: (student T test) two-paired P value 0.0002); T=4 h, mock versus MMS: (student T test) two-paired P value <0.0001). (C) Plot of DNA content (PI, propidium iodide) in mock (blue) and HU-treated (purple) cells as a function of exposure time. Elutriated G1 phase cells were treated with 20 mM HU 1 h after isolation (vertical arrow, mid-S phase addition) and samples were collected every 30 min for 4.5 h. 30,000 cells were scored at each time point. (D) Statistical analysis of flow cytometry side scatter (SSC) in mock (blue) and HU-treated (purple) cells. HU was added during S phase and samples were collected at 1 h intervals. The results of three independent experiments (n=3) are compiled. (E) Visual representation of flow cytometry side scatter (SSC) and forward scatter (FSC) in cells synchronized by centrifugal elutriation. Controls: mock-treated G1 cells (T=0 h after elutriation), mock-treated S phase cells (T=1 h after elutriation), and mock-treated cells 6 h after elutriation. Experimental samples: HU addition for 6 h beginning at T=0 h (HU/G1 phase), or for 6 h beginning at T=1 h (HU/S phase). The higher complexity of HU-treated cells was not observed at any stage of the cell cycle in untreated controls (see Figure 3.5). (F) Left panel: the area for 100 cell images was measured in mock and HU-treated cells. The average area was determined and subjected to statistical analysis. A 30% increase in cell size was observed in HU-treated cells (T=8 h, mock versus HU: (student T test) two-paired P value <0.0001). Right panel: representative micrograph illustrating the size difference between mock-treated S phase and S phase cells arrested with HU for 8 h. (G) Production of macronuclear extrusion bodies. DAPI staining was used to identify cells with DNA masses that were not associated with the micro- or macronucleus (macronuclear extrusion bodies). (T=4 h, mock versus HU. Student T test, two-paired P value: 0.2249).

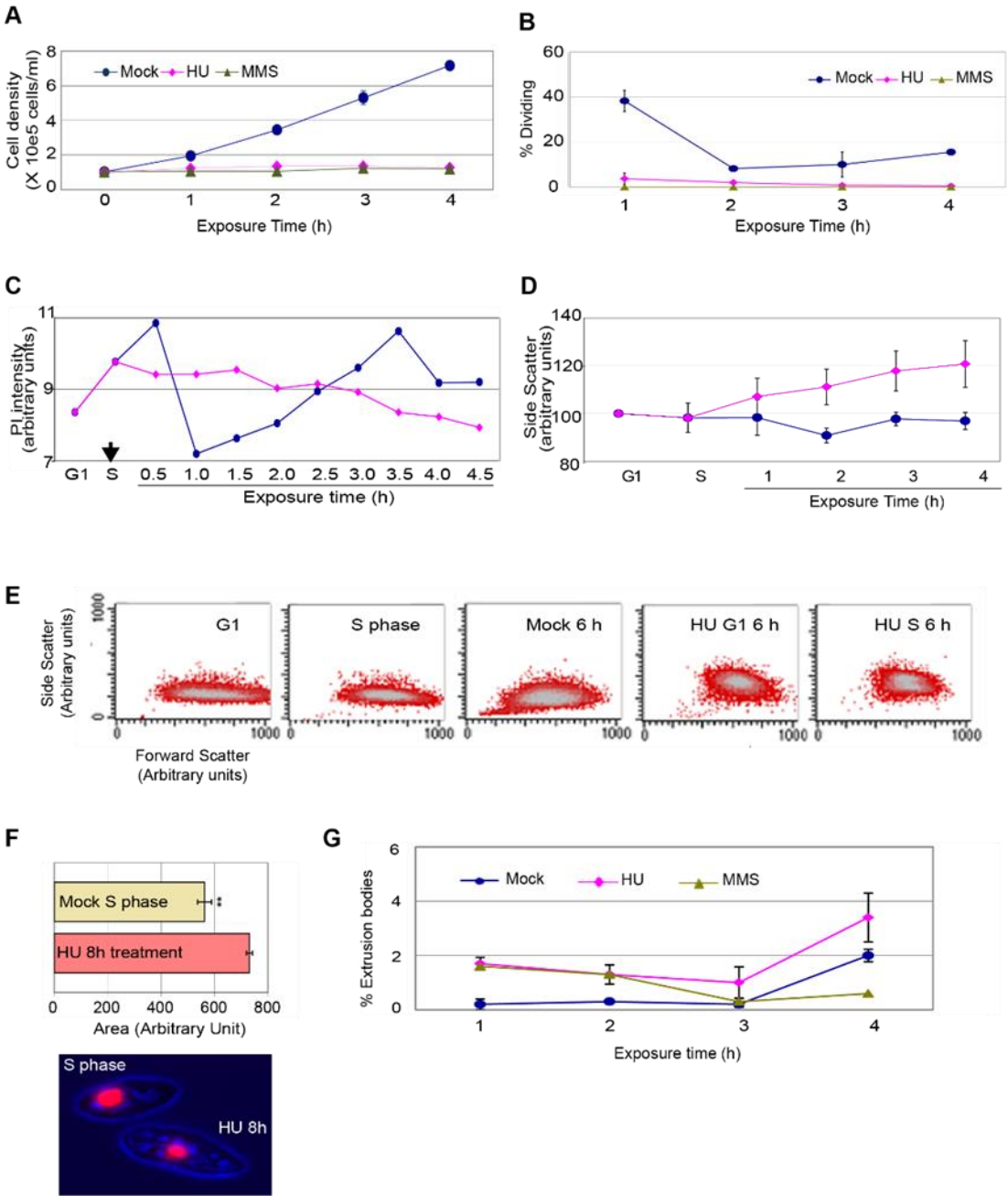
A
Cell density (X 10e5 cells/ml)
Mock
HU
MMS
Exposure Time (h)
B
% Dividing
Exposure Time (h)
C
PI intensity (arbitrary units)
G1
S
Exposure time (h)
D
Side Scatter (arbitrary units)
Exposure Time (h)
E
Side Scatter (Arbitrary units)
G1
S phase
Mock 6 h
HU G1 6 h
HU S 6 h
Forward Scatter (Arbitrary units)
F
Mock S phase
HU 8h treatment
Area (Arbitrary Unit)
S phase
HU 8h
G
% Extrusion bodies
Exposure time (h)

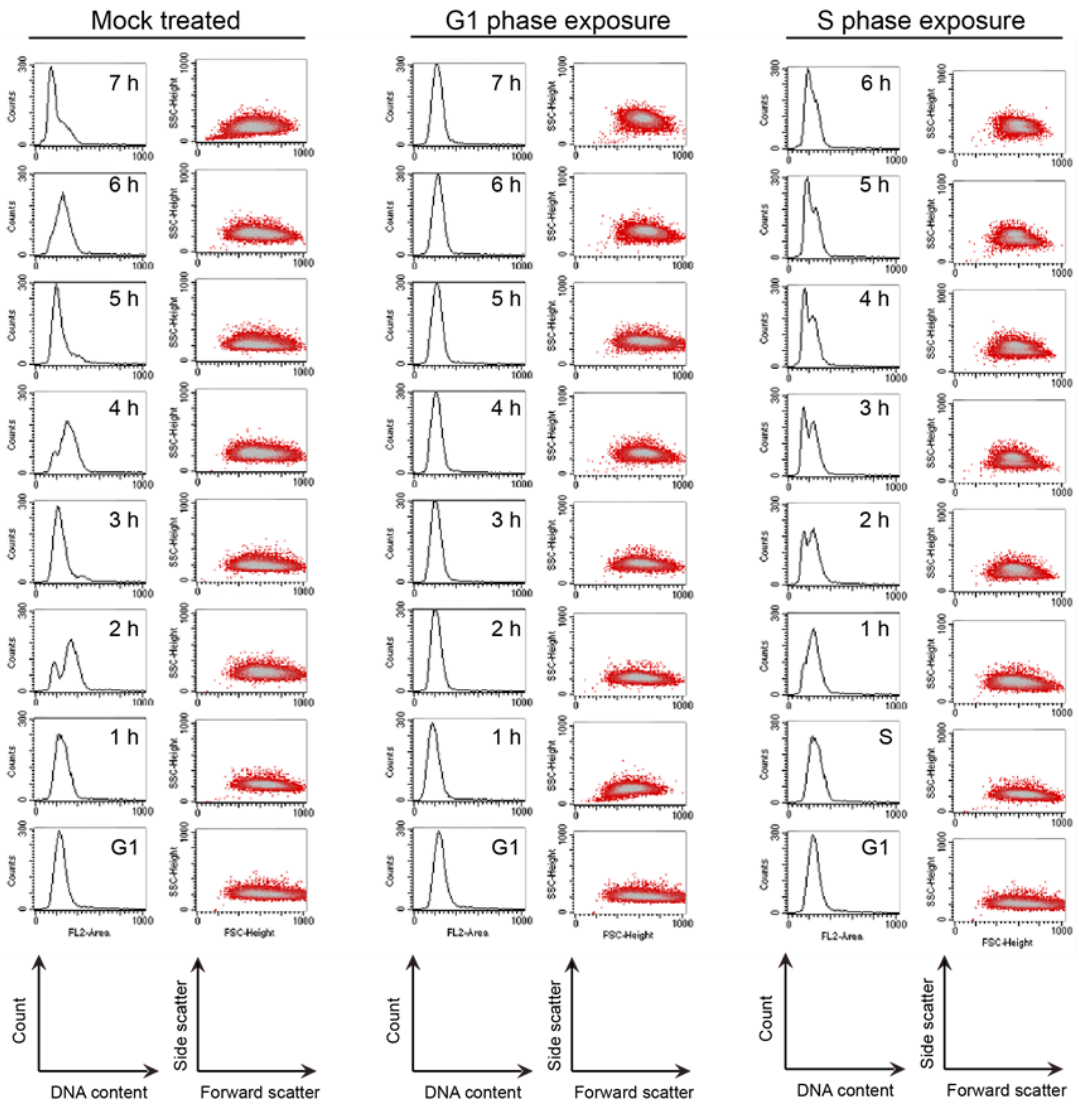

Figure 3.5. Forward and side scatter flow cytometry parameters. (A) Mock, (B) G1 HU-treated, and (C) mid-S phase HU-treated cells were subjected to flow cytometry analysis at hourly intervals. Flow cytometry analyses: left panel- DNA content (PI intensity), right panel- plot of SSC (Y axis) versus FSC (X axis). HU treated cells exhibited an increase in SSC, regardless of the time of drug addition. A subset of these data are depicted in Figure 3.4E.

cells exceeded that of any stage in the cell cycle in mock-treated controls, and was not dependent on the time of HU addition (Figure 3.4E; Figure 3.5, G1 or S phase exposure to HU). Fifth, consistent with cell division arrest, the average size of HU-arrested cells was larger than mock-treated G2 phase controls (Figure 3.4F, $P < 0.0001$); however the average size of the macronucleus was equivalent in mock and HU-treated cells ($P = 0.1896$). Finally, DAPI staining revealed a modest, but statistically insignificant increase in the formation of chromatin exclusion bodies (CEBs) (Figure 3.4G). CEBs are generated to lower macronuclear DNA content without cell division (Bodenbender et al, 1992). A modest increase in CEBs cannot account for the large fraction of cells that exhibited an apparent decrease in DNA content. The collective data demonstrate that HU and MMS-treated *Tetrahymena* do not undergo cell division or adjust their DNA content through known ciliate-specific mechanisms.

Stabilization of nascent strands and down-regulation of histone H3 acetylation

Two additional mechanisms were considered to explain the observed change in apparent DNA content in S phase arrested cells: active degradation of DNA and global compaction of chromatin. DNA fiber analysis was used to examine DNA synthesis and determine the fate of pulse labeled DNA over time. As a starting point, we re-fed starved, G1-arrested cells with media containing HU for 4 h. HU-arrested cells were simultaneously pulse-labeled with IdU for 1-4 h, and DNA fibers were examined for incorporation of IdU into nascent strands. Whereas cells in an asynchronous population generated long IdU tracts after labeling for 20 min (Figure 3.6A, upper image, red tracts), no incorporation was detected in HU-treated cells, regardless of the timing or

duration of labeling (Figure 3.6A, middle (1 h IdU) and lower (4 h IdU) images). However, CldU was readily incorporated following HU removal (green tracts). We conclude that HU arrests replication forks rather than slows down the rate of fork progression.

To examine the fate of nascent strands in HU-treated cells, synchronized mid-S phase cells were pulse labeled with IdU for 10 min prior to the addition of HU, and DNA fibers were prepared 1 and 4 h after HU addition. As a control, cells were collected directly after IdU removal without HU treatment. Nascent strands were readily detected in DNA fibers from HU and mock-treated cells. The length of labeled tracts was measured in over 350 randomly chosen DNA fibers per sample condition. The median length of labeled DNA tracks did not decrease following HU addition, suggesting that the nascent strands were not actively degraded (Figure 3.6B). Visual inspection of microscope fields revealed that the overall density of labeled fibers was similar in mock and HU-treated cells. We conclude that nascent DNA strands are not selectively targeted for degradation in HU-treated cells. While this experiment does not rule out the possibility that DNA is degraded non-selectively, the rapid resumption of DNA synthesis following HU removal (see below, Figures 3.9-3.11, Figure 3.8) indicates that the overall integrity of chromosomes is maintained.

Phosphorylation of histone H2A.X occurs at stalled replication forks and is reliable marker for activation of the ATR checkpoint response (Cimprich & Cortez, 2008). Hyper-phosphorylation is associated with chromatin condensation, DNA fragmentation and apoptosis in metazoan cells (Talasz et al, 2002). As expected,

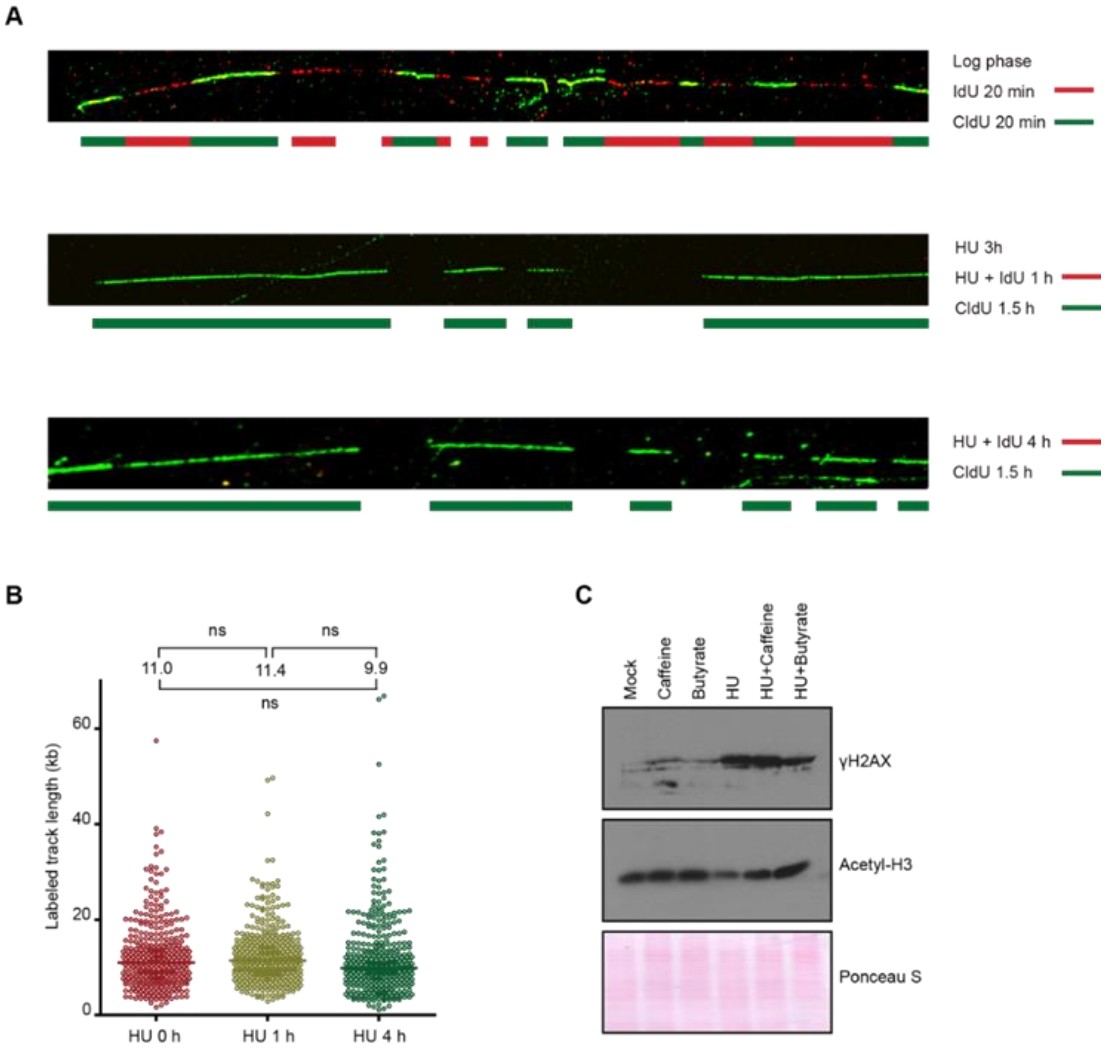

Figure 3.6. Effect of HU on DNA replication (nascent strand synthesis and stability) and acetylation of histone H3. (A) DNA fiber analysis in the presence or absence of HU. Cells were synchronized at the G1/S border by starvation and re-feeding, and cultured in the presence of 20 mM HU and 400 μM IdU for 4 h, or 20 mM HU for 3h, then 20 mM HU plus 400 μM IdU for 1h. HU and IdU were removed, and cells were further cultured for 90 min in media containing 100 μM CldU. DNA fibers were visualized as described in Materials and Methods (IdU, red; CldU, green). As a control, an untreated log phase culture was sequentially pulse labeled for 20 min in media containing IdU and CldU. (B) Mid-S phase cells were pulse labeled with 100 μM CldU for 10 min prior to the addition of HU, and DNA fibers were prepared 0, 1 and 4 h after HU treatment. The length of individual labeled DNA tracts was plotted and the median tract length was calculated as subjected to statistical analysis. (C) Western blot analysis with phospho-gamma H2A.X and acetylated histone H3 antibodies. Synchronized starved/re-fed cells were treated for 4 h with the indicated drug or drug combination (20 mM HU, 1mM caffeine, 50 mM sodium butyrate) and cells were lysed in SDS loading buffer. Twenty micrograms of protein was loaded in each lane. Ponceau S staining was used to verify protein transfer and served as a crude validation for equal protein loading prior to antibody probing.

phosho-gamma H2A.X levels were elevated HU-treated *Tetrahymena* (Figure 3.6C). Surprisingly, caffeine, an ATR inhibitor, did not suppress H2A.X phosphorylation; however, the histone deacetylase inhibitor, sodium butyrate largely inhibited this response (Figure 3.6C, gamma H2A.X; Figure 3.7D, Rad 51p). To explore this further, we examined histone H3 acetylation using a modification-specific monoclonal antibody. Histone H3 acetylation levels were depressed in HU-treated cells (Figure 3.6C; Figure 3.7C). This response was blocked when sodium butyrate was added at the time of HU addition. Histone deacetylation has been shown to promote compaction of human chromosomes by disrupting interactions with the nuclear envelope (Malik et al, 2014). More importantly, since acetylation promotes origin activation in other species, including late firing and dormant replication origins (Aggarwal & Calvi, 2004; Aparicio et al, 2004; Mantiero et al, 2011), the global deacetylation of *Tetrahymena* histone H3 might suppress ORC-dependent origins of DNA replication.

ORC and MCM proteins are degraded during HU-induced replication stress

In recently published work we provided evidence for the co-regulation of ORC and MCM complexes (Lee et al, 2015). Using macronuclear gene replacement, for example, we discovered that a 5-fold reduction in Orc1p leads to a comparable decrease in the steady state level of Mcm6p and Orc2p. Furthermore, under normal physiological conditions, ORC and MCM protein levels coordinately increase during the early stages of wild type development in conjugating cells, and are subsequently down regulated during the late stages of endoreplication in exconjugants.

To better understand the *Tetrahymena* checkpoint response, ORC and MCM protein levels were examined in HU and MMS treated cell synchronized at the G1/S border by centrifugal elutriation or during subsequent mid-S phase drug addition (Figure 3.7). The abundance of the MCM complex was relatively constant in MMS-arrested *Tetrahymena* (Figure 3.1B, G1 and S phase drug addition; Figure 3.7B, lower panel). These results are consistent with studies in yeast and higher eukaryotes, where MCM proteins are reversibly phosphorylated to transiently slow or arrest replication forks and inhibit new origin firing (Ibarra et al, 2008; Komata et al, 2009).

HU-treated *Tetrahymena* elicited a very different checkpoint response. Mcm6p levels rapidly declined in HU-arrested cells (Figure 3.1B, G1 and S phase drug addition; Figure 3.7B). Moreover, Orc1p (Figure 3.7C; Figure 3.9C, HU arrest) and Orc2p (Figure 3.9C, HU arrest) were degraded in a time-dependent manner. The degradation of Orc1p was inhibited by the addition of caffeine to HU treated cells (Figure 3.7D), implicating ATR in the regulation of ORC. Rad51p was modestly induced in HU + caffeine treated cells, consistent with ATR involvement (Figure 3.7D). While the Mcm6p signal is weak in the HU+ caffeine treated sample, the collective data indicate that ORC and MCM proteins are co-regulated in response to the DNA damaging agents, HU and MMS. The HU and MMS responses clearly differ, suggesting that the DNA damage and replication stress pathways bifurcate downstream of ATR. Two questions immediately arose: are HU-treated cells competent to re-enter the cell cycle and faithfully replicate their chromosomes? What events must occur for ORC and MCM-depleted cells to progress through S phase?

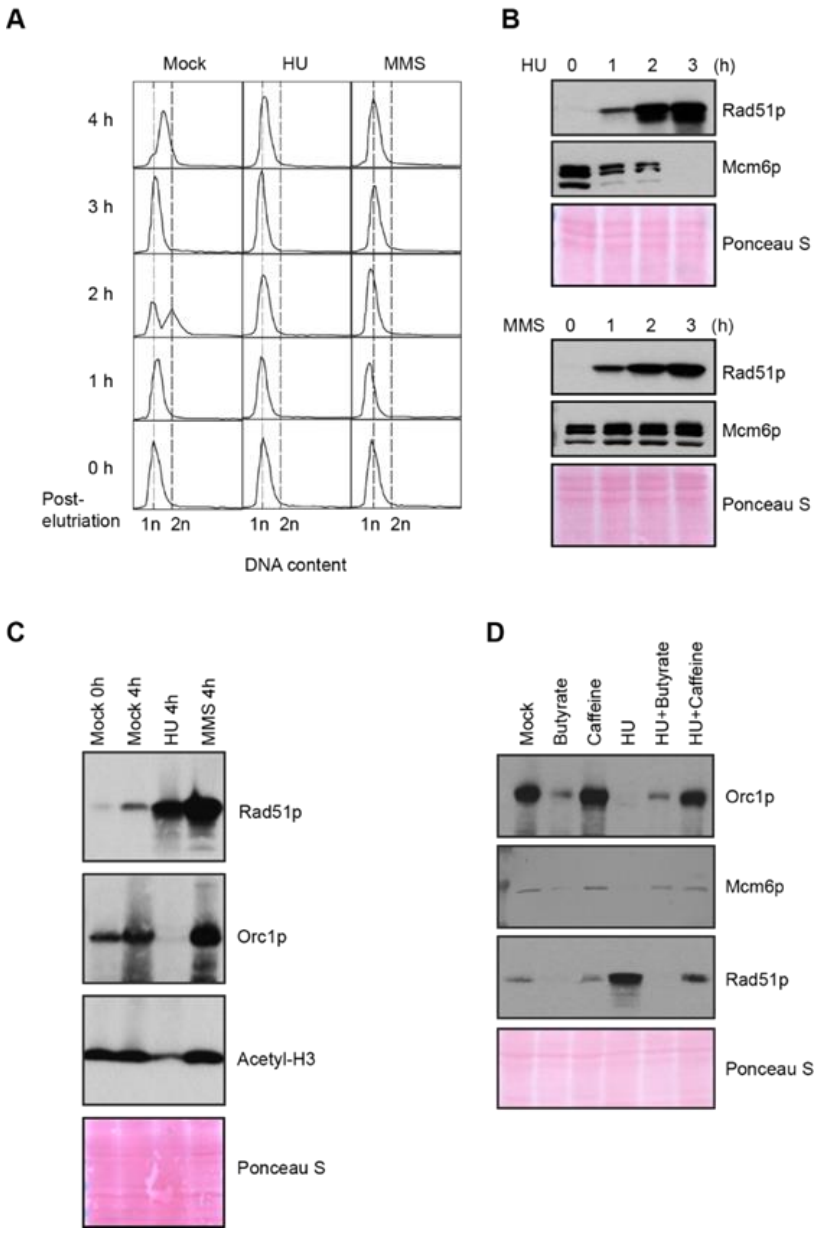

Figure 3.7. Effect of HU and MMS on pre-RC proteins in treated G1 cultures. HU (20 mM) or MMS (0.06%) were added immediately to an elutriated G1 phase population and cells were cultured for 4 h. (A) Flow cytometry analysis at 1 h intervals. (B) Western blot analysis with Rad51p and Mcm6p antibodies. Twenty micrograms of protein was loaded in each lane, as determined by Lowry protein assay, and Ponceau S staining was used to assess protein transfer prior to antibody probing. (C) Western blot analysis with Rad51p, Orc1p and acetylated histone H3 antibodies. Cells were synchronized by starvation and re-feeding, and cultured for 4 h +/- HU. (D) Western blot analysis of cells treated with 20 mM HU in the presence or absence of ATR and histone deacetyltransferase inhibitors (1 mM caffeine and 50 mM sodium butyrate, respectively). Synchronization was achieved by starvation and re-feeding, and cells were subsequently cultured for 4 h. Western blot analysis with antibodies directed against Orc1p, Mcm6p and Rad51p.

DNA replication precedes ORC and MCM replenishment during HU recovery

The HU induced decrease in Orc1p and Mcm6p was much greater than changes that occur under selective pressure in the ORC1 knockdown mutant (Lee et al, 2015). This precipitous drop in ORC and MCMs raised the possibility that origin licensing might be irreparably compromised in HU-treated cells. We first examined this possibility on cells that had transitioned past the G1/S border prior to cell cycle arrest. Synchronized S phase cells were exposed to HU for 4 h, and subsequently released into drug free media (recovery period). Flow cytometry was used to monitor subsequent cell cycle progression, and western blotting assessed the abundance of Rad51p and Mcm6p. Remarkably, the recovering cell population quickly resumed DNA replication and completed S phase within 2 h (Figure 3.8A), prior to the replenishment of Mcm6p (Figure 3.8B, 0-2 h, no caffeine). These cells replicated, divided, and entered the second S phase without delay, as Mcm6p levels were eventually restored (Figure 3.8B, 4 h, no caffeine).

DNA synthesis and cell cycle progression during the recovery phase was not dependent on inhibition of ATR, although the first cell cycle proceeded more quickly in caffeine-treated cells (Figure 3.8A). Whereas Rad51p levels gradually declined during the recovery period, Rad51p remained elevated when caffeine was added (Figure 3.8B). Hence, while activation of ATR leads to degradation of the replicative helicase subunit, Mcm6p (Figure 3.1B), new synthesis of Mcm6p is not required for subsequent genome-wide replication. Moreover, suppression of ATR is not required for new DNA synthesis,

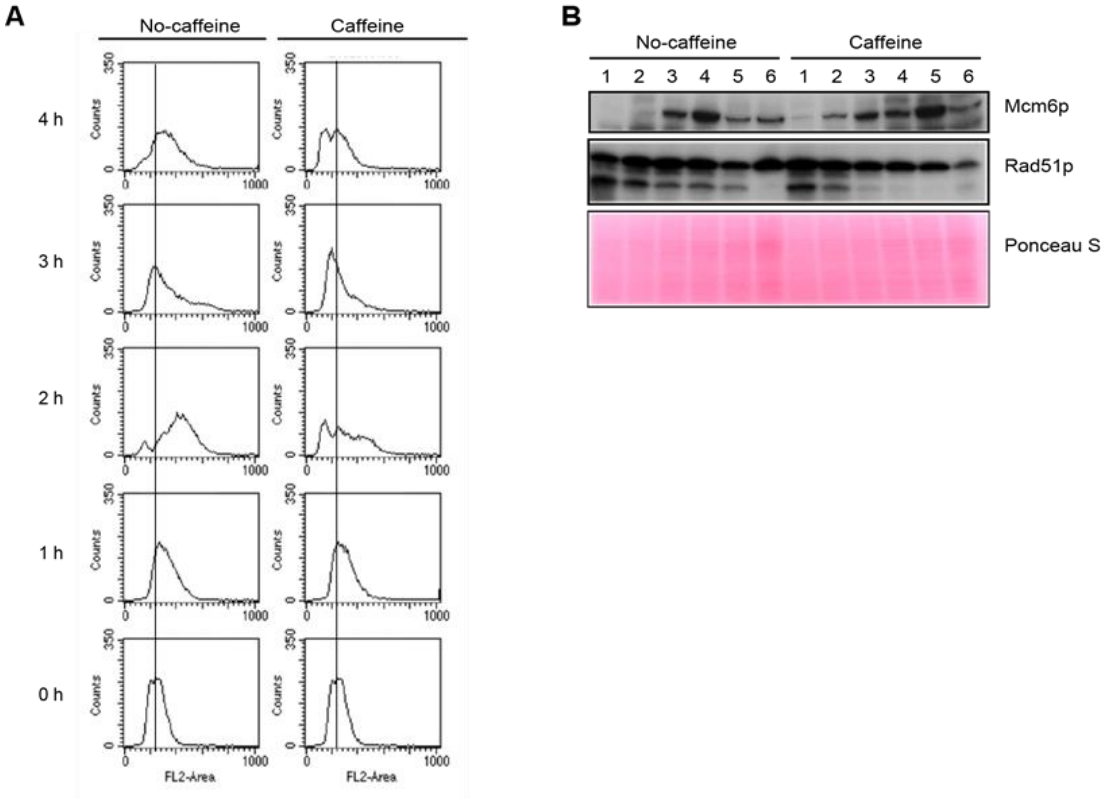

Figure 3.8. Recovery from HU-induced cell cycle arrest. Elutriated cells were allowed to progress to mid-S phase and 20 mM HU was added for 8 h. Cells were washed twice and resuspended in HU-free media supplemented with (+) or lacking 1mM caffeine. Samples were taken at 1 h intervals. (A) Flow cytometry analysis of HU-arrested and released cells. (B) Western blot analysis of Rad51p and Mcm6p. Lower panel: Ponceau S staining of PVDF membranes prior to antibody probing.

in spite of the high levels of damage sustained during HU exposure (Figure 3.6C, phospho-gamma H2A.X).

We next addressed the requirements for ORC during the first S phase following HU removal. G1 arrested cells were used as the starting point for this analysis for two reasons. First, since Orc1p levels naturally cycle in an unperturbed cell population (Figure 3.9B, mock-treated control), peaking at G1 and disappearing by late S phase, HU addition to G1 synchronized cells would eliminate this variable. Second, by adding HU to G1 phase cells, we could monitor the entire S phase immediately following drug removal. Mock-treated starved/re-fed cells generated a characteristic DNA cell cycle profile (Figure 3.9A), in which cells enter S phase and down regulated Orc1p within 90 min, and subsequently synthesize new Orc1p during G2 phase (180 min) (Figure 3.9B). The flow cytometry profile of HU-treated and released cells was indicative of a healthy synchronous cell cycle. DNA content increased within 60 min after HU removal and a new G1 phase population appeared prior to the replenishment of ORC (Figures 3.9A and 3.9B, T= 120 min, T= 150 min). In a separate experiment, we probed for Orc2p. Orc1p and Orc2p were down regulated in HU-treated cells (Figure 3.9C). Like Orc1p, Orc2p levels did not increase prior to the completion of the first S phase during the recovery from HU-induced genotoxic stress. The unexpected behavior of pre-RC components raised the possibility that replication might occur by an ORC-independent mechanism.

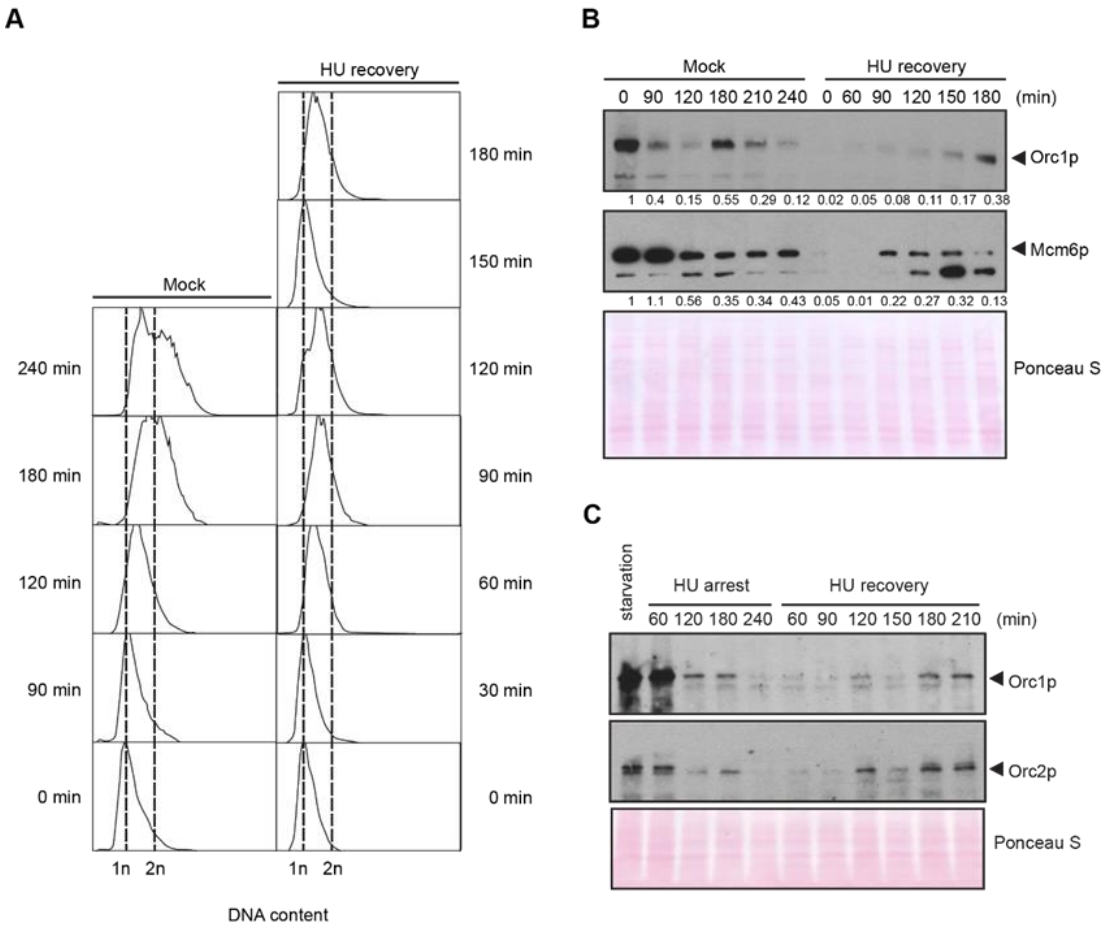

Figure 3.9. Kinetics of DNA replication and pre-RC replenishment following HU removal. A G1 population, synchronized by starvation and re-feeding, was treated with 20 mM HU for 4 h in 2% PPYS media. Cells were washed twice with HU-free media, re-suspended in their original volume and cultured for an additional 3 h in media lacking HU. Mock-treated, starved/re-fed cells were used as a control. (A) Flow cytometry analysis of mock-treated cells (left panel, starved/re-fed cells) and HU-treated cells following removal of the drug (right panel, HU recovery). (B) Western blot analysis with Orc1p and Mcm6p antibodies. Note the cell cycle oscillation of Orc1p in mock-treated cells, and the absence of Orc1p replenishment prior to completion of the first cell cycle in the HU recovery population. Twenty micrograms of protein was loaded in each lane, as determined by Lowry protein assay, and Ponceau S staining was used to assess protein transfer prior to antibody probing. (C) Western blot analysis of Orc1p and Orc2p levels during exposure to 20 mM HU in growth media (HU arrest), and following HU removal (HU recovery). Cells were synchronized by starvation and re-feeding. Twenty micrograms of protein was loaded in each lane.

The rDNA replication origin is inactive and is passively replicated in ORC-depleted cells

The *Tetrahymena* rDNA minichromosome (Figure 3.10A, schematic) serves as an excellent substrate to examine the effect of depleting ORC subunits. As shown previously, wild type strains initiate replication exclusively from nucleosome-free regions in the 5' non-transcribed spacer (NTS) in this palindromic 21 kb minichromosome (Figure 3.10A, Domain 1 and Domain 2) (MacAlpine et al, 1997). ORC recruitment to rDNA origins occurs by an unconventional mechanism. An integral RNA subunit of ORC, designated 26T RNA, undergoes Watson-Crick base pairing with type IA and IB elements, which are present at rDNA origins and absent in non-rDNA chromosomes (Donti et al, 2009; Mohammad et al, 2007). Mutations in 26T RNA disrupt ORC recruitment to Domain 1 and Domain 2 origins (Mohammad et al, 2007). Under these conditions, the rDNA origin is silenced on a subpopulation of cells, but this minichromosome is still replicated. Hence, a backup pathway (and possibly a cryptic origin) exists, that can be readily monitored through the analysis of replication intermediate (RI) patterns.

Neutral/neutral (N/N) two-dimensional gel electrophoresis was used to assess rDNA origin activity in ORC-depleted cells during the recovery from HU-induced replication stress. The characteristic bubble-to-Y arc RI pattern was observed in the *HindIII* 5' NTS fragment from mock-treated S phase cells (Figure 3.10B, S phase, probe 1, arrowhead identifies the bubble arc). This pattern was not detected in ORC-depleted cells that had been released from the HU block. Instead, the predominant RI pattern that

Figure 3.10. Two-dimensional gel electrophoresis analysis of rDNA replication intermediates following removal of HU. Cells were synchronized at the G1/S border by starvation and cultured in growth media in the absence or presence of 20 mM HU. DNA was prepared from mock-treated starved cells, mock-treated S phase cells, and HU-treated cells at defined intervals following HU removal. (A) Upper diagram: schematic of the 21 kb rDNA minichromosome and location of relevant restriction sites and probes for Southern blot analysis. Macronuclear rDNA minichromosomes contain two copies of the rRNA coding region and adjacent 5' and 3 'non-transcribed spacer (NTS) regions in an inverted orientation. The 35S rRNA precursor encodes the 17S, 5.8S and 26S rRNAs (grey areas- mature RNA coding regions, black and white stippled areas- processed RNA precursor regions, hatched area- self-splicing 26S rRNA intron). Telomeric DNA repeats (vertical hashes) are present at chromosome termini. Blowup of the 1.9 kb 5 NTS. Thick arrow- rRNA promoter; grey ovals- position of phase nucleosomes in vegetative rDNA minichromosomes (Palen & Cech, 1984), black boxes- type 1 repeats. Domains 1 and 2 (thin arrows) are 430 bp imperfect tandem repeats with 230 bp nuclease hypersensitive regions. The positions of four probes for N/N and N/A 2D gel analysis are shown. Lower diagram: schematic of typical RI patterns detected by N/N 2D gel electrophoresis. Simple Y arc (arrow): passive replication of the probed DNA fragment interval due to initiation elsewhere in the chromosome. Bubble arc (arrowhead): initiation at a central position in the probed DNA fragment. Bubble-to-Y arc: initiation at an asymmetric position in the examined fragment (low MW RIs: bubble arc (arrowhead), high MW RIs: Y arc). Composite: active (complete bubble arc, arrowhead) and passive (complete Y arc, arrow) replication within the probed DNA fragment. X and Double Y: the X spike (arrowhead) is generated from branch migration recombinant intermediates, and the double Y (open arrow) is generated by two converging replication forks. (B) RI patterns detected with the 5' NTS probe 1 on HindIII digested DNA from mock treated quiescent (starvation) and replicating cell populations (S phase). (C) 5' NTS analysis on DNA from HU-treated cells 0-120 min after HU removal. See flow cytometry profiles (Figure 3.9A) and western blots (Figure 3.9B) for cell cycle progression and abundance of Orc1p and Mcm6p, respectively. (D) Two-dimensional N-N gel analysis of the 5.5 kb rRNA coding region ClaI fragment (position 2168-7629, probe 2). (E) Two dimensional neutral-alkaline (N/A) analysis of RIs derived from the rRNA coding region ClaI fragment. Probe 3 spans nucleotides 2169 to 3670, and probe 4 spans nucleotides 5214-6676. Schematic of nascent-strand RIs resolved by N/A 2D gel electrophoresis. The 1n spot corresponds to non-replicating DNA. The vertical smear is derived from nicked, non-replicating DNA, and the horizontal smear represents the parental strand in RIs of different length. The diagonal arc corresponds to nascent-strand replication intermediates that are liberated from the parental strand by alkali denaturation prior to electrophoresis in the second dimension.

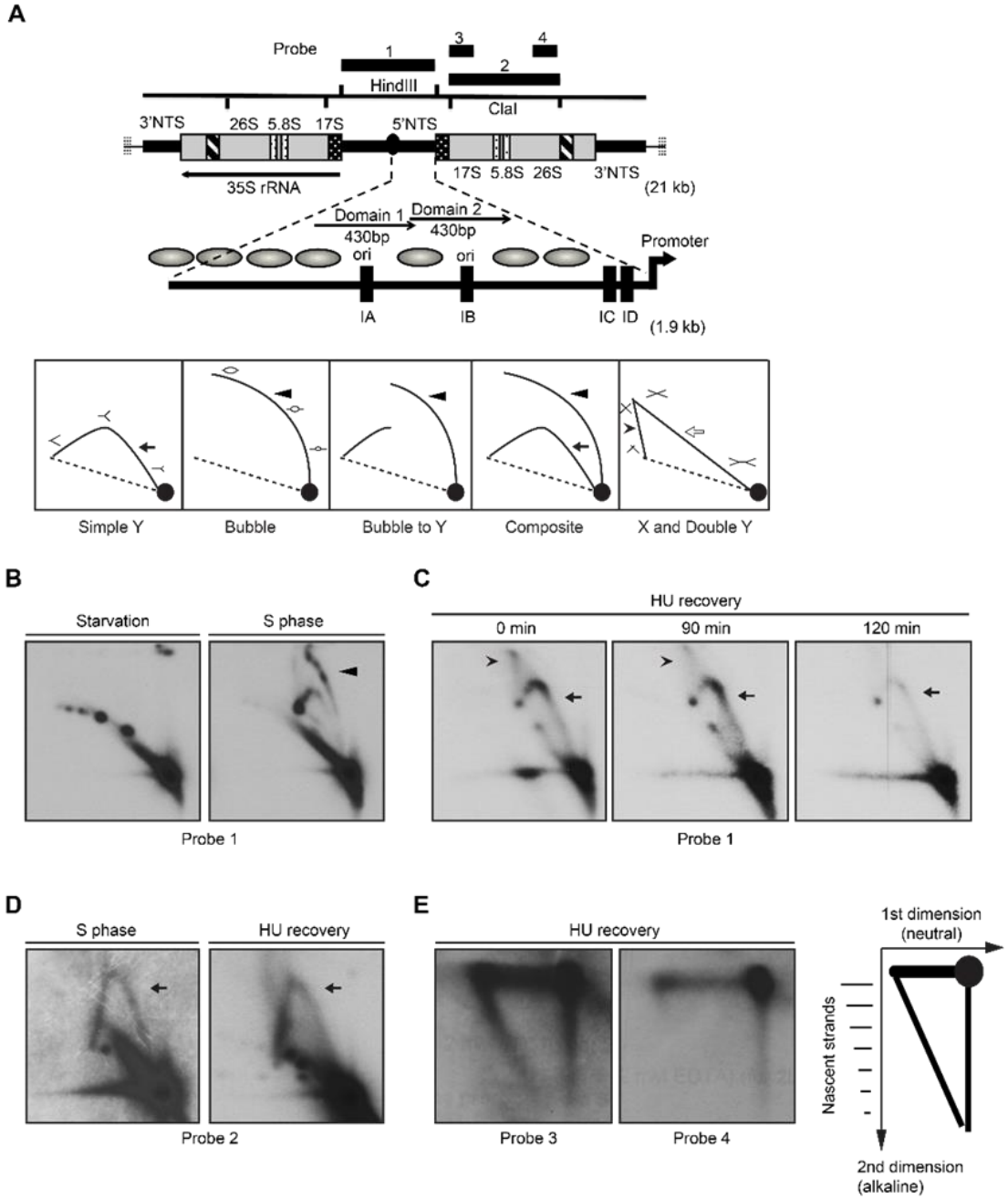
A
Probe
1
2
3
4
HindIII
ClaI
3'NTS
26S 5.8S 17S
5'NTS
17S 5.8S 26S
3'NTS
(21 kb)
35S rRNA
Domain 1
430bp
Domain 2
430bp
ori
ori
Promoter
IA
IB
IC ID
(1.9 kb)
Simple Y
Bubble
Bubble to Y
Composite
X and Double Y
B
Starvation
S phase
Probe 1
C
HU recovery
0 min
90 min
120 min
Probe 1
D
S phase
HU recovery
Probe 2
E
HU recovery
Probe 3
Probe 4
1st dimension
(neutral)
Nascent strands
2nd dimension
(alkaline)

formed corresponds to a simple Y arc (Figure 3.10C, 0-120 min; filled arrow), indicative of passive replication of 5' NTS. A faint double Y arc pattern (open arrow) was also detected, consistent with converging replication forks emanating from initiation events near the rRNA promoter or distal to the restriction enzyme cut site. Finally, an X spike was detected (arrowhead), indicative of branch migration in stalled replication forks or DNA molecules generated by homologous recombination. We conclude that the rDNA origin is inactivated in ORC-depleted cells.

To test for the presence of a cryptic origin in the rRNA coding region, N/N 2D gels were used to examine the 5.5 kb *ClaI* coding region fragment (Figure 3.10A, schematic). No origins (bubble arcs) were detected in this region in mock-treated controls or cells recovering from HU-induced replication stress. Instead, a simple Y arc was observed (Figure 3.10D, probe 2).

Neutral alkaline (N/A) gel electrophoresis specifically visualizes nascent strands and can reveal the direction of replication fork progression through a given DNA interval. N/A gel analysis of *ClaI*-digested DNA was used to distinguish between four possibilities: random initiation, initiation from cryptic origins in the coding region, initiation from more distal sites (3' NTS or the telomere), and initiation from the promoter-proximal region. Whereas both short and long nascent strands were detected with 5' NTS proximal probe 3, only high molecular weight RIs were detected with the more 3' proximal probe 4 (Figure 3.10E). The collective data suggest that replication initiates proximal to the rRNA promoter.

New initiation events predominate in ORC-depleted non-rDNA chromosomes

DNA fiber analysis was used to distinguish between two models for genome-wide replication following HU depletion of ORC and MCMs: elongation of forks that initiated prior to or during HU exposure, and new initiation events. Cells were synchronized in G1 by starvation and re-feeding and HU was immediately added to the media. Following 4 h exposure, the HU was removed and nascent DNA strands were sequentially labeled with IdU and CldU. New initiation events will generate DNA fibers in which the red pulse labeled segment (IdU) is flanked by green (CldU) on both sides. Elongation of existing forks will produce a green-red-gap-red-green signature, in which the gapped region corresponds to a DNA segment that was replicated prior to the pulse/chase. Both images were detected during the HU recovery, prior to replenishment of ORC and MCMs (Figure 3.11A). New initiation events were more frequently observed (6 out of 7 events in the randomly chosen images). These data argue that bidirectional replication initiation is the predominant mechanism for genome-wide duplication of macronuclear chromosomes during the recovery from HU-induced replication stress.

DNA fibers were also used to quantitatively examine replication initiation and fork elongation in mock-treated controls (high ORC and MCMs) and during the first S phase after HU removal (low ORC and MCMs). The physical distance between replication initiation sites (inter-origin distance, IOD) was measured in individual DNA molecules, and the speed of elongating replication forks (fork velocity, FV) was assessed (Tuduri et al, 2010). In previously published work, we reported a median inter-origin

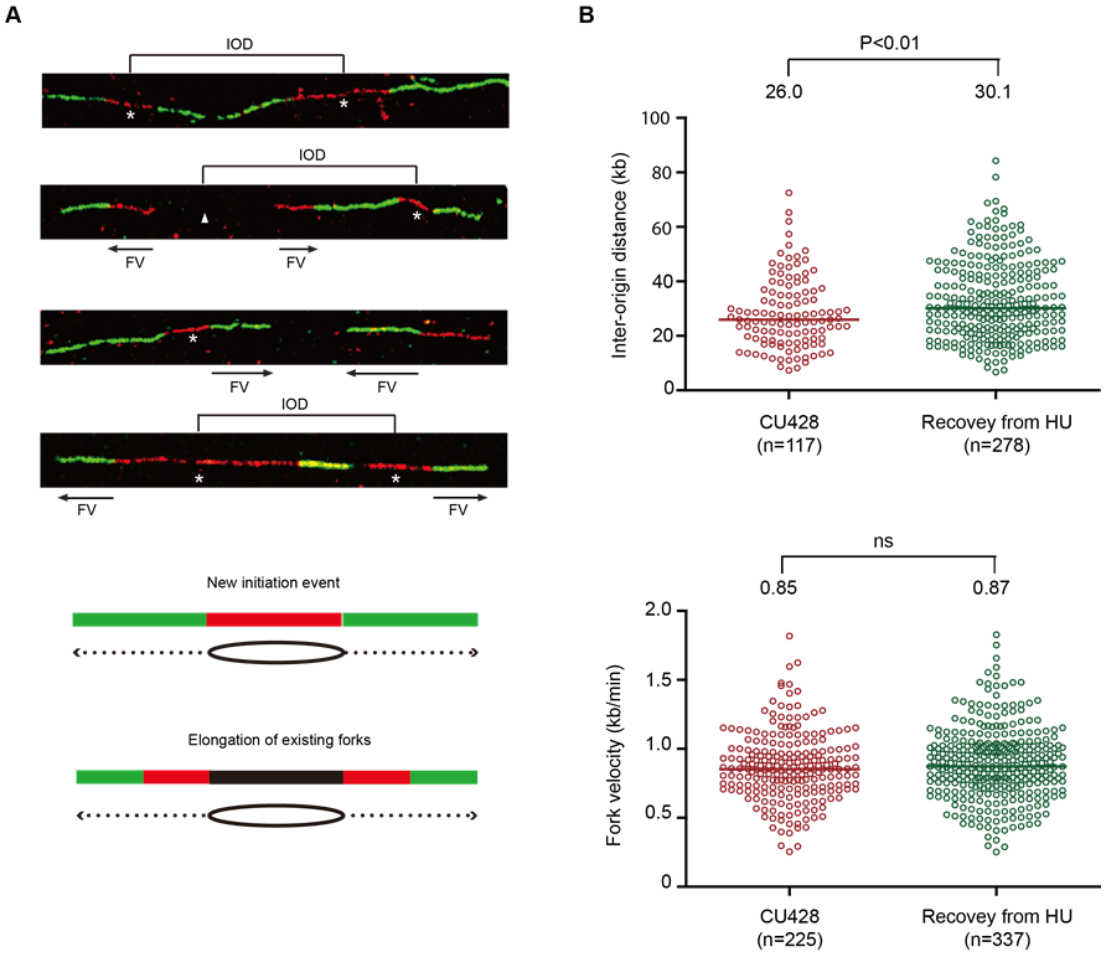

Figure 3.11. DNA fiber analysis of mock-treated cells and cells recovering from HU-induced replication stress. An asynchronous cell population was used to measure inter-origin distances and fork rates in mock-treated cells by sequential labeling with IdU and CldU for 10 min each (see Materials and Methods). HU-treated cells were synchronized at the G1/S border by starvation and re-feeding, and released into 20 mM HU for 4 h. Cells were washed free of HU, and incubated for 60 min prior to the sequential addition of IdU and CldU for 10 min each. (A) Representative DNA fibers images. (B) Compilation of DNA fiber image data and statistical analysis. Inter-origin distance was defined as the distance between the centers of two red segments in either green-red-green-red-green or green-red-gap-red-green tracks. Fork velocity was determined by measuring the length of the green segment in red-green tracks or the red segments in green-red-gap-red-green tracks. GraphPad Prism software was used to analyze the statistical significance, and the p-values shown in Figures were determined by two-tailed unpaired t-test.

distance of 24.3 kb and fork elongation rate of 0.83 kb/min for mid-log phase vegetative cells. A 5-fold reduction in Orc1p and corresponding drop in Mcm6p had no effect on inter-origin distance, but resulted in a decreased rate in fork elongation (Lee et al, 2015). We performed a similar analysis on cells recovering from HU-arrest, prior to the replenishment of Orc1p, Orc2p and Mcm6p. Whereas the fork elongation rates for mock and HU-recovering cells were indistinguishable (Figure 3.11B), the median inter-origin distance increased by 16% in HU treated, released cells (from 26.0 kb to 30.1 kb; $p<0.01$). Hence, although the conventional DNA replication program is perturbed, new initiation events are the major contributor to genome-wide replication under low ORC conditions. Since the rDNA origin is passively replicated during HU recovery (Figure 3.10C), we speculate that the new initiation events in non-rDNA chromosomes are generated by an ORC-independent mechanism.

Discussion

The failure to completely replicate chromosomes leads to genome instability. While aberrant DNA replication decreases fitness and is selected against, aneuploidy can lead to unchecked cell proliferation by altering the expression of proto-oncogenes and tumor suppressor genes (Ly et al, 2014). Intra-S phase DNA damage/replication stress checkpoint responses protect chromosomes by transiently arresting DNA replication. A cornerstone of these responses is the reversible phosphorylation of the MCM2-7 complex. In the work presented here, we show that replication stress triggers a very different ATR-dependent response in *Tetrahymena*. Mcm6p, Orc1p and Orc2p are degraded. Paradoxically, DNA synthesis rapidly resumes following release from

genotoxic stress, and a full round of DNA replication occurs prior to replenishment of these essential pre-RC components. These findings expand the repertoire of eukaryotic checkpoint responses, and suggest that a novel mechanism for replication initiation remains to be discovered.

Distinctive attributes of the Tetrahymena *checkpoint response*

A remarkable feature of ciliates is the presence of two functionally distinct nuclei within a single cytoplasm. During vegetative growth, the transcriptionally silent, diploid micronucleus and the actively transcribed, polyploid macronucleus replicate at different stages of the cell cycle. Their respective chromosomes are segregated at different times and by unrelated mechanisms. The mitotic micronucleus divides during macronuclear G1 and amitotic macronuclear division is coupled to cytokinesis. Since the macronucleus confers the cellular phenotype, macronuclear DNA damage or replication stress should decrease fitness. However, aberrant macronuclear division with lagging chromosomes, a signature of incomplete replication, is readily tolerated (Donti et al, 2009; Smith et al, 2004).

The high copy number of macronuclear chromosomes (45 C) may provide a buffer against errors in DNA replication and chromosome transmission. Indeed, *Tetrahymena* has evolved mechanisms to correct genic balances, such as the ability to partially re-replicate the macronucleus without cell division (Cleffmann, 1975; Doerder & DeBault, 1978) or eliminate excess DNA in the form of chromatin extrusion bodies (Cleffmann, 1980). Within the framework of these seemingly chaotic cell cycles, the apical ATR checkpoint kinase triggers a robust intra-S phase checkpoint response that

arrests DNA replication in both the micronucleus and macronucleus when challenged with agents that induce DNA damage and replication stress (Yakisich et al, 2006).

The administration of MMS or HU midway through macronuclear S phase leads to rapid cell cycle arrest (Figure 3.1C), induction of the break-induced repair protein, Rad51p (Figures 3.1A and 3.1B), and phosphorylation of gamma H2A.X (Figure 3.6). ORC and MCM subunits are stable in MMS-treated *Tetrahymena*; however they are actively degraded during HU exposure (Figures 3.1B, 3.6B and 3.6C). The different fate of ORC and MCMs in HU and MMS-treated cells is indicative of bifurcation of the pathway downstream of ATR. Although the details differ, HU and MMS also activate different downstream pathways in other eukaryotes (Branzei & Foiani, 2009).

In contrast to other model eukaryotes, *Tetrahymena* DNA content neither remains constant nor gradually increases (Alvino et al, 2007; Mickle et al, 2007) during prolonged HU exposure. Instead the apparent DNA content decreases over time, assuming a G1 value in a large subpopulation of cells (Figure 3.1C-E, Figure 3.2). What could account for these changes? Precocious cell division has been ruled out (Figure 3.4A-F), and DNA fiber analysis revealed that nascent DNA strands are not selectively degraded (Figure 3.6B). Global changes in the acetylation status of histone H3 occur in HU-treated cells (Figures 3.6C and 3.7C). Studies in diploid maize cells previously demonstrated that chromatin compaction can diminish propidium iodide fluorescence intensity (Biradar & Rayburn, 1994). Diminished interactions between chromosomes and the nuclear envelope promote chromatin compaction in cultured human cells, manifesting as aggregated chromatin clusters (Malik et al, 2014).

Previous studies in *Tetrahymena* revealed that histone acetylation impacts on the fate of macronuclear chromosomes. Experimentally-induced down regulation of the *Tetrahymena* histone deacetylase, THD1, leads to an increase in chromatin extrusion body formation and diminished integrity of the macronucleus (Wiley et al, 2005). Whether this reflects an increase in acetylation in eliminated DNA or altered expression of genes that are modulated by histone acetylation is not known. We favor the later model for two reasons. First, the modest increase in CEBs observed in HU-treated *Tetrahymena* (Figure 3.4G; mock treated: 1%, HU-treated 3%) cannot account for the time-dependent decrease in apparent DNA content. Second, while heterochromatin formation is essential for the selective removal of ~5000 internally eliminate sequence elements (IESs) in the developing macronucleus (Taverna et al, 2002), CEB formation correlates with an increase, rather than decrease, in acetylated histone H3 status, a marker for euchromatin. We posit that histone H3 deacetylation and chromatin compaction are largely responsible for the apparent decrease in DNA content in HU-treated cells. How this would impact subsequent rounds of DNA replication is matter of speculation.

A key feature of the intra-S phase checkpoint response in yeast and higher eukaryotes is the reversible phosphorylation-dependent inhibition of the replicative helicase, through ATR/CHK1-dependent phosphorylation of Mcm2p and Mcm3p (Cortez et al, 2004; Shechter & Gautier, 2004; Stead et al, 2012). In this study we show that checkpoint activation in *Tetrahymena* is associated with the degradation of MCM and ORC subunits. While Orc1p normally turns over during S phase, Orc2p levels do

not oscillate across the cell cycle (Donti et al, 2009). Recent studies revealed that the abundance of ORC and MCM proteins are dynamically co-regulated (Lee et al, 2015). Partial depletion of Orc1p by gene disruption leads to a concomitant decrease in Orc2p and Mcm6p levels during the vegetative stage of the life cycle. Unexpectedly, ORC and MCM naturally fluctuate to a greater degree during conjugation, and poorly correlate with the demands for DNA replication: ORC and MCM are elevated early in development when the replication load is low, and precipitously decline when the replication load increases (Lee et al, 2015). Aberrantly migrating (RNase A + mung bean nuclease-sensitive) RIs are generated in the endoreplicating macronucleus, suggesting that RNA-DNA hybrids accumulate, similar to yeast senataxin mutants (Alzu et al, 2012; Lee et al, 2015). Hence, the initiation of DNA replication is dynamically re-programmed during *Tetrahymena* development. Our analysis of cells recovering from HU-induced replication stress suggests that the capacity to replicate under low ORC and MCM conditions is retained during the vegetative phase of the life cycle.

Replication stress has been shown to trigger different, species-specific checkpoint responses and recovery mechanisms. For example, while HU inhibits replication initiation in *S. cerevisiae*, it only slows replication forks in *S. pombe* (Alvino et al, 2007). Furthermore, most late firing origins in *S. pombe* are regulated by a RAD3 (ATR) independent mechanism (Mickle et al, 2007). Mammalian ATR inhibits replication initiation and elongation (Feijoo et al, 2001; Heffernan et al, 2002); however, replication origins are far from equivalent, since neighboring origins are differentially sensitive to HU depletion of dNTP pools (Anglana et al, 2003). The unifying features in

these species are the stabilization of late firing origins and reversible phosphorylation of MCM subunits (Cortez et al, 2004; Randell et al, 2010; Snaith et al, 2000). Once the source of stress is removed, the conventional DNA replication program resumes (Diffley et al, 2000; Levenson & Hamlin, 1993).

HU-induced degradation of ORC and MCMs provides unprecedented challenges to the *Tetrahymena* DNA replication machinery. Pre-RCs are not re-established prior to the initiation and completion of the first S phase following HU removal (Figures 3.9 and 3.8). The distance between initiation sites increases during the recovery phase, and the sole origin in the rDNA minichromosome is silenced (Figures 3.10 and 3.11). No cryptic origins were uncovered in the 21 kb rDNA minichromosome, however; leading strand synthesis proceeds toward the telomeres, suggesting that replication initiates proximal to the rRNA promoter.

Models for replication initiation under limiting ORC conditions

Several models are considered for DNA replication with limiting amounts of *Tetrahymena* ORC. In the first model, replication initiation and elongation are uncoupled in HU-treated cells. Stalled replication forks generated during HU arrest are simply elongated during the recovery phase. Whereas initiation and elongation are transiently uncoupled in *Drosophila* follicle cells (Claycomb et al, 2002), two pieces of data disfavor this model in *Tetrahymena*. First, during the recovery from HU-induced stress, new initiation events were detected by 2D gel analysis in rDNA minichromosome, and the 5' NTS origin did not serve as the initiation site (Figure 3.10). More importantly, the

predominant CldU/IdU/CldU pattern in non-rDNA DNA fibers generated during HU recovery corresponds to new initiation events (Figure 3.11A).

In the second model, a small subpopulation of origins is refractory to ORC and MCM depletion. Initiation events during HU recovery occur at cryptic or firing late origins, analogous to origins that are used by *S. cerevisiae* upon HU removal (Karnani & Dutta, 2011). These origins would need to function at low ORC concentrations, and consequently, they should have a high affinity for ORC and be less dependent on epigenetic factors (Hoggard et al, 2013). *Tetrahymena*'s innate ability to partially re-replicate the macronuclear genome, despite S phase-specific degradation of Orc1p, is consistent with this model (Cleffmann, 1975; Donti et al, 2009); however, the global decrease in histone acetylation during HU exposure suggests a strong epigenetic component. Further studies are needed to determine the relative contribution of chromatin-associated and pre-deposition histones to the H3 acetylation profile in HU-arrested *Tetrahymena* (Jasencakova et al, 2010).

A third model posits that the genome is duplicated in an ORC-independent manner. Archaebacteria and animal viruses provide the only precedents. *Haloferax volcanii* strains lacking all four ORC-dependent chromosomal origins exhibit increased fitness relative to strains with 1-4 intact origins (Hawkins et al, 2013). Cell viability in the originless mutant is dependent on RadA recombinase, which is non-essential in wild type strains. In this view, the converging replication forks and branch migration intermediates in the *Tetrahymena* rDNA 5' NTS (Figure 3.9B) could represent recombination substrates or intermediates that prime DNA replication. Based on the

measured inter-origin distance (Figure 3.11), approximately 250,000 recombination events would be required to replicate a single polyploid macronucleus. Alternatively, DNA replication could be primed by a covalently bound protein, as in adenovirus (Challberg et al, 1980), tRNA molecules (avian sarcoma virus) (Cordell et al, 1979), or non-coding RNA. While there is no precedent for the last scenario, dicer-generated small (27-30 nt) non-coding RNAs play novel roles in ciliates, directing the removal of ~6000 IES elements in the developing *Tetrahymena* macronucleus (Malone et al, 2005; Mochizuki & Gorovsky, 2005). Small (23-24 nt) non-coding RNAs of unknown function are similarly produced during the vegetative cell cycle (Lee & Collins, 2006). The 287 nt non-coding RNA, 26T RNA, is an integral component of ORC, selectively directing the complex to complementary DNA sequences at the amplified rDNA origin (Mohammad et al, 2007). The underlying mechanism for replication initiation in ORC-depleted cells awaits further studies.

The *Tetrahymena* system has several interesting unanticipated parallels in which endoreplication is a common theme. DSB-inducing agents induce ATR in *Arabidopsis thaliana* to activate the endoreplication program rather than arrest the cell cycle (Adachi et al, 2011). While *Drosophila* ORC is normally present in endoreplicating nurse cells (Sher et al, 2012), ORC2-deficient mutant cells undergo multiple rounds of endoreplication by an undetermined mechanism (Park & Asano, 2008). The archaebacteria *H. volvanii*, which efficiently propagates originless chromosomes is polyploid, and can tolerate significant variation in chromosome copy number (Hawkins et al, 2013). We propose that polyploid cells are inherently more tolerant than diploid

cells to DNA damage and replication stress, and can propagate chromosomes by unconventional mechanisms that function to a lesser degree in diploid species or tissues. High-throughput mapping of replication origins should provide novel insights into underlying mechanism(s) for replication initiation site selection in *Tetrahymena*.

Material and methods

Cell cycle synchronization and DNA damage checkpoint activation

Tetrahymena strain CU428 was obtained from the *Tetrahymena* Stock Center. Standard methods were used to cultivate cells and visualize cells by light and fluorescence microscopy (Yakisich et al, 2006). Cell cycle synchronization was achieved by starvation and re-feeding or by centrifugal elutriation as previously described (Donti et al, 2009). For DNA damage checkpoint activation, standard growth media was supplemented with either 20 mM hydroxyurea (HU, Sigma Chemical) or 0.06% methylmethansulphonate (MMS, Sigma Chemical). Stock solutions of caffeine and sodium butyrate (Sigma-Aldrich) were prepared in water. The working concentrations of caffeine and sodium butyrate were 1 mM and 50 mM, respectively. For cell division analysis, DAPI-stained cells were examined microscopically at defined intervals after drug treatment and removal.

Flow cytometry

Flow cytometry analysis was performed on Becton Dickinson FACSAria II flow cytometer (BD Biosciences), using propidium iodide to monitor DNA content. Data were analyzed using BD FACSDiva™ software. Histograms were plotted, in which the y-axis represents the number of events and the x-axis represents the relative DNA

content. Forward and side scatter data were graphed to visualize the distribution of individual cells within the population.

Western blot analysis

Whole cell extracts were prepared by lysing cells in 1% SDS lysis buffer (50 mM Tris at pH 8.0, 150 mM NaCl, 1 mM EDTA, 1% NP-40, 1% sodium deoxycholate, 1% SDS) for 15 min on ice. Protein concentrations were determined using the modified Lowry protein assay reagents (Bio-Rad). Unless otherwise stated, equal amounts of total protein (20 μg) were loaded in each lane and samples were subjected to SDS-PAGE and transferred to nitrocellulose membranes (Whatman Protran BA85, GE Healthcare). Prior to probing, membranes were stained with Ponceau S staining (Sigma-Aldrich) to confirm equivalent sample loading and protein transfer. Immunodetection of *Tetrahymena* Orc1p (1:5,000), Orc2 (1:5,000) and Mcm6p (1:10,000) were carried out using polyclonal rabbit antibodies raised against immunogenic *Tetrahymena* peptides (Covance). Antibodies directed against Rad51 (51RAD01, Thermo Scientific, 1:5,000 dilution), phospho-gamma H2A.X (2F3, BioLegend, 1:1,000 dilution), and acetyl-histone H3 (polyclonal antibody #06599, Millipore, 1:10,000 dilution) were obtained from the indicated commercial sources). Blots were incubated with the primary antibodies at 4 ℃ overnight, washed and incubated for 3 h at 4 ℃ with horseradish peroxidase-conjugated goat anti-rabbit or goat anti-mouse IgG (Jackson ImmunoResearch). Membrane bound secondary antibodies were visualized using ECL reagents (PerkinElmer) according to the manufacturer's instructions. Densitometry of

blots was performed using ImageJ software (version 1.47v for Macintosh, National Institutes of Health).

Two-dimensional (2D) gel analysis of DNA replication intermediates

Total genomic DNA was isolated from *Tetrahymena* cultures as previously described to preserve DNA replication intermediates (RI) (Zhang et al, 1997). For RI enrichment, 200 μg of genomic DNA were digested with *HindIII* (rDNA 5' NTS analysis) or *ClaI* (rDNA coding region analysis) for 4 h and applied to the 200-μl packed volume benzoylated naphthoylated DEAE (BND)-cellulose (Sigma-Aldrich). Caffeine-eluted DNA samples were precipitated with isopropanol, using 20 μg glycogen as a carrier. Total DNA recovery was estimated to be ~5% of input.

Neutral-neutral (N/N) and neutral-alkaline (N/A) 2D gel electrophoresis were performed as previously described (MacAlpine et al, 1997). Approximately 3-10 μg of BND cellulose-enriched DNA was loaded for each 2D gel experiment. For N/N analysis, the first dimension gel (0.4% agarose) was run in 1X TAE buffer (40 mM Tris, 20 mM acetic acid, and 1 mM EDTA) at 1.5 V/cm for 20 h at RT. The second dimension gel (1% agarose) was run in 1X TBE buffer (90 mM Tris, 90 mM boric acid, 2 mM EDTA) containing 0.5 mg/ml ethidium bromide at 3 V/cm for 18 h at 4 ℃. For N/A analysis, the second dimension separation was performed at 4 ℃ in recirculating buffer (40 mM NaOH, 2 mM EDTA) at 1.5 V/cm for 20 h.

DNA was transferred overnight to a charged nylon membrane (Hybond-XL, Amersham) in alkaline buffer by capillary blotting. Membranes were prehybridized at 37 ℃ for 4 h in 1M NaCl, 1% SDS, 10% dextran sulfate, 5 mM Tris [pH 7.5], 100 μg/ml

of denatured salmon sperm DNA and 25% formamide. rDNA 5' NTS and coding region probes were labeled by random priming and added directly to the prehybridization solution. After 18 h, membranes were washed three times in 2X SSC/1% SDS solution for 15 min each at 42 ℃, and once in 0.4X SSC/0.1% SDS solution for 15 min at 42 ℃. Blot were exposed to X-ray film with an intensifying screen at -70 ℃ or analyzed with a phosphorimager.

DNA fiber analysis

Tetrahymena was cultured in 2% PPYS media to the density of 1.5x10e5 cells/ml. For pulse chase experiments, cells were sequentially pulse labeled with 400 μM IdU (Sigma) and 100 μM CldU (MP Biomedicals) at 30°C. The media was removed and cells were washed once with 1X PBS between each labeling step. For DNA fiber processing, cells were washed twice with PBS, the cell density was adjusted to $1x10^6$ cells/ml. Preparation and immunostaining of DNA fibers was performed as described previously described (Chastain et al, 2006; Schwab & Niedzwiedz, 2011; Stewart et al, 2012) with the following modifications. Briefly, after fixation and HCl treatment, slides were washed three times with 1X PBS, and blocked with 5% BSA in PBS for 30 min. Mouse anti-BrdU (1:50, Becton Dickson) and rat anti-BrdU (Accurate Chemical, 1:100 dilution) antibodies in 5% BSA were then added onto slides. After 1 h incubation, the slides were washed three times again with 1X PBS, and incubated for 30 min with secondary antibodies: Alexa Fluor 568 goat anti-mouse IgG (Invitrogen/Molecular Probes, 1:100 dilution) and Alexa Fluor 488 goat anti-rat IgG (Invitrogen/Molecular Probes, 1:100 dilution). Finally, slides were washed three times with 1X PBS,

dehydrated with an ethanol series, and mounted with SlowFade Gold antifade solution (Invitrogen). During immunostaining, all antibodies were diluted in 5% BSA in 1X PBS, all incubations were performed at 37 ℃, and all wash steps were done at RT. DNA fiber images were obtained on a Nikon A1R+ confocal microscope at 600X magnification. Measurements of track length were performed with Nikon NIS-Elements software. Red-green-red tracks represent origins that initiated DNA replication during the IdU pulse. Red-green-gap-green-red tracts represent origins that initiated DNA replication prior to the IdU pulse. Inter-origin distance was defined as the distance between the centers of two red segments in either green-red-green-red-green or green-red-gap-red-green tracks. Fork velocity was determined by measuring the length of the green segment in red-green tracks or the red segments in green-red-gap-red-green tracks. GraphPad Prism software was used to analyze the statistical significance, and the p-values shown in Figures were determined by two-tailed unpaired t-test.

CHAPTER IV

DEVELOPMENTALLY REGULATED DNA REPLICATION PROGRAMS: GENE AMPLIFICATION AND ENDOREPLICATION

Overview

Whereas chromosomes are duplicated once and only once during conventional cell cycle, two alternative programs exist to increase DNA copy on a genome-wide or locus-specific scale: endoreplication and gene amplification. These alternative replication programs are sequentially linked in specialized metazoan cells. In the work described herein, I examined endoreplication and gene amplification in the unicellular eukaryote *Tetrahymena thermophila*. I determined the kinetics for amplification of the rDNA minichromosome and the temporal window for rDNA amplification relative to endoreplication of the remaining macronuclear chromosomes. Early rounds of rDNA replication occur by locus-specific gene amplification when other chromosomes are being endoreplicated, and both programs are shut down simultaneously. rDNA replication is then switched from amplification to endoreplication upon refeeding. During this switch, ORC levels are low, and the rDNA origin that was used for amplification is not being used. The replication intermediates that are seen in the rDNA during Endo II have the same signature as the replication intermediates that are seen in vegetative cells lacking a histone monomethyltransferase. I propose that epigenetic modifications of the chromatin may play a role in endocycling cells.

Introduction

DNA replication is a process to duplicate genetic material for inheritance. A conventional mitotic cell cycle contains G1, S, G2 and M phases. During S phase, DNA replication occurs and the entire genome must be replicated once and only once per cell cycle. DNA replication starts at specific sites in chromosomes named origins of replication. The origin recognition complex (ORC), which contains six subunits and is conserved across different eukaryotes (Bell & Stillman, 1992; Gossen et al, 1995; Moon et al, 1999; Rowles et al, 1996), binds to replication origins and dictates where replication initiates. ORC recruits other factors such as Cdc6 and Cdt1 to facilitate loading of the replicative helicase MCM2-7 to form the "licensed" pre-replication complex (pre-RC) (Sclafani & Holzen, 2007). Activation of the "licensed" pre-RC requires the recruitment of Cdc45 and GINS to MCM2-7 (Ilves et al, 2010). Other components of replisome such as DNA polymerase α and primase are then recruited. In *S. cerevisiae* and higher eukaryotes, phosphorylation or degradation of Orc1p prevents re-replication (Fernandez-Cid et al, 2013; Mendez et al, 2002). Export of MCM2-7 from nucleus is another way to block re-replication in *S. cerevisiae* (Labib et al, 1999; Nguyen et al, 2000).

In addition to the conventional mitotic cell cycle, different DNA replication programs exist in eukaryotes, such as endoreplication (or endocycles) and gene amplification. Endocycles are composed of alternating G and S phases without mitosis, and the genome replicates once during each S phase. Endocycling occurs in specialized cells during eukaryotic development to generate polyploid cells. In mammals and flies,

these cells play a supportive role, providing nutrients and proteins for the developing embryo or fetus. Endoreplication and polyploidy occur in plants, animal tissues and ciliates, such as plant endosperms and trichomes, *Drosophila* follicle cells, rodent trophoblasts, and *Tetrahymena* macronuclear anlagen (Fox & Duronio, 2013). Studies on endocycles in *Drosophila* follicle cells have shown that Notch signaling is the regulator for transition from mitotic cell cycles to endocycles (Deng et al, 2001; Lopez-Schier & St Johnston, 2001). Notch signaling controls the transition mainly through inducing expression of Fzr/Cdh1, an activator of the anaphase-promoting complex/cyclosome (APC/C), and suppressing expression of mitotic CDK (Deng et al, 2001; Shcherbata et al, 2004). Moreover, oscillation of Cyclin E/Cdk2 activity is the driving force for endoreplication (Follette et al, 1998; Weiss et al, 1998). In *Drosophila*, E2F1 is responsible for expression and oscillation of Cyclin E (Zielke et al, 2011).

Developmentally programmed gene amplification is a specialized replication program to increase the amount of a certain DNA segment in the genome by firing origins at specific loci many times. The purpose is to increase DNA template for transcription to generate the large quantities of RNA and/or structural proteins required during development. Developmentally programmed gene amplification is often preceded by genome-wide endoreplication and takes place in terminally differentiated cells, such as amplification of the *Drosophila* chorion genes (Calvi et al, 1998), and *Sciara coprophila* cocoon genes (Wu et al, 1993). In *Drosophila* follicle cells, after three rounds of endoreplication from stage 7 to stage 10A, gene amplification at specific loci initiates at stage 10B when genome-wide replication initiation has been inactivated

(Calvi et al, 1998). The timing of gene amplification is strictly controlled, and the origin firing and fork elongation are separated. Origin firing occurs during stages 10B and 11, but the forks are only elongated about 5 kb from the origins. Theses forks are subsequently elongated during stages 12 and 13 to amplify around 40 kb of DNA (Claycomb et al, 2002). One exception to the timing is the amplicon DAFC-62D, with an additional round of origin firing during stage 13 to provide more template for late gene transcription (Claycomb et al, 2004). Finally, the "onionskin" structure with a gradient of amplified DNA is formed (Calvi et al, 1998; Liang et al, 1993; Osheim et al, 1988). Replication initiation must be stringently regulated for the transition from genome-wide endoreplication to site specific gene amplification.

Epigenetic modifications play an important role in modulating DNA replication. In *S. cerevisiae*, histone deacetylase Rpd3 directs regulation of replication timing, and histone acetylation promotes late origin firing (Knott et al, 2009). In human cells, histone acetyltransferase Hbo1 interacts with multiple components of pre-RC, and it is involved in pre-RC formation and licensing of replication origins (Burke et al, 2001; Miotto & Struhl, 2010). In *Drosophila* follicle cells, histone acetylation is critical for specifying origins for chorion gene amplification (Aggarwal & Calvi, 2004). When histone deacetylase Rpd3 is tethered to the origin of chorion genes, the origin activity decreases.

Tetrahymena thermophila, a ciliated protozoan, is a powerful model system to study DNA replication. *Tetrahymena* contains two structurally and functionally distinct nuclei in a single cell. The germline micronucleus (MIC) is composed of five

transcriptionally silent chromosomes and the somatic macronucleus (MAC) is composed of approximately 180 transcriptionally active chromosomes (Gorovsky & Woodard, 1969; Mayo & Orias, 1981; Yao & Gorovsky, 1974). Besides the vegetative cell cycle, *Tetrahymena* undergoes a sexual life cycle upon starvation and mixing of cells expressing different mating type genes (Allewell et al, 1976). During conjugation, the MIC undergoes meiosis. Four pronuclei are generated, three of which are degraded by programmed nuclear death (PND) (Akematsu & Endoh, 2010; Cole & Sugai, 2012). The remaining pronuclei undergoes one round of mitosis, generating two genetically identical stationary and migratory pronuclei. The pronuclei are reciprocally exchanged between mating pairs to produce the zygotic micronucleus. This nucleus undergoes two round of mitosis to generate four MICs, two of which develop into new MACs and two maintain their micronuclear identity. The process of converting a micronucleus into macronucleus is termed macronuclear development. Many important events occur during this process, including ribosomal DNA (rDNA) amplification and non-rDNA endoreplication. During MAC development, the micronuclear genome experiences massive DNA rearrangement (Chalker & Yao, 2011). Chromosomes are fragmented at specific sites and *de novo* telomere addition occurs at the ends of fragments. Moreover, internal eliminated sequences (IESs), which consist of the repetitive sequences, are removed from the micronuclear genome. Concurrently, heterochromatin is converted into euchromatin. In total, ~180 macronuclear chromosomes are generated, and these chromosomes undergo two phases of endoreplication to increase their copy number to 45 C. By comparison, the 10.3 kb ribosomal DNA (rDNA) locus is excised from

flanking DNA and rearranged into a 21 kb head-to head palindromic minichromosome (Yasuda & Yao, 1991). The rDNA undergoes developmentally programmed gene amplification to obtain about 9,000 C. The exact kinetics for rDNA amplification has not been determined. It is unknown whether rDNA amplification is associated with endoreplication. During macronuclear development, chromatin remodeling occurs during transition from the MIC to the MAC, and heterochromatin is converted into euchromatin. It is unknown when exactly the epigenetic changes such as histone modifications are completely finished. The epigenetic status may affect origin utilization during development.

How is the rDNA selectively chosen for gene amplification? One model posits that the mechanisms for ORC recognition of the rDNA and the non-rDNA origin differ. In contrast to other eukaryotes, *Tetrahymena* ORC contains an integral RNA subunit, named 26T RNA. 26T RNA corresponds to the terminal 282 nucleotides of 26S rRNA. ORC binding to the rDNA chromosome is mediated by Watson-Crick base pairing between 26T RNA and the Type I element T-rich strand in the 5' nontranscribed spacer (NTS) of rDNA (Mohammad et al, 2007). In addition to the rDNA origin, a non-rDNA replicon ARS1 has been identified. This replicon lacks sequence complementary to 26T RNA (Donti et al, 2009). Therefore, ORC recognizes the non-rDNA origin by a different mechanism. Moreover, ORC binds to rDNA and non-rDNA origins at different stages during the cell cycle (Donti et al, 2009). Another model for the selective amplification of rDNA is that amplification specific sequences or trans-acting factors are involved. For example, in *Drosophila*, an amplification control element ACE3 is a replication

enhancer necessary for gene amplification (Orrweaver et al, 1989). The Myb complex associates with ACE3 and origin sequences and is required for gene amplification (Beall et al, 2002).

It is advantageous to use *Tetrahymena* to study gene amplification and endoreplication. Massive amounts of synchronized cells can be achieved easily compared to *Drosophila* where a certain type of cells with low quantity needs to be dissected in tissues. More importantly, as an early branching single celled eukaryote, *Tetrahymena* has distinctly featured gene amplification and endoreplication programs. Firstly, compared to locus specific amplification in *Drosophila* follicle cells, *Tetrahymena* rDNA forms a single minichromosome for amplification. Secondly, there are two different phases of endoreplication: one occurs during early development, and the other one occurs during late development upon refeeding. Thirdly, unlike higher eukaryotes, gene amplification and endoreplication in *Tetrahymena* are not associated with terminal differentiation. After development, progeny switch back to the vegetative cell cycle. Thus, any unresolved DNA structure such as the "onionskin" structure can cause a problem for cell division. Study on distinct replication programs in *Tetrahymena* would shed light on how DNA replication is regulated in specialized replication programs in eukaryotes.

ORC and MCM complexes are dynamically regulated during *Tetrahymena* development (Lee et al, 2015). ORC and MCM levels are upregulated dramatically in early development including postzygotic mitosis and Endoreplication phase I (Endo I). They then drop to their lowest level in Endoreplication phase II (Endo II) during late

development. However, the load for DNA replication in Endo II is high. An ORC-independent mechanism may be utilized for replication initiation. In addition, aberrant replication intermediates have been detected during Endo II, further supporting that the DNA replication program is fundamentally altered.

In the work presented in this chapter, I used quantitative PCR analysis to determine the precise temporal profiles for the copy number change of rDNA and non-rDNA chromosomes during the time windows for rDNA amplification and genome-wide endoreplication during *Tetrahymena* development. DNA fiber analysis was employed to examine the replication features of chromosomes during the different endoreplication stages, which differ with respect to the abundance of ORC and MCM proteins. I find that replication initiates more frequently, but that the rate of replication fork elongation slows down during Endo II, when ORC and MCM protein levels are reduced. I also determined that the aberrantly migrating replication intermediates that I previously observed during Endo II are generated during the vegetative cell cycle in histone monomethyltransferase defective, TXR1Δ strains (Gao et al, 2013). I speculate that the underlying changes in replication in the TXR1Δ are mechanistically related to the changes in the replication program during MAC development.

Results

qPCR analysis of rDNA amplification profile during development

In order to gain insight into the mechanism for rDNA amplification, I started by determining the time window for rDNA amplification during MAC development. qPCR analysis was utilized to quantitatively measure the copy number change of rDNA. Since

the parental MAC still exists in the cell when rDNA amplification occurs in the developing MAC, rDNA molecules in both the parental and progeny MACs could serve as qPCR templates. To eliminate any background signal from the parental MACs, rDNA chromosomes in the developing MAC need to be distinguished. *Tetrahymena* heterokaryon strains containing different polymorphisms in MIC and MAC were used for this purpose, because the developing MAC is generated from the MIC during development. Two heterokaryons, SB1934 and SB4202, both of which contain two polymorphic forms of rDNA: C3 rDNA in the micronucleus and B rDNA in the macronucleus were mated, and genomic DNA was collected at different time points for qPCR analysis. Since there is a 42 bp DNA insertion in C3 rDNA, the primer set for qPCR was designed for specific amplification of C3 rDNA rather than B rDNA, which eliminates all background signal from parental (B rDNA) macronuclei. A primer set which can be utilized to amplify a product specific to the integrate micronuclear rDNA locus was used as a micronuclear genome control. The $2^{-\Delta\Delta Ct}$ method was used for quantification of the rDNA copy number (Livak & Schmittgen, 2001). There are two major periods for rDNA replication: the first period ends at 16 h post-mixing, with the rDNA copy number increases from 2 C to 500 C; the second period occurs after refeeding, when the rDNA copy number increases further from 500 C to 2,000 C in my analysis (Figure 4.1A). Between these two periods, the copy number of the rDNA is maintained at around 500 C, which indicates that no replication occurs after 16 h post-mixing, until cell are re-fed. Whereas there is a 250-fold increase in rDNA copy number

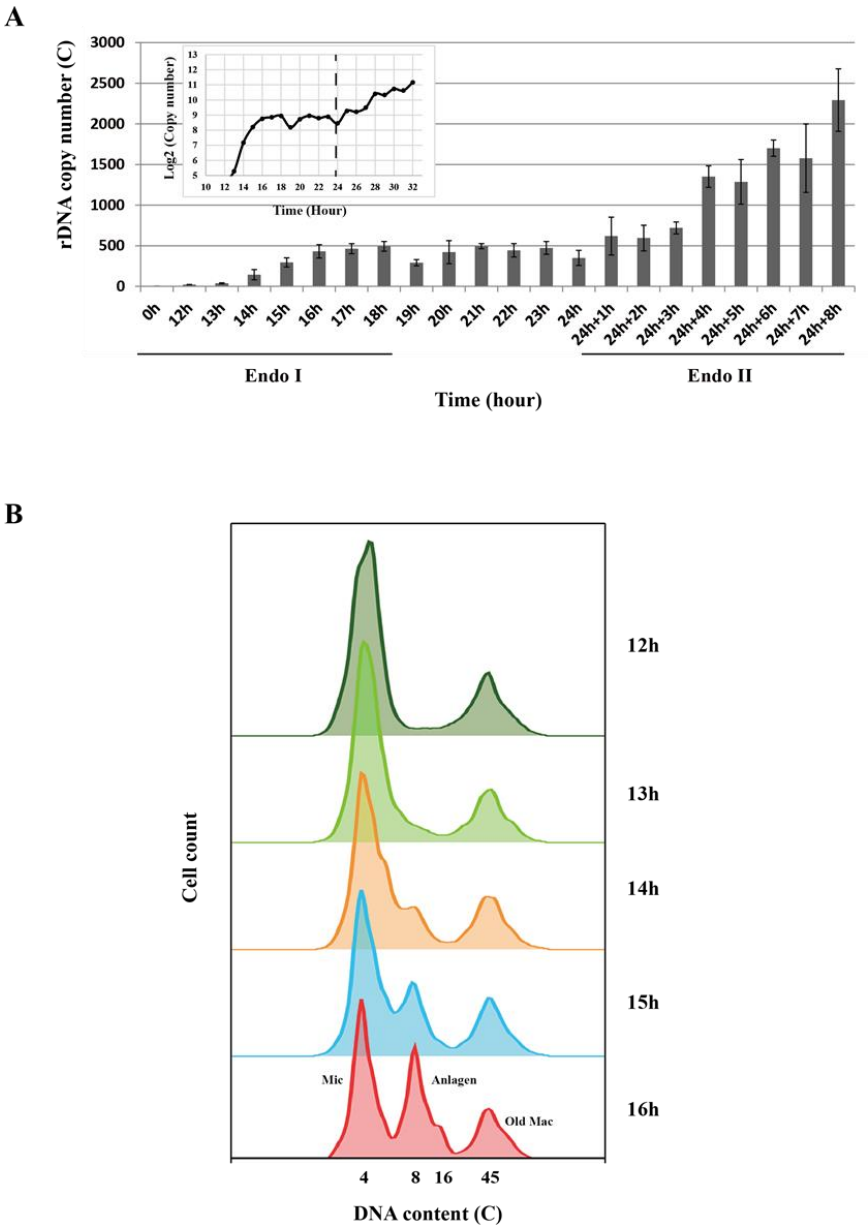

Figure 4.1. rDNA amplification overlaps with Endoreplication I. (A) qPCR analysis on rDNA copy number change during *Tetrahymena* development; Samples were collected at 0 h, 12 h-24 h postmxing. At 24 h, cells were re-fed, and samples were collected at 0 h-8 h after refeeding. rDNA copy number of each sample was normalized to the sample at 0 h post-mixing (4C). Micronuclear genome copy number was used as an internal control for 2-ΔΔCt method. The embedded figure shows the rDNA copy number change in a log2 scale, and the dash line indicates refeeding time. (B) Flow cytometry analysis on genomic DNA content during Endo I; (C) A representative image of EdU labeling of anlagen nuclei. Nuclei was shown in blue color and EdU labeling was shown in red. Cells during Endo I have four nuclei in one cell (the right bottom cell). Two of them are newly generated micronuclei without EdU labeling, and the other two are developing macronuclei with EdU labeling. (D) EdU labeling image showing DNA replication during Endo I.

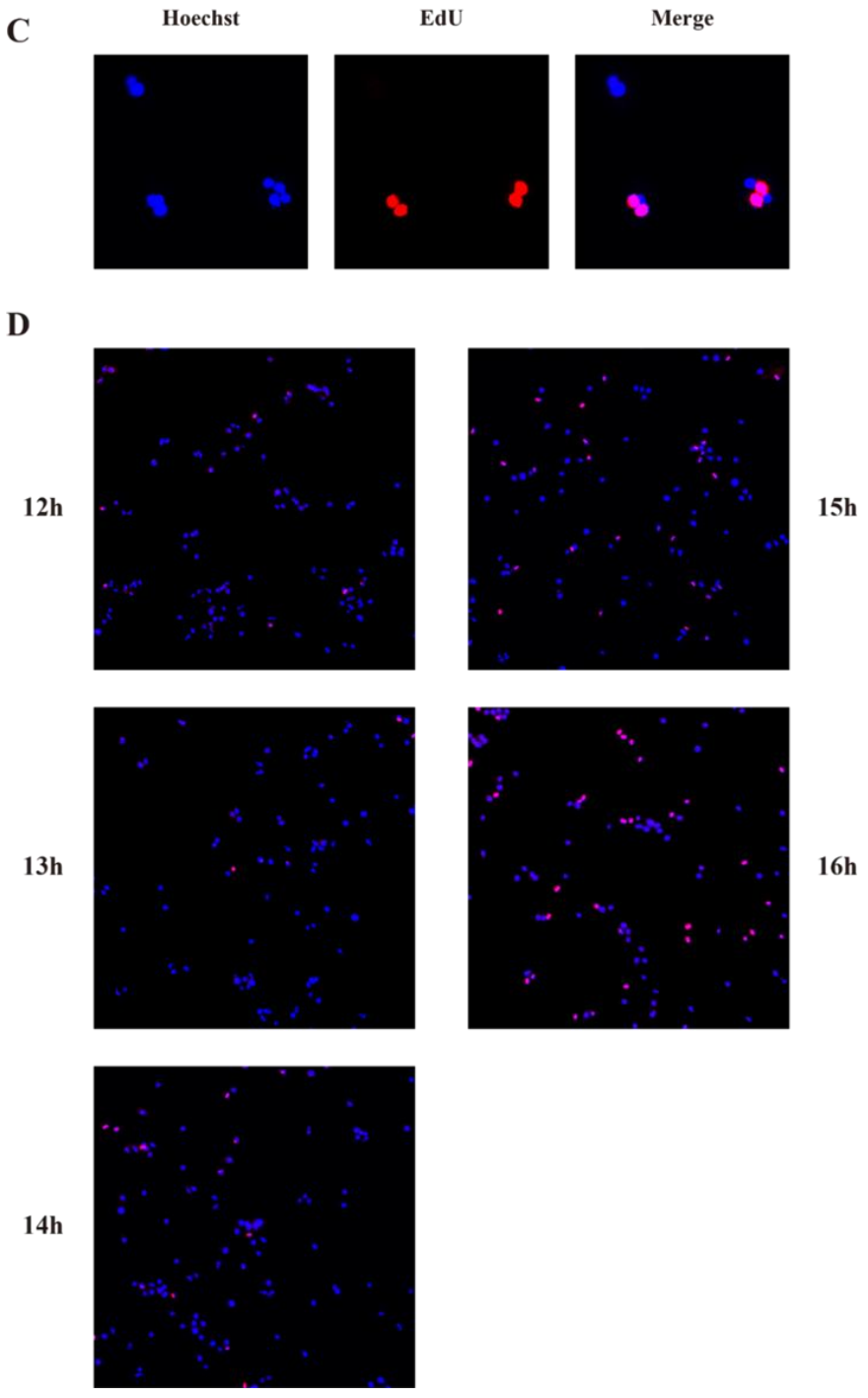

Figure 4.1. Continued.

during the first period, there is only 4 to 5-fold increase after refeeding. In addition, cytophotometric analysis and flow cytometry analysis have shown that genomic DNA signal for bulk DNA increases from 2 C to 16 C during Endo I, and from 16 C to around 32 C-64 C during Endo II (Lee et al, 2015; Yin et al, 2010). qPCR results suggest that the first period of rDNA replication is the actual amplification stage and coincident with Endo I. The second period of rDNA replication during Endo II does not appear to be a bona fide gene amplification since the rate of increase in copy number of rDNA and non-rDNA chromosomes is comparable.

To confirm that the time window of rDNA amplification and Endo I overlaps, a nucleoside analog of thymidine, 5-ethynyl-2'-deoxyuridine (EdU) was used to pulse-label cells to measure active DNA synthesis at hourly intervals during development. At the same time, cells were collected, lysed, stained with propidium iodide (PI), and analyzed by flow cytometry to determine the DNA content of different nuclei. EdU began to incorporate noticeably into macronuclear anlagen at 14 h post-mixing and incorporation increased dramatically during 15 h and 16 h (Figure 4.1C, D). Flow cytometry analysis data showed a similar pattern, the peak of anlagen nuclei appeared at 14 h and increased rapidly from 15 h to 16 h (Figure 4.1B). EdU and flow cytometry data reveal that the timing for genome-wide endoreplication corresponds to the period when the rate of rDNA copy number increase is greatest determined by qPCR. Collectively, the data suggest that rDNA gene amplification and genome-wide endoreplication occur concurrently. A limitation of this experiment is that we measured rDNA by qPCR and non-rDNA abundance by flow cytometry using propidium iodide.

Monitoring rDNA and non-rDNA copy number change simultaneously by qPCR would provide us with more accurate quantitative data and better assess the time window for both replication programs.

Instability of exogenous DNA tags in micronuclear chromosomes

Preliminary data (Figure 4.1) has shown that there are two developmental periods where rDNA minichromosome replication occurs, the first one of which is the actual amplification stage and is coincident with Endo I. The rDNA copy number was determined by qPCR, and non-rDNA content was counted from bulk DNA using flow cytometry. To directly compare increase in copy number in endoreplicating non-rDNA and amplifying rDNA chromosomes, I inserted DNA sequence tags into plasmids carrying copies of rDNA and non-rDNA MAC chromosomes. DNA fragments White1 and White2 from *Drosophila white* gene were used to tag rDNA and non-rDNA chromosomes respectively. These DNA fragments have significantly higher GC content than endogenous *Tetrahymena* seuqences, so they can serve as better qPCR targets for copy number determination. I then introduced these sequences into germline MIC using biolistic transformation. The transformants were first screened by paromomycin resistance provided by a co-transformed plasmid, and then screened by PCR using White1/2 specific primers (Figure 4.3A, B). True transformants were passaged for over 100 fissions to generate sexually mature strains for subsequent use.

Round I genomic exclusion was used to generate heterokaryons (Allen, 1967) (diagramed in Figure 4.2). The heterozygous transformant which contains White1/2 tags

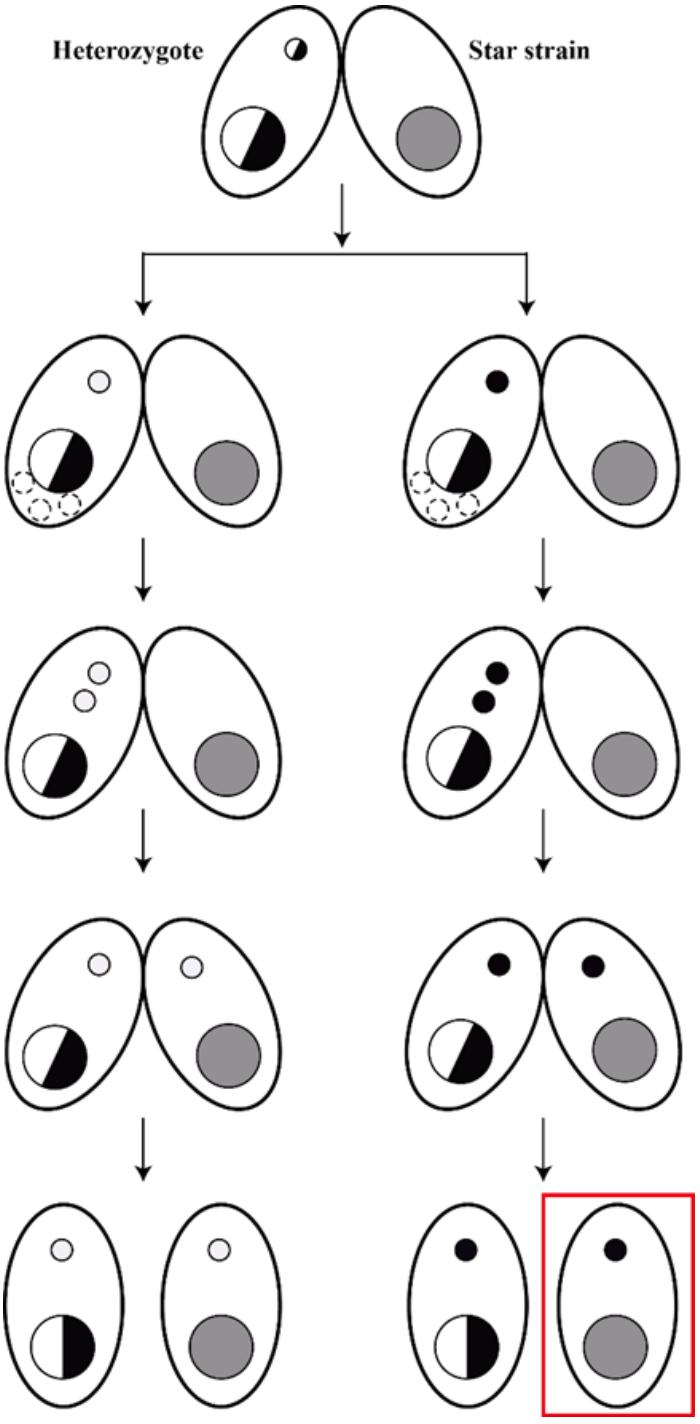

Figure 4.2. Schematic of round I genomic exclusion. The black and white colors stand for two heterozygous alleles. The grey colored circle stands for the MAC of the star strain, which is different from the MAC in the heterozygote. Heterokaryon strain needed is indicated in the red box.

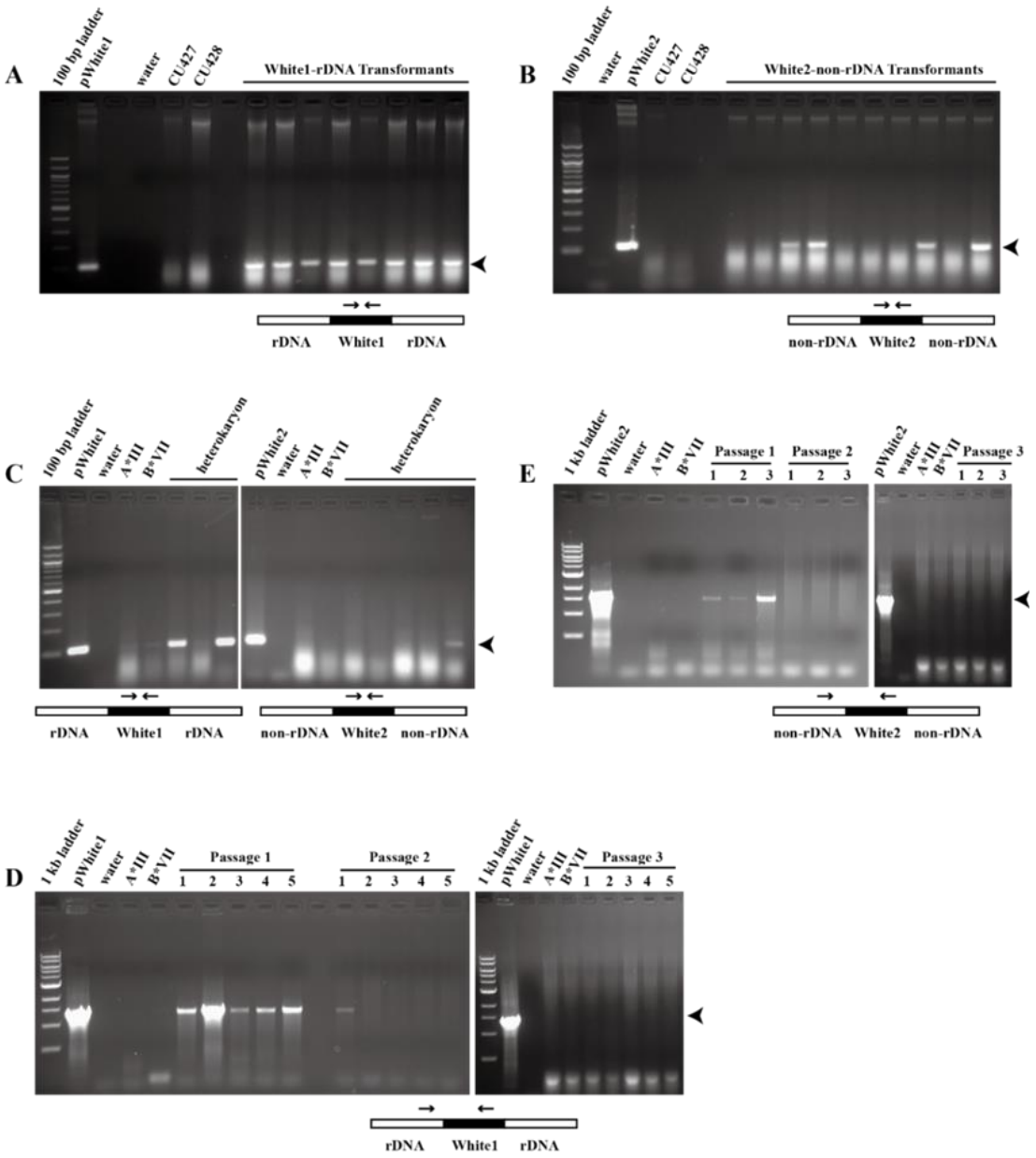

Figure 4.3. Instability of exogenous DNA tags in micronuclear chromosomes in *Tetrahymena.* (A) PCR screening of White1-rDNA transformants. (B) PCR screening of White2-non-rDNA transformants. (C) PCR screening of White1-rDNA and White2-non-rDNA heterokaryons from round I genomic exclusion. (D) PCR analysis of stability of White1 DNA tag in heterokaryons. (E) PCR analysis of stability of White2 DNA tag in heterokaryons. A*III and B*VII serve as the negative controls. PCR primer sets used are indicated below each panel. Numbers indicate different transformant lines in panels A and B, or different clonal lines of heterokaryon in panels D and E. Arrowhead indicates the position of the expected PCR product.

in both MIC and MAC was mated with a star strain which contain a defective MIC. During mating, the White1/2 tagged heterozygous MIC undergoes meiosis and mitosis and is converted into either wild type or White1/2 tagged homozygous MIC. The replica of the nucleus is transferred to the star strain. The MAC in both mating sides were maintained as before. Finally, the star strain side becomes into a heterokaryon which contains homozygous White1/2 tag in the MIC but not in the MAC.

After round I genomic exclusion, the star side was distinguished from the heterozygote side based on their different mating types. Further screening of heterokaryons containing a homozyogous micronuclei with the tagged chromosome was achieved by PCR analysis using White1/2 specific primers. Heterokaryons with White1 tagged rDNA or White2 tagged non-rDNA were successfully created (Figure 4.3C), but the DNA tags were unstable in the strains and lost after the second passage (Figure 4.3D, E). In order to confirm this result, the transformation with White1 tagged rDNA was repeated. Micronuclear specific primers were used this time to distinguish wild type rDNA and tagged rDNA, ensuring that all positive transformants are germline transformants rather than anlagen or somatic transformants. Transformants were used to generate heterokaryons, but no heterokaryon with stable White1 tagged rDNA was successfully created (data not shown). The DNA tag was perfectly maintained in the original heterozygous transformants. Taken together, foreign GC rich DNA tags were successfully inserted into the 3' NTS region of micronuclear rDNA or a non-rDNA chromosome, and they were well maintained in heterozygous transformant lines during the vegetative cell cycle. However, the DNA tags were not able to be maintained in

heterokaryons. These foreign DNA tags may be eliminated from *Tetrahymena* genome through an unknown mechanism (see Discussion). At the same time, many heterokaryons such as the H3.2-GFP strain used later on, have been successfully generated by other researchers. Therefore, elimination of foreign DNA tags from MIC must be selective.

qPCR analysis on rDNA amplification and non-rDNA endoreplication profile during development

Since foreign GC-rich tags cannot be stably maintained in heterokaryons, here I took advantage of two existing heterokaryon strains: SB1934 and H3.2-GFP to perform conjugation (Figure 4.4). As described before, strain SB1934 is a heterokaryon containing C3-specific rDNA sequence in the MIC and B rDNA sequence in the MAC, so specific primers can be used to exclusively amplify the C3 rDNA allele. Strain H3.2-GFP contains the green fluorescent protein (GFP) coding sequence inserted at 3' end of the *hht2* gene to encode a C-terminal GFP tagged histone H3 gene (*HHT2*) (Cui et al, 2006). This *hht2-gfp* cassette exists only in the MIC and not the MAC and the strain was generated by round I genomic exclusion (Allen, 1967). Therefore, it can be used as the qPCR template specifically for assessing copy number changes in a non-rDNA chromosome during macronuclear development. Conjugation between these two strains was performed and genomic DNA was isolated from the mating cells at 2-hour intervals. qPCR analysis was carried out as described before to determine the copy number changes of both non-rDNA and rDNA chromosomes for comparative analysis. Because

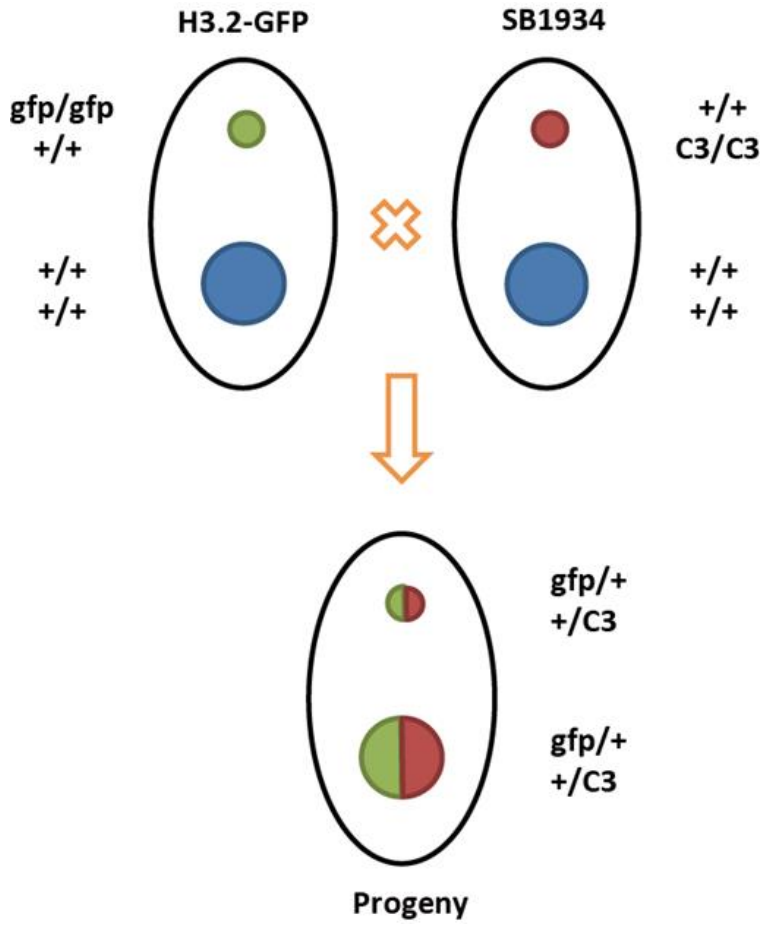

Figure 4.4. Schematic of mating between H3.2-GFP and SB1934.

both *gfp* and C3 sequence exist only in the MIC, there was no background signal from parental MAC during development, which ensured the accuracy of the qPCR analysis.

During first 24 h post-mixing, rDNA copy number increases from 2 C to approximately 550 C (Figure 4.5A). Specifically, rDNA copy number starts to increase from 2 C at 10 h, reaches over 300 C at 18 h, then increases gradually to 550 C between 18 h and 24 h. This data is consistent with previous qPCR results (Figure 4.1A). A slight delay has been seen here, which may be due to lower synchrony of the mating. After refeeding, from 24 h to 32 h, rDNA copy number reaches around 2400 C from 600 C, which is also consistent with previous results (Figure 4.1A). Therefore, based on the copy number change of the rDNA during development, it is confirmed that rDNA copy number is highest early in development. To relate these data to endoreplication time, the change of non-rDNA copy number was also carefully monitored (Figure 4.5A). The non-rDNA copy number starts to increase from 2 C at 12 h, to 4 C at 14 h, 8 C at 16 h. Consistent with 2-hour endoreplication cycles, the increase from 8 C to 16 C takes 8 h (16-24 h). Upon refeeding, the non-rDNA abundance increases to 32 C in an 8 h interval (24-32 h). In other words, there is an 8-fold increase for non-rDNA during Endo I; and 2-fold increase for non-rDNA during Endo II. The overall replication patterns of rDNA and non-rDNA are very similar during the refeeding interval (24-32 h).

In order to better compare the replication rate of rDNA and non-rDNA across development, a simple exponential model $C_t=C_0\ (1+R)^t$, where C_0 is the copy number at the beginning, C_t is the copy number at time t, R is the replication rate, and t is the time, is used to explain the copy number change of chromosomes. A log-linear model can be

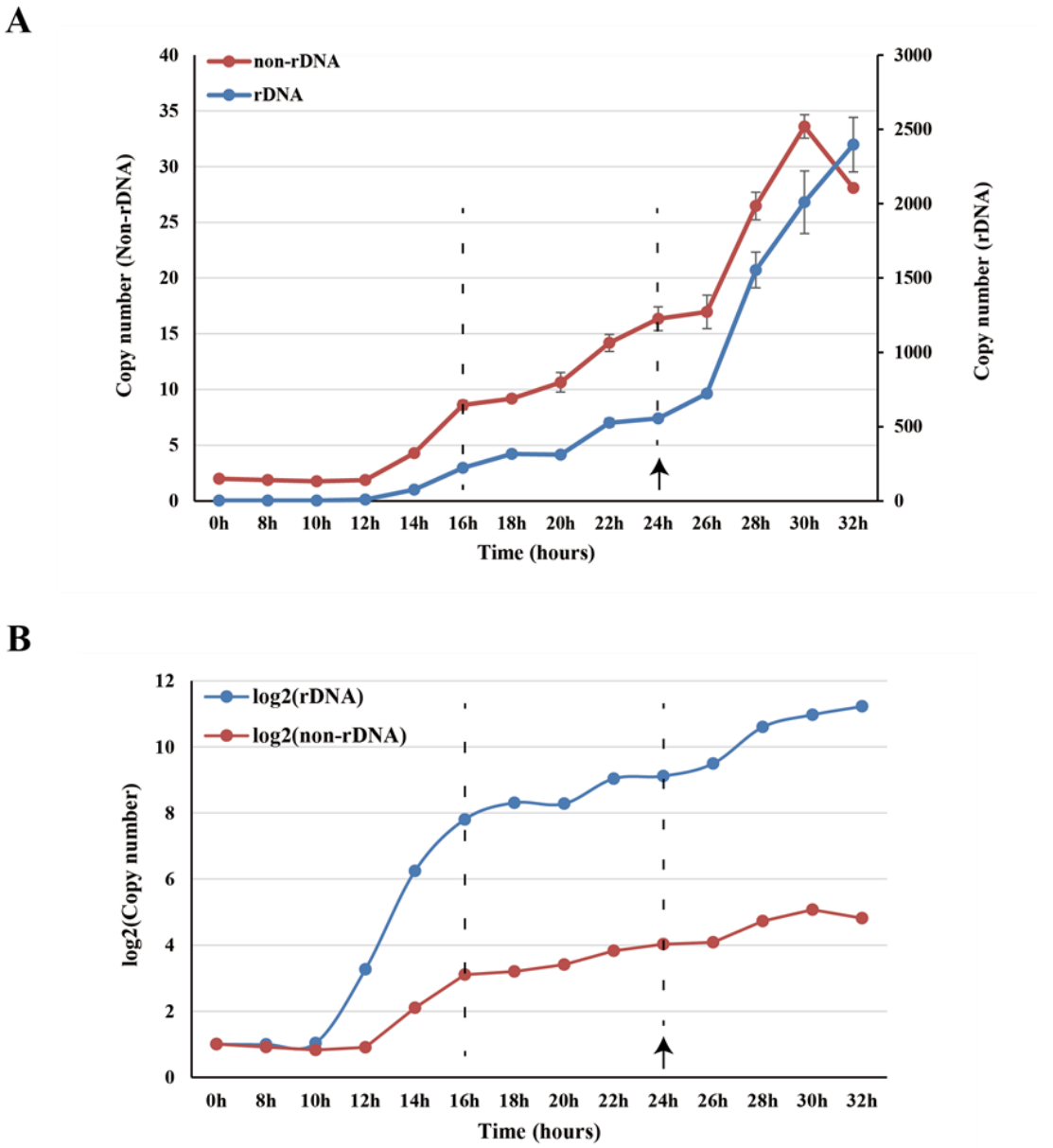

Figure 4.5. Copy number change of rDNA and non-rDNA chromosomes during *Tetrahymena* development. Copy numbers of both rDNA and non-rDNA at 0 h were set as 2 C. (A) Actual copy number change of rDNA and non-rDNA during *Tetrahymena* development. Left Y-axis stands for non-rDNA copy number and right Y-axis for rDNA copy number. SB1934 and H3.2-GFP strains were mated at 0 h, and genomic DNA was collected during conjugation. Cells were re-fed at 24 h (arrow), and were grown an additional 8 h after refeeding (32 h). (B) Log_2 scale of rDNA and non-rDNA copy number in A.

used to estimate replication rate, since $\log_2 (C_t) = \log_2 [C_0] + \log_2 (1 + R)^t$. As shown in Figure 4.5B, the curve from Figure 4.5A was re-plotted in $\log_2$ scale versus time, where the slope of the curve can stand for the replication rate. The fastest replication stage for both rDNA and non-rDNA occurs during early development, specifically, 10-16 h for rDNA and 12-16 h for non-rDNA. However, the replication rate is much higher for the rDNA locus relative to the non-rDNA locus that was examined. In addition, an increase in rDNA copy number is observed two hour earlier than non-rDNA replication (10 h versus 12 h). This argues that rDNA gene amplification precedes non-rDNA endoreplication, and the regulation of rDNA amplification is different from non-rDNA endoreplication. During 16-24 h, the replication rates for both processes are very low. The fold changes for both rDNA and non-rDNA are very modest, which may be a reflection of asynchrony within the population. This apparent plateau may be reflective of depletion of DNA precursors. After refeeding (24-32 h), the replication rate of rDNA and non-rDNA increases, but at a much slower rate than early development. The difference of the two processes becomes less noticeable. Therefore, rDNA replication during late development may employ the same replication mechanism as non-rDNA, specifically endoreplication. Taken together, earlier onset of rDNA indicates differential regulation of rDNA amplification and non-rDNA endoreplication. Similar change pattern of both rDNA and non-rDNA suggests that these two processes are correlated. This brings up the questions: how would gene amplification be affected in an endoreplication defective mutant, and vice versa (see Discussion).

Slow fork movement during Endo II

qPCR analysis on the copy number change of rDNA and non-rDNA chromosomes revealed that the rDNA is selectively amplified early in development (Endo I), and rDNA molecules are subsequently replicated by the same mechanism as non-rDNA chromosomes late in development (Endo II). In addition, aberrant replication intermediates (RIs) appear in rDNA molecules during Endo II, and the 5' NTS origin is passively replicated in sub-population of rDNA molecules (Lee et al, 2015). Moreover, the protein levels of ORC and MCMs are lowest in Endo II. These results inspired us to investigate the regulation of replication initiation and elongation on a genome-wide scale by DNA fiber analysis.

In DNA fiber analysis, the average distance between two adjacent firing origins can be measured. By studying many individual DNA fibers, we can determine whether there is a change of the overall origin density in the endocycling MAC. Furthermore, the length of a single labeled track can be used to assess the fork velocity (see Material and Methods). Three samples, one from late Endo I and the other two from Endo II, have been collected for both inter-origin distance and fork velocity analyses. The median inter-origin distances for vegetative S phase, late Endo I (15.5 h), early Endo II (3.5 h after refeeding) and late Endo II (6.5 h after refeeding) are 26.9, 24.2, 23.8, and 24.5 kb respectively (Figure 4.6A), and the average IODs are 29.5 ± 13.7, 27.7 ± 14.8, 25.3 ± 10.8, and 25.5 ± 11.6 kb. In general, the IOD decreases by approximate 10% in endoreplication compared to vegetative S phase, suggesting more origins are utilized during late endoreplication. This difference is statistically significant, which was

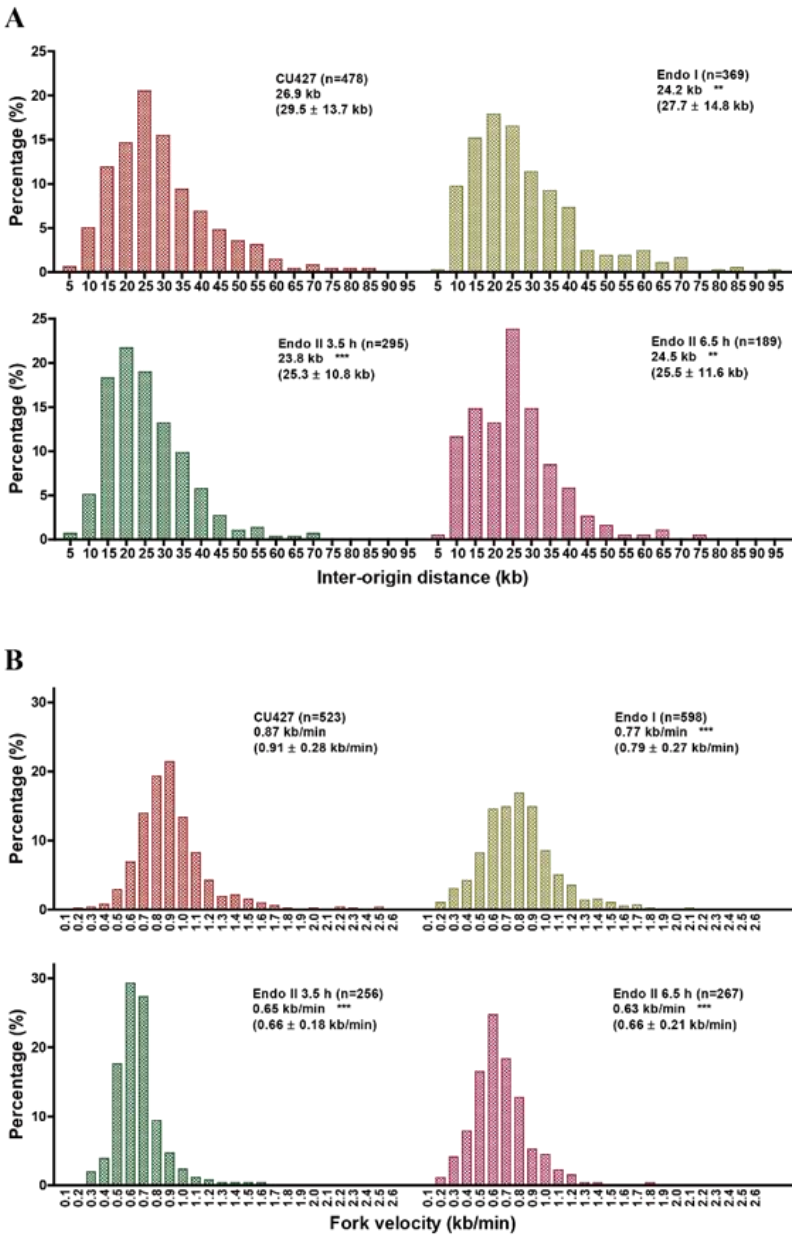

Figure 4.6. DNA fiber analysis on endoreplicating cells. The mating culture from CU428 x CU427 at different developmental stages was collected for the analysis. Endo I, cells were labeled at 15.5 h post-mixing; Endo II 3.5 h and 6.5 h, cells were labeled respectively at 3.5 h and 6.5 h after refeeding. Log phase CU427 was used as a control. (A), Inter-origin distance (IOD) comparison between log phase and endoreplicating cells. (B), Fork velocity comparison between log phase and endoreplicating cells. The frequency distribution of DNA fibers with different IODs or fork velocities is presented. For each group, the median IOD or fork velocity is indicated. The mean with S. D. is indicated in parenthesis. n, the total number of DNA fibers scored. Statistical significance was determined using the Kruskal-Wallis test followed by Dunn's test. Each sample from endoreplicating cells is compared to log phase CU427. **, $p < 0.01$; ***, $p < 0.001$.

determined by the Kruskal-Wallis test. In addition, there is no difference in IODs among the three samples from different stages of endoreplication, indicating that changes in origin utilization might be started in late Endo I. Downregulation of ORC and MCM proteins during late Endo I is consistent with this hypothesis (Chapter II, Figure 2.9).

The median fork velocities for vegetative S phase, Endo I, early Endo II and late Endo II are 0.87, 0.77, 0.65, 0.63 kb/min respectively, and the average fork velocities are 0.91 ±0.28, 0.79 ±0.27, 0.66 ±0.18, 0.66 ±0.21 kb/min (Figure 4.6B). Therefore, the fork velocity in late Endo I is 11% slower than the fork velocity in vegetative S phase (Figure 4.6B, upper-right panel vs. upper-left panel). This difference is extended to 25%-28% in Endo II (Figure 4.6B, bottom-left and bottom-right panels). These data suggest that fork velocity is gradually reduced during *Tetrahymena* development, which is supported by the previously observed result that MCM protein levels are gradually decreasing from late Endo I to late Endo II (Chapter II, Figure 2.9). In addition, aberrant rDNA replication intermediates show up as early as 16 h (Chapter II Figure 2.11), which falls into the late stage of Endo I. Taken together, these data suggest that alteration in origin usage and fork elongation exists not only in rDNA molecules but also in the entire non-rDNA genome.

rDNA RIs of log phase TXR1Δ resemble those of WT Endo II

In collaboration with Yifan Liu's group, we previously identified aberrant replication intermediates (RIs) in a strain TXR1Δ, which is defective in histone H3K27 monomethylation (Gao et al, 2013). This mutant exhibits a defect in replication fork elongation and generates extensive mass of single stranded DNA (ssDNA) during S

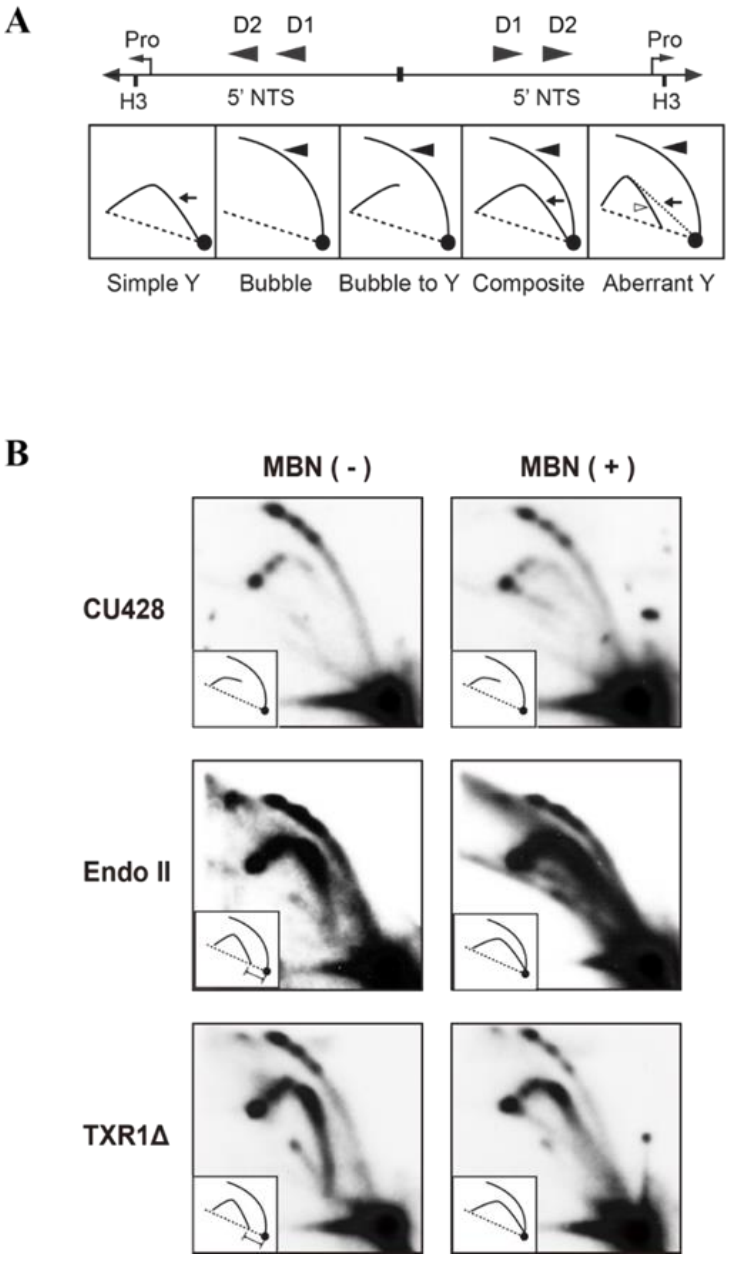

Figure 4.7. Two-dimensional gel analysis of rDNA replication intermediates (RIs) in TXR1Δ cells. (A). Schematic of the rDNA 5'NTS fragment generated by restriction digestion used for 2D gel in (B). H3, Hind *III* digestion sites; D1 and D2, domain I and domain II, containing the rDNA replication origins; Pro, promoter of the rDNA gene. Different types of RIs may be detected by 2D gel analysis: simple Y (arrow), replication from outside of 5'NTS (passive replication); bubble (filled arrowhead) or bubble to Y, replication inside of 5' NTS (active replication); composite, both active and passive replication of 5' NTS; aberrant Y (unfilled arrowhead), simple Y containing partially replicated DNA. Diagonal dashed line, migration of linear duplex DNA fragments; dotted arc, reference pattern for simple Y. (B) 2D gel analysis on untreated and mung bean nuclease (MBN) digested rDNA RIs in CU428 log phase, Endo II and TXR1Δ log phase cells.

phase presumably by uncoupling helicase activity from the polymerase. Aberrant rDNA RIs were detected in vegetative TXR1Δ. By comparing aberrant rDNA RIs in TXR1Δ and Endo II, I found that the migrating patterns were very similar (Figure 4.7). Mung Bean nuclease digestion followed by 2D gel analysis shows that the migration of rDNA RIs (pre-treated with RNase A) in both TXR1Δ and Endo II changes, indicating ssDNA or RNA-DNA hybrids are generated at the replication fork in both cases. It seems that the TXR1Δ has more of these aberrant RIs than is seen in the Endo II sample. In addition, after Mung Bean nuclease treatment, a portion of aberrant RIs were converted into simple Y arcs, indicating passive replication occurs in a sub-population of rDNA molecules in both the TXR1Δ vegetative S phase and endoreplicating wild type cells. Collectively, these data confirm that there are single stranded regions in the 5' NTS of the rDNA in TXR1Δ. It is possible that RIs detected in Endo II are generated by the same mechanism as the RIs in TXR1Δ log phase cells.

Altered replication initiation and elongation in TXR1Δ

Previous experiments to study replication initiation and elongation in TXR1Δ strains relied on 2D gel analysis to assess replication initiation and elongation in just the rDNA minichromosome. These experiments revealed that ssDNA accumulates at 5' NTS of rDNA in TXR1Δ, and passive replication occurs in a sub-population of cells. However, there are limitations to this approach. First, only a specific rDNA locus was measured. Secondly, fork elongation was not quantitatively measured. In order to explore the genome-wide change in replication in TXR1Δ cells, DNA fiber analysis was employed to study origin utilization and fork elongation. The median IODs in vegetative

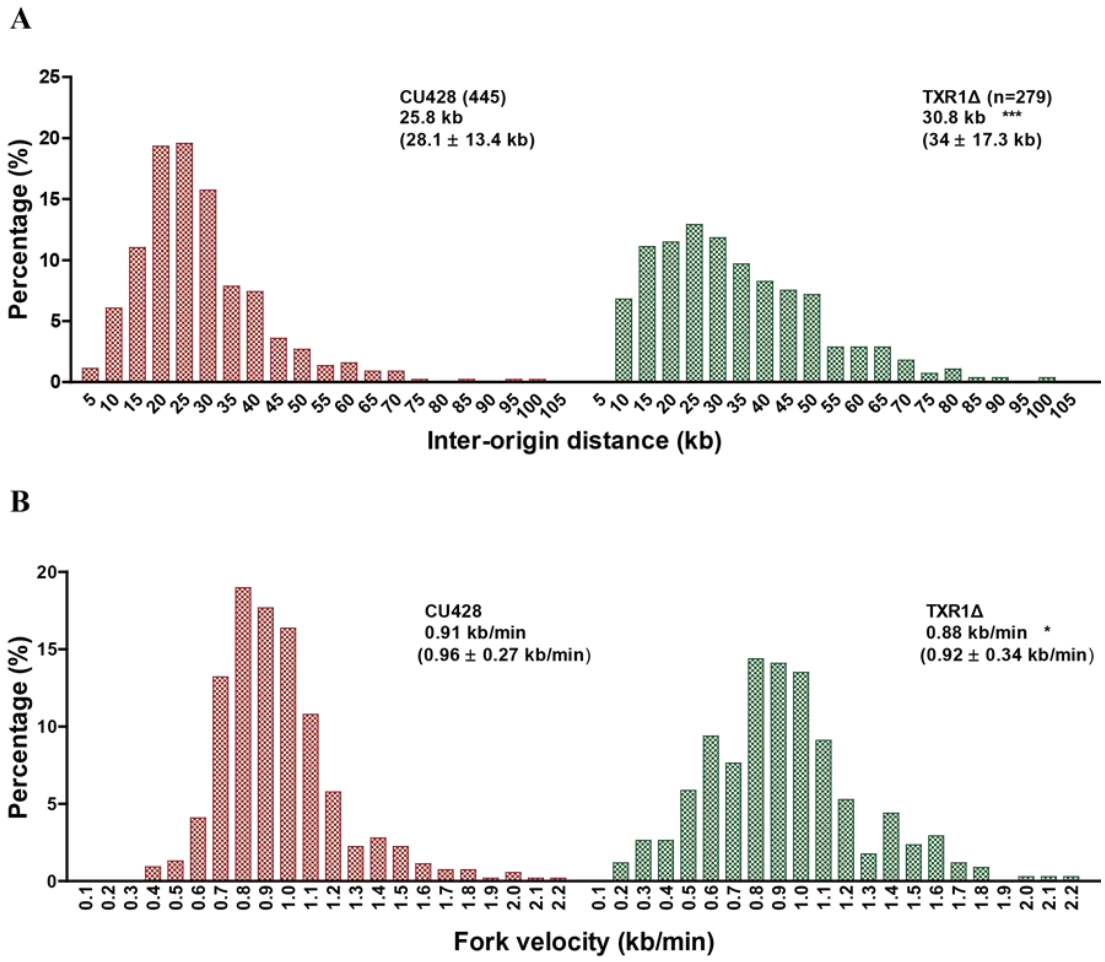

Figure 4.8. DNA fiber analysis on TXR1Δ cells. (A), Inter-origin distance (IOD) comparison between WT and TXR1Δ cells. (B), Fork velocity comparison between WT and TXR1Δ cells. The frequency distribution of DNA fibers with different IODs or fork velocities is presented. For each group, the median IOD or fork velocity is indicated. The mean with S. D. is indicated in parenthesis. n, the total number of DNA fibers scored. Statistical significance was determined using the Mann Whitney test. *, $p \leq 0.05$; **, $p < 0.01$; ***, $p < 0.001$.

S phase of wild type cells and TXR1Δ cells are 25.8 kb and 30.8 kb respectively, and the average IODs are 28.l ± 13.4 kb and 34 ± 17.3 kb (Figure 4.8A). Compared to wild type cells, IOD increases by 19% in TXR1Δ. Within 20-30 kb size range, there are 14% fewer fibers in TXR1Δ compared to the wild type strain. However, there are 15% more fibers that are over 40 kb in the TXR1Δ strain. These data suggest that fewer origins are used in TXR1Δ than wild type. For fork movement, the median fork velocity in TXR1Δ is 0.88 kb/min (the average fork velocity is 0.92 ± 0.34 kb/min), and the median fork velocity in the wild type strain is 0.91 kb/min (the average fork velocity is 0.96 ± 0.27 kb/min) (Figure 4.8B). Although the difference of the fork velocity is small, TXR1Δ has more forks with lower speed (Figure 4.8B, 14% more in 0-0.7 kb/min range while 16% fewer in 0.7-1.2 kb/min range in TXR1Δ), indicating that replication elongation is affected at some but not all elongating forks. This result is correlated with the 2D gel result that passive replication occurs in a sub-population of rDNA molecules. In conclusion, DNA fiber analysis revealed that replication initiation and elongation are altered in TXR1Δ strains.

Discussion

The model organism *Tetrahymena thermophila* has been used in our group to study many aspects of DNA replication. Unique features of this model system make our study possible: the co-habitation of two functionally distinct nuclei in a single cell, two different life cycles-vegetative cell cycle and conjugation, and distinct replication programs during development. In this chapter, several questions related to developmentally regulated DNA replication programs in *Tetrahymena* have been

investigated. The temporal window for rDNA amplification relative to other DNA replication programs, specifically endoreplication was determined. The initiation program for rDNA replication during Endo II is distinctly different from rDNA amplification and vegetative replication program. Besides rDNA chromosomes, differentially regulated DNA replication exists in non-rDNA chromosomes during Endo II.

Interdependence between rDNA amplification and endoreplication

The precise profile of the copy number change for rDNA and non-rDNA chromosomes has been quantified throughout macronuclear development. The changing features of the respective rDNA and non-rDNA copy number have several implications. First, selective amplification of the rDNA mainly occurs during early development. Although the rDNA copy number still increases after cells are refed, the replication rate is much slower. It is probable that rDNA replication after refeeding is governed by the same set of rules as non-rDNA chromosomes. Secondly, rDNA amplification starts prior to the onset of endoreplication of non-rDNA chromosomes. This is different from the amplification of the chorion genes in *Drosophila* follicle cells, where several rounds of endoreplication precede locus-sepcific gene amplification and genome-wide endoreplication is repressed when only locus-specific gene amplification occurs (Calvi et al, 1998). Thirdly, rDNA amplification and endoreplication plateau at the same time, indicating these two processes are likely to be co-regulated.

It is still unknown whether rDNA amplification is dependent on non-rDNA endoreplication, and vice versa. The Anlagen Stage Induced 2 (ASI2) gene is

developmentally regulated in *Tetrahymena* and encodes a putative signal transduction receptor. ASI2 is up-regulated during macronuclear development and endoreplication is arrested in the ASI2 knockout mutant (Li et al, 2006; Yin et al, 2010). In order to check rDNA amplification in cells in which Endo I is blocked, somatic ASI2 knockout strains with C3 rDNA in MIC were generated. C3 rDNA from developing MAC could be exclusively monitored by qPCR. However, the MIC in these knockout strains shows instability. Micronuclear specific targets used for internal controls for macronuclear rDNA were missing in MIC determined by qPCR analysis. As an alternative approach, siRNA directed ASI2 knockdown could be utilized to solve this problem. The rDNA amplification-defective *rmm11* mutants can be used to determine effect on endoreplication when rDNA amplification was blocked. These mutants are heterokaryons with C3 rDNA in MIC and B rDNA in MAC, so qPCR analysis can be used to monitor rDNA copy number, and flow cytometry analysis and DAPI staining can be utilized to determine whether endoreplication is impaired.

rDNA amplification timing and mechanism

Unlike chorion gene amplification in *Drosophila* follicle cells, where origin firing and elongation are temporally separated (Claycomb et al, 2004; Claycomb et al, 2002), continuous origin firing and elongation were detected during rDNA amplification in *Tetrahymena*. This is supported by the observation the same replication rate is maintained during the amplification window in starved, mating cells. However, the overall time window for rDNA amplification is still tightly controlled during development. This is supported by previous study on a mutant strain *rmm11* (Kapler &

Blackburn, 1994). This strain contains a point mutation on the cis-element required for excision of rDNA from micronuclear locus. The severe amplification defect was caused by the point mutation which delays rather than blocks the rDNA excision. This delay could cause the excised rDNA to miss the time window for amplification. In addition, the replication rate of rDNA replication during Endo II is much lower, and separated from rDNA amplification by a plateau. I speculate that lack of nutrients and dNTPs for replication is the reason for appearance of the plateau. If the progeny are re-fed early, the rDNA may be amplified to a higher degree since the late replication event of the rDNA is now pushed into the time window for amplification.

What is the mechanism for the selective amplification of rDNA? Previous study has shown that *Tetrahymena* ORC contains an integral RNA subunit mediating ORC binding to the rDNA chromosome by base pairing to the complementary sequence, but such sequence does not exist on the non-rDNA chromosome (Donti et al, 2009; Mohammad et al, 2007). Thus, one hypothesis for rDNA amplification mechanism is that the specific binding manner of ORC to rDNA determines the selective amplification of rDNA but not non-rDNA chromosomal DNA replication during development. In order to test this hypothesis, the type I element from 5' NTS of rDNA has been cloned, inserted into the ARS1 replicon on a plasmid and the chimeric plasmid was transformed into *Tetrahymena* during development. As a result, the type I element was not able to confer the amplification ability of the rDNA to the non-rDNA autonomously replicating sequence (data not shown). However, whether there is any inhibitory element in the episome is unknown.

The second hypothesis of rDNA amplification is that the palindromic structure of the rDNA chromosome is required for amplification. One rationale behind this hypothesis is that palindromic structure is unique for the rDNA molecule but does not exist on the non-rDNA chromosomes. An 11 kb molecule containing a single copy of rDNA has been detected during development, but relative amount is low compared with the 21 kb palindromic rDNA molecule based on Southern blot results (Pan & Blackburn, 1981). The 11 kb molecule may be the intermediate or by-product generated during rDNA amplification. Although the 11 kb rDNA molecule has the ability to autonomously replicate, whether it can be amplified without forming the palindromic structure is still unknown. Quantitative analysis on the copy number of the 11 kb molecule during development would provide useful information on the mechanism of rDNA amplification. In addition, palindromic structure is formed and required during gene amplification in budding yeast and human cells (Rattray et al, 2005; Tanaka et al, 2007a). Whether a similar mechanism is employed by *Tetrahymena* for rDNA amplification needs to be tested further.

Another model to explain rDNA amplification in *Tetrahymena* is the RFB-dependent rDNA amplification model, which has been proposed for rDNA amplification in *S. cerevisiae* (Ganley et al, 2009). Fob1 (replication fork blocking) protein is an essential trans-acting factor required for rDNA amplification (Kobayashi et al, 1998; Kobayashi & Horiuchi, 1996). Fob1 binds at RFB and induces a double strand break (DSB) which in further leads to copy number change of rDNA. In *Tetrahymena*, an RFB was identified near the center of the palindrome, and it is activated only during rDNA

amplification (Zhang et al, 1997). It is possible that RFB is required for rDNA amplification. In an RFB mutant, a fragile site is generated in micronuclear genome and the rDNA locus is lost, so macronuclear rDNA chromosome cannot be generated (Yakisich & Kapler, 2006). To test this model, specific trans-acting factors which bind RFB need to be identified.

Replication initiation and elongation of Endo II

Previous study indicates that passive replication occurs in a sub-population of rDNA molecules during Endo II (Lee et al, 2015). Here change of genome-wide origin usage was determined, and slightly higher origin density was detected. This result is surprising because both the levels of Orc1p and Mcm6p are lowest in Endo II. In *Drosophila* follicle cells, endoreplication can occur normally when Orc1 or Orc2 is depleted (Park & Asano, 2008). I propose that ORC-independent replication initiation might be exploited during Endo II. In addition, genome-wide fork elongation was also tested, the average fork rate in Endo II is slower than vegetative cell cycles. With lower level of Mcm6p (Lee et al, 2015), we anticipated that replication forks would move more slowly, similar to ORC1 mutant strains that I examined during the vegetative cycle. Studies from rDNA replication in Endo II have shown that aberrant replication intermediates accumulate, and these RIs are sensitive to Mung Bean nuclease digestion, indicating single stranded regions exist in RIs (Alzu et al, 2012). I speculate that the aberrant RIs are related to slow fork elongation. It is important to test whether these aberrant RIs exist in non-rDNA chromosomes.

Similar aberrant rDNA RIs was also detected in log phase TXR1Δ (Gao et al, 2013). These aberrant RIs are sensitive to Mung Bean nuclease, indicating the single stranded DNA exist in rDNA RIs. Reduce monomethylation level of histone H3 lysine 27 in TXR1Δ may change nucleosome assembly around origins to affect origin utilization. As a result, moderate decrease of the origin density was observed in TXR1Δ. Recent study in *Tetrahymena* on DNA replication under genotoxic stress has shown that global changes in the acetylation status of histone H3 occurs upon hydroxyurea (HU) treatment (Chapter III, Figures 3.6C and 3.7C). Decreased histone H3 acetylation has been detected in HU-treated cells where Orc1 and Mcm6 levels are extremely low. Low levels of these proteins remain in the first S phase after HU removal. rDNA molecule utilizes a dormant origin, and the genome-wide origin density decreases. I postulate that acetylation level of histone H3 probably has not resumed, and altered chromatin compaction affects origin utilization. Here the change of another epigenetic marker (H3K27me1) leads to similar change on origin usage. Whether monomethylation of H3K27 changes under genotoxic stress needs to be investigated. Furthermore, although average fork rate does not change, TXR1Δ has more short elongating fibers. I speculate that a portion, but not all, of the elongating forks move more slowly.

Reasons behind slow replication in Endo II

It is comprehensible that replication forks move more slowly in TXR1Δ, where the epigenetic status of chromosomes is disturbed. However, why do replication forks move slowly during Endo II? Since macronuclear development is the process to generate fully functional euchromatic MAC from a heterochromatic MIC precursor, chromatin

epigenetic status such as histone H3 K27 monomethylation might still not well established during Endo II. To test whether aberrant rDNA RIs and slow fork rates in Endo II and TXR1Δ are attributed to the same mechanism, monomethylation level of H3 K27 on rDNA molecules can be tested by ChIP assay during Endo II.

Another possible reason for slow replication in Endo II is that replication and transcription compete with each other. During Endo II, cells are still in juvenile stage. On one hand, cells are endoreplicating to increase the copy number of chromosomes; one the other hand, cells need to transcribe genes to generate plenty of RNAs, which are then translated into proteins. Cells need to coordinate massive replication and transcription processes, and one or both processes might be compromised to some extent. This hypothesis is supported by the following findings. In *S. cerevisiae*, RNA helicase senataxin is involved in coordinating replication fork movement with transcription (Alzu et al, 2012). In senataxin mutant, aberrant RIs with RNA-DNA hybrids accumulate. These RIs show similar aberrant Y arcs with rDNA RIs in Endo II by 2D gel analysis, and are sensitive to RNase/MBN digestion. Therefore, I speculate that competition between massive replication and transcription might cause slower replication of Endo II than log phase cells, and aberrant RIs may accumulated temporarily. This model can be tested by blocking transcription by adding RNA polymerase inhibitors to mating cells.

Genome surveillance of Tetrahymena *micronucleus*

To serve specific experimental purposes, foreign DNA is often introduced into the micronuclear or macronuclear genome of *Tetrahymena*. However, it has been

reported that foreign DNA can be eliminated from *Tetrahymena* (Liu et al, 2005; Yao et al, 2003). RNA-guided elimination is employed to prevent foreign DNA from integrating into somatic genome during development. This is similar to the elimination of endogenous IESs during macronuclear development. Non-coding RNAs are generated from MIC, and transported into old MAC to scan the macronuclear genome. RNAs that cannot base pair with the macronuclear genomic DNA are kept and migrated to the anlagen MAC to eliminate IESs and foreign DNA. The degree of elimination of foreign DNA depends on the position inserted and the dosage of the DNA sequence (Liu et al, 2005). The elimination of foreign DNA that I observed in this work is a different situation. It occurs during vegetative cell cycle rather than conjugation, and occurs in MIC not MAC. Two DNA fragments from *Drosophila white* gene were inserted into two different positions of micronuclear genome, and both are unstable in heterokaryons. This indicates that the intrinsic feature of the DNA tags determines the instability rather than the positions of their insertion. Moreover, the DNA tags were surprisingly stable in the heterozygote. This raises two hypotheses for the mechanism of elimination. The first hypothesis is that the DNA tags become unstable when they are homozygous in MIC. If the hypothesis is true, strains that are homozygous for the DNA tag in the MIC will not be obtained. This can be tested by mating with two tagged heterozygous strains. Clonal lines could be established from the progeny, and PCR analysis with MIC specific primers would be utilized to distinguish the wild type rDNA locus and the tagged rDNA locus. If the DNA tag can be stably maintained in homozygous status, I expect three quarters of the progeny have at least one copy of the DNA tag, and one third of which

has both copies of the DNA tag in MIC. The second hypothesis is that a similar RNA-guided elimination mechanism exists in mitotic cell cycle to secure the MIC. The non-coding RNAs are generated from the macronuclear genome, and transported into MIC to scan the DNA sequences that do not exists in MAC. However, it is unknown how cells distinguish foreign DNA from endogenous IESs. The higher GC content of the DNA tags might be recognized. Further investigation could be performed to answer these questions. Heterokaryon strains are valuable and often used by researchers. For example, lethal mutations can be preserved in these strains. Therefore, researchers should be aware of the issues discussed here, when using heterokaryon strains.

Material and methods

Tetrahymena *culture and strains*

Tetrahymena strains were cultured in 2% PPYS media (2% proteose peptone, 0.2% yeast extract, 0.003% sequestrine) at 30ºC. 250 μg/ml penicillin, 100 μg/ml streptomycin and 250 ng/ml amphotericin B (Antibiotic-Antimycotic, Life Technologies) was added to prevent cell culture contamination. For starvation, *Tetrahymena* cells were collected from log phase culture, washed twice with 10 mM Tris-HCl (pH 7.4), and starved in the same buffer supplemented with 250 μg/ml penicillin, 100 μg/ml streptomycin and 250 ng/ml amphotericin B for 18 h. For mating, *Tetrahymena* cells were starved 18 h described, mixed with equal number at the final cell density of 2.5 x 10^5cell/ml and then incubated under stationary conditions at 30ºC.

All *Tetrahymena* strains used in this study are listed in Table 4.1.

Table 4.1. *T. thermophila* strains used in this study.

strain	Micronuclear genotype	Macronuclear phenotype
CU427	chx1-1/chx1-1	paromomycin-sensitive cycloheximide-sensitive
CU428	*mpr1-1/mpr1-1*	paromomycin-sensitive 6-methylpurine-sensitive
B2086		paromomycin-sensitive
SB1934	rDNA [C3]/rDNA [C3]; mpr1-1/mpr1-1	paromomycin-sensitive 6-methylpurine-sensitive rDNA [B]
SB4202	pmr1[C3]-1/pmr1[C3]-1; CHX1[C3]/CHX1[C3]	paromomycin-sensitive cycloheximide-resistant rDNA [B]
g-H3.2+GFP-3	hht2[3'neo2, GFPc] / hht2[3'neo2, GFPc]	paromomycin-sensitive
A*III	star	Wild type
B*VII	star	Wild type

Biolistic transformation

Tetrahymena biolistic transformantion were performed according to standard protocols (Bruns & Cassidy-Hanley, 2000; Chalker, 2012). For vegetative transformation, cells were starved before transformation. For germline and macronuclear anlagen transformation, cells were starved and mated. Germline transformation were normally performed at 2.5 to 4 h after mixing cells, with the feature of crescent micronuclei, while macronuclear anlagen transformation were carried out at 8 to 10 h, with the feature of two micronuclei and two anlagen macronuclei in a single cell. The exact timing for transformation was determined by monitoring mating pairs by acridine orange (0.001%) staining under a fluorescence microscope.

DNA were coated onto gold particles (0.6 μm, Biorad) based on the standard protocol (Bruns & Cassidy-Hanley, 2000; Chalker, 2012), washed with 70% EtOH, and resuspended in 100% EtOH. DNA-coated gold particles were distributed onto the center of the macrocarrier (microparticle carrier disk, Biorad) and the particles were completely dried by ambient exposure and placed onto the surface of the macrocarrier. The macrocarriers were immobilized into the Hepta adaptor of the PDS-1000 / He™ and Hepta™ Systems (Biorad). Cells were collected by centrifugation at 3,000 rpm for 2 min, washed once with 10 mM Tris-HCl, resuspended in 1 ml of 10 mM HEPES (pH 7.5), and equally distributed onto a sterile Whatman filter paper pre-wetted with 1 ml of 10 mM Tris-HCl (pH 7.4). The Whatman paper was supported by a 100 mm diameter petridish. The petridish was placed in the chamber of the PDS-1000 / He™ and Hepta™ Systems, then the gold particles coated with DNA were introduced into *Tetrahymena*

cells by firing the biolistic bombardment according to the manufacturer's instructions (Biorad). After transformation, the cells were transferred into 10 ml Tris-HCl (pH 7.4) and incubated at 30^{o}C for approximately 18 h to complete development. The cells were then re-fed with equal volume of 4% PPYS, and incubated at 30^{o}C with shaking (100 rpm) for 6 h before adding selective drugs.

Construction of micronuclear White1/2 tagged rDNA/non-rDNA cell lines

Plasmid pD5H8 were used to generate *Drosophila white* gene fragment tagged rDNA (3' NTS region). This plasmid contains a NotI restriction site at 3'NTS of the rDNA (Gaertig & Gorovsky, 1992). *White* gene DNA fragment designated White1 was cloned by PCR and inserted into the NotI site. SphI and SalI were used to release the White1 flanked with rDNA for *Tetrahymena* transformation. To tag the non-rDNA chromosome, another DNA fragment from *White* gene named White2 was inserted into plasmid pCR2.1 containing the flanking DNA sequence from 3' NTS of a 38 kb target chromosome (NCBI, Nucleotide: Scf_8254072). KpnI and Xho I were used to release the White2 with the flanking sequence for transformation.

The pNeo4 plasmid contains a codon-optimized *neo* (neomycin phosphotransferase) gene (Mochizuki, 2008), 5' flanking region of metallothionein (MTT1) gene including an inducible MTT1 promoter. Upon $CdCl_2$ induction, *neo4* gene is expressed and confers paromomycin resistance. 3' flanking region of endogenous MTT1 gene was cloned and inserted into 3' end of the *neo4* gene to generate plasmid pNeo4-3' MTT1, so *neo4* gene would be targeted for integrating into micronuclear copy

of the MTT1 locus after transformation by homologous recombination and be expressed under MTT1 promoter in the progeny macronucleus.

Germline transformations were performed 3-4 h after mixing CU428 and B2086 strains, White1/White2 tagged DNA fragments were co-transformed with pNeo4-3' MTT1 into *Tetrahymena* cells. After recovery from transformation, 1.0 μg/ml $CdCl_2$ was added into the culture to induce *neo4* expression for 2 h. Paromomycin (100 μg/ml) was then added to kill the non-transformed cells. Further screening of the White1/2 transformants were done by PCR analysis using White1/2 specific primers.

Single cell isolates were generated from positive transformants and PCR analysis was used to confirm that the cell line contains White1 or White2 fragment. Homozygous White1/2 tagged germline strains were generated by round I genomic exclusion, also named star cross (Allen, 1967). The star cross was performed between the single cell isolates and the star strain A*III or B*VII. Star strains are the *Tetrahymena* strains which have a defective micronucleus. During star cross, the micronucleus from a normal strain undergoes meiosis and mitosis, and is transferred to the star strain. During this process, the White1/2 tagged heterozygous micronucleus is converted into either wild type or White1/2 tagged homozygous micronucleus, and the nucleus is also transferred to the star strain. During star mating, cells were fed at 6 h after mating to make sure the cells only finish the round I genomic exclusion without further mating. After round I genomic exclusion, the macronucleus was still maintained as before. Finally, the star strain side becomes a heterokaryon which contains homozygous White1/2 tag in the micronucleus, but not in the macronucleus.

Genomic DNA isolation

Genomic DNA was isolated from *Tetrahymena* cells according to a previously described protocol (Zhang et al, 1997). Cells were collected by centrifugation at 3,000 rpm for 3 min, washed once with ice-cold 10 mM Tris-HCl (pH 7.4), and resuspended in the same buffer. Equal volume of NDS lysis buffer (10 mM Tris, 0.5 M EDTA, 2% SDS, pH 9.5) was added. Proteinase K (Sigma-Aldrich) was added at the final concentration of 200 μg/ml, and the sample was incubated at 37^{o}C overnight. After that equal volume of TE buffer (10 mM Tris, 1mM EDTA, pH 8.0) was added to dilute the sample. Phenol/chloroform/isoamyl alcohol (25:24: 1) and chloroform were used sequentially to extract DNA. DNA was then precipitated in ethanol and resuspended in TE buffer. RNase A was added to the sample at the final concentration of 10 μg/ml, and the sample was incubated for 1 h at 37^{o}C. Finally, genomic DNA was re-precipitated in ethanol and resuspended in TE buffer.

Southern blot analysis

Total genomic DNA (50 μg) was digested with appropriate restriction enzymes. DNA was run on 0.6% or 0.8% agarose gel in 1xTAE buffer (40 mM Tris, 20 mM acetic acid, and 1 mM EDTA) at 1.5-2.0 V/cm for 18 h at RT. The agarose gel was soaked in 0.25 M HCl for 30 min, and then in transfer buffer (0.5 M NaOH, 1.5 M NaCl) for 15 min twice. DNA was transferred to Hybond XL membrane (GE Healthcare) by capillary blotting in alkaline transfer buffer for 20 h. The membrane was then rinsed with 0.2 M Tris-HCl, pH7.4/2x SSC for 5 min, and air-dried O/N. Once dried, the membranes were incubated at 37^{o}C O/N in pre-hybridization solution (1 M NaCl, 25% formamide, 10%

dextran sulfate, 1% SDS, 5 mM Tris-HCl [pH 7.4], 100 μg/ml boiled salmon sperm DNA). DNA probes were radio-labeled with alpha-[^{32}P] dATP using NEBlot kit (New England BioLabs), purified by G-50 spin column, denatured, and added to the pre-hybridization solution. The membrane was probed for 24 h at 37^{o}C before wash. The membrane was subsequently washedat 42^{o}C using 2x SSC (two washes), followed by 2x SSC/1% SDS (two washes), and 0.4X SSC/0.1% SDS (two washes). The blot was exposed to x-ray film at -80^{o}C O/N.

5-ethynyl-2'-deoxyuridine (EdU) labeling

Click-iT EdU Alexa Fluor 594 Imaging Kit (Life Technologies) was used to identify cells undergoing DNA replication using the EdU labeling assay. Basically, EdU was added to the mating culture at the final concentration of 100 μM, and mating cells were labeled at 30^{o}C for 20 min. The cells were then washed, fixed, and reacted with Click-It reagent according to manufacturer's instructions (Life Technologies). Hoechst 33342 was used to stain the nuclei. Both Hoechst staining and EdU labeling were detected using a fluorescent microscope.

Quantitative PCR (qPCR)

qPCR were performed in 96 well plates on the StepOnePlus Real-Time PCR Systems (Applied Biosystems). qPCR was done in a 10 μl reaction including 5 μl Power SYBR® Green PCR Master Mix (Applied Biosystems), with 1-5 ng genomic DNA as a template, and 200 nM forward and reverse primers. Each DNA sample was assayed in triplicate. Water was used to replace genomic DNA for the negative control.

Flow cytometry

DNA content of micronuclei, and analagen macronuclei of mating cells were determined by flow cytomeric analysis. A total of $5x10^5$ cells were collected from mating culture during development by centrifugation at 3,000 rpm for 3 min. Then cells were washed once using 10 mM Tirs-HCl (pH7.4), and pellet the cells again by centrifugation. TMS buffer (0.5 ml of 10 mM Tris-HCl [pH 7.4], 10 mM $MgCl_2$, 3 mM $CaCl_2$, 0.25 M sucrose, 0.2% NP-40) was added to lyse the cells while maintaining intact nuclei. Propidium iodide and RNase A were then added to the samples at a final concentration of 20 μg/ml and 200 μg/ml respectively, and the samples were incubated in the dark at room temperature for 30 min. Samples were analyzed on Becton Dickinson FACSAria II flow cytometer (BD Biosciences). A total of twenty thousand events were collected for each sample for data analysis. Data analyses were performed using Flowjo version 10 software. The number of events versus the relative DNA content was plotted in histograms.

DNA fiber analysis

Tetrahymena cells were pulse-labeled with 400 μM IdU (Sigma) at 30ºC for 10 min. Then cells were washed once with 1 ×PBS. Cells were resuspended in pre-warmed fresh media (for vegetative cells) or 10 mM Tirs-HCl (pH7.4) (for mating cells) with 100 μM CldU (MP Biomedicals) and labeled for 10 min. After two washes with PBS, the cell density was adjusted to 1×10^6 cell/ml. Preparation and immunostaining of DNA fibers were performed as previously described (Chastain et al, 2006; Schwab & Niedzwiedz, 2011; Stewart et al, 2012) with the following modifications. Briefly, after

fixation and HCl treatment, slides were washed three times with 1 ×PBS, and 5% BSA in PBS was used to block slides for 30 min. Mouse α-BrdU (1:50, Becton Dickson) which recognizes IdU and rat α-BrdU (1:100, Accurate Chemical) which recognizes CldU in 5% BSA were then added onto slides. After 1 h incubation, the slides were washed three times with 1 ×PBS, and were incubated for 30 min with secondary antibodies: Alexa Fluor 568 goat anti-mouse IgG (1: 100, Invitrogen/Molecular probes) and Alexa Fluor 488 goat anti-rat IgG (1: 100, Invitrogen/Molecular probes). Next, the slides were washed three times with 1 ×PBS and dehydrated with ethanol series and mounted with SlowFade Gold antifade (Invitrogen). During immunostaining, all antibodies were diluted in 5% BSA in 1x PBS, all incubations were performed at 37^{o}C, and all wash steps were done at RT.

DNA fiber images were taken by a Nikon A1R+ confocal microscope with 600x magnification. Measurements of track length were performed with Nikon NIS-Elements software. Inter-origin distance was defined as the distance between the centers of two red segments in either green-red-green-red-green or green-red-gap-red-green tracks. Fork velocity was determined by measuring the length of the green segment in a red-green track or red segments in a green-red-gap-red green track. GraphPad Prism software was used to analyze the statistical significance, and the p-values shown in figures were determined by Mann-Whitney test for single comparisons or Kruskal-Wallis test for multiple comparisons.

Two-dimensional (2D) gel electrophoresis of DNA replication intermediates (RIs)

Total genomic DNA was prepared as described before (Zhang et al, 1997). Genomic DNA (200 μg) was digested by HindIII at 37°C for 4 h, precipitated by ethanol, and resuspended in 400 μl of TNE buffer (100 mM NaCl, 10 mM Tris, 1 mM EDTA, pH 8.0). The digested DNA was then applied to 200 μl of benzoylated naphthoylated DEAE (BND)-cellulose (Sigma-Aldrich). RIs was bound to the BND-cellulose, and non-specific binding DNA fragments were washed out with 400 μl of TNE buffer for five times. 200 μl of 1.8% caffeine in TNE was used to elute RIs from BND-cellulose. DNA was then precipitated with isopropanol, washed with 70% ethanol and resuspended in TE buffer. For B rDNA strains, the enriched RIs were directly applied onto gel electrophoresis. For strains containing C3 rDNA in the developing MAC and B rDNA in the parental MAC, RIs were further digested by SphI to separate parental B rDNA from progeny C3 rDNA 5' NTS fragments.

For Mung Bean nuclease (MBN) treatment, 3 μg of BND cellulose-enriched RIs was digested with 5 U of MBN (New England BioLabs) at 30 ℃ for 30 min. SDS was added to the final concentration of 0.01% to inactivate MBN.

Neutral-neutral 2D gel electrophoresis was performed according to previous description (Zhang et al, 1997). Typically, 5-10 μg of BND cellulose-enriched RIs were loaded on a 0.4% agarose gel, and the first dimensional gel was run in 1xTAE buffer at 1.5 V/cm for 18 h at RT. The gel was visualized by ethidium bromide staining, and gel slice from each lane was cut with correct size range of RIs and rotated 90 degree for second dimension gel electrophoresis. Gel slices were inserted into 1% agarose gel, and

the second dimensional gel electrophoresis was performed in 1xTBE buffer (89 mM Tris, 89 mM boric acid, 2 mM EDTA, pH 8.0) containing 0.5 μg/ml ethidium bromide at 3 V/cm for 18 h at 4ºC. Southern blot analysis was carried out to detect the patterns of RIs.

CHAPTER V

SUMMARY AND DISCUSSION

Overview

DNA replication is an important process to duplicate genetic material for inheritance. In eukaryotes, replication initiation is tightly regulated to guarantee that DNA is replicated once and only once per cell cycle. Origin recognition complex (ORC) is the initiator and dictates where replication occurs. ORC recruits other factors to load MCM2-7 helicase at the replication origin and form pre-replication complex (pre-RC), licensing the origin in G1 phase. Further activation of MCM2-7 is required to initiate replication. Once the origin is utilized, phosphorylation or degradation of pre-RC components prevent re-replication of the genome during the same cell cycle. Besides a conventional mitotic cell cycle, which contains G1, S, G2, and M phases, there are specialized replication programs to serve specific purposes, such as endoreplication and gene amplification. Endoreplication (or endocycle) consists of alternating G and S phases without mitosis to generate polyploid nuclei, while gene amplification is a specialized replication program that increases the copy number of a certain locus in the genome by firing the same origins repeatedly. Both replication programs are often found in tissues that support the developing embryo or fetus, and their purpose is to provide the requisite nutrients and proteins. Although endocycling has been found in many eukaryotes, and the signaling pathways and regulation of endocycle have been largely investigated, the control of replication initiation during endoreplication has been less reported. One report in *Drosophila* suggests that ORC is dispensable for endoreplication

(Park & Asano, 2008). In my dissertation research, I used the model organism *Tetrahymena* to study the regulation of replication in different replication programs, including endoreplication and gene amplification. DNA replication under disturbed conditions, such as in the Orc1p knockdown strain, under genotoxic stress, and in the histone methyltransferase defective mutant strain TXR1Δ, were also studied. By studying and comparing these replication programs, I uncovered strong evidence for unconventional replication initiation events during endoreplication and the recovery from hydroxyurea-induced replication stress. My data suggest that replication initiation under these conditions is ORC independent. Using DNA fiber imaging, changes in origin utilization and fork elongation were also detected during endoreplication. Altogether, the findings in this research broaden our horizon of eukaryotic replication control, and provide useful information on how *Tetrahymena* use different strategies to achieve specialized replication programs.

My collaborative studies with two former students, Po-Hsuen Lee and Pamela Sandoval on regulation of different replication programs were performed at three levels. First, the protein levels of pre-RC components ORC and MCM complex were determined by western blotting analysis. Secondly, a well-studied rDNA replicon was chosen to determine origin usage in this specific locus by two dimensional (2D) gel analysis. Thirdly, DNA fiber analysis was employed to determine origin utilization and replication elongation on a genome-wide scale. By combining data from these three levels, we were able to determine the possible mechanisms involved in differential regulation of DNA replication.

DNA replication in the ORC1 knockdown strain

To start with, the vegetative cell cycle was studied in an Orc1p knockdown stain. A 5-fold decrease in Orc1p was observed in this strain, and the protein levels of Orc2p and Mcm6p reduced correspondingly (Figure 2.1). DNA fiber analysis showed that genome-wide origin density does not change, but the replication fork moves more slowly (Figure 2.5). This result is different from the case in *S. cerevisiae*, where 30% fewer origins were detected in an ORC2 mutant strain (Shimada et al, 2002). Furthermore, protein level of MCM complex did not change in the yeast mutant. In addition, origin usage of the rDNA minichromosome does not change in ORC1 knockdown strain. These data suggest that fork elongation rather than initiation is perturbed with moderate reduction of the protein levels of ORC and MCM complex. Co-regulation of ORC and MCM subunits could be tested by expressing ORC1 under an inducible promoter. Whether overexpression of Orc1p causes up-regulation of MCM subunits can be determined. Furthermore, whether fork elongation can be recovered could be tested. Alternatively, Mcm6p can be knocked down to see whether Orc1p or Orc2p is down-regulated.

Endoreplication

Compared to the moderate reduction of ORC and MCMs in the ORC1 knockdown strain, the levels of these two proteins are much lower during endocycles of late development. ORC and MCMs are dynamically regulated during development, with high levels at early development including Endo I, low levels at later stages of development (Endo II) (Figures 2.9 and 2.10). These results are unexpected, because the

amount of DNA replication during these two stages are opposite to the protein levels of the ORC and MCMs. However, DNA fiber analysis showed that more origins are firing during Endo II. How could endoreplication initiate with limiting amounts of ORC? One possibility is that an ORC-independent mechanism is utilized. In *Drosophila* salivary gland cells, endoreplication is not affected when Orc1p or Orc2p are knocked out (Park & Asano, 2008). Although the mechanism of replication initiation is still unknown, these findings in *Drosophila* support ORC-independent initiation in metazoa.

One model to explain the ORC-independent initiation is that endoreplication-specific chromosomal structure might be used for new origin firing. It has been proposed that D-loops or R-loops in bacteria can mediate a DnaA-independent loading of DnaB onto arrested replication forks (Masai & Arai, 1996; Sandler & Marians, 2000). D-loops are generated from homologous recombination at double strand breaks. 2D gel analysis on rDNA replication intermediates (RIs) revealed that aberrant RIs accumulate during Endo II (Figure 2.11). These RIs are sensitive to Mung Bean nuclease, indicating ssDNA or DNA/RNA hybrids exists in the RIs (Figure 2.11). Therefore, these D-loops/R-loops could support replication initiation. Additionally, western blot analysis has shown that Rad51p is upregulated during development, with the highest peak at late Endo I (Figure 2.9), which is consistent with the gene expression profile in the *Tetrahymena* Genome Database. During Endo II, Rad51p is still maintained at relatively high level, while other proteins such as alpha-tubulin (Atu1p) decrease (Figures 2.9 and 2.10). These data indicate that homologous recombination occurs during endoreplication. I postulate that HR peaks in late Endo I, when Rad51p level is the highest. At this time, cells probably

use up all dNTPs required for DNA synthesis, and wait for nutrients to support further endoreplication. If this is true, the aberrant RIs of rDNA may be absent when cells are re-fed early, and lower level of Rad51p may be detected. This can be tested by measuring Rad51p by Western blotting, monitoring endoreplication by flow cytometry, analyzing rDNA RIs by 2D gel electrophoresis, and determining rDNA copy number by qPCR. In addition, homologous recombination based replication initiation has been reported in an archaeon *Haloferax volcanii* when all the origins are deleted (Hawkins et al, 2013). Replication initiates at more dispersed regions and recombinase RadA is required. Similarly, a derivative of *S. cerevisiae* chromosome III with all ARSs deleted can still propagate (Dershowitz et al, 2007). Moreover, in *S. cerevisiae*, ORC is not required for break-induced replication (BIR) which is an important homologous recombination pathway to repair double-strand breaks (DSBs) (Lydeard et al, 2010). However, BIR acts at stalled forks rather than replication sites.

To test whether the recombination based initiation occurs during late development, a heterokaryon mutant with RAD51 knocked out only in MIC could be generated. During early conjugation, wild type Rad51p is generated from parental MACs to support normal early events, such as meiosis. While in Endo II or late Endo I, the parental MACs are degraded and new MACs are generated from MICs, there is no functional Rad51p. First, copy number change of rDNA and non-rDNA chromosomes can be determined by qPCR. If there is no increase in copy number during late development, this will suggest that endoreplication depends on Rad51p. Secondly, 2D gel analysis of rDNA RIs can be performed to check whether the aberrant RIs are

present or absent. Absence of aberrant RIs will indicate that formation of the RIs depends on Rad51p. Thirdly, genome-wide nascent strand sequencing can be carried out to determine endoreplication-specific initiation sites (Cayrou et al, 2012b). Current research in the lab is focusing on identifying replication origins throughout the macronuclear genome during the vegetative phase of the life cycle when the level of ORC protein is high, using centrifugal elutriation to synchronize cells in S phase. Our collaborator Yifan Liu' group is developing a project to map all of the ORC binding sites by Chromatin Immunoprecipitation (ChIP). The predication we would make is that there would be good correlation between initiation sites and ORC binding sites. Similarly, elutriation can be utilized to separate mating pairs (or exconjugants) for non-mated cells to obtain endocycling cells with high purity. By comparing the origin maps of vegetative S phase and endocycling cells, we will identify endoreplication-specific origins. If homologous recombination is required to fire these origins, I expect to see no enrichment of nascent strand DNA at these sites in the RAD51 knockout strain by qPCR analysis.

Another model to explain the ORC-independent initiation is that an alternative replication initiation protein is used specifically for Endo II. In order to test this model, nascent strand sequencing can be used to identify the endoreplication-specific origins as described above. Electrophoretic mobility shift assay (EMSA) could be carried out by incubation of radio-labeled DNA sequences of a replication origin with nuclear extracts from either vegetative cell cycle or Endo II. If the specific initiation protein exists, I expect to see gel shift occurs for the Endo II sample, but not the vegetative sample.

Furthermore, one way to identify the initiation protein is the chromatin affinity purification-mass spectrometry (ChAP-MS). This method was developed by Dr. Alan Tackett (University of Arkansas) to study the dynamic regulation of protein-DNA interactions at a single locus in *S. cerevisiae* (Byrum et al, 2012). First, as described above, nascent strand sequencing could be used to identify the endoreplication-specific origins. Then, I will create a *Tetrahymena* strain that contains a lexA binding site at an endoreplication-specific origin, and expresses a lexA repressor-protein A fusion protein for affinity purification of intact chromatin. Endo II cells could be treated with formaldehyde to crosslink proteins to DNA. The origin region can be enriched by incubation of sheared chromatin with IgG-coated Dyna beads. Proteins associated with the origin can be analyzed by high-resolution mass spectrometry to reveal their identity. Finally, if such protein has been identified, knockdown or knockout strains would be generated to determine whether the origin can still be utilized when the initiation protein is lacking. I expect to see the failure of origin utilization when the initiator is lacking. In addition, ChAP-MS can be used to identify not only endoreplication-specific initiators but also histone modifications associated with the replication origins, if there are specific epigenetic components involved in origin determination.

HU-induced DNA replication

In my dissertation research, an unconventional replication program in response to genotoxic stress was also investigated. Under hydroxyurea (HU) treatment, ORC and MCMs are degraded (Figures 3.1, 3.7, and 3.9). Once HU is removed, genome-wide replication occurs prior to replenishment of ORC and MCMs (Figure 3.9). In yeast and

higher eukaryotes, the checkpoint responses are very different: MCMs are reversibly phosphorylated to arrest replication forks and inhibit new origin firing (Cortez et al, 2004; Ibarra et al, 2008). So how does DNA replication occur after removal of HU, but before ORC and MCMs are restored? Passive replication of the rDNA chromosome indicates that a dormant origin is used instead of the normal origin (Figure 3.10). Our current data suggest that replication might initiate in proximity to the rDNA promoter. On a genome-wide scale, less origins are firing (Figure 3.11). These data suggest that replication initiation is altered. I propose that an ORC-independent, recombination-based mechanism is used for replication initiation. In addition, decreased acetylation level of histone H3 under HU treatment has been detected (Figures 3.6C and 3.7C). It has been shown that histone deacetylation promotes compaction of human chromosomes from the nuclear envelope (Malik et al, 2014). Moreover, histone deacetylase Rpd3 is involved in regulation of replication timing for late firing origins in *S. cerevisiae* (Aparicio et al, 2004). Deletion of Rpd3 leads to early activation of late origins. In *Drosophila* follicle cells, acetylation of histone H3 specifies and activates origins for chorion gene amplification (Aggarwal & Calvi, 2004). I speculate that during the first S phase after HU removal, acetylation of histone H3 has still not resumed, which is involved in determination of origin usage. To test this, the acetylation level of H3 after HU removal needs to be measured in the rDNA origin and promoter regions via a ChIP assay using antibody against acetylated histone H3.

Although changes in origin utilization have been observed during this unconventional cell cycle, unexpectedly, the fork velocity is similar to the normal

vegetative cell cycle. How could replication forks progress normally without Mcm6p or very little Mcm6p? Studies have shown that MCMs are excessive in other eukaryotes (Edwards et al, 2002; Forsburg, 2004), and excessive MCMs can license dormant origin firing in response to replication stress (Ge et al, 2007; Ibarra et al, 2008). In *Drosophila* S2 cells, over 95% reduction of the levels of MCM3, 5 and 6 do not significantly affect DNA replication or increase DNA damage (Crevel et al, 2011). These studies indicate that low level of MCMs in HU treated *Tetrahymena* cells may be enough to support DNA replication once HU is removed. However, as mentioned before, levels of MCMs are less reduced in an ORC1 knockdown strain and during Endo II, yet fork rate decreases in both cases. These results suggest that MCMs are not superfluous in *Tetrahymena*. One caveat here is that only Mcm6p was monitored in our experiments, we do not know the protein levels of other MCM subunits. We can add HA tag at the N-terminal or C-terminal of other MCM subunits and determine the protein levels using antibodies against the HA tag.

Based on these findings, I hypothesize that a specialized helicase or MCM homolog can act as a substitute and is responsible for or facilitates replication elongation. Two candidates are MCM8 and MCM9. Recent studies have shown that the MCM8-MCM9 complex plays an important role in homologous recombination repair at DNA damage sites (Lutzmann et al, 2012; Nishimura et al, 2012; Park et al, 2013). Studies on the roles of MCM8 and MCM9 in DNA replication have generated contradictory conclusions. While some studies indicate that MCM8 and MCM9 interact with components of pre-RC and are involved in pre-RC assembly (Lutzmann & Mechali,

2008; Volkening & Hoffmann, 2005), other studies show that they are not essential for replication licensing (Hartford et al, 2011; Maiorano et al, 2005). In *Drosophila* S2 cells, depletion of MCM8 causes a 30% reduction in the number of replication forks, but cell cycle progression and cell viability are normal (Crevel et al, 2007). In *Xenopus*, MCM8 has helicase activity and is involved in the elongation phase of DNA replication (Maiorano et al, 2005). Paralogs of MCM8 and MCM9 do not exist in yeast and some other fungi, but they do exist in ciliates (Liu et al, 2009). I speculate that MCM8 or/and MCM9 are involved in fork elongation during the first S phase recovered from HU treatment, when some or all subunits of MCM2-7 are degraded. To test this hypothesis, an inducible siRNA construct targeting MCM8/MCM9 could be generated and introduced into a *Tetrahymena* strain. Induction of this siRNA could be performed either during HU treatment or after HU removal. Changes in origin usage and fork elongation can be determined by DNA fiber analysis. rDNA RIs can be examined by 2D gel analysis. I expect to see slow fork elongation. Furthermore, Mcm6p or/and other MCM subunits could be overexpressed in MCM8/9 knockdown background to see how fork rate is affected.

If other MCM homologs are involved in replication elongation, do these MCM proteins facilitate replication elongation in the ORC1 knockdown strain or in Endo II? Based on the levels of Mcm6p and fork rates that were observed in these replication programs, this might be not the case. There must be a threshold to trigger this specific function of MCM8/9, which probably depends on the degree of DNA damage or the level of ORC depletion.

DNA replication in TXR1Δ

In this dissertation, the replication features of a histone monomethyltransferase defective strain TXR1Δ were studied, in order to explore not only the importance of this protein in DNA replication, but also the mechanism for endoreplication. TXR1 has been identified by our collaborator Dr. Yifan Liu's group. In *Tetrahymena*, it is the sole homolog of Arabidopsis ATXR5 and ATXR6, which are the histone methyltransferases responsible for histone H3 lysine 27 monomethylation (Gao et al, 2013; Jacob et al, 2009). In the TXR1Δ strains, massive amounts of single stranded DNA accumulate in intergenic regions, including replication origins. rDNA RIs in vegetative TXR1Δ are similar to those in Endo II (Gao et al, 2013). RIs from both samples were sensitive to Mung Bean nuclease digestion (Figure 4.7), indicating presence of ssDNA and possibly the accumulation of DNA-RNA hybrids. Moreover, moderate reduction in origin density was observed in non-rDNA chromosomes in the TXR1Δ strains. These results suggest that histone H3 lysine monomethylation plays an important role in modulating origin usage. In addition, slow fork movement was detected in a subpopulation of TXR1Δ. Similarities between rDNA RIs in vegetative TXR1Δ and Endo II brings up a question: are histone modifications, such as monomethylation of H3 lysine 27 discussed here, established in Endo II? Immunofluorescence with antibody against histone H3K27me1 can be performed to check the level of this modification across development and vegetative cell cycle. The result will provide more information on whether aberrant RIs in TXR1Δ and Endo II are generated by the same mechanism.

Gene amplification

In other organisms that undergo developmentally programed gene amplification, locus-specific over-replication is preceded by endoreplication of the entire genome (Calvi et al, 1998). This raises the question of whether endoreplication is required for gene amplification in *Tetrahymena*, and vice versa. To answer this question, the time window for rDNA amplification relative to non-rDNA endoreplication was determined first. During *Tetrahymena* development, rDNA gene amplification starts two hours earlier than the onset of non-rDNA endoreplication and both replication programs plateau at the same time (Figure 4.5). Since there must be a balance between DNA synthesis and protein synthesis, it is reasonable that rDNA is amplified first, and then both rDNA amplification and non-rDNA endoreplication occur. The rates of amplification during these two different stages are the same, indicating that origin firing and elongation are not temporally separated, which is not the case for chorion gene amplification in *Drosophila* follicle cells (Claycomb et al, 2002).

Studies have shown that Anlagen Stage Induced 2 (ASI2), encoding a putative signal transduction receptor, is required for endoreplication in *Tetrahymena*, and endoreplication is arrested in ASI2 knockout mutant (Li et al, 2006; Yin et al, 2010). During development, Asi2p produced from the parental MAC is required for Endo I, and Asi2p generated from the developing MAC is needed for Endo II. To test whether rDNA amplification is affected in ASI2 knockout strains, gene replacement has been used to disrupt somatic ASI2 in strains with C3 rDNA in MIC. Although ASI2 was successfully disrupted, instability of MIC was observed in these knockouts. Therefore, I was not able

to determine the copy number change of rDNA by qPCR analysis. An alternative experiment that can be carried out to generate ASI2 mutants is to introduce DNA sequences that encode an inducible siRNA against ASI2 into the MIC or MAC of *Tetrahymena* C3 strains. Endoreplication would be blocked, and the degree of rDNA amplification can be determined by qPCR analysis. If rDNA amplification (especially for the late stage) depends on endoreplication, I expect to see low degree of rDNA amplification. Alternatively, I may see dramatic increase in rDNA copy number if there is competition between rDNA amplification and non-rDNA endoreplication for trans-acting factors that control replication initiation and fork elongation.

To test whether rDNA amplification is required for Endo II, we can mate heterokaryon strains that contain an amplification-defective allele in MIC but have wild type MAC, and look at endocycling through qPCR or flow cytometry analysis. In these strains, there is a point mutation on the cis-element required for excision of rDNA from micronuclear locus (Kapler & Blackburn, 1994). The mutation delays the excision process, and rDNA misses the time window for amplification. Since when rDNA amplification is blocked, protein synthesis will be affected eventually, I expect that Endo II will be impaired.

Similar to endoreplication, rDNA amplification is followed by a plateaued period until refeeding when rDNA starts to increase the copy number again. We know that early refeeding causes disappearance of the plateau period for endoreplication (Yin et al, 2010). I expect to see the same phenomenon for rDNA. However, early refeeding may push late rDNA replication event into the amplification time window. I speculate that

rDNA will be amplified to a higher degree upon early refeeding. This could be assessed by qPCR analysis with primer sets specific for rDNA and non-rDNA chromosomes.

How is the rDNA minichromosome selectively chosen for amplification? Coincidence of rDNA amplification and endoreplication suggests that unique features of the rDNA chromosome enable amplification. In *Tetrahymena*, the mechanisms of ORC binding to rDNA and non-rDNA chromosomes are different (Donti et al, 2009). Base pairing between rDNA and the 26T RNA subunit is required for rDNA recognition but not for non-rDNA chromosomes. This specialized recognition could be responsible for the rDNA amplification. A gain-of-function assay has been utilized to test whether cis-elements from rDNA chromosomes can provide the amplification ability to a non-rDNA ARS replicon on an episome. Preliminary data indicate that cis-elements cannot turn the replicon into an amplicon. However, whether there is any inhibitory element in the episome is unknown. Another hypothesis for selective rDNA amplification is that specific trans-acting factors or epigenetic modifications determine the amplification of rDNA. To test this model, ChAP-MS as described before, can be used to identify these factors by comparing trans-acting factors or epigenetic modifications of the rDNA origin and the non-rDNA origin.

Summary

In summary, I studied different replication programs in *Tetrahymena* in my dissertation research. The major focus was on the endoreplication program which occurs naturally. Starvation induced conjugation in *Tetrahymena* is a strategy to face stress. On the other hand, endoreplication used to rebuild the genome shows abnormality to some

extent corresponding to the "stress", such as alteration of origin usage, slow replication fork movement, aberrant replication intermediates. To further uncover the mechanism of replication control during endoreplication or under genotoxic stress, genome-wide nascent strand sequencing should be employed to mapping replication origins.

Different genome-wide approaches have been developed in recent years to analyze DNA replication in eukaryotes. One of these approaches is chromatin immunoprecipitation (ChIP) of ORC or MCMs followed by sequencing (ChIP-seq) or microarray (ChIP-chip) analysis. This method has been used to identify about 300 ORC-bound sites in *S. cerevisiae* (Eaton et al, 2010; Wyrick et al, 2001). Another method is 5-bromo-2'-deoxyuridine immunoprecipitation (BrdU-IP) followed by microarray or comparative genomic hybridization (CGH). The approach is often used in presence of HU to look at early firing origins. It has been used in budding yeast to determine the role of histone deacetylase Rpd3 in the time of origin firing (Knott et al, 2009). This method has also been used to look at the coordination between transcription and early replication in *Drosophila*. It was found that origins tend to replicate in early S phase if adjacent genes are actively transcribed (MacAlpine et al, 2004). The third approach is nascent strand sequencing with λ-exonuclease digestion for enrichment. This approach has been used to analyze metazoan replication origins. The study revealed that in *Drosophila* and mouse cells, origins cluster near CpG islands regardless of methylation status (Cayrou et al, 2011).

Tetrahymena has both natural (endoreplication) and inducible (stress-induced) programs in which DNA replication occurs under conditions where the essential proteins

(ORC and MCMs) are dramatically reduced. This provide us with a rich resource of material and experimental conditions to explore conventional and potentially alternative DNA replication programs in eukaryotes.

REFERENCES

Adachi S, Minamisawa K, Okushima Y, Inagaki S, Yoshiyama K, Kondou Y, Kaminuma E, Kawashima M, Toyoda T, Matsui M, Kurihara D, Matsunaga S, Umeda M (2011) Programmed induction of endoreduplication by DNA double-strand breaks in *Arabidopsis*. *Proc Natl Acad Sci U S A* **108:** 10004-10009

Aggarwal BD, Calvi BR (2004) Chromatin regulates origin activity in *Drosophila* follicle cells. *Nature* **430:** 372-376

Ahn JY, Li X, Davis HL, Canman CE (2002) Phosphorylation of threonine 68 promotes oligomerization and autophosphorylation of the Chk2 protein kinase via the forkhead-associated domain. *J Biol Chem* **277:** 19389-19395

Akematsu T, Endoh H (2010) Role of apoptosis-inducing factor (AIF) in programmed nuclear death during conjugation in *Tetrahymena thermophila*. *BMC Cell Biol* **11:** 13

Allen SL (1967) Genomic exclusion: a rapid means for inducing homozygous diploid lines in *Tetrahymena pyriformis*, syngen 1. *Science* **155:** 575-577

Allewell NM, Oles J, Wolfe J (1976) A physicochemical analysis of conjugation in *Tetrahymena pyriformis*. *Exp Cell Res* **97:** 394-405

Alt FW, Kellems RE, Bertino JR, Schimke RT (1978) Selective multiplication of dihydrofolate reductase genes in methotrexate-resistant variants of cultured murine cells. *J Biol Chem* **253:** 1357-1370

Altschuler MI, Yao MC (1985) Macronuclear DNA of *Tetrahymena thermophila* exists as defined subchromosomal-sized molecules. *Nucleic Acids Res* **13:** 5817-5831

Alvino GM, Collingwood D, Murphy JM, Delrow J, Brewer BJ, Raghuraman MK (2007) Replication in hydroxyurea: it's a matter of time. *Mol Cell Biol* **27:** 6396-6406

Alzu A, Bermejo R, Begnis M, Lucca C, Piccini D, Carotenuto W, Saponaro M, Brambati A, Cocito A, Foiani M, Liberi G (2012) Senataxin associates with replication forks to protect fork integrity across RNA-polymerase-II-transcribed genes. *Cell* **151:** 835-846

Anglana M, Apiou F, Bensimon A, Debatisse M (2003) Dynamics of DNA replication in mammalian somatic cells: nucleotide pool modulates origin choice and interorigin spacing. *Cell* **114:** 385-394

Aparicio JG, Viggiani CJ, Gibson DG, Aparicio OM (2004) The Rpd3-Sin3 histone deacetylase regulates replication timing and enables intra-S origin control in *Saccharomyces cerevisiae*. *Mol Cell Biol* **24:** 4769-4780

Aparicio OM (2013) Location, location, location: it's all in the timing for replication origins. *Genes Dev* **27:** 117-128

Arias EE, Walter JC (2006) PCNA functions as a molecular platform to trigger Cdt1 destruction and prevent re-replication. *Nat Cell Biol* **8:** 84-90

Bakkenist CJ, Kastan MB (2003) DNA damage activates ATM through intermolecular autophosphorylation and dimer dissociation. *Nature* **421:** 499-506

Beall EL, Manak JR, Zhou S, Bell M, Lipsick JS, Botchan MR (2002) Role for a *Drosophila* Myb-containing protein complex in site-specific DNA replication. *Nature* **420:** 833-837

Bell SP, Stillman B (1992) ATP-dependent recognition of eukaryotic origins of DNA replication by a multiprotein complex. *Nature* **357:** 128-134

Berbenetz NM, Nislow C, Brown GW (2010) Diversity of eukaryotic DNA replication origins revealed by genome-wide analysis of chromatin structure. *PLoS Genet* **6:** e1001092

Berezney R, Dubey DD, Huberman JA (2000) Heterogeneity of eukaryotic replicons, replicon clusters, and replication foci. *Chromosoma* **108:** 471-484

Biradar DP, Rayburn AL (1994) Flow cytometric probing of chromatin condensation in maize diploid nuclei. *New Phytol* **126:** 31-35

Blow JJ, Dutta A (2005) Preventing re-replication of chromosomal DNA. *Nat Rev Mol Cell Biol* **6:** 476-486

Blumenthal AB, Clark EJ (1977) Discrete sizes of replication intermediates in *Drosophila* cells. *Cell* **12:** 183-189

Bodenbender J, Prohaska A, Jauker F, Hipke H, Cleffmann G (1992) DNA elimination and its relation to quantities in the macronucleus of *Tetrahymena*. *Dev Genet* **13:** 103-110

Branzei D, Foiani M (2009) The checkpoint response to replication stress. *DNA Repair (Amst)* **8:** 1038-1046

Britton JS, Edgar BA (1998) Environmental control of the cell cycle in *Drosophila*: nutrition activates mitotic and endoreplicative cells by distinct mechanisms. *Development* **125:** 2149-2158

Brownell JE, Zhou J, Ranalli T, Kobayashi R, Edmondson DG, Roth SY, Allis CD (1996) *Tetrahymena* histone acetyltransferase A: a homolog to yeast Gcn5p linking histone acetylation to gene activation. *Cell* **84:** 843-851

Bruns PJ, Brussard TE (1981) Nullisomic *Tetrahymena*: eliminating germinal chromosomes. *Science* **213:** 549-551

Bruns PJ, Cassidy-Hanley D (2000) Biolistic transformation of macro- and micronuclei. *Methods Cell Biol* **62:** 501-512

Burke TW, Cook JG, Asano M, Nevins JR (2001) Replication factors MCM2 and ORC1 interact with the histone acetyltransferase HBO1. *J Biol Chem* **276:** 15397-15408

Burma S, Chen BP, Murphy M, Kurimasa A, Chen DJ (2001) ATM phosphorylates histone H2AX in response to DNA double-strand breaks. *J Biol Chem* **276:** 42462-42467

Byrum SD, Raman A, Taverna SD, Tackett AJ (2012) ChAP-MS: a method for identification of proteins and histone posttranslational modifications at a single genomic locus. *Cell Rep* **2:** 198-205

Byun TS, Pacek M, Yee MC, Walter JC, Cimprich KA (2005) Functional uncoupling of MCM helicase and DNA polymerase activities activates the ATR-dependent checkpoint. *Genes Dev* **19:** 1040-1052

Cadoret JC, Meisch F, Hassan-Zadeh V, Luyten I, Guillet C, Duret L, Quesneville H, Prioleau MN (2008) Genome-wide studies highlight indirect links between human replication origins and gene regulation. *Proc Natl Acad Sci U S A* **105:** 15837-15842

Calvi BR, Lilly MA, Spradling AC (1998) Cell cycle control of chorion gene amplification. *Genes Dev* **12:** 734-744

Cayrou C, Coulombe P, Puy A, Rialle S, Kaplan N, Segal E, Mechali M (2012a) New insights into replication origin characteristics in metazoans. *Cell Cycle* **11:** 658-667

Cayrou C, Coulombe P, Vigneron A, Stanojcic S, Ganier O, Peiffer I, Rivals E, Puy A, Laurent-Chabalier S, Desprat R, Mechali M (2011) Genome-scale analysis of metazoan replication origins reveals their organization in specific but flexible sites defined by conserved features. *Genome Res* **21:** 1438-1449

Cayrou C, Gregoire D, Coulombe P, Danis E, Mechali M (2012b) Genome-scale identification of active DNA replication origins. *Methods* **57:** 158-164

Cech TR, Brehm SL (1981) Replication of the extrachromosomal ribosomal RNA genes of *Tetrahymena thermophilia*. *Nucleic Acids Res* **9:** 3531-3543

Chalker DL (2012) Transformation and strain engineering of *Tetrahymena*. *Methods Cell Biol* **109:** 327-345

Chalker DL, Yao MC (2001) Nongenic, bidirectional transcription precedes and may promote developmental DNA deletion in *Tetrahymena thermophila*. *Genes Dev* **15:** 1287-1298

Chalker DL, Yao MC (2011) DNA elimination in ciliates: transposon domestication and genome surveillance. *Annu Rev Genet* **45:** 227-246

Challberg MD, Desiderio SV, Kelly TJ, Jr. (1980) Adenovirus DNA replication *in vitro*: characterization of a protein covalently linked to nascent DNA strands. *Proc Natl Acad Sci U S A* **77:** 5105-5109

Chastain PD, 2nd, Heffernan TP, Nevis KR, Lin L, Kaufmann WK, Kaufman DG, Cordeiro-Stone M (2006) Checkpoint regulation of replication dynamics in UV-irradiated human cells. *Cell Cycle* **5:** 2160-2167

Chehab NH, Malikzay A, Appel M, Halazonetis TD (2000) Chk2/hCds1 functions as a DNA damage checkpoint in G(1) by stabilizing p53. *Genes Dev* **14:** 278-288

Chen Z, Speck C, Wendel P, Tang C, Stillman B, Li H (2008) The architecture of the DNA replication origin recognition complex in *Saccharomyces cerevisiae*. *Proc Natl Acad Sci U S A* **105:** 10326-10331

Cherry JM, Blackburn EH (1985) The internally located telomeric sequences in the germ-line chromosomes of *Tetrahymena* are at the ends of transposon-like elements. *Cell* **43:** 747-758

Chuang RY, Kelly TJ (1999) The fission yeast homologue of Orc4p binds to replication origin DNA via multiple AT-hooks. *Proc Natl Acad Sci U S A* **96:** 2656-2661

Chung PH, Yao MC (2012) *Tetrahymena thermophila* JMJD3 homolog regulates H3K27 methylation and nuclear differentiation. *Eukaryot Cell* **11:** 601-614

Cimprich KA, Cortez D (2008) ATR: an essential regulator of genome integrity. *Nat Rev Mol Cell Biol* **9:** 616-627

Claycomb JM, Benasutti M, Bosco G, Fenger DD, Orr-Weaver TL (2004) Gene amplification as a developmental strategy: isolation of two developmental amplicons in *Drosophila*. *Dev Cell* **6:** 145-155

Claycomb JM, MacAlpine DM, Evans JG, Bell SP, Orr-Weaver TL (2002) Visualization of replication initiation and elongation in *Drosophila*. *J Cell Biol* **159:** 225-236

Claycomb JM, Orr-Weaver TL (2005) Developmental gene amplification: insights into DNA replication and gene expression. *Trends Genet* **21:** 149-162

Cleffmann G (1975) Amount of DNA produced during extra S phases in *Tetrahymena*. *J Cell Biol* **66:** 204-209

Cleffmann G (1980) Chromatin elimination and the genetic organisation of the macronucleus in *Tetrahymena thermophila*. *Chromosoma* **78:** 313-325

Clyne RK, Kelly TJ (1995) Genetic analysis of an ARS element from the fission yeast *Schizosaccharomyces pombe*. *EMBO J* **14:** 6348-6357

Cole E, Sugai T (2012) Developmental progression of *Tetrahymena* through the cell cycle and conjugation. *Methods Cell Biol* **109:** 177-236

Conover RK, Brunk CF (1986) Macronuclear DNA molecules of *Tetrahymena thermophila*. *Mol Cell Biol* **6:** 900-905

Cordell B, Swanstrom R, Goodman HM, Bishop JM (1979) tRNATrp as primer for RNA-directed DNA polymerase: structural determinants of function. *J Biol Chem* **254:** 1866-1874

Cortez D (2005) Unwind and slow down: checkpoint activation by helicase and polymerase uncoupling. *Genes Dev* **19:** 1007-1012

Cortez D, Glick G, Elledge SJ (2004) Minichromosome maintenance proteins are direct targets of the ATM and ATR checkpoint kinases. *Proc Natl Acad Sci U S A* **101:** 10078-10083

Crevel G, Hashimoto R, Vass S, Sherkow J, Yamaguchi M, Heck MM, Cotterill S (2007) Differential requirements for MCM proteins in DNA replication in *Drosophila* S2 cells. *PLoS One* **2:** e833

Crevel I, Crevel G, Gostan T, de Renty C, Coulon V, Cotterill S (2011) Decreased MCM2-6 in *Drosophila* S2 cells does not generate significant DNA damage or cause a marked increase in sensitivity to replication interference. *PLoS One* **6:** e27101

Cui B, Liu Y, Gorovsky MA (2006) Deposition and function of histone H3 variants in *Tetrahymena thermophila*. *Mol Cell Biol* **26:** 7719-7730

Delacroix S, Wagner JM, Kobayashi M, Yamamoto K, Karnitz LM (2007) The Rad9-Hus1-Rad1 (9-1-1) clamp activates checkpoint signaling via TopBP1. *Genes Dev* **21:** 1472-1477

Deng WM, Althauser C, Ruohola-Baker H (2001) Notch-Delta signaling induces a transition from mitotic cell cycle to endocycle in *Drosophila* follicle cells. *Development* **128:** 4737-4746

Dershowitz A, Snyder M, Sbia M, Skurnick JH, Ong LY, Newlon CS (2007) Linear derivatives of *Saccharomyces cerevisiae* chromosome III can be maintained in the absence of autonomously replicating sequence elements. *Mol Cell Biol* **27:** 4652-4663

Diffley JF, Bousset K, Labib K, Noton EA, Santocanale C, Tercero JA (2000) Coping with and recovering from hydroxyurea-induced replication fork arrest in budding yeast. *Cold Spring Harb Symp Quant Biol* **65:** 333-342

Diffley JF, Cocker JH, Dowell SJ, Rowley A (1994) Two steps in the assembly of complexes at yeast replication origins *in vivo*. *Cell* **78:** 303-316

Doerder FP, DeBault LE (1978) Life cycle variation and regulation of macronuclear DNA content in *Tetrahymena thermophila*. *Chromosoma* **69:** 1-19

Doerder FP, Ditaranto J, DeBault LE (1981) Evolutionary constraints on quantitative variation and regulation of macronuclear DNA content in the genus *Tetrahymena*. *J Cell Sci* **49:** 177-193

Donti TR, Datta S, Sandoval PY, Kapler GM (2009) Differential targeting of *Tetrahymena* ORC to ribosomal DNA and non-rDNA replication origins. *EMBO J* **28:** 223-233

Doyon Y, Cayrou C, Ullah M, Landry AJ, Cote V, Selleck W, Lane WS, Tan S, Yang XJ, Cote J (2006) ING tumor suppressor proteins are critical regulators of chromatin acetylation required for genome expression and perpetuation. *Mol Cell* **21:** 51-64

Drury LS, Perkins G, Diffley JF (1997) The Cdc4/34/53 pathway targets Cdc6p for proteolysis in budding yeast. *EMBO J* **16:** 5966-5976

Drury LS, Perkins G, Diffley JF (2000) The cyclin-dependent kinase Cdc28p regulates distinct modes of Cdc6p proteolysis during the budding yeast cell cycle. *Curr Biol* **10:** 231-240

Eaton ML, Galani K, Kang S, Bell SP, MacAlpine DM (2010) Conserved nucleosome positioning defines replication origins. *Genes Dev* **24:** 748-753

Eaton ML, Prinz JA, MacAlpine HK, Tretyakov G, Kharchenko PV, MacAlpine DM (2011) Chromatin signatures of the *Drosophila* replication program. *Genome Res* **21:** 164-174

Edwards MC, Tutter AV, Cvetic C, Gilbert CH, Prokhorova TA, Walter JC (2002) MCM2-7 complexes bind chromatin in a distributed pattern surrounding the origin recognition complex in *Xenopus* egg extracts. *J Biol Chem* **277:** 33049-33057

Evrin C, Clarke P, Zech J, Lurz R, Sun J, Uhle S, Li H, Stillman B, Speck C (2009) A double-hexameric MCM2-7 complex is loaded onto origin DNA during licensing of eukaryotic DNA replication. *Proc Natl Acad Sci U S A* **106:** 20240-20245

Falck J, Mailand N, Syljuasen RG, Bartek J, Lukas J (2001) The ATM-Chk2-Cdc25A checkpoint pathway guards against radioresistant DNA synthesis. *Nature* **410:** 842-847

Feijoo C, Hall-Jackson C, Wu R, Jenkins D, Leitch J, Gilbert DM, Smythe C (2001) Activation of mammalian Chk1 during DNA replication arrest: a role for Chk1 in the intra-S phase checkpoint monitoring replication origin firing. *J Cell Biol* **154:** 913-923

Fernandez-Cid A, Riera A, Tognetti S, Herrera MC, Samel S, Evrin C, Winkler C, Gardenal E, Uhle S, Speck C (2013) An ORC/Cdc6/MCM2-7 complex is formed in a multistep reaction to serve as a platform for MCM double-hexamer assembly. *Mol Cell* **50:** 577-588

Follette PJ, Duronio RJ, O'Farrell PH (1998) Fluctuations in cyclin E levels are required for multiple rounds of endocycle S phase in *Drosophila*. *Curr Biol* **8:** 235-238

Forsburg SL (2004) Eukaryotic MCM proteins: beyond replication initiation. *Microbiol Mol Biol Rev* **68:** 109-131

Forsburg SL (2008) The MCM helicase: linking checkpoints to the replication fork. *Biochem Soc Trans* **36:** 114-119

Fox DT, Duronio RJ (2013) Endoreplication and polyploidy: insights into development and disease. *Development* **140:** 3-12

Furnari B, Rhind N, Russell P (1997) Cdc25 mitotic inducer targeted by chk1 DNA damage checkpoint kinase. *Science* **277:** 1495-1497

Gaertig J, Gorovsky MA (1992) Efficient mass transformation of *Tetrahymena thermophila* by electroporation of conjugants. *Proc Natl Acad Sci U S A* **89:** 9196-9200

Gallagher RC, Blackburn EH (1998) A promoter region mutation affecting replication of the *Tetrahymena* ribosomal DNA minichromosome. *Mol Cell Biol* **18:** 3021-3033

Ganley AR, Ide S, Saka K, Kobayashi T (2009) The effect of replication initiation on gene amplification in the rDNA and its relationship to aging. *Mol Cell* **35:** 683-693

Gao S, Xiong J, Zhang C, Berquist BR, Yang R, Zhao M, Molascon AJ, Kwiatkowski SY, Yuan D, Qin Z, Wen J, Kapler GM, Andrews PC, Miao W, Liu Y (2013) Impaired replication elongation in *Tetrahymena* mutants deficient in histone H3 Lys 27 monomethylation. *Genes Dev* **27:** 1662-1679

Ge XQ, Jackson DA, Blow JJ (2007) Dormant origins licensed by excess Mcm2-7 are required for human cells to survive replicative stress. *Genes Dev* **21:** 3331-3341

Geng Y, Yu Q, Sicinska E, Das M, Schneider JE, Bhattacharya S, Rideout WM, Bronson RT, Gardner H, Sicinski P (2003) Cyclin E ablation in the mouse. *Cell* **114:** 431-443

Gibson DG, Bell SP, Aparicio OM (2006) Cell cycle execution point analysis of ORC function and characterization of the checkpoint response to ORC inactivation in *Saccharomyces cerevisiae*. *Genes Cells* **11:** 557-573

Gorovsky MA, Woodard J (1969) Studies on nuclear structure and function in *Tetrahymena pyriformis*: I. RNA synthesis in macro- and micronuclei. *J Cell Biol* **42:** 673-682

Gossen M, Pak DT, Hansen SK, Acharya JK, Botchan MR (1995) A *Drosophila* homolog of the yeast origin recognition complex. *Science* **270:** 1674-1677

Hammond MP, Laird CD (1985) Control of DNA replication and spatial distribution of defined DNA sequences in salivary gland cells of *Drosophila melanogaster*. *Chromosoma* **91:** 279-286

Harrison JC, Haber JE (2006) Surviving the breakup: the DNA damage checkpoint. *Annu Rev Genet* **40:** 209-235

Hartford SA, Luo Y, Southard TL, Min IM, Lis JT, Schimenti JC (2011) Minichromosome maintenance helicase paralog MCM9 is dispensible for DNA replication but functions in germ-line stem cells and tumor suppression. *Proc Natl Acad Sci U S A* **108:** 17702-17707

Hawkins M, Malla S, Blythe MJ, Nieduszynski CA, Allers T (2013) Accelerated growth in the absence of DNA replication origins. *Nature* **503:** 544-547

Heffernan TP, Simpson DA, Frank AR, Heinloth AN, Paules RS, Cordeiro-Stone M, Kaufmann WK (2002) An ATR- and Chk1-dependent S checkpoint inhibits replicon initiation following UVC-induced DNA damage. *Mol Cell Biol* **22:** 8552-8561

Heichinger C, Penkett CJ, Bahler J, Nurse P (2006) Genome-wide characterization of fission yeast DNA replication origins. *EMBO J* **25:** 5171-5179

Heller RC, Kang S, Lam WM, Chen S, Chan CS, Bell SP (2011) Eukaryotic origin-dependent DNA replication *in vitro* reveals sequential action of DDK and S-CDK kinases. *Cell* **146:** 80-91

Hoggard T, Shor E, Muller CA, Nieduszynski CA, Fox CA (2013) A Link between ORC-origin binding mechanisms and origin activation time revealed in budding yeast. *PLoS Genet* **9:** e1003798

Huang RY, Kowalski D (1993) A DNA unwinding element and an ARS consensus comprise a replication origin within a yeast chromosome. *EMBO J* **12:** 4521-4531

Huberman JA, Riggs AD (1966) Autoradiography of chromosomal DNA fibers from Chinese hamster cells. *Proc Natl Acad Sci U S A* **55:** 599-606

Hyrien O, Maric C, Mechali M (1995) Transition in specification of embryonic metazoan DNA replication origins. *Science* **270:** 994-997

Ibarra A, Schwob E, Mendez J (2008) Excess MCM proteins protect human cells from replicative stress by licensing backup origins of replication. *Proc Natl Acad Sci U S A* **105:** 8956-8961

Iizuka M, Matsui T, Takisawa H, Smith MM (2006) Regulation of replication licensing by acetyltransferase Hbo1. *Mol Cell Biol* **26:** 1098-1108

Ilves I, Petojevic T, Pesavento JJ, Botchan MR (2010) Activation of the MCM2-7 helicase by association with Cdc45 and GINS proteins. *Mol Cell* **37:** 247-258

Jacob F, Brenner S, Cuzin F (1963) On the regulation of DNA replication in bacteria. *Cold Spring Harbor Symposia on Quantitative Biology* **28:** 329-348.

Jacob Y, Feng S, LeBlanc CA, Bernatavichute YV, Stroud H, Cokus S, Johnson LM, Pellegrini M, Jacobsen SE, Michaels SD (2009) ATXR5 and ATXR6 are H3K27 monomethyltransferases required for chromatin structure and gene silencing. *Nat Struct Mol Biol* **16:** 763-768

Jallepalli PV, Brown GW, Muzi-Falconi M, Tien D, Kelly TJ (1997) Regulation of the replication initiator protein p65cdc18 by CDK phosphorylation. *Genes Dev* **11:** 2767-2779

Jasencakova Z, Scharf AN, Ask K, Corpet A, Imhof A, Almouzni G, Groth A (2010) Replication stress interferes with histone recycling and predeposition marking of new histones. *Mol Cell* **37:** 736-743

Kaplan N, Moore IK, Fondufe-Mittendorf Y, Gossett AJ, Tillo D, Field Y, LeProust EM, Hughes TR, Lieb JD, Widom J, Segal E (2009) The DNA-encoded nucleosome organization of a eukaryotic genome. *Nature* **458:** 362-366

Kapler GM, Blackburn EH (1994) A weak germ-line excision mutation blocks developmentally controlled amplification of the rDNA minichromosome of *Tetrahymena thermophila*. *Genes Dev* **8:** 84-95

Karnani N, Dutta A (2011) The effect of the intra-S-phase checkpoint on origins of replication in human cells. *Genes Dev* **25:** 621-633

Karrer KM (2012) Nuclear dualism. *Methods Cell Biol* **109:** 29-52

Knoblich JA, Sauer K, Jones L, Richardson H, Saint R, Lehner CF (1994) Cyclin E controls S phase progression and its down-regulation during *Drosophila* embryogenesis is required for the arrest of cell proliferation. *Cell* **77:** 107-120

Knott SR, Viggiani CJ, Tavare S, Aparicio OM (2009) Genome-wide replication profiles indicate an expansive role for Rpd3L in regulating replication initiation timing or efficiency, and reveal genomic loci of Rpd3 function in *Saccharomyces cerevisiae*. *Genes Dev* **23:** 1077-1090

Kobayashi T, Heck DJ, Nomura M, Horiuchi T (1998) Expansion and contraction of ribosomal DNA repeats in *Saccharomyces cerevisiae*: requirement of replication fork blocking (Fob1) protein and the role of RNA polymerase I. *Genes Dev* **12:** 3821-3830

Kobayashi T, Horiuchi T (1996) A yeast gene product, Fob1 protein, required for both replication fork blocking and recombinational hotspot activities. *Genes Cells* **1:** 465-474

Komata M, Bando M, Araki H, Shirahige K (2009) The direct binding of Mrc1, a checkpoint mediator, to Mcm6, a replication helicase, is essential for the replication checkpoint against methyl methanesulfonate-induced stress. *Mol Cell Biol* **29:** 5008-5019

Kong D, DePamphilis ML (2001) Site-specific DNA binding of the *Schizosaccharomyces pombe* origin recognition complex is determined by the Orc4 subunit. *Mol Cell Biol* **21:** 8095-8103

Kumagai A, Dunphy WG (2000) Claspin, a novel protein required for the activation of Chk1 during a DNA replication checkpoint response in *Xenopus* egg extracts. *Mol Cell* **6:** 839-849

Labib K (2010) How do Cdc7 and cyclin-dependent kinases trigger the initiation of chromosome replication in eukaryotic cells? *Genes Dev* **24:** 1208-1219

Labib K, Diffley JF, Kearsey SE (1999) G1-phase and B-type cyclins exclude the DNA-replication factor Mcm4 from the nucleus. *Nat Cell Biol* **1:** 415-422

Lee CH, Chung JH (2001) The hCds1 (Chk2)-FHA domain is essential for a chain of phosphorylation events on hCds1 that is induced by ionizing radiation. *J Biol Chem* **276:** 30537-30541

Lee DG, Bell SP (1997) Architecture of the yeast origin recognition complex bound to origins of DNA replication. *Mol Cell Biol* **17:** 7159-7168

Lee JH, Paull TT (2005) ATM activation by DNA double-strand breaks through the Mre11-Rad50-Nbs1 complex. *Science* **308:** 551-554

Lee JK, Moon KY, Jiang Y, Hurwitz J (2001) The *Schizosaccharomyces pombe* origin recognition complex interacts with multiple AT-rich regions of the replication origin DNA by means of the AT-hook domains of the spOrc4 protein. *Proc Natl Acad Sci U S A* **98:** 13589-13594

Lee PH, Meng X, Kapler GM (2015) Developmental regulation of the *Tetrahymena thermophila* origin recognition complex. *PLoS Genet* **11:** e1004875

Lee SR, Collins K (2006) Two classes of endogenous small RNAs in *Tetrahymena thermophila*. *Genes Dev* **20:** 28-33

Lei M, Kawasaki Y, Tye BK (1996) Physical interactions among Mcm proteins and effects of Mcm dosage on DNA replication in *Saccharomyces cerevisiae*. *Mol Cell Biol* **16:** 5081-5090

Levenson V, Hamlin JL (1993) A general protocol for evaluating the specific effects of DNA replication inhibitors. *Nucleic Acids Res* **21:** 3997-4004

Li S, Yin L, Cole ES, Udani RA, Karrer KM (2006) Progeny of germ line knockouts of ASI2, a gene encoding a putative signal transduction receptor in *Tetrahymena*

thermophila, fail to make the transition from sexual reproduction to vegetative growth. *Dev Biol* **295:** 633-646

Li X, Zhao Q, Liao R, Sun P, Wu X (2003) The SCF(Skp2) ubiquitin ligase complex interacts with the human replication licensing factor Cdt1 and regulates Cdt1 degradation. *J Biol Chem* **278:** 30854-30858

Liang C, Spitzer JD, Smith HS, Gerbi SA (1993) Replication initiates at a confined region during DNA amplification in *Sciara* DNA puff II/9A. *Genes Dev* **7:** 1072-1084

Linskens MH, Huberman JA (1988) Organization of replication of ribosomal DNA in *Saccharomyces cerevisiae*. *Mol Cell Biol* **8:** 4927-4935

Lipford JR, Bell SP (2001) Nucleosomes positioned by ORC facilitate the initiation of DNA replication. *Mol Cell* **7:** 21-30

Liu Y, Mochizuki K, Gorovsky MA (2004) Histone H3 lysine 9 methylation is required for DNA elimination in developing macronuclei in *Tetrahymena*. *Proc Natl Acad Sci U S A* **101:** 1679-1684

Liu Y, Richards TA, Aves SJ (2009) Ancient diversification of eukaryotic MCM DNA replication proteins. *BMC Evol Biol* **9:** 60

Liu Y, Song X, Gorovsky MA, Karrer KM (2005) Elimination of foreign DNA during somatic differentiation in *Tetrahymena thermophila* shows position effect and is dosage dependent. *Eukaryot Cell* **4:** 421-431

Livak KJ, Schmittgen TD (2001) Analysis of relative gene expression data using real-time quantitative PCR and the 2(-Delta Delta C(T)) Method. *Methods* **25:** 402-408

Loidl J, Mochizuki K (2009) *Tetrahymena* meiotic nuclear reorganization is induced by a checkpoint kinase-dependent response to DNA damage. *Mol Biol Cell* **20:** 2428-2437

Loidl J, Scherthan H (2004) Organization and pairing of meiotic chromosomes in the ciliate *Tetrahymena thermophila*. *J Cell Sci* **117:** 5791-5801

Lopez-Schier H, St Johnston D (2001) Delta signaling from the germ line controls the proliferation and differentiation of the somatic follicle cells during *Drosophila* oogenesis. *Genes Dev* **15:** 1393-1405

Lubelsky Y, Sasaki T, Kuipers MA, Lucas I, Le Beau MM, Carignon S, Debatisse M, Prinz JA, Dennis JH, Gilbert DM (2011) Pre-replication complex proteins assemble at regions of low nucleosome occupancy within the Chinese hamster dihydrofolate reductase initiation zone. *Nucleic Acids Res* **39:** 3141-3155

Lutzmann M, Grey C, Traver S, Ganier O, Maya-Mendoza A, Ranisavljevic N, Bernex F, Nishiyama A, Montel N, Gavois E, Forichon L, de Massy B, Méchali M (2012) MCM8- and MCM9-deficient mice reveal gametogenesis defects and genome instability due to impaired homologous recombination. *Mol Cell* **47:** 523-534

Lutzmann M, Mechali M (2008) MCM9 binds Cdt1 and is required for the assembly of prereplication complexes. *Mol Cell* **31:** 190-200

Ly T, Ahmad Y, Shlien A, Soroka D, Mills A, Emanuele MJ, Stratton MR, Lamond AI (2014) A proteomic chronology of gene expression through the cell cycle in human myeloid leukemia cells. *Elife* **3:** e01630

Lydeard JR, Lipkin-Moore Z, Sheu YJ, Stillman B, Burgers PM, Haber JE (2010) Break-induced replication requires all essential DNA replication factors except those specific for pre-RC assembly. *Genes Dev* **24:** 1133-1144

MacAlpine DM, Rodriguez HK, Bell SP (2004) Coordination of replication and transcription along a *Drosophila* chromosome. *Genes Dev* **18:** 3094-3105

MacAlpine DM, Zhang Z, Kapler GM (1997) Type I elements mediate replication fork pausing at conserved upstream sites in the *Tetrahymena thermophila* ribosomal DNA minichromosome. *Mol Cell Biol* **17:** 4517-4525

MacAlpine HK, Gordan R, Powell SK, Hartemink AJ, MacAlpine DM (2010) *Drosophila* ORC localizes to open chromatin and marks sites of cohesin complex loading. *Genome Res* **20:** 201-211

Mailand N, Falck J, Lukas C, Syljuasen RG, Welcker M, Bartek J, Lukas J (2000) Rapid destruction of human Cdc25A in response to DNA damage. *Science* **288:** 1425-1429

Maiorano D, Cuvier O, Danis E, Mechali M (2005) MCM8 is an MCM2-7-related protein that functions as a DNA helicase during replication elongation and not initiation. *Cell* **120:** 315-328

Malik P, Zuleger N, de las Heras JI, Saiz-Ros N, Makarov AA, Lazou V, Meinke P, Waterfall M, Kelly DA, Schirmer EC (2014) NET23/STING promotes chromatin compaction from the nuclear envelope. *PLoS One* **9:** e111851

Malone CD, Anderson AM, Motl JA, Rexer CH, Chalker DL (2005) Germ line transcripts are processed by a Dicer-like protein that is essential for developmentally programmed genome rearrangements of *Tetrahymena thermophila*. *Mol Cell Biol* **25:** 9151-9164

Mantiero D, Mackenzie A, Donaldson A, Zegerman P (2011) Limiting replication initiation factors execute the temporal programme of origin firing in budding yeast. *EMBO J* **30:** 4805-4814

Marahrens Y, Stillman B (1992) A yeast chromosomal origin of DNA replication defined by multiple functional elements. *Science* **255:** 817-823

Marheineke K, Hyrien O (2004) Control of replication origin density and firing time in *Xenopus* egg extracts: role of a caffeine-sensitive, ATR-dependent checkpoint. *J Biol Chem* **279:** 28071-28081

Marsh TC, Cole ES, Stuart KR, Campbell C, Romero DP (2000) RAD51 is required for propagation of the germinal nucleus in *Tetrahymena thermophila*. *Genetics* **154:** 1587-1596

Masai H, Arai K (1996) Mechanisms of primer RNA synthesis and D-loop/R-loop-dependent DNA replication in *Escherichia coli*. *Biochimie* **78:** 1109-1117

Masai H, Matsumoto S, You Z, Yoshizawa-Sugata N, Oda M (2010) Eukaryotic chromosome DNA replication: where, when, and how? *Annu Rev Biochem* **79:** 89-130

Mayo KA, Orias E (1981) Further evidence for lack of gene expression in the *Tetrahymena* micronucleus. *Genetics* **98:** 747-762

Mechali M (2010) Eukaryotic DNA replication origins: many choices for appropriate answers. *Nat Rev Mol Cell Biol* **11:** 728-738

Meister P, Taddei A, Ponti A, Baldacci G, Gasser SM (2007) Replication foci dynamics: replication patterns are modulated by S-phase checkpoint kinases in fission yeast. *EMBO J* **26:** 1315-1326

Mendez J, Zou-Yang XH, Kim SY, Hidaka M, Tansey WP, Stillman B (2002) Human origin recognition complex large subunit is degraded by ubiquitin-mediated proteolysis after initiation of DNA replication. *Mol Cell* **9:** 481-491

Merriam EV, Bruns PJ (1988) Phenotypic assortment in *Tetrahymena thermophila*: assortment kinetics of antibiotic-resistance markers, tsA, death, and the highly amplified rDNA locus. *Genetics* **120:** 389-395

Miao W, Xiong J, Bowen J, Wang W, Liu Y, Braguinets O, Grigull J, Pearlman RE, Orias E, Gorovsky MA (2009) Microarray analyses of gene expression during the *Tetrahymena thermophila* life cycle. *PLoS One* **4:** e4429

Mickle KL, Ramanathan S, Rosebrock A, Oliva A, Chaudari A, Yompakdee C, Scott D, Leatherwood J, Huberman JA (2007) Checkpoint independence of most DNA replication origins in fission yeast. *BMC Mol Biol* **8:** 112

Mihaylov IS, Kondo T, Jones L, Ryzhikov S, Tanaka J, Zheng J, Higa LA, Minamino N, Cooley L, Zhang H (2002) Control of DNA replication and chromosome ploidy by geminin and cyclin A. *Mol Cell Biol* **22:** 1868-1880

Mimura S, Seki T, Tanaka S, Diffley JF (2004) Phosphorylation-dependent binding of mitotic cyclins to Cdc6 contributes to DNA replication control. *Nature* **431:** 1118-1123

Miotto B, Struhl K (2010) HBO1 histone acetylase activity is essential for DNA replication licensing and inhibited by Geminin. *Mol Cell* **37:** 57-66

Miyake T, Loch CM, Li R (2002) Identification of a multifunctional domain in autonomously replicating sequence-binding factor 1 required for transcriptional activation, DNA replication, and gene silencing. *Mol Cell Biol* **22:** 505-516

Mochizuki K (2008) High efficiency transformation of *Tetrahymena* using a codon-optimized neomycin resistance gene. *Gene* **425:** 79-83

Mochizuki K, Fine NA, Fujisawa T, Gorovsky MA (2002) Analysis of a piwi-related gene implicates small RNAs in genome rearrangement in *Tetrahymena*. *Cell* **110:** 689-699

Mochizuki K, Gorovsky MA (2005) A Dicer-like protein in *Tetrahymena* has distinct functions in genome rearrangement, chromosome segregation, and meiotic prophase. *Genes Dev* **19:** 77-89

Mochizuki K, Novatchkova M, Loidl J (2008) DNA double-strand breaks, but not crossovers, are required for the reorganization of meiotic nuclei in *Tetrahymena*. *J Cell Sci* **121:** 2148-2158

Mohammad M, Saha S, Kapler GM (2000) Three different proteins recognize a multifunctional determinant that controls replication initiation, fork arrest and transcription in *Tetrahymena*. *Nucleic Acids Res* **28:** 843-851

Mohammad M, York RD, Hommel J, Kapler GM (2003) Characterization of a novel origin recognition complex-like complex: implications for DNA recognition, cell cycle control, and locus-specific gene amplification. *Mol Cell Biol* **23:** 5005-5017

Mohammad MM, Donti TR, Sebastian Yakisich J, Smith AG, Kapler GM (2007) *Tetrahymena* ORC contains a ribosomal RNA fragment that participates in rDNA origin recognition. *EMBO J* **26:** 5048-5060

Moon KY, Kong D, Lee JK, Raychaudhuri S, Hurwitz J (1999) Identification and reconstitution of the origin recognition complex from *Schizosaccharomyces pombe*. *Proc Natl Acad Sci U S A* **96:** 12367-12372

Morrison TL, Yakisich JS, Cassidy-Hanley D, Kapler GM (2005) TIF1 Represses rDNA replication initiation, but promotes normal S phase progression and chromosome transmission in *Tetrahymena*. *Mol Biol Cell* **16:** 2624-2635

Nam EA, Cortez D (2011) ATR signalling: more than meeting at the fork. *Biochem J* **436:** 527-536

Nguyen VQ, Co C, Irie K, Li JJ (2000) Clb/Cdc28 kinases promote nuclear export of the replication initiator proteins Mcm2-7. *Curr Biol* **10:** 195-205

Nguyen VQ, Co C, Li JJ (2001) Cyclin-dependent kinases prevent DNA re-replication through multiple mechanisms. *Nature* **411:** 1068-1073

Nieduszynski CA, Knox Y, Donaldson AD (2006) Genome-wide identification of replication origins in yeast by comparative genomics. *Genes Dev* **20:** 1874-1879

Nishimura K, Ishiai M, Horikawa K, Fukagawa T, Takata M, Takisawa H, Kanemaki Masato T (2012) Mcm8 and Mcm9 form a complex that functions in homologous recombination repair induced by DNA interstrand crosslinks. *Mol Cell* **47:** 511-522

Nishitani H, Lygerou Z, Nishimoto T, Nurse P (2000) The Cdt1 protein is required to license DNA for replication in fission yeast. *Nature* **404:** 625-628

Nishitani H, Sugimoto N, Roukos V, Nakanishi Y, Saijo M, Obuse C, Tsurimoto T, Nakayama KI, Nakayama K, Fujita M, Lygerou Z, Nishimoto T (2006) Two E3 ubiquitin ligases, SCF-Skp2 and DDB1-Cul4, target human Cdt1 for proteolysis. *EMBO J* **25:** 1126-1136

Ohtani K, DeGregori J, Leone G, Herendeen DR, Kelly TJ, Nevins JR (1996) Expression of the HsOrc1 gene, a human ORC1 homolog, is regulated by cell proliferation via the E2F transcription factor. *Mol Cell Biol* **16:** 6977-6984

Okuno Y, Satoh H, Sekiguchi M, Masukata H (1999) Clustered adenine/thymine stretches are essential for function of a fission yeast replication origin. *Mol Cell Biol* **19:** 6699-6709

Oliver AW, Paul A, Boxall KJ, Barrie SE, Aherne GW, Garrett MD, Mittnacht S, Pearl LH (2006) Trans-activation of the DNA-damage signalling protein kinase Chk2 by T-loop exchange. *EMBO J* **25:** 3179-3190

Orias E (1991) Evolution of amitosis of the ciliate macronucleus: gain of the capacity to divide. *J Protozool* **38:** 217-221

Orr-Weaver TL, Johnston CG, Spradling AC (1989) The role of Ace3 in *Drosophila* chorion gene amplification. *EMBO J* **8:** 4153-4162

Osheim YN, Miller OL, Jr., Beyer AL (1988) Visualization of *Drosophila melanogaster* chorion genes undergoing amplification. *Mol Cell Biol* **8:** 2811-2821

Paixao S, Colaluca IN, Cubells M, Peverali FA, Destro A, Giadrossi S, Giacca M, Falaschi A, Riva S, Biamonti G (2004) Modular structure of the human lamin B2 replicator. *Mol Cell Biol* **24:** 2958-2967

Palen TE, Cech TR (1984) Chromatin structure at the replication origins and transcription-initiation regions of the ribosomal RNA genes of *Tetrahymena*. *Cell* **36:** 933-942

Pan WC, Blackburn EH (1981) Single extrachromosomal ribosomal RNA gene copies are synthesized during amplification of the rDNA in *Tetrahymena*. *Cell* **23:** 459-466

Pan WJ, Gallagher RC, Blackburn EH (1995) Replication of an rRNA gene origin plasmid in the *Tetrahymena thermophila* macronucleus is prevented by transcription through the origin from an RNA polymerase I promoter. *Mol Cell Biol* **15:** 3372-3381

Pappas DL, Jr., Frisch R, Weinreich M (2004) The NAD(+)-dependent Sir2p histone deacetylase is a negative regulator of chromosomal DNA replication. *Genes Dev* **18:** 769-781

Parisi T, Beck AR, Rougier N, McNeil T, Lucian L, Werb Z, Amati B (2003) Cyclins E1 and E2 are required for endoreplication in placental trophoblast giant cells. *EMBO J* **22:** 4794-4803

Park J, Long DT, Lee KY, Abbas T, Shibata E, Negishi M, Luo Y, Schimenti JC, Gambus A, Walter JC, Dutta A (2013) The MCM8-MCM9 complex promotes RAD51 recruitment at DNA damage sites to facilitate homologous recombination. *Mol Cell Biol* **33:** 1632-1644

Park SY, Asano M (2008) The origin recognition complex is dispensable for endoreplication in *Drosophila*. *Proc Natl Acad Sci U S A* **105:** 12343-12348

Patil NS, Hempen PM, Udani RA, Karrer KM (1997) Alternate junctions and microheterogeneity of Tlr1, a developmentally regulated DNA rearrangement in *Tetrahymena thermophila*. *J Eukaryot Microbiol* **44:** 518-522

Preer JR, Preer LB (1979) The size of macronuclear DNA and its relationship to models for maintaining genic balance. *The Journal of Protozoology* **26:** 14-18

Quinn LM, Herr A, McGarry TJ, Richardson H (2001) The *Drosophila* Geminin homolog: roles for Geminin in limiting DNA replication, in anaphase and in neurogenesis. *Genes Dev* **15:** 2741-2754

Randell JC, Fan A, Chan C, Francis LI, Heller RC, Galani K, Bell SP (2010) Mec1 is one of multiple kinases that prime the Mcm2-7 helicase for phosphorylation by Cdc7. *Mol Cell* **40:** 353-363

Rao H, Stillman B (1995) The origin recognition complex interacts with a bipartite DNA binding site within yeast replicators. *Proc Natl Acad Sci U S A* **92:** 2224-2228

Rattray AJ, Shafer BK, Neelam B, Strathern JN (2005) A mechanism of palindromic gene amplification in *Saccharomyces cerevisiae*. *Genes Dev* **19:** 1390-1399

Remus D, Beall EL, Botchan MR (2004) DNA topology, not DNA sequence, is a critical determinant for *Drosophila* ORC-DNA binding. *EMBO J* **23:** 897-907

Remus D, Beuron F, Tolun G, Griffith JD, Morris EP, Diffley JF (2009) Concerted loading of Mcm2-7 double hexamers around DNA during DNA replication origin licensing. *Cell* **139:** 719-730

Rowles A, Chong JP, Brown L, Howell M, Evan GI, Blow JJ (1996) Interaction between the origin recognition complex and the replication licensing system in *Xenopus*. *Cell* **87:** 287-296

Saha S, Kapler GM (2000) Allele-specific protein-DNA interactions between the single-stranded DNA-binding protein, ssA-TIBF, and DNA replication determinants in *Tetrahymena*. *J Mol Biol* **295:** 423-439

Sandler SJ, Marians KJ (2000) Role of PriA in replication fork reactivation in *Escherichia coli*. *J Bacteriol* **182:** 9-13

Schaeffer V, Althauser C, Shcherbata HR, Deng WM, Ruohola-Baker H (2004) Notch-dependent Fizzy-related/Hec1/Cdh1 expression is required for the mitotic-to-endocycle transition in *Drosophila* follicle cells. *Curr Biol* **14:** 630-636

Schwab RA, Niedzwiedz W (2011) Visualization of DNA replication in the vertebrate model system DT40 using the DNA fiber technique. *J Vis Exp* **56:** e3255

Sclafani RA, Holzen TM (2007) Cell cycle regulation of DNA replication. *Annu Rev Genet* **41:** 237-280

Segurado M, de Luis A, Antequera F (2003) Genome-wide distribution of DNA replication origins at A+T-rich islands in *Schizosaccharomyces pombe*. *EMBO Rep* **4:** 1048-1053

Senga T, Sivaprasad U, Zhu W, Park JH, Arias EE, Walter JC, Dutta A (2006) PCNA is a cofactor for Cdt1 degradation by CUL4/DDB1-mediated N-terminal ubiquitination. *J Biol Chem* **281:** 6246-6252

Sequeira-Mendes J, Diaz-Uriarte R, Apedaile A, Huntley D, Brockdorff N, Gomez M (2009) Transcription initiation activity sets replication origin efficiency in mammalian cells. *PLoS Genet* **5:** e1000446

Shcherbata HR, Althauser C, Findley SD, Ruohola-Baker H (2004) The mitotic-to-endocycle switch in *Drosophila* follicle cells is executed by Notch-dependent regulation of G1/S, G2/M and M/G1 cell-cycle transitions. *Development* **131:** 3169-3181

Shechter D, Gautier J (2004) MCM proteins and checkpoint kinases get together at the fork. *Proc Natl Acad Sci U S A* **101:** 10845-10846

Sher N, Bell GW, Li S, Nordman J, Eng T, Eaton ML, Macalpine DM, Orr-Weaver TL (2012) Developmental control of gene copy number by repression of replication initiation and fork progression. *Genome Res* **22:** 64-75

Sher N, Von Stetina JR, Bell GW, Matsuura S, Ravid K, Orr-Weaver TL (2013) Fundamental differences in endoreplication in mammals and *Drosophila* revealed by analysis of endocycling and endomitotic cells. *Proc Natl Acad Sci U S A* **110:** 9368-9373

Sheu YJ, Stillman B (2006) Cdc7-Dbf4 phosphorylates MCM proteins via a docking site-mediated mechanism to promote S phase progression. *Mol Cell* **24:** 101-113

Sheu YJ, Stillman B (2010) The Dbf4-Cdc7 kinase promotes S phase by alleviating an inhibitory activity in Mcm4. *Nature* **463:** 113-117

Shimada K, Pasero P, Gasser SM (2002) ORC and the intra-S-phase checkpoint: a threshold regulates Rad53p activation in S phase. *Genes Dev* **16:** 3236-3252

Shimuta K, Nakajo N, Uto K, Hayano Y, Okazaki K, Sagata N (2002) Chk1 is activated transiently and targets Cdc25A for degradation at the *Xenopus* midblastula transition. *EMBO J* **21:** 3694-3703

Shirahige K, Hori Y, Shiraishi K, Yamashita M, Takahashi K, Obuse C, Tsurimoto T, Yoshikawa H (1998) Regulation of DNA-replication origins during cell-cycle progression. *Nature* **395:** 618-621

Simpson RT (1990) Nucleosome positioning can affect the function of a cis-acting DNA element *in vivo*. *Nature* **343:** 387-389

Smith JJ, Yakisich JS, Kapler GM, Cole ES, Romero DP (2004) A beta-tubulin mutation selectively uncouples nuclear division and cytokinesis in *Tetrahymena thermophila*. *Eukaryot Cell* **3:** 1217-1226

Snaith HA, Brown GW, Forsburg SL (2000) *Schizosaccharomyces pombe* Hsk1p is a potential cds1p target required for genome integrity. *Mol Cell Biol* **20:** 7922-7932

Sonneville R, Querenet M, Craig A, Gartner A, Blow JJ (2012) The dynamics of replication licensing in live *Caenorhabditis elegans* embryos. *J Cell Biol* **196:** 233-246

Spradling AC (1981) The organization and amplification of two chromosomal domains containing *Drosophila* chorion genes. *Cell* **27:** 193-201

Stead BE, Brandl CJ, Sandre MK, Davey MJ (2012) Mcm2 phosphorylation and the response to replicative stress. *BMC Genet* **13:** 36

Stewart JA, Wang F, Chaiken MF, Kasbek C, Chastain PD, 2nd, Wright WE, Price CM (2012) Human CST promotes telomere duplex replication and general replication restart after fork stalling. *EMBO J* **31:** 3537-3549

Stinchcomb DT, Struhl K, Davis RW (1979) Isolation and characterisation of a yeast chromosomal replicator. *Nature* **282:** 39-43

Stoeber K, Tlsty TD, Happerfield L, Thomas GA, Romanov S, Bobrow L, Williams ED, Williams GH (2001) DNA replication licensing and human cell proliferation. *J Cell Sci* **114:** 2027-2041

Stucki M, Clapperton JA, Mohammad D, Yaffe MB, Smerdon SJ, Jackson SP (2005) MDC1 directly binds phosphorylated histone H2AX to regulate cellular responses to DNA double-strand breaks. *Cell* **123:** 1213-1226

Tada S, Li A, Maiorano D, Mechali M, Blow JJ (2001) Repression of origin assembly in metaphase depends on inhibition of RLF-B/Cdt1 by geminin. *Nat Cell Biol* **3:** 107-113

Takahashi TS, Wigley DB, Walter JC (2005) Pumps, paradoxes and ploughshares: mechanism of the MCM2-7 DNA helicase. *Trends Biochem Sci* **30:** 437-444

Talasz H, Helliger W, Sarg B, Debbage PL, Puschendorf B, Lindner H (2002) Hyperphosphorylation of histone H2A.X and dephosphorylation of histone H1 subtypes in the course of apoptosis. *Cell Death Differ* **9:** 27-39

Tanaka H, Cao Y, Bergstrom DA, Kooperberg C, Tapscott SJ, Yao MC (2007a) Intrastrand annealing leads to the formation of a large DNA palindrome and determines the boundaries of genomic amplification in human cancer. *Mol Cell Biol* **27:** 1993-2002

Tanaka S, Diffley JF (2002) Interdependent nuclear accumulation of budding yeast Cdt1 and Mcm2-7 during G1 phase. *Nat Cell Biol* **4:** 198-207

Tanaka S, Umemori T, Hirai K, Muramatsu S, Kamimura Y, Araki H (2007b) CDK-dependent phosphorylation of Sld2 and Sld3 initiates DNA replication in budding yeast. *Nature* **445:** 328-332

Taverna SD, Coyne RS, Allis CD (2002) Methylation of histone h3 at lysine 9 targets programmed DNA elimination in *Tetrahymena*. *Cell* **110:** 701-711

Tercero JA, Diffley JF (2001) Regulation of DNA replication fork progression through damaged DNA by the Mec1/Rad53 checkpoint. *Nature* **412:** 553-557

Theis JF, Newlon CS (1997) The ARS309 chromosomal replicator of *Saccharomyces cerevisiae* depends on an exceptional ARS consensus sequence. *Proc Natl Acad Sci U S A* **94:** 10786-10791

Thoma F, Bergman LW, Simpson RT (1984) Nuclease digestion of circular TRP1ARS1 chromatin reveals positioned nucleosomes separated by nuclease-sensitive regions. *J Mol Biol* **177:** 715-733

Tower J (2004) Developmental gene amplification and origin regulation. *Annu Rev Genet* **38:** 273-304

Tuduri S, Tourriere H, Pasero P (2010) Defining replication origin efficiency using DNA fiber assays. *Chromosome Res* **18:** 91-102

Tugal T, Zou-Yang XH, Gavin K, Pappin D, Canas B, Kobayashi R, Hunt T, Stillman B (1998) The Orc4p and Orc5p subunits of the *Xenopus* and human origin recognition complex are related to Orc1p and Cdc6p. *J Biol Chem* **273:** 32421-32429

Ullah Z, Kohn MJ, Yagi R, Vassilev LT, DePamphilis ML (2008) Differentiation of trophoblast stem cells into giant cells is triggered by p57/Kip2 inhibition of CDK1 activity. *Genes Dev* **22:** 3024-3036

Vas A, Mok W, Leatherwood J (2001) Control of DNA rereplication via Cdc2 phosphorylation sites in the origin recognition complex. *Mol Cell Biol* **21:** 5767-5777

Vashee S, Cvetic C, Lu W, Simancek P, Kelly TJ, Walter JC (2003) Sequence-independent DNA binding and replication initiation by the human origin recognition complex. *Genes Dev* **17:** 1894-1908

Volkening M, Hoffmann I (2005) Involvement of human MCM8 in prereplication complex assembly by recruiting hcdc6 to chromatin. *Mol Cell Biol* **25:** 1560-1568

Wang L, Lin CM, Brooks S, Cimbora D, Groudine M, Aladjem MI (2004) The human beta-globin replication initiation region consists of two modular independent replicators. *Mol Cell Biol* **24:** 3373-3386

Weiss A, Herzig A, Jacobs H, Lehner CF (1998) Continuous Cyclin E expression inhibits progression through endoreduplication cycles in *Drosophila*. *Curr Biol* **8:** 239-242

Wiley EA, Myers T, Parker K, Braun T, Yao MC (2005) Class I histone deacetylase Thd1p affects nuclear integrity in *Tetrahymena thermophila*. *Eukaryot Cell* **4:** 981-990

Wilmes GM, Archambault V, Austin RJ, Jacobson MD, Bell SP, Cross FR (2004) Interaction of the S-phase cyclin Clb5 with an "RXL" docking sequence in the initiator protein Orc6 provides an origin-localized replication control switch. *Genes Dev* **18:** 981-991

Wilmes GM, Bell SP (2002) The B2 element of the *Saccharomyces cerevisiae* ARS1 origin of replication requires specific sequences to facilitate pre-RC formation. *Proc Natl Acad Sci U S A* **99:** 101-106

Wohlschlegel JA, Dwyer BT, Dhar SK, Cvetic C, Walter JC, Dutta A (2000) Inhibition of eukaryotic DNA replication by geminin binding to Cdt1. *Science* **290:** 2309-2312

Wolfe J (1982) The conjugation junction of *Tetrahymena*: Its structure and development. *J Morphol* **172:** 159-178

Wu N, Liang C, DiBartolomeis SM, Smith HS, Gerbi SA (1993) Developmental progression of DNA puffs in *Sciara coprophila*: amplification and transcription. *Dev Biol* **160:** 73-84

Wuarin J, Buck V, Nurse P, Millar JB (2002) Stable association of mitotic cyclin B/Cdc2 to replication origins prevents endoreduplication. *Cell* **111:** 419-431

Wyrick JJ, Aparicio JG, Chen T, Barnett JD, Jennings EG, Young RA, Bell SP, Aparicio OM (2001) Genome-wide distribution of ORC and MCM proteins in *S. cerevisiae*: high-resolution mapping of replication origins. *Science* **294:** 2357-2360

Xiong J, Lu X, Lu Y, Zeng H, Yuan D, Feng L, Chang Y, Bowen J, Gorovsky M, Fu C, Miao W (2011) *Tetrahymena* Gene Expression Database (TGED): a resource of microarray data and co-expression analyses for *Tetrahymena*. *Sci China Life Sci* **54:** 65-67

Yakisich JS, Kapler GM (2006) Deletion of the *Tetrahymena thermophila* rDNA replication fork barrier region disrupts macronuclear rDNA excision and creates a fragile site in the micronuclear genome. *Nucleic Acids Res* **34:** 620-634

Yakisich JS, Sandoval PY, Morrison TL, Kapler GM (2006) TIF1 activates the intra-S-phase checkpoint response in the diploid micronucleus and amitotic polyploid macronucleus of *Tetrahymena*. *Mol Biol Cell* **17:** 5185-5197

Yao MC, Chao JL (2005) RNA-guided DNA deletion in *Tetrahymena*: an RNAi-based mechanism for programmed genome rearrangements. *Annu Rev Genet* **39:** 537-559

Yao MC, Choi J, Yokoyama S, Austerberry CF, Yao CH (1984) DNA elimination in *Tetrahymena*: a developmental process involving extensive breakage and rejoining of DNA at defined sites. *Cell* **36:** 433-440

Yao MC, Fuller P, Xi X (2003) Programmed DNA deletion as an RNA-guided system of genome defense. *Science* **300:** 1581-1584

Yao MC, Gorovsky MA (1974) Comparison of the sequences of macro- and micronuclear DNA of *Tetrahymena pyriformis*. *Chromosoma* **48:** 1-18

Yao MC, Kimmel AR, Gorovsky MA (1974) A small number of cistrons for ribosomal RNA in the germinal nucleus of a eukaryote, *Tetrahymena pyriformis*. *Proc Natl Acad Sci U S A* **71:** 3082-3086

Yao MC, Yao CH, Monks B (1990) The controlling sequence for site-specific chromosome breakage in *Tetrahymena*. *Cell* **63:** 763-772

Yao MC, Zheng K, Yao CH (1987) A conserved nucleotide sequence at the sites of developmentally regulated chromosomal breakage in *Tetrahymena*. *Cell* **48:** 779-788

Yasuda LF, Yao MC (1991) Short inverted repeats at a free end signal large palindromic DNA formation in *Tetrahymena*. *Cell* **67:** 505-516

Yin L, Gater ST, Karrer KM (2010) A developmentally regulated gene, ASI2, is required for endocycling in the macronuclear anlagen of *Tetrahymena*. *Eukaryot Cell* **9:** 1343-1353

Zegerman P, Diffley JF (2007) Phosphorylation of Sld2 and Sld3 by cyclin-dependent kinases promotes DNA replication in budding yeast. *Nature* **445:** 281-285

Zhang Z, Macalpine DM, Kapler GM (1997) Developmental regulation of DNA replication: replication fork barriers and programmed gene amplification in *Tetrahymena thermophila*. *Mol Cell Biol* **17:** 6147-6156

Zhu W, Chen Y, Dutta A (2004) Rereplication by depletion of geminin is seen regardless of p53 status and activates a G2/M checkpoint. *Mol Cell Biol* **24:** 7140-7150

Zielke N, Kim KJ, Tran V, Shibutani ST, Bravo MJ, Nagarajan S, van Straaten M, Woods B, von Dassow G, Rottig C, Lehner CF, Grewal SS, Duronio RJ, Edgar BA (2011) Control of *Drosophila* endocycles by E2F and CRL4(CDT2). *Nature* **480:** 123-127

Zou L, Elledge SJ (2003) Sensing DNA damage through ATRIP recognition of RPA-ssDNA complexes. *Science* **300:** 1542-1548

APPENDIX A

The work described in Chapter II, was published in PLOS Genetics (11: e1004875, January 8, 2015) and I was a co-first author. Here I summarize my specific contributions to this work and their significance.

One of the important contributions I made required the utilization of a method called DNA fiber analysis to examine DNA replication initiation and elongation through pulse- and chase-labeling in individual DNA fibers. Compared to traditional approaches used in the lab to study DNA replication, such as two dimensional gel electrophoresis which focuses on a specific replication origin, DNA fiber analysis could provide us with information on initiation and elongation on a genome-wide scale. Although this method has been used in other organisms, this is the first time that the approach was applied to ciliates. I have optimized different conditions, such as labeling period and the way to spread fibers, to find the best working procedure for *Tetrahymena* cells. In this chapter, by using DNA fiber analysis, I found that the origin density was not affected in ORC1 knockdown strain where there was five-fold reduction of Orc1p (Figure 2.5B). This was surprising because fewer origins were utilized in the ORC2 mutant in *S. cerevisiae*. I also found that the replication fork rate decreases in the ORC1 knockdown strain (Figure 2.5B), and this may be due to the coordinate downregulation of MCMs in this strain. These data suggest that replication elongation rather than initiation is perturbed in ORC1 knockdown strain. The data also indicate that MCMs are not excessive in *Tetrahymena*, which is different from other higher eukaryotes.

Secondly, I followed up Po-Hsuen Lee's initial observations that levels of Orc1p and Mcm6p fluctuate during development. I used alpha-tubulin protein (Atu1p) as a reference to quantify the changes of Orc1p and Mcm6p by western blot analysis (Figures 2.9 and 2.10). I chose Atu1p because previous study has shown that this protein does not fluctuate in mating cells or exconjugates before refeeding (Endo II). In this work, I found that the abundance of Atu1p was dramatically reduced late in Endo II (Figures 2.9 and 2.10), similar to Orc1p. I also determined the protein level of Rad51p across development, and found that Rad51p was not greatly reduced in Endo II. The different change patterns of these proteins upon refeeding indicate that the low levels of Orc1p and Mcm6p are not due to a loading problem. The protein levels of Orc1p and Mcm6p are lowest late in Endo II when the demands for DNA synthesis is high (Figures 2.9 and 2.10). This data suggest an ORC-independent mechanism might be used for replication initiation. Moreover, I determined that Rad51p peaks late in Endo I (Figures 2.9 and 2.10). This data supports that homologous recombination occurs late in Endo I, when nutrients and dNTPs are lacking, and suggests that homologous recombination might mediate ORC-independent replication initiation.

Another important contribution I made to this work was that I discovered that aberrant rDNA replication intermediates (RIs) are generated during Endo II (Figure 2.11) by 2D gel electrophoresis. These RIs are sensitive to Mung Bean nuclease (MBN) digestion, indicating that ssDNAs or DNA-RNA hybrids exist (Figure 2.11). I speculate that these aberrant RIs may arise from some minor elongation problems during Endo II. After MBN treatment, aberrant RIs are converted to simple Y arcs. This data suggest

that the known replication origins are not utilized during Endo II, when levels of ORC proteins are very low. Hence, my collective data suggest that replication initiation and elongation are altered during endoreplication.

APPENDIX B

The work described in Chapter III, is a manuscript that has been submitted to PLOS Genetics, and I am a co-first author. Here I summarize my specific contributions to this work and their significance.

I used DNA fiber analysis to address mechanistic questions related to the effect of hydroxyurea (HU) on origin firing and fork elongation as well as the specific DNA replication program after HU removal, prior to replenishment of ORC and MCM proteins. DNA fiber analysis in starved and re-fed cells under HU treatment provided no evidence for incorporation of IdU (Figure 3.6A). In contrast to *S. cerevisiae*, where HU slows replication forks, HU appears to arrest replication fork elongation in *Tetrahymena*. Moreover, ORC and MCM proteins are degraded under HU treatment. This brings up a question: how would DNA replication occur after HU removal since the pre-RC components are degraded? To answer this question, I used DNA fiber analysis to determine replication initiation and elongation in the first S phase after HU removal when ORC and MCM proteins are not replenished. Although there was no fork elongation in HU arrested G1 cells, both fork elongation and new origin firing were detected once HU was removed (Figure 3.11). The collective data suggest that new origin firing is ORC-independent. I found that the inter-origin distance is larger than normal S phase (Figure 3.11), which confirmed that replication initiation in this specialized replication program is altered. Surprisingly, the fork rate is not affected (Figure 3.11). Since the levels of MCM proteins are not restored, I propose that an

alternative helicase, such as MCM8 or/and MCM9 is responsible for replication elongation.

In addition, when Pamela Sandoval added HU to cells in mid-S phase, she saw the DNA replication profile changes. The DNA content did not increase or stay constant. Instead, she saw a decrease in DNA content in S phase arrested cells under HU treatment. I performed DNA fiber analysis to ask whether the newly synthesized DNA has been selectively degraded. I saw no evidence for that (Figure 3.6B), suggesting that other mechanisms could be involved. One possibility raised by my co-author Po-Hsuen Lee is that compaction through global histone acetylation might be responsible.